

Chloroplast engineering in the green alga *Chlamydomonas* for production of novel recombinant products

Luyao Yang

Institute of Structural and Molecular Biology

University College London

A thesis submitted for the degree of

Doctor of Philosophy (PhD)

April 2025

Declaration

I, Luyao Yang, confirm that the work presented in my thesis is my own.
Where information has been derived from other sources, I confirm that this has been indicated in the thesis.

Abstract

The edible microalga *Chlamydomonas reinhardtii* has emerged as a promising platform for producing high-value compounds and has been applied broadly, such as recombinant therapeutics and biomaterials. Growth rates and disease control are two major limiting factors in aquaculture, but both could be addressed through oral delivery of affordable therapeutics. Fish growth hormones (fGHs) have been shown to promote the growth of fish and shellfish, and specific double-stranded RNA (dsRNA) molecules designed to key viral genes can serve as RNA-based vaccines. When taken up by animals, the dsRNA can trigger the RNA interference (RNAi) mechanism and produce small interfering RNA (siRNA) that silence viral genes. The study sets out to produce fGHs and dsRNAs in the chloroplast of *C. reinhardtii* to develop a system for whole-cell bio-encapsulation and oral delivery. Initial studies used shrimp as a model and focused on the optimisation of fGHs and dsRNA administration doses, shrimp growth and viral challenge performance, as well as optimisation of a low-cost 'hanging bag' photobioreactor system used for scale-up production of the algae to produce sufficient dried biomass for further shrimp feeding trials. Furthermore, a novel recipient strain *psaA*** was developed and tested to optimise the chloroplast transformation method for the simple generation of marker-free transformants.

Spider silk protein is a biomaterial in wide applications as its outstanding mechanical features are biodegradable and biocompatible. However, spider silk production has many limitations, especially the challenging, time-consuming, and expensive collecting process. Recombinant production was attempted in various systems, with

microalga *C. reinhardtii* as one of the promising organisms. Several types of recombinant spider silk proteins attract extra attention, particularly major ampullate spidroin (*MaSp*), such as *MaSp1* and *MaSp2*. Transgenic lines of *C. reinhardtii* that appear to accumulate the different sizes of repetitive *MaSp1* protein were created and cultivated under photoheterotrophic and photoautotrophic growth conditions.

Impact Statement

My thesis, titled "*Chloroplast Engineering in the Green Alga Chlamydomonas for Production of Novel Recombinant Products*," addresses key challenges in sustainable biotechnology through innovations in chloroplast engineering. By advancing genetic modification methods in *Chlamydomonas*, my research provides a foundation for scalable, eco-friendly protein production, offering alternatives to conventional, resource-intensive practices.

Academic Impact

This research makes significant contributions to molecular biology, focusing on chloroplast engineering and synthetic biology. It introduces a novel approach to codon reassignment and optimization, preventing reversion mutations and expanding the toolkit for chloroplast transformation. By developing a versatile recipient cell line, *psaA*^{**} (double-stop), and a codon-optimized spider silk gene, this work enhances the stability and efficiency of chloroplast genetic modifications. The methods and insights offer valuable resources for future studies and provide a blueprint for producing diverse recombinant proteins relevant to therapeutic and agricultural applications.

Economic and Societal Impact

This research focuses on edible chloroplast-encapsulated fish growth hormone and an anti-viral shrimp vaccine, with transformative potential for aquaculture. Viral outbreaks cause significant losses worldwide in this sector, and this project offers a

cost-effective, easy-to-administer solution with the shrimp vaccine, enhancing aquaculture resilience to disease. These applications contribute to food security by offering scalable, practical solutions to meet industry needs.

Environmental Impact

Using *Chlamydomonas* as a bio-factory for recombinant proteins presents a sustainable alternative to traditional production practices that require substantial chemical and energy inputs. Chloroplast engineering in algae reduces greenhouse gas emissions and minimizes waste, aligning with green biotechnology principles. These sustainable methods reduce environmental impact and encourage responsible biotech advancements.

In summary, my thesis advances scientific understanding of chloroplast engineering while establishing a sustainable platform with broad applications. It supports economic growth, environmental sustainability, and improved food security, positioning this research as a promising step toward more responsible biotechnology.

Acknowledgements

I am deeply grateful for the support, encouragement, and guidance I have received throughout my PhD journey. This work would not have been possible without the many individuals who generously contributed their time, expertise, and encouragement. Though this may be a long list of acknowledgments, it cannot fully convey my gratitude to everyone.

First and foremost, I would like to thank my supervisor, Prof. Saul Purton, for his invaluable guidance, patience, and unwavering support throughout this project. His mentorship has been a source of inspiration, and his insights have profoundly shaped my understanding of molecular biology and biotechnology. I am also grateful to my secondary supervisor, Dr. Brenda Parker, and my thesis committee chair, Dr. Andrew Osborne, for their guidance and support.

I am equally grateful to the members of the Purton Lab, whose camaraderie, advice, and collaborative spirit enriched my research experience. Special thanks to our lab manager, Thushyanthi Sivagnanam, for her dedication and assistance; Dr. Henry Taunt, for helping me establish myself in the lab; Dr. Harry Jackson, who inspired me to uphold professionalism and scientific rigor daily and offered patient guidance on the fish growth hormone project; Dr. Jing Cui, for her selfless encouragement, mentorship, and preliminary trials on the spider silk protein project; Dr. Lydia Mapstone, who demonstrated my first experiment in the Purton Lab and served as a role model for women entrepreneurs; and Dr. Tamar Schwarz and Dr. Julianie Stapelberg Rogers, for their inspiration and companionship in the lab. I would also like to thank my peers:

Miss Pokchut Kulsokumbot, whose kindness and understanding continually encouraged me, as well as Mr. Gabriel Scoglio, Miss Rinad Alhedaithy, Miss Anaëlle Vilatte, and Miss Inés Zouhaïr, for their camaraderie and support. To our summer students, Miss Liepa Siupsinskaite, for her contributions to the spider silk project, and Miss Kanticha Jutharee (Mae), for her valuable assistance on my psaA** project, I extend my sincere thanks.

I would like to thank my collaborators, Dr. Vanvimon Saksmerprome and Dr. Patai Charoonnart (Ploy), for hosting me during the animal trials in Thailand and for their valuable collaboration. I am also grateful to Dr. Carlos Fajardo Quiñones for his collaboration on the dsRNA project.

My heartfelt gratitude goes to my family. To my late grandparents, Yeye, Nainai, and Laoye, whom I sadly lost during my PhD journey – I hope I have made you proud, and I know you are watching over me. To my parents, for being models of dedication and passion in their careers. Their unwavering support has given me the strength to persevere, and their faith in me has been my greatest motivation. To my beloved dogs, Xiaobai and Chocolate, thank you for bringing joy to my family while I am abroad. To my uncle Quan and his family, for their generous support, both financially and emotionally, along this journey. A special thanks to my best friend, Miss Xue Han, for over 17 years of friendship, and all my best wishes for her career and happiness.

To my friends, thank you for being my sounding board and helping me find balance throughout this demanding journey. Special thanks to Mr. Patrick Goh for his companionship throughout my PhD, for unconditionally bearing with my sensitive and

emotional moments, and for supporting me selflessly—may your kindness be blessed. My gratitude also goes to Miss Lulu Sun for her care and companionship during my final writing year; best wishes to her on her own PhD journey. Thank you to Miss Eileen Wang for her encouragement and unfailing kindness. I am also deeply appreciative of Mr. Jacky Huang for his insights, support, and companionship. Each of you has contributed to this journey in your own way, and I am profoundly grateful.

I would like to thank my colleagues at Synthetica Biotech LTD—Mr. Dabier Miya, Mrs. Tea Sankovic, and Mrs. Jane Purton—for their trust and support. I am excited about the path ahead for Synthetica and wish us all the best for a bright future.

I am grateful to Prof. Qi Cheng and Qi's Academy for their financial support, which enabled me to pursue this research. Their commitment to advancing scientific knowledge and supporting early-career researchers has been instrumental in making this work possible.

Last but not least, I would like to thank myself, Luyao, for my hard work, diligence, and resilience throughout this journey, despite the challenges. And thank you to my best mate, *Chlamy*, for making this research possible, even if you were occasionally a bit uncooperative!

Thank you all for making this achievement possible.

Table of Contents

Declaration	2
Abstract	3
Impact Statement	5
Acknowledgements.....	7
Table of Contents	10
List of Tables	14
List of Figures.....	15
List of Appendices	18
List of Abbreviations.....	19
1 Introduction.....	24
1.1 The chloroplast of microalgae.....	24
1.1.1 What are microalgae?.....	24
1.1.2 The chloroplast and photosynthesis of microalgae.....	28
1.1.3 <i>Chlamydomonas reinhardtii</i> as a model organism.....	30
1.2 The chloroplast engineering of <i>C. reinhardtii</i>	35
1.2.1 The chloroplast genome of <i>C. reinhardtii</i>	35
1.2.2 DNA delivery into the chloroplast of <i>C. reinhardtii</i>	39
1.2.3 STEP Toolkit in <i>C. reinhardtii</i> chloroplast	43
1.3 The microalga <i>C. reinhardtii</i> as a platform for novel products	47
1.3.1 Advantages of using <i>C. reinhardtii</i> for recombinant production	47
1.3.2 Synthesis of recombinant products in <i>C. reinhardtii</i> chloroplast.....	50
1.3.3 Challenges of <i>C. reinhardtii</i> chloroplast for recombinant production	55
1.4 Aims and objectives.....	56
2 Materials and Methods.....	60
2.1 <i>Chlamydomonas reinhardtii</i> strains, cultivation, and storage	60
2.2 <i>Escherichia coli</i> strains, culture and storage	62
2.3 Molecular techniques.....	64
2.3.1 DNA assembly	64

2.3.2	Nucleic acids extraction	69
2.4	DNA analysis	71
2.4.1	Diagnostic restriction enzymes digestion.....	71
2.4.2	Agarose gel electrophoresis and gel purification	72
2.4.3	DNA sequencing	73
2.5	RNA analysis	74
2.5.1	Analytical polyacrylamide gel electrophoresis	74
2.5.2	Agarose gel electrophoresis	74
2.5.3	Fluorescent RNA analysis	75
2.6	Gene delivery.....	76
2.6.1	<i>E. coli</i> competent cells and heat shock transformation.....	76
2.6.2	Chloroplast transformation.....	76
2.7	Protein analysis	78
2.7.1	Protein purification	78
2.7.2	Western blotting	79
2.8	Downstream processing	81
2.8.1	Hanging bag' photobioreactor.....	81
2.8.2	Freeze drying	83
2.9	Shrimp feeding trial.....	83
2.9.1	Experimental Setup	84
2.9.2	Feeding Regimen	84
2.9.3	Growth Performance and Health Assessment.....	85
2.9.4	Statistical Analysis	85
2.10	Bioinformatic analysis	86
2.10.1	Protein alignment.....	86
2.10.2	Algal growth data analysis	87
3	psaA^{**}: an improved recipient strain for simple generation of marker-free transformants	89
3.1	Introduction	89
3.2	Experimental procedures.....	99

3.2.1	<i>C. reinhardtii</i> strains and growth conditions	99
3.2.2	Plasmid construction	99
3.2.3	<i>C. reinhardtii</i> transformation	100
3.2.4	Luminescence assays	101
3.2.5	Western blot analysis	101
3.3	Results	102
3.3.1	Generation of <i>psaA</i> ^{**} – a marker-free <i>C. reinhardtii</i> PSI mutant carrying two TGA stop codons in <i>psaA</i> -3	102
3.3.2	<i>psaA</i> ^{**} serves as a transformation recipient strain using high light selection	107
3.3.3	<i>psaA</i> ^{**} as a marker-free recipient cell with rapid transformation feature	110
3.4	Discussion	116
3.4.1	Summary of Key Findings	116
3.4.2	Comparison with Existing Methods	117
3.4.3	Limitations of <i>psaA</i> ^{**} strain	119
3.4.4	Future Directions	121
4	Production of recombinant fish growth hormone (fGH) in the chloroplast of microalga <i>C. reinhardtii</i>	128
4.1	Introduction	128
4.2	Results	135
4.2.1	Choice of fGH sequences	135
4.2.2	Plasmid assembly of fGHs-expressing cassette	135
4.2.3	Generation of stable, scar-less, and marker-free <i>C. reinhardtii</i> strain	139
4.2.4	Western blot analysis of (HA)-tagged fGHs	140
4.2.5	Growth performance of shrimp larvae fed transplastomic microalga <i>C. reinhardtii</i>	142
4.3	Discussion	147
5	Production of recombinant spider silk protein in the chloroplast of <i>C. reinhardtii</i>	152
5.1	Introduction	152
5.2	Results	163

5.2.1	Construction and assembly strategy of MaSp1-expressing <i>C. reinhardtii</i>	163
5.2.2	Construction of MaSp1-expressing <i>C. reinhardtii</i>	166
5.2.3	Improving synthesis of spider silk proteins by enhancing tRNA ^{Gly} levels in the chloroplast	168
5.3	Discussion	176
6	The <i>C. reinhardtii</i> chloroplast as a platform to produce double-stranded RNA (dsRNA)	181
6.1	Introduction	181
6.2	Results.....	186
6.2.1	'One-step One-pot' platform to clone dsRNA targets	186
6.2.2	Creating dsRNAs-expressing <i>C. reinhardtii</i> for silencing viral genes during shrimp infection	188
6.2.3	Investigating the gene-silencing mechanism in <i>C. reinhardtii</i> chloroplast: Can chloroplast-expressed dsRNAs silence nuclear-encoded genes?	197
6.2.4	Quantification methods of dsRNA yield in <i>C. reinhardtii</i>	204
6.3	Discussion	206
6.3.1	Optimizing dsRNA length and multiple dsRNA Constructs.....	207
6.3.2	Gene-silencing mechanisms and the role of dsRNA under stress conditions .	207
6.3.3	Enhancing dsRNA yield with psaA** expression system.....	208
6.3.4	Broad Implications of a dsRNA Platform	209
7	Final discussion	212
7.1	Summary of main findings	212
7.2	Further research	214
7.2.1	Future directions of psaA** system.....	214
7.2.2	Future direction of fish growth hormone (FGH)	216
7.2.3	Future directions of spider silk protein	218
7.2.4	Future directions of dsRNA platform.....	219
7.3	Concluding remarks.....	222
	Appendices	225
	Reference	286

List of Tables

Table 1.1 Selectable markers and strategies used for chloroplast transformation in <i>Chlamydomonas reinhardtii</i> , adapted from Esland et al, 2018.....	42
Table 1.2 Approaches to achieve robust expression of recombinant proteins in <i>C. reinhardtii</i>	53
Table 2.1 A summary of <i>C. reinhardtii</i> strains used in this study	60
Table 2.2 A summary of <i>E. coli</i> strains used in this study	63
Table 3.1 Comparison of advantages and disadvantages of <i>psaA**</i> and other transformation recipient cells developed in the Purton lab.	92
Table 4.1 GHs of different species	130
Table 5.1 Comparative analysis of mechanical properties of spider silk, metals, alloys, and fibre materials.	152
Table 5.2 Comparative analysis of different spider silk proteins in spider draglin. Adapted from Ramezaniaghdam et al., 2022.	156

List of Figures

Figure 1.1 Phenotypic diversity of microalgae.....	27
Figure 1.2 Evolution of Primary Endosymbiosis in Photosynthetic Eukaryotes.	29
Figure 1.3 Cellular structure of the microalga <i>Chlamydomonas reinhardtii</i>	31
Figure 1.4 Timeline of significant research breakthroughs using <i>C. reinhardtii</i>	34
Figure 1.5 The genome map of <i>C. reinhardtii</i> chloroplast genome.	36
Figure 1.6 The intergrtion of foreign DNA into neutral sites of chloroplast of <i>C. reinhardtii</i>	37
Figure 1.7 Systematic workflow for transgene construction, insertion, and expression in the <i>C. reinhardtii</i> chloroplast	38
Figure 1.8 Biolistic® PDS-1000/He particle delivery system and bombardment process (Bio-Rad Laboratories, Hercules, CA.)	40
Figure 1.9 The levels of STEP toolkit.	44
Figure 1.10 Schematic workflow of the ‘design-build-test’ strategy in <i>C. reinhardtii</i> chloroplast.	45
Figure 1.11 Schematic workflow of <i>C. reinhardtii</i> chloroplast as a platform for novel recombinant products.....	46
Figure 1.12 Schematic RNA interference pathway (Fajardo et al., 2024).	54
Figure 3.1 Comparison of recipient <i>C. reinhardtii</i> strains.	94
Figure 3.2 Photosynthetic restoration for insertion of GOIs by codon reassignment using tRNA marker trnWUCA.	95
Figure 3.3 The schematic structure of plasmid ppsaA** pLY410.	104
Figure 3.4 Plasmid constructs and plastome integration strategies for the generation of psaA**, and demonstration of photosynthetic restoration by codon reassignment.	105
Figure 3.5 Comparative spot test analysis of <i>C. reinhardtii</i> psaA** mutant and parental strain CC-1690 under different conditions.....	108
Figure 3.6 Transformation of psaA** mutant with NLUC in a photosynthetic restoration vector.	109
Figure 3.7 PCR and phenotype analysis of the photosynthetically restored line psaA**::NLUC.	112
Figure 3.8 Luminescence assay and western blotting analysis of psaA**::Nluc strains.....	115

Figure 3.9 The comparison between original design of <i>trnWUCA</i> Young et al. (2015) and full restoring 3' UTR.	123
Figure 4.1 The overview of the production of fish growth hormone (fGHs) in the chloroplast of <i>C. reinhardtii</i>	132
Figure 4.2 Design of fGH-expressing cassette and gene of interests (GOIs) variants used for production of transgenic <i>C. reinhardtii</i>	138
Figure 4.3 Light-restoration Strategy for generation of marker-less transformants using the HT72 recipient cells and PCR confirmation of GOI integration and homoplasmy of pLYfGH transformants.	140
Figure 4.4 Western blot analysis of HA-tagged <i>C. reinhardtii</i> FGH transformants.	141
Figure 4.5 Growth performance of shrimp larva fed transplastomic microalga <i>C. reinhardtii</i>	146
Figure 5.1 Schematic representation of different types of spider silk and their role in spider webs, including an example of the seven types of native silk glands and threads from the spider <i>Araneus diadematus</i> : major ampullate silk (blue). Adapted from Zheng & Ling, 2018 and Ramezaniaghdam et al., 2022.	155
Figure 5.2 The schematic structure of MaSp protein sequences and their structure. Adapted from Van Beek et al., 2002; Gray et al. 2016; Yarger et al., 2018 and Ramezaniaghdam et al., 2022	157
Figure 5.3 Schematic overview of spider silk protein production in <i>C. reinhardtii</i>	161
Figure 5.4 Recombinant expression of Spider silk protein (MaSp1) in <i>C. reinhardtii</i>	162
Figure 5.5 Assembly strategy of the vectors with various MaSp1 repetitive domain from <i>Nephila clavipes</i> was developed to express spider silk protein.	165
Figure 5.6 PCR confirmation of GOI integration and homoplasmy of MaSp1 transformants.	166
Figure 5.7 PCR confirmation of R1 homoplasmy for CC1690::MaSp1 transformant lines..	167
Figure 5.8 Western blot analysis of recombinant MaSp1 multimers (2–6 mer) expressed in the chloroplast of <i>C. reinhardtii</i> CC1690.	168
Figure 5.9 Strategy for enhancing recombinant expression of <i>MaSp1</i> gene by targeting the pathway to Glycyl-tRNA ^{Gly}	169
Figure 5.10 Gene insertion for <i>MaSp1</i> in the chloroplast genome using a photosynthesis restoration strategy: comparison of <i>MaSp1</i> constructs with and without <i>trnG2</i>	172

Figure 5.11 PCR Confirmation of MaSp1 integration and homoplasmy in HT72 transformants without (left panel) and with (right panel) the trnG2 gene.	173
Figure 5.12 Western blot analysis of <i>MaSp1</i> multimer expression in <i>E. coli</i> DH5α with and without trnG2 enrichment.	174
Figure 5.13 Western blot analysis of wild-type <i>C. reinhardtii</i> (CC-1690), HT72:: <i>MaSp1</i> 6-mer, and HT72::trnG2 + <i>MaSp1</i> 6-mer transformants at varying cell densities.....	176
Figure 6.1 The completing p2xTRBL vector allows cloning of any DNA fragment between convergent <i>rrnS</i> promoters to create a dual transcription cassette.....	186
Figure 6.2 Schematic overview of shrimp antiviral dsRNAs production in <i>Chlamydomonas reinhardtii</i>	190
Figure 6.3 Schematic and PCR validation of chloroplast-targeted dsRNA and viral protein expression constructs in <i>Chlamydomonas reinhardtii</i> HT72.	191
Figure 6.4 Survival rates of shrimp fed with different feeds against WSSV and YHV viral challenges over 7 days.....	196
Figure 6.5 Hypothesis schematic overview of chloroplast-expressed dsRNAs trigger gene silencing of nuclear-encoded genes.....	198
Figure 6.6 Chloroplast-expressed double-stranded RNA expressing Y-5 and Arg7.	200
Figure 6.7 Phenotype prediction (upper) and testing results (lower) of the chloroplast-expressed double-stranded Y-5 and ARG7 strains.....	201
Figure 6.8 Chloroplast-expressed aptamer-integrated double-stranded RNA expressing systems and fluorescent assay.	204

List of Appendices

Appendix 1 Composition of Tris-acetate-phosphate (TAP) medium modified from (Gorman and Levine, 1965; Harris, 2009)	225
Appendix 2 Composition of Sueoka high-salt (HSM) medium modified from (Harris, Stern and George N., 2009).....	225
Appendix 3 DNA sequence of plasmid pLY410 (for making <i>psaA**</i>)	226
Appendix 4 Summary of primers used for genotyping PCR and DNA sequencing for <i>psaA**</i> work.....	238
Appendix 5 Sequencing results of <i>psaA**</i> strain.	239
Appendix 6 Coding sequence and protein sequence of codon optimised <i>fGH</i> gene for the <i>C. reinhardtii</i> chloroplast.	240
Appendix 7 List of components and amino acid sequences in the MaSp1 constructs, adapted from Foong et al., 2020.	244
Appendix 8 Coding sequence codon optimised <i>MaSp1</i> gene for the <i>C. reinhardtii</i> chloroplast.	246
Appendix 9 DNA sequence of plasmid pLY118 (dxTRBL, 5191 bp)	248
Appendix 10 Recipe for 50× Tris-Acetate-EDTA (TAE) Buffer.....	256
Appendix 11 Protocols for OneTaq PCR, Q5 High-Fidelity PCR, and OneTaq One-Step RT-PCR.....	259
Appendix 12 Plasmid map of NLuc and Nluc**	267

List of Abbreviations

5-FC	5-Fluorocytosine
ADG	Average Daily Gain
AAS	Amino Acid Sequence
ARG7	Argininosuccinate Lyase Gene
BCCP	Biotin Carboxyl Carrier Protein
bp	Base Pair
BSA	Bovine Serum Albumin
CDS	Coding Sequence
Chl	Chlorophyll
CpPos-Neg	Chloroplast Positive-Negative Selection
CRISPR	Clustered Regularly Interspaced Short Palindromic Repeats
CTD	C-Terminal Domain
DH5 α	<i>Escherichia coli</i> DH5 α
DFHBI	3,5-Difluoro-4-hydroxybenzylidene Imidazolinone
DICER	Dicer Ribonuclease
dsRNA	Double-Stranded RNA
EDTA	Ethylenediaminetetraacetic Acid
fGH	Fish Growth Hormone
FCR	Feed Conversion Ratio

FITC	Fluorescein Isothiocyanate
FMDV	Foot-and-Mouth Disease Virus
GFP	Green Fluorescent Protein
GC	Guanine-Cytosine
GOI	Gene of Interest
GRAS	Generally Recognized As Safe
GMO	Genetically Modified Organism
Gly	Glycine
HA	Hemagglutinin
HSM	High Salt Minimal Medium
HT	Heat-Tolerant
IPTG	Isopropyl β -D-1-Thiogalactopyranoside
IR	Inverted Repeat
kDa	Kilodalton
LB	Lysogeny Broth Medium
Lv	Level
MaSp	Major Ampullate Spidroin
mCherry	Monomeric Cherry Fluorescent Protein
miRNA	MicroRNA
nLuc	NanoLuc Luciferase
NTD	N-Terminal Domain

NUPTs	Nuclear Integrants of Plastid DNA
OD	Optical Density
ORF	Open Reading Frame
PAGE	Polyacrylamide Gel Electrophoresis
PCR	Polymerase Chain Reaction
petB	Cytochrome b ₆ /f Complex Subunit B Gene
PsaA	Photosystem I Subunit A
psaA**	psaA Double-Stop Mutant
psbH	Photosystem II Subunit H Gene
psbA	Photosystem II Subunit A Gene
ptxD	Phosphite Oxidoreductase Gene
RISC	RNA-Induced Silencing Complex
RNAi	RNA Interference
rbcl Gene	Ribulose-1,5-Bisphosphate Carboxylase/Oxygenase Large Subunit
rrnS	Ribosomal RNA Small Subunit Gene
RLU	Relative Luminescence Units
SDS	Sodium Dodecyl Sulfate
siRNA	Small Interfering RNA
SGR	Specific Growth Rate
Strep-Tag II	Streptavidin-Binding Peptide Tag

STEP	SynBio Toolkit for Engineering Plastomes
TAE	Tris-Acetate-EDTA Buffer
TAP	Tris-Acetate-Phosphate Medium
TBE	Tris-Borate-EDTA Buffer
TGA	Thymine-Guanine-Adenine (Opal Stop Codon)
trnG	Transfer RNA Glycine Gene
trnW ^{UCA}	Modified Tryptophan Transfer RNA (Anticodon UCA)
TSP	Total Soluble Protein
UTR	Untranslated Region
WSSV	White Spot Syndrome Virus
YHV	Yellow Head Virus
WT	Wild-Type

Chapter 1

Introduction

1 Introduction

1.1 The chloroplast of microalgae

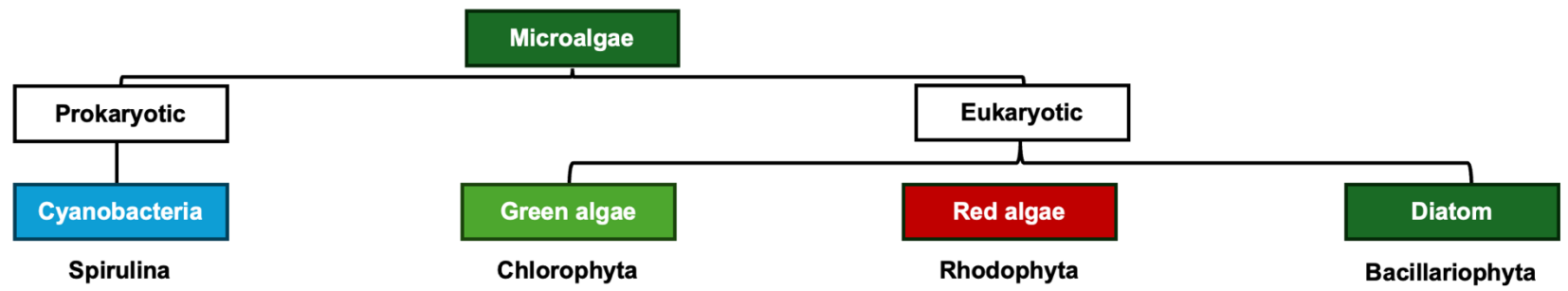
1.1.1 What are microalgae?

Microalgae are photosynthetic eukaryote microorganisms that exist mainly in aquatic environments (Figure 1.1). Microalgae are found in oceans, rivers, lakes, and even extreme environments such as hot springs and salt flats, where their unique physiological adaptations allow them to thrive in conditions inhospitable to many other organisms. Though generally microscopic and unicellular, they display considerable diversity in morphology, size, and metabolic capabilities, which allows them to occupy diverse ecological niches (Liang et al., 2023). The microalgae include phylogenic groups such as the Chlorophyta (green algae), which are closely related to higher plants and possess chlorophyll a and b as primary light-absorbing pigments, the Rhodophyta (red algae), and the Bacillariophyta (diatoms). In a broader definition, microalgae also include the prokaryotic group, cyanobacteria (previously termed 'blue green' algae) due to their shared photosynthetic processes and ecological roles (Falkowski & Raven, 2013; Smith, 2003).

Microalgae are primary producers in aquatic ecosystems contributing to the base of the food web by converting sunlight into biomass. Unlike land plants and chlorophyte algae, the many other microalgal groups found within these ecosystems display a wide range of diverse features which contribute to their photosynthetic versatility and adaptability. For example, the chloroplasts retain additional membrane layers and use

unique pigments such as phycobilins and novel chlorophylls and carotenoids for light harvesting (Maréchal, 2018). Microalgae directly support zooplankton, small fish and crustacea, and, indirectly, higher trophic levels, including larger fish and marine mammals. They also play a critical role in carbon cycling, as microalgae capture CO₂ from the atmosphere and sequester it within oceanic sediments, mitigating greenhouse gas levels and aiding in climate change management (Chisti, 2007; Wehr & Sheath, 2002). Furthermore, microalgae are also essential to nutrient cycling; they assimilate nitrogen and phosphorus during growth and release these nutrients back into the environment upon decomposition, thereby supporting ecosystem health (Liang et al., 2023).

The biochemical diversity of microalgae and their ease of cultivation have positioned them as promising candidates for numerous biotechnological applications (Einhaus et al., 2024). Their potential spans the pharmaceutical, energy, agriculture, and environmental sectors, where they could be utilized for high-value compounds, commodity bioproducts and biofuels, and could be employed in different bioremediation efforts such as carbon capture, wastewater clean-up and removal of heavy metals (Liang et al., 2023).



Arthrospira maxima

Chlamydomonas reinhardtii

Porphyridium purpureum

Phaeodactylum tricornutum

Chlorella reisi

Figure 1.1 Phenotypic diversity of microalgae.

Microalgae can vary widely in shape and size, ranging from a few to several hundred micrometres. By a broader definition, microalgae include both prokaryotic (cyanobacteria) and eukaryotic organisms. Here, only a selection is shown (from left to right): Cyanobacteria cyanobacterium (spirulina) *Arthrospira maxima* (scale bar = 50 μm); the green alga *Chlamydomonas reinhardtii* (scale bar = 20 μm) and *Chlorella reisiigii* (scale bar = 10 μm), the red alga *Porphyridium purpureum* (scale bar = 10 μm) and the diatom *Phaeodactylum tricornutum* (scale bar = 10 μm). Image credit: CCAP.

1.1.2 The chloroplast and photosynthesis of microalgae

Chloroplasts are vital organelles in plant and algal cells and are the site of photosynthesis, converting light energy into chemical energy that supports life on Earth (Blankenship, 2008; Chaffey, 2003). Structurally, chloroplasts are optimized for this process, containing (in green algae and plants) a double membrane that protects internal components and allows selective transport of materials. Inside, the stroma houses the thylakoid membranes that are organized into stacks, or grana, which increase surface area for light absorption and facilitate the light-dependent reactions of photosynthesis (Nelson & Yocum, 2006; Raven, 1999).

The endosymbiotic theory (Figure 1.2) explains the origin of chloroplasts, proposing that they evolved over 1.5 billion years' ago from ancient cyanobacteria that were engulfed by an ancestral eukaryotic cell. Over time, this symbiotic relationship led to the cyanobacterium evolving into a chloroplast, transferring much of its genetic material to the host's nucleus. Evidence for this includes genetic and structural similarities, such as circular DNA and ribosomal composition, shared by chloroplasts and cyanobacteria (Gray, 2012; Howe & Barbrook, 2007; Sugiura, 2003).

Beyond photosynthesis, chloroplasts contribute to synthesizing fatty acids, amino acids, and secondary metabolites such as chlorophyll and carotenoids, which protect against photooxidative damage and support cellular functions (Daniell et al., 2016; DellaPenna & Pogson, 2006). Advances in chloroplast genetic engineering using the model alga *Chlamydomonas reinhardtii* and land plants such as *Nicotiana tabacum* (tobacco) have allowed for targeted modifications to the chloroplast genome, enabling

the production of valuable biotechnological products, including novel metabolites and therapeutic proteins (Dyo & Purton, 2018; Bock, 2022).



Figure 1.2 Evolution of Primary Endosymbiosis in Photosynthetic Eukaryotes.

Illustration of primary endosymbiosis, where an ancestral heterotrophic eukaryote engulfed an ancient cyanobacterium, leading to the formation of primary chloroplasts. This process gave rise to major algal lineages, including the Glaucophyta, the red algae (Rhodophyta), and the green algae (Chlorophyta). The involvement of an ancestral Chlamydia-like organism may have contributed to the integration process. (Adapted from Maréchal, 2018).

1.1.3 *Chlamydomonas reinhardtii* as a model organism

Chlamydomonas reinhardtii is a unicellular green alga in the Chlorophyta phylum and a widely recognized model organism in photosynthesis and cellular biology research (Salomé & Merchant, 2019). Known for its biflagellate structure, which enables motility, *C. reinhardtii* is both simple and versatile to work with in the laboratory, making it ideal for experimental studies. Its ease of cultivation and genetic manipulation, with growth possible in both liquid and solid media under photoautotrophic or heterotrophic conditions, supports a broad range of research setups (Goodenough, 2023). Notably, *C. reinhardtii* has been extensively used in chloroplast engineering, providing a model system for chloroplast gene expression and the production of recombinant proteins, owing to its well-characterized chloroplast genome (Merchant et al., 2007; Rochaix, 1997).

Figure 1.3 illustrates the structure of a typical *C. reinhardtii* cell, showcasing various specialized organelles essential for its survival and adaptability. At its centre lies the nucleus, housing a ~111 Mb haploid genome composed of 17 chromosomes that encode some 17,700 genes (Craig et al., 2023) including the ~3000 that encode components of the chloroplast (Dobrogojski et al., 2020). The chloroplast itself surrounds the nucleus and occupies ~50% of the cell volume. It contains its own genetic system with ~100 genes (section 1.2.1) and is primarily responsible for driving photosynthesis, converting sunlight into chemical energy. Within the chloroplast, the pyrenoid facilitates carbon fixation, a crucial step in photosynthesis, by concentrating CO₂ around ribulose-1,5-bisphosphate carboxylase/oxygenase (Rubisco) (S. He et

al., 2023). Mitochondria are distributed throughout the cell, providing energy via cellular respiration. The contractile vacuole maintains osmotic balance by expelling excess water, and the Golgi body is involved in processing and transporting proteins and lipids (Salomé & Merchant, 2019). Starch granules serve as energy storage, and the cell wall offers structural support. The two cilia enable movement and taxis, allowing the cell to navigate and respond to its environment, while the eyespot (stigma) aids in orienting the cell toward optimal light for photosynthesis. The plasma membrane encloses the cell, regulating substance exchange, with the glycoprotein-rich cell wall providing structural integrity to the cell (Niklas et al., 2017).

Figure 1.3 Cellular structure of the microalga *Chlamydomonas reinhardtii*.

The internal structure of a microalgal cell, showcasing key organelles involved in various cellular processes. Notable features include the chloroplast, which is responsible for photosynthesis; the nucleus; the pyrenoid, involved in carbon fixation; and the contractile vacuole, which helps regulate water balance. Additional structures include basal bodies, Golgi

body, mitochondria, starch granules, eyespot for light sensing, and cilium for movement. This complex cellular organization enables microalgae to thrive in diverse aquatic environments. Image credit: Debbie Maizels. <https://doi.org/10.7554/eLife.39233.002>.

Additionally, *C. reinhardtii* has been granted 'Generally Recognized As Safe' (GRAS) status by the US Food and Drug Administration (Masi et al., 2023a) with similar approval in China and Singapore, making it suitable for various applications, including the production of pharmaceuticals and nutraceuticals (Rasala & Mayfield, 2011). The combination of its rapid growth rate, short generation time, and genetic flexibility makes it a valuable resource for studies in cell biology, genetics, and biochemistry (Goodenough, 2023).

This adaptability of *C. reinhardtii* also allows it to grow under varying conditions, such as light or dark environments and in the presence or absence of specific nutrients, enabling it to serve as a robust model for investigating physiological processes (Goodenough, 2023). Historically, it has played a pivotal role in photosynthesis research, elucidating mechanisms of light capture, electron transport, and ATP synthesis, and has provided insights into chloroplast biogenesis and the coordination of nuclear and chloroplast gene expression (Rochaix, 1997). Its biflagellate structure also makes it valuable for studying flagellar motility, contributing to the discovery of proteins involved in flagellar and cilia assembly and regulation (Goodenough, 2023).

Techniques for the genetic engineering of the nuclear genome are well advanced in *C. reinhardtii* (Perozeni & Baier, 2023) and recent advances in genetic tools, including RNA interference (RNAi) and CRISPR-Cas9 genome editing, have further enhanced *C. reinhardtii*'s research potential, allowing precise genome manipulation for gene

function studies and the production of recombinant proteins (Jinkerson & Jonikas, 2015). These developments underscore *C. reinhardtii*'s significance as a model organism and its ongoing contributions to biotechnology and basic research (Figure 1.4).

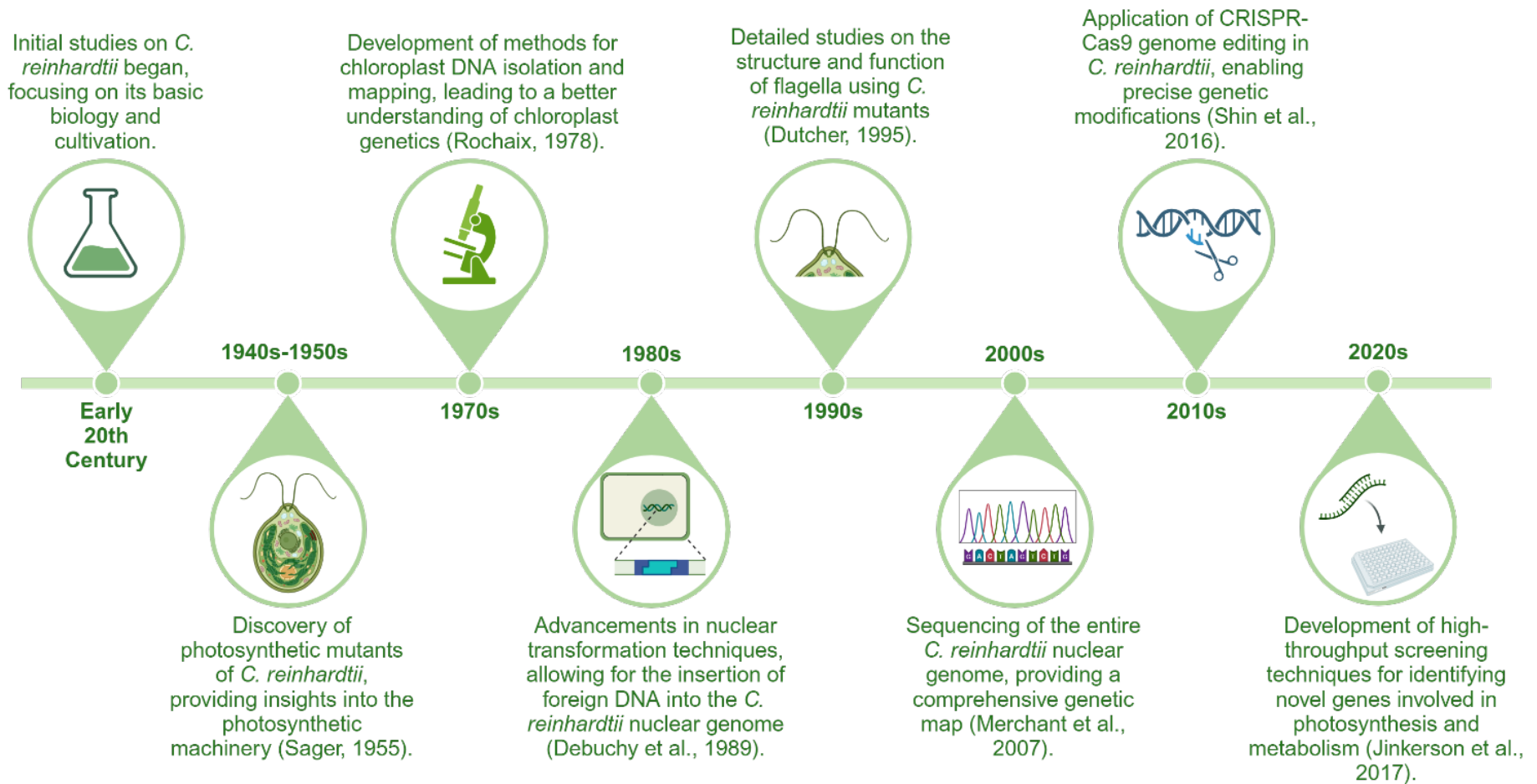


Figure 1.4 Timeline of significant research breakthroughs using *C. reinhardtii*.

1.2 The chloroplast engineering of *C. reinhardtii*

Chloroplast engineering in *Chlamydomonas reinhardtii* offers a valuable new approach in sustainable biotechnology, utilizing the unique chloroplast environment to express recombinant proteins and produce valuable compounds. This process leverages specific features within the chloroplast's genome and regulatory sequences, which enhance gene expression efficiency and stability, providing a robust platform for genetic manipulation (Dyo & Purton, 2018; Jackson et al., 2021; Rasala et al., 2011).

1.2.1 The chloroplast genome of *C. reinhardtii*

The chloroplast genome of *C. reinhardtii* is relatively small and circular, around 200 kilobases in size (Figure 1.5). It encodes 100 genes with the 70 protein-coding genes mainly encoding proteins involved in the light reactions of photosynthesis and ATP synthesis, or components of the organelle's transcription-translation apparatus. RNA genes encode the complement of 26 tRNAs and four rRNAs required for translation (Gallaher et al., 2018). Unlike the nuclear genome, the chloroplast genome has a compact organization with minimal non-coding regions and is inherited maternally. Furthermore, many of the genes are co-transcribed with the primary transcripts rapidly processed to yield monocistronic mature mRNAs (Cavauiuolo et al., 2017). Introducing transgenes into the chloroplast genome therefore requires the identification of suitable insertion sites. Such sites would be specific regions of the genome that do not disrupt the expression of essential genes, either directly through disruption of an endogenous gene or indirectly through interference with transcription of co-expressed genes

located downstream of an insertion site. In the chloroplast genome of *C. reinhardtii*, several neutral sites have been identified and validated. These include sites between *psbH* and *trnE2* (Wannathong et al., 2016), *psbA* and *rrn5* (Jackson et al., 2022), and *Wendyll* (*orf202*) and *psaA-3* (Taunt et al., 2023) making it a model organism for chloroplast engineering. Inserting foreign genes at these neutral sites ensures the stable and predictable expression of the transgene and that the introduced DNA does not perturb photosynthesis or other vital chloroplast functions.

Figure 1.5 The genome map of *C. reinhardtii* chloroplast genome.

The chloroplast genome of *Chlamydomonas reinhardtii*. Generated from Genbank entry BK000554 using OGDRAW (ogdraw.mpimp-golm.mpg.de). The arrows indicated the neutral sites of *C. reinhardtii* genome. Genes are coloured according to function (e.g. photosystem II genes in dark green), with genes transcribed anticlockwise on the outer side of the circle; those transcribed clockwise on the inner side (Jackson et al., 2021; Taunt et al., 2018).

Homologous recombination occurs readily in the chloroplast of chlorophytes, allowing the precise and targeted insertion of foreign DNA into these neutral sites via two recombination events, as shown in figure 1.6.

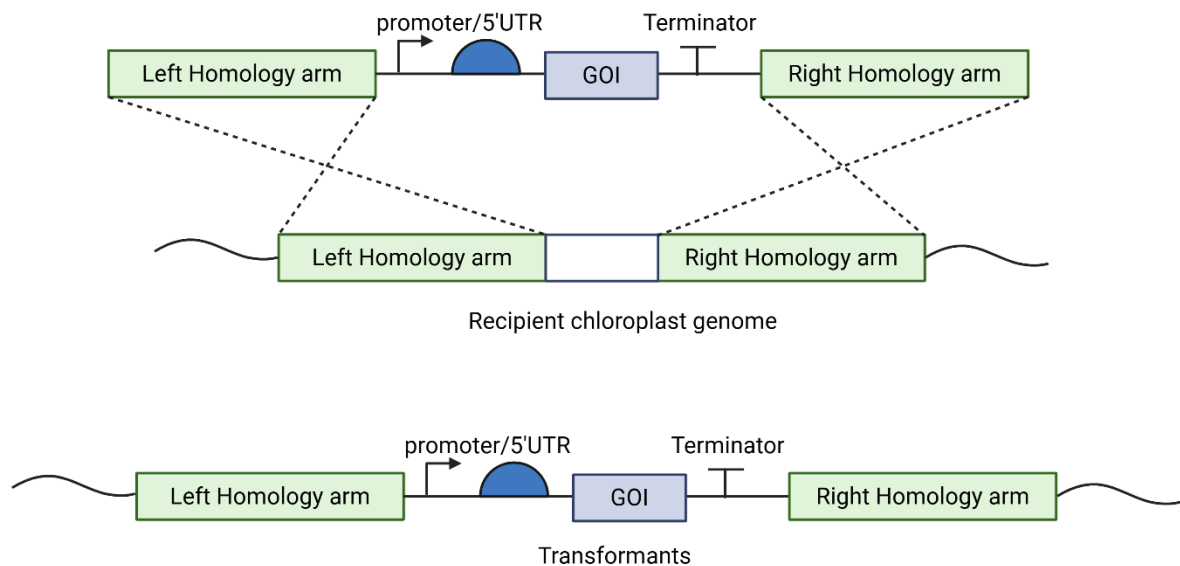


Figure 1.6 The intergrtion of foreign DNA into neutral sites of chloroplast of *C. reinhardtii*.

The minimum size of each homology region required for efficient recombination has been shown to be ~0.25 kb (Jackson et al., 2022). Typically, the homology regions are designed to be ~1.0 kb in size (Cullen et al., 2007), although a systematic study of size versus recombination efficiency has yet to be reported.

The design of transgenes for expression in the *Chlamydomonas reinhardtii* chloroplast follows a structured workflow that balances biological efficiency with practical implementation (Figure 1.7). Codon optimisation is a key initial step, aligning the coding sequence with the codon usage bias of the chloroplast genome to enhance translational efficiency (Fages-Lartaud et al., 2022; Young & Purton, 2016).

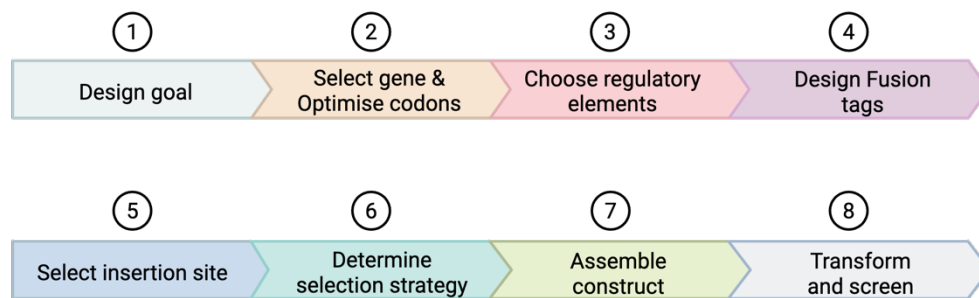


Figure 1.7 Systematic workflow for transgene construction, insertion, and expression in the *C. reinhardtii* chloroplast

Equally critical is the strategic selection of cis-acting elements, which regulate the expression of the transgene. Promoter choice significantly impacts transcriptional activity; commonly used promoters include *psaA*, *rbcL*, and *atpA*, each offering different expression strengths and regulatory dynamics (Einhaus et al., 2021; Rasala et al., 2011). The 5' untranslated region (5'UTR) affects mRNA stability and ribosome recruitment, with elements such as the *atpA* or *rbcL* 5'UTRs frequently employed for their proven efficiency (Jackson et al., 2022; Taunt et al., 2023; Vilatte et al., 2023). The 3'UTR stabilises transcripts and influences termination; *psaB* and *rbcL* 3'UTRs are popular choices (Jackson et al., 2021; Jackson et al., 2022). Additionally, the

intergenic expression element (IEE), where applicable, can enhance expression when inserted between regulatory sequences.

Further design considerations include the fusion of epitope tags (e.g., FLAG, HA) or affinity tags (e.g., His-tag, Strep-tag) to facilitate detection and purification. Optional inclusion of protease cleavage sites enables post-expression removal of tags, while translational fusions with fluorescent proteins (e.g., GFP, mCherry) can support localisation studies or real-time expression monitoring.

The versatility of transplastomics in *C. reinhardtii* is further enhanced by the development of combinatorial DNA assembly pipelines (as discussed in the next section) and simple methods for marker-free delivery of transgene clusters into the chloroplast genome (Jackson et al., 2021). The high ploidy and gene expression levels in the algal chloroplast, combined with the ability to precisely target transgenes via homologous recombination, make it an attractive system for recombinant protein expression (Charoonnart et al., 2018, 2023).

1.2.2 DNA delivery into the chloroplast of *C. reinhardtii*

Several methods are employed for delivery of foreign DNA into the chloroplast of *C. reinhardtii*, with biolistic particle delivery (gene gun) and glass bead-mediated transformation being the most common. The gene gun method (Figure 1.8) involves the bombardment of a lawn of algal cells with DNA-coated particles, which penetrate the cell wall, cell membrane and two chloroplast membranes. Glass bead-mediated

transformation, on the other hand, involves agitating a suspension of algal cells with DNA and glass beads, using a lab vortex (Changko, 2021; Mayfield, 1990). It is assumed that the abrasive action of the beads creates transient holes in the cells allowing DNA to cross the multiple membranes and enter the chloroplast (Larrea-Alvarez et al., 2021).

Figure 1.8 Biolistic® PDS-1000/He particle delivery system and bombardment process (Bio-Rad Laboratories, Hercules, CA.)

Selection markers are essential for identifying and isolating successfully transformed chloroplast genomes in *Chlamydomonas reinhardtii* (See Table 1.1). One of the most widely used markers is *aadA*, which confers resistance to spectinomycin and streptomycin (Goldschmidt-Clermont, 1991). This gene, originally derived from *E. coli*,

enables robust selection of transformants and is typically flanked by recombination sites, allowing for its removal post-selection to generate marker-free transgenic lines (Larrea-Alvarez, 2018). Similarly, the *aphA-6* gene provides resistance to kanamycin and amikacin (Bateman & Purton, 2000) , offering an alternative to *aadA*-based selection systems.

In addition to heterologous antibiotic resistance genes, endogenous ribosomal RNA gene variants such as *rnnS* and *rnnL* have been utilized to confer resistance to spectinomycin, streptomycin, kanamycin, or erythromycin (Newman et al., 1990). Herbicide resistance has also been engineered through mutations in *psbA*, enabling selection on compounds like metribuzin, 3-(3,4-dichlorophenyl)-1,1-dimethylurea (DCMU), and phenmedipham (Newman et al., 1992; Przibilla et al., 1991).

Restoration of photosynthesis through complementation of essential photosynthetic genes—including *atpB*, *petB*, *psaB*, *psbA*, *psbH*, *rbcL*, and *tscA*—represents another effective marker-free strategy, particularly in recipient strains carrying deletions or mutations in these genes (Bertalan et al., 2015; Bingham et al., 1991; Boynton et al., 1988; H. C. Chen & Melis, 2013; Robertson et al., 1990; Wannathong et al., 2016).

A more recent innovation is the use of suppressor tRNA-based systems. The modified tRNA *trnWUCA* enables translational readthrough of an opal (UGA) stop codon mutation introduced into the chloroplast *psaA-3* gene, thus restoring photosynthesis and allowing for selection without antibiotics (Young & Purton, 2016).

Additional markers include *ARG9*, which rescues arginine prototrophy in *ARG9* mutant strains (Remade et al., 2009), and *ptxD*, which confers the ability to utilize phosphite as a sole phosphorus source, offering an environmentally friendly selection strategy (Changko, 2020). Negative selection can also be employed using *codA*, where expression of this gene renders cells sensitive to 5-fluorocytosine (Young & Purton, 2014).

Together, these systems provide a diverse toolkit for chloroplast engineering in *C. reinhardtii*, enabling researchers to tailor selection strategies to specific experimental goals and regulatory considerations.

Table 1.1 Selectable markers and strategies used for chloroplast transformation in *Chlamydomonas reinhardtii*, adapted from Esland et al, 2018.

Marker	Phenotype	References
<i>aadA</i>	Streptomycin and spectinomycin resistance	(Goldschmidt-Clermont, 1991)
<i>aphA-6</i>	Kanamycin and amikacin resistance	(Bateman & Purton, 2000)
<i>rrnS</i> and <i>rrnL</i> variants	Resistance to spectinomycin, streptomycin, kanamycin, or erythromycin	(Newman et al., 1990)
<i>psbA</i> variants	Resistance to various herbicides e.g., metribuzin, 3-(3,4-dichlorophenyl)-1,1-dimethylurea (DCMU), phenmedipham	(Newman et al., 1992; Przibilla et al., 1991)
Essential photosynthesis genes e.g., <i>atpB</i> , <i>petB</i> , <i>psaB</i> , <i>psbA</i> , <i>psbH</i> , <i>rbcL</i> , <i>tscA</i>	Restored photosynthesis in recipient strain	(Bertalan et al., 2015; Bingham et al., 1991; Boynton et al., 1988; H. C. Chen & Melis, 2013; Robertson et al., 1990; Wannathong et al., 2016)

<i>trnWUCA</i>	Restored photosynthesis by translational read-through of opal mutation in <i>psaA-3</i>	(Young & Purton, 2016)
<i>ARG9</i>	Rescued arginine prototrophy in an <i>ARG9</i> mutant strain	(Remade et al., 2009)
<i>ptxD</i>	Ability to use phosphite as a source of phosphorus	(Changko et al., 2020)
<i>codA</i>	Sensitivity to 5-fluorocytosine	(Young & Purton, 2014)

Advancements in marker-free transformation techniques have further enhanced the utility of chloroplast transformation. These methods enable the introduction of multiple transgenes without the need for selectable markers, facilitating more complex genetic modifications and metabolic engineering (Bateman & Purton, 2000; Goldschmidt-Clermont, 1991; Larrea-Alvarez, 2018).

1.2.3 STEP Toolkit in *C. reinhardtii* chloroplast

The Toolkit developed in the Purton group for the *C. reinhardtii* chloroplast is termed STEP (SynBio Toolkit for Engineering Plastomes) and is based on the ‘start-stop’ assembly method developed for bacterial engineering [Click or tap here to enter text..](#) Based on Golden Gate cloning technology, STEP uses a standardized, modular system to facilitate the assembly of DNA parts, such as promoters, coding sequences, terminators, and regulatory elements. Using specific restriction type IIS enzymes and standardized overhangs, multiple DNA fragments can be precisely assembled in a one-pot reaction, making it fast and efficient to construct complex genetic circuits and expression cassettes. This toolkit is particularly valuable for the *C. reinhardtii* chloroplast because it allows for high throughput testing of various constructs, enabling researchers to quickly explore and optimize gene expression.

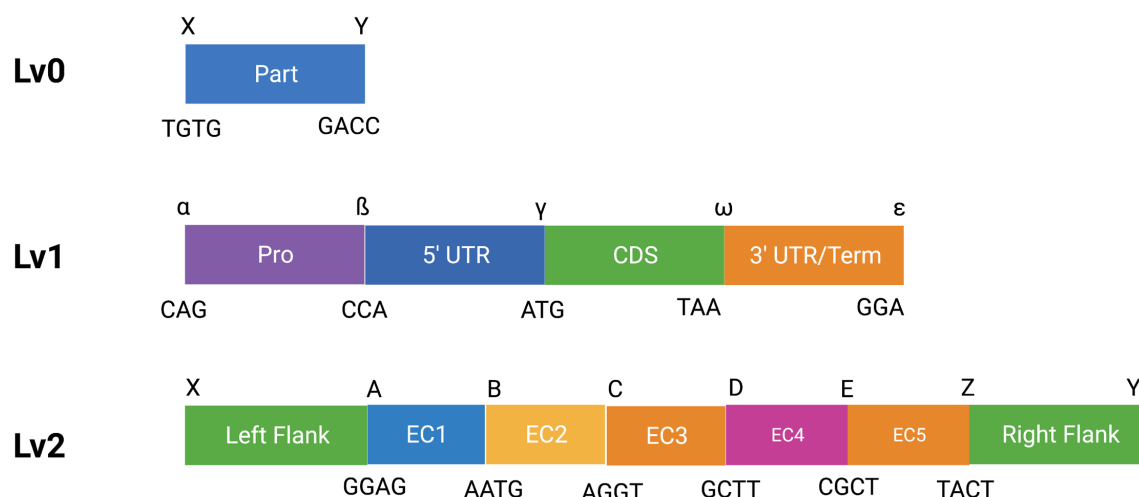


Figure 1.9 The levels of STEP toolkit.

The STEP Toolkit aligns well with the "design-test-build" cycle (Figure 1.10), a key concept in synthetic biology that emphasizes iterative improvement (Baig et al., 2020). In the *design* phase, scientists create specific genetic constructs tailored for desired functions or traits, such as improved protein expression or metabolic pathway engineering. During the *build* phase, the constructs are assembled using a MoClo Toolkit, leveraging the toolkit's modular parts and streamlined cloning process. The *test* phase involves introducing these constructs into the organism and analyzing the outcome to assess gene expression, protein yield, or other performance indicators. Based on these results, researchers can then *redesign* or modify constructs as needed, beginning a new cycle of iteration to further refine and optimize the system.

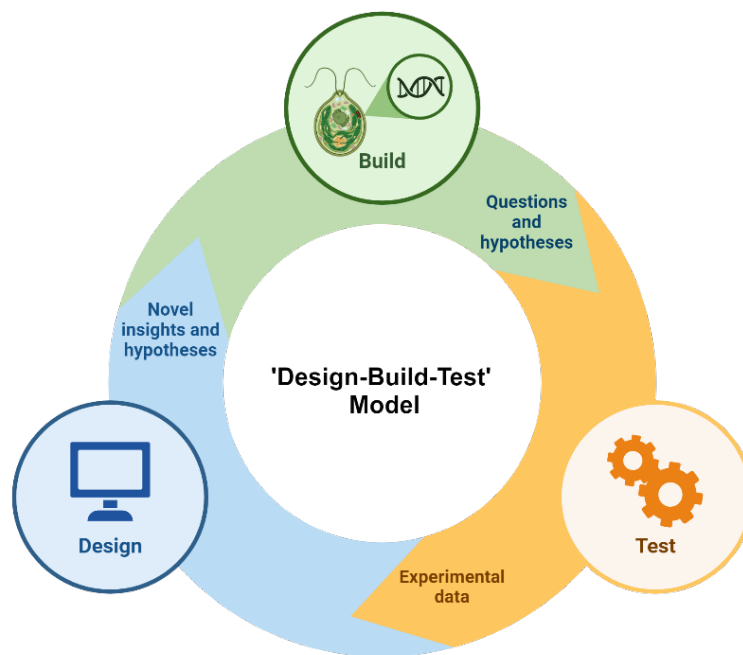


Figure 1.10 Schematic workflow of the 'design-build-test' strategy in *C. reinhardtii* chloroplast.

This iterative "design-test-build" cycle facilitated by the STEP toolkit enables efficient optimization of chloroplast genetic constructs, supporting a wide range of applications, from therapeutic proteins, RNAs and metabolites, to industrial enzymes and commodity products (Wannathong et al., 2016; Charoonnart et al., 2018, 2023; Sandoval-Vargas et al., 2019; Fajardo et al., 2024). By allowing for rapid testing and reassembly of genetic parts, the toolkit accelerates research progress and enhances the potential of *C. reinhardtii* and its chloroplast as a chassis for synthetic biology and biotechnology applications as illustrated in Figure 1.11 and discussed in the next section.

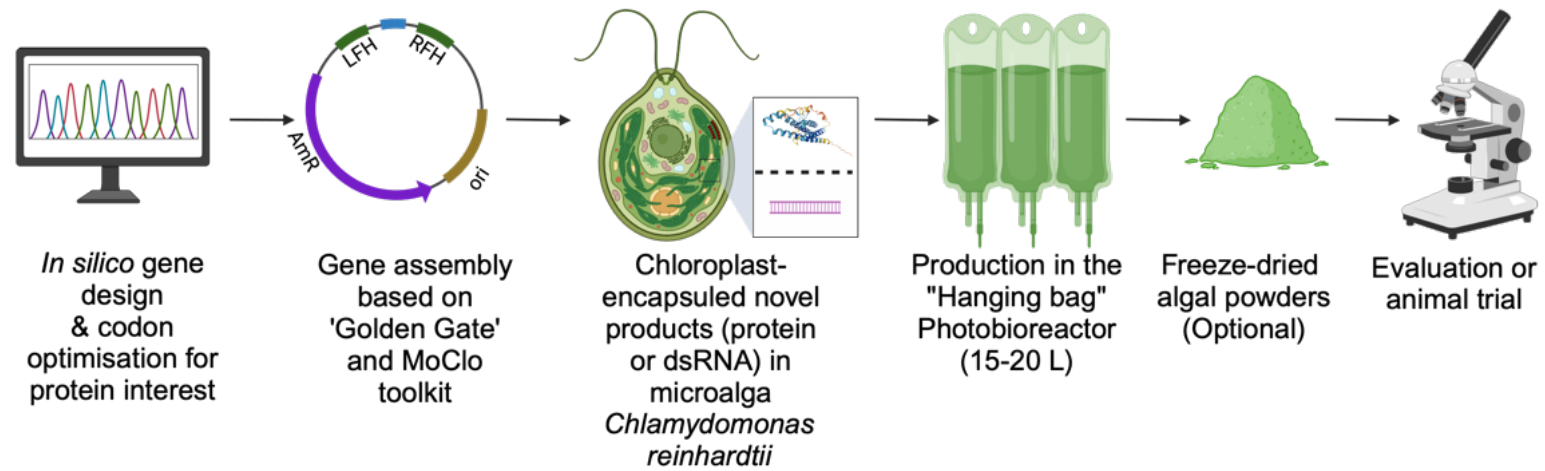


Figure 1.11 Schematic workflow of *C. reinhardtii* chloroplast as a platform for novel recombinant products.

1.3 The microalga *C. reinhardtii* as a platform for novel products

C. reinhardtii has garnered significant attention as a versatile platform to produce a wide range of recombinant products. Its ease of cultivation, genetic manipulability, and capacity for high-level expression of foreign genes make it an attractive host for biotechnological applications (Arias et al., 2023; Barolo et al., 2024; Ma et al., 2022).

1.3.1 Advantages of using *C. reinhardtii* for recombinant production

C. reinhardtii offers several unique advantages to produce recombinant proteins and nucleic acids, in particular within the chloroplast compartment. This section details these benefits, emphasizing the organism's suitability for large-scale and cost-effective biotechnological applications. The distinct features of *C. reinhardtii* make it a powerful tool for various industries, ranging from pharmaceuticals to agriculture.

1. **Photosynthetic Growth:** *C. reinhardtii* can grow autotrophically, using sunlight as an energy source and CO₂ as a carbon source. This offers the potential for cost-effective and environmentally sustainable large-scale production, as it requires simple inorganic inputs of CO₂, H₂O and basic nutrients together with sunlight. Alternatively, *C. reinhardtii* is capable of heterotrophic growth using conventional fermentation technologies when supplied with acetate as a source of fixed carbon. This offers the potential for much higher yields and productivities (Barolo et al., 2024) and the use of well-established industrial fermentation infrastructures rather than photobioreactors.

2. **Chloroplast Genetic Engineering:** The chloroplast genome of *C. reinhardtii* is easily accessible for genetic modifications and the tools and technologies for efficient engineering have been developed over the last 35 years (Taunt et al., 2023). This allows the precise, targeted integration of transgenes into neutral sites in the genome via homologous recombination, and stable and predictable levels of transgene expression. This stability is particularly beneficial for recombinant production, as it avoids the need for any selective agents to maintain transgene expression and ensures consistent batch-to-batch levels of the recombinant protein.
3. **High-Level Protein Expression:** The chloroplast of *C. reinhardtii* is capable of high protein synthesis rates, which allows to produce large quantities of recombinant proteins. Chloroplasts also provide a compartmentalized environment, which can help in accumulating high levels of the target protein without affecting other cellular processes.
4. **Simple Cultivation Requirements:** *C. reinhardtii* grows well in simple media and does not require complex or expensive growth factors, reducing production costs. Its cultivation can also be scaled up in photobioreactors, providing a feasible pathway from lab-scale research to industrial-scale production.
5. **Eukaryotic Protein Processing:** The chloroplast is of prokaryotic origin, but can perform some post-translational modifications including correct folding, disulphide bond formation and multi-subunit assembly: processes that are problematic in established prokaryotic platforms such as *E. coli* (Rosano & Ceccarelli, 2014), making the chloroplast more suitable than bacterial systems for producing complex proteins.

6. **Reduced Risk of Contamination:** Unlike *E. coli* or mammalian cell systems, *C. reinhardtii* does not possess endotoxins - reducing the risk of contamination with these toxic compounds - and is not prone to infectious agents (e.g. viral pathogens and prions), respectively. Indeed, *C. reinhardtii* has been shown to be completely non-toxic and has been given GRAS status for various food and feed applications (Fields et al., 2020; Lee et al., 2022; Murbach et al., 2018). The use of a harmless, non-toxic host reduces the risk of contamination in the final product and simplifies the purification process, particularly in medical or pharmaceutical applications.
7. **Versatility in Producing Various Compounds:** *C. reinhardtii* can be engineered to produce a wide range of valuable products, including therapeutic proteins, biofuels, vaccines, and bioactive compounds. This versatility expands its utility across diverse biotechnology fields (Masi et al., 2023).
8. **Rapid Growth Cycle and Short Generation Time:** The relatively short lifecycle of *C. reinhardtii* allows for faster experimental cycles, enabling rapid testing and iteration in research, which is ideal for synthetic biology and metabolic engineering projects.
9. **Accumulation of recombinant products in the chloroplast:** The algal chloroplast naturally serves as a compartment for accumulation of storage compounds such as starch and triacylglycerides. It is therefore a good site for accumulation of recombinant proteins, RNAs and metabolites without perturbing the biology of the rest of the cell. Examples of this application include the synthesis and accumulation of immunotoxins in the chloroplast that would otherwise be toxic if present in the cytosol (Taunt et al. 2018), and the stable accumulation of long double-stranded RNAs in the chloroplast where nucleo-cytosolic production would be expected to be compromised by rapid processing to small RNAs by Dicer (Zhang et al., 2015),

as discussed in section 1.3.2.2 below. Finally, accumulation in the chloroplast offers the opportunity for natural bioencapsulation of the product by drying the algal cells to produce a stable, but non-viable particle in which the recombinant product is encapsulated by multiple membranes and a cell wall. This offers opportunities for oral delivery of the active compound (Charoonnart et al., 2018, 2019, 2023; Fajardo et al., 2024), and for avoidance of a costly cold chain as the drying stabilises the compound (Vilatte et al., 2023).

1.3.2 Synthesis of recombinant products in *C. reinhardtii* chloroplast

The chloroplast of *Chlamydomonas reinhardtii* has emerged as a promising platform for synthesizing a wide range of recombinant proteins, including monoclonal antibodies (mAbs), therapeutic antibodies, enzymes, and vaccines. As discussed above, this photosynthetic microalga offers a controlled environment for producing complex proteins, with several advantages over other systems such as bacteria or yeast. For example, the algal chloroplast has shown potential as a bioreactor for vaccine production. By expressing antigens in the chloroplast, *C. reinhardtii* can produce vaccines that are stable and cost-effective, ideal for large-scale production. Chloroplast-produced vaccines are particularly advantageous because they do not contain contaminating endotoxins or animal-derived components, making them safer for human use. Additionally, chloroplast-produced vaccines can be formulated as oral vaccines, providing a needle-free alternative that could improve accessibility in low-resource settings (Arias et al., 2023; Barolo et al., 2024; Ma et al., 2022; Shamriz & Ofoghi, 2017).

1.3.2.1 Optimising recombinant protein production in the chloroplast

Recombinant protein expression levels in cell platforms are influenced by multiple factors, such as transgene instability (Larrea-Alvarez & Purton, 2020), issues with transcription or translation, protein toxicity and stability issues, improper or absent post-translational modifications, formation of inclusion bodies, and protein inactivity (Mendez Leyva, 2019). To overcome these challenges, a range of innovative strategies have been applied within microalgal expression systems to boost recombinant protein production, both in the chloroplast and in the nucleus. These strategies include host or strain engineering, utilizing strong promoters, selectable markers, reporter genes, advanced cloning vectors, codon optimization, protein tagging, and optimizing culture media, as summarized in Table 1.2.

Approach	Function	Examples	References
Selectable markers	<ul style="list-style-type: none"> Improve transformation efficiency 	NIT1; ARG7; ble; ptxD; aadA; aadA-codA	(J. E. Blankenship & Kindle, 1992; Jackson et al., 2022; Lumbreras et al., 1998; Purton & Rochaix, 1995; Sandoval-Vargas et al., 2019b)
Reporters	<ul style="list-style-type: none"> Enable high accumulation of proteins of interest Monitor gene activity 	Nanoluc luciferase gene; Fluorescent protein (mCherry, mVenus and GFP); Gus; Ars	(Franklin et al., 2002; Humby et al., 2009; Kim et al., 2020; Klein et al., 1992; Niemeyer et al., 2023)
Protein tags	<ul style="list-style-type: none"> Increase protein solubility and enable affinity purification 	FLAG, His, MBP, MAT, Myc, Strep tag II	(H. Chen et al., 2023; Derrien et al., 2012; Jia et al., 2022; Rasala et al., 2012; Song et al., 2005)
Promoters	<ul style="list-style-type: none"> Drive high-level expression of transgenes Reduce toxic gene products by regulating expression levels 	<i>rrnS</i> , <i>psaA</i> , <i>atpA</i> , <i>atpB</i>	(Jackson et al., 2022; Wannathong et al., 2016)
Untranslated regions (5' UTR/3' UTR)	<ul style="list-style-type: none"> Enhance the expression of recombinant genes 	<i>psaA</i> , <i>psbA</i> , <i>chlL</i>	(Jackson et al., 2022; Wannathong et al., 2016)
Terminators	<ul style="list-style-type: none"> Improve transgene expression by stabilizing transcript homeostasis 	<i>rbcL</i> , <i>atpA</i> , <i>psaA</i> , <i>petA</i> , <i>petD</i>	(Jackson et al., 2022; Wannathong et al., 2016)
Codon optimization	<ul style="list-style-type: none"> Facilitate more efficient and robust expression of genes by matching codon usage with <i>Chlamydomonas</i> chloroplast codon preferences 		(Fages-Lartaud et al., 2022; Weiner et al., 2018, 2020)

Approach	Function	Examples	References
Vector construction	<ul style="list-style-type: none"> • Enable homologous recombination for precise insertion of transgenes into the chloroplast genome 		(Charoonnart et al., 2023; Jackson et al., 2022; Taunt et al., 2023)
Engineering host/strains	<ul style="list-style-type: none"> • Use photosynthetic mutants or engineered strains to optimize transformation and expression efficiency 	HT72/TN72 HNT6	(Taunt et al., 2023; Wannathong et al., 2016)
Media optimization	<ul style="list-style-type: none"> • Support high-cell density cultures, improving aeration and increasing protein yield • Improve protein folding and activity through controlled nutrient supply (fed-batch) • Optimize nutrient composition to prevent stress-induced protein inactivity and enhance overall expression 		(Cui et al., 2022; Torres-Tiji et al., 2022)

Table 1.2 Approaches to achieve robust expression of recombinant proteins in *C. reinhardtii*.

1.3.2.2 Double-stranded RNA (dsRNA)-based recombinant products

Figure 1.12 Schematic RNA interference pathway (Fajardo et al., 2024).

In addition to proteins, *C. reinhardtii* has been utilized to produce recombinant nucleic acids, including RNA molecules used for gene silencing and therapeutic purposes.

C. reinhardtii can be engineered to produce double-stranded RNA (dsRNA) molecules for RNA interference applications. These dsRNA molecules can silence specific genes in target organisms, offering a method for pest control and disease treatment (Molnar et al., 2010).

The production of therapeutic RNA molecules, such as small interfering RNA (siRNA) and microRNA (miRNA) in *C. reinhardtii* is a promising area of research. These molecules can regulate gene expression and have potential applications in treating

various diseases (Cerutti et al., 2011). The ability to produce these therapeutic RNAs in a cost-effective and scalable manner makes *C. reinhardtii* an attractive alternative to traditional production systems. For example, siRNAs produced in *C. reinhardtii* could be used to target and silence disease-causing genes in human cells, providing a novel approach to gene therapy.

One of the major advantages of producing recombinant nucleic acids in *C. reinhardtii* is the organism's ability to perform post-transcriptional modifications, which are essential for the stability and functionality of RNA molecules. This feature, combined with the ease of genetic manipulation in *C. reinhardtii*, allows to produce highly specific and functional RNA molecules tailored to target particular genes or pathways.

1.3.3 Challenges of *C. reinhardtii* chloroplast for recombinant production

While the chloroplast of *C. reinhardtii* offers a unique and promising platform for recombinant protein production, several challenges limit its broader application in biotechnology, underscoring the need for the development of simpler and more cost-effective recipient cell lines that can address current limitations and be customized for specific applications.

First, creating simple and inexpensive recipient cells would allow for more scalable, low-cost production, which is especially important for applications where economic feasibility is a priority. Such cells would be designed to maintain genetic stability, achieve high-yield expression, and thrive under minimal, non-sterile conditions, ultimately making them accessible for larger-scale industrial use.

Second, addressing the need for complex protein-based therapeutics, including the expression of challenging compounds like repetitive proteins or oral-delivery therapeutics, remains a priority. Repetitive proteins, often desirable for their structural properties, are notoriously difficult to express due to issues with genetic instability, transcript slippage, and protein folding. Similarly, protein-based oral-delivery therapeutics require specific design considerations to ensure they remain stable through the digestive system and can be efficiently absorbed. Engineering specialized recipient cells that can stably produce these proteins while ensuring correct folding and high yields could facilitate their use in a range of therapeutic and industrial applications.

Lastly, novel RNA therapeutics represent an emerging frontier in biotechnology. RNA-based products, such as double-stranded RNAs for gene silencing or mRNA vaccines, hold significant therapeutic potential but require a stable and high-yield production platform. Developing recipient cells capable of efficiently synthesizing RNA molecules would enable the production of these therapeutics in a cost-effective manner, potentially allowing for breakthroughs in gene therapy, pest control, and disease prevention. By addressing these diverse needs, advancements in recipient cell lines can help overcome current challenges associated with *C. reinhardtii* chloroplast engineering, unlocking its full potential in biotechnology.

1.4 Aims and objectives

The overall aim of this thesis is to advance the understanding and application of chloroplast engineering in the green alga *C. reinhardtii* to produce novel recombinant

products. By leveraging the unique advantages of *C. reinhardtii*, this research seeks to develop efficient and scalable methods for producing high-value novel recombinant products, specifically proteins and nucleic acids with applications in various industries. The specific, measurable objectives of this research are aligned with the key findings and methodologies detailed in each result chapter of the thesis.

Overall Aim: To develop and optimize chloroplast engineering techniques in *C. reinhardtii* for the efficient production of recombinant proteins and nucleic acids, thereby demonstrating the organism's potential as a versatile platform for biotechnological applications.

- Objective 1: To create an improved recipient strain *psaA*** of *C. reinhardtii* for simple generation of marker-free transformants.
 - Related Chapter: Chapter 3: An improved recipient strain for simple generation of marker-free transformants: *psaA***
- Objective 2: To achieve high-yield production of recombinant fish growth hormone (fGH) in the chloroplast of *C. reinhardtii*.
 - Related Chapter: Chapter 4: Production of recombinant fish growth hormone (fGH) in the chloroplast of microalga *C. reinhardtii*
- Objective 3: To optimize the production of recombinant spider silk protein in the chloroplast of *C. reinhardtii*.
 - Related Chapter: Chapter 5: Production of recombinant spider silk protein in the chloroplast of microalga *C. reinhardtii*

- Objective 4: To explore the use of *C. reinhardtii* chloroplasts as a platform for producing double-stranded RNA (dsRNA) for gene silencing applications.
 - Related Chapter: Chapter 6: *C. reinhardtii* chloroplast as a platform to produce double-stranded RNA (dsRNA)

Each of these objectives is designed to address specific challenges and opportunities in chloroplast engineering and recombinant production using *C. reinhardtii*. By systematically pursuing these goals, this research aims to demonstrate the versatility and efficiency of *C. reinhardtii* as a biotechnological platform, providing valuable insights and methodologies that can be applied across various industries.

Chapter 2

Materials and Methods

2 Materials and Methods

2.1 *Chlamydomonas reinhardtii* strains, cultivation, and storage

The *C. reinhardtii* strains used in this work are detailed in Table 2.1. Stocks were maintained on 1.5% agar plates containing Tris-acetate Phosphate (TAP) medium (Goodenough, 2023) under dim light (5-10 $\mu\text{E}/\text{m}^2/\text{s}$) at 20 °C. The strains can be found in the Chlamydomonas Resource Centre (www.Chlamycollection.org/) listed under their culture collection codes.

Table 2.1 A summary of *C. reinhardtii* strains used in this study

Strain name	Culture code	Comments	Reference
Wild-type (WT)	CC-1690	Used to build recipient strain CC1690:: <i>psaA</i> ** (Chapter 3); Used for CpNeg-Pos strategy for fGH (Chapter 4) and MaSp1 (Chapter 5) transformants	(Sager, 1955) https://www.chlamycollection.org/product/cc-1690-wild-type-mt-sager-21-gr/
<i>Y.I.T.D</i>	CC-4033	Phenotype: Yellow in the dark; Used to building recipient strain CC-4033:: <i>psaA</i> ** (Chapter 3);	https://www.chlamycollection.org/product/cc-4033-y5-nit-mt/
<i>cw15</i>	CC-1833	Phenotype: wall deficient; used to building recipient strain <i>cw15</i> :: <i>psaA</i> **, can grow on nitrate Genotype: From CC-1690 21 gr mt+ x CC-1615 <i>cw15 nit2 mt-</i> ; the <i>cw15</i> mutation ultimately derives from CC-400.	https://www.chlamycollection.org/product/cc-1833-cw15-nit-mt/

TN72	CC-5168	<p>Phenotype: acetate-requiring, light sensitive (ΔPSII mutant); cell-wall deficient strain carrying the cw15</p> <p>Genotype: psbH::aadA knockout; suitable for transformation using the glass beads method</p> <p>Used to build dsRNA transformants (Chapter 6)</p>	<p>(Wannathong et al., 2016)</p> <p>https://www.chlamycollection.org/product/cc-5168-cw15-%E2%88%86psbh-strain-tn72/</p>
HT72	CC-6055	<p>Phenotype: acetate-requiring, light sensitive (ΔPSII mutant); cell-walled wild-type strain CC-1690</p> <p>Genotype: psbH::aadA knockout; suitable for transformation using the microparticle bombardment method;</p> <p>recipient strain <i>psaA</i>** (Chapter 3);</p>	<p>https://www.chlamycollection.org/product/cc-6055-psbhaada-knockout-ht72/</p>
HNT6	CC-5937	<p>Phenotype: acetate-requiring, light sensitive (ΔPSI mutant); Background strain is CC-1690;</p> <p>Genotype: <i>psaA-3::aadA</i> knockout in which part of the <i>psaA-3</i> coding region and 3' UTR is replaced with the <i>aadA</i> cassette through chloroplast transformation.</p>	<p>(Taunt et al., 2023)</p> <p>https://www.chlamycollection.org/product/cc-5937-psaa-3aada-knockout-hnt6/</p>

C. reinhardtii strains were cultured in either TAP or High Salt Minimal (HSM) (Appendix 1 and 2) growth medium depending on application. Liquid cultures were grown under constant light conditions at 25 °C with 120 rpm rotary agitation and an average light intensity of 25-50 μ E/m²/s in an illuminated incubator shaker (Innova 4340, New Brunswick Scientific). To obtain a continuous growth status, liquid cultures were incubated by Algem HT24 or Algem pro photobioreactors (Algenuity) under optimal

conditions. Growth on nutrient agar plates (TAP or HSM) containing 1.5% bacto agar (w/v) at 25 °C with various light conditions depending on the phenotype of the strains. Starter *C. reinhardtii* cultures were made by inoculating 20 ml TAP medium with a sterile laboratory inoculating loop from nutrient agar plates and growing until mid-log phase before sub-cultured into fresh medium.

Light sensitive *C. reinhardtii* strains were conducted on nutrient agar plates with 1.5% bacto agar (w/v) at 25°C with dim light (5 $\mu\text{E}/\text{m}^2/\text{s}$) with re-streaking to fresh TAP plates every 6-8 weeks. Additionally, the GeneArt® Cryopreservation Kit for Algae (Thermo Fisher) was used for long-term storage: its specialized cryoprotective reagents minimize intracellular ice crystal formation to protect cell integrity, while controlled cooling (via Mr. Frosty® container) allows strains to be stored at -70°C or liquid nitrogen without compromising post-thaw viability.

Cell density was determined using a haemocytometer (Hawksley, Improved Neubauer, BS.738, Depth 0.1 mm, 1/400 mm²), counted by microscope (ZEISS, Axio Lab.A1) at 400x magnification. The cells were fixed by treated with iodine (19.7 mM iodine in 95% (v/v) ethanol). Optical density measurements were made at 750 nm by spectrophotometer (ATi Unicam UV2 UV/VIS Spectrometer, Thermo Electron Corporation) to avoid the interference of the absorbance of chlorophyll a and b.

2.2 *Escherichia coli* strains, culture and storage

The *E. coli* strains used in this work are detailed in Table 2.2. *E. coli* DH5 α was routinely used for cloning, *E. coli* HT115 (DE3) and BL21 strains were also used for

dsRNA and protein expression respectively. *E. coli* was grown in Lysogeny Broth (LB) Broth medium supplemented with antibiotics when necessary. Liquid cultures were grown overnight at 37 °C with 200 rpm rotary agitation in a shaking incubator (Cole-Parmer™ Stuart™ SI60D Forced Air Incubator, 60 L and IKA Vibrax VXR Orbital Shaker). Single colony on 1.5% (w/v) LB agar plate was inoculated using sterile pipette tips. *E. coli* strains were stored as 20% (v/v) glycerol stocks at -70 °C. Cell density was measured by optical density at 600 nm using spectrophotometer (ATi Unicam UV2 UV/VIS Spectrometer, Thermo Electron Corporation).

Table 2.2 A summary of *E. coli* strains used in this study

Strain name	Genotype	Comments	Reference
DH5α	F– ϕ 80/ <i>lacZ</i> ΔM15 Δ(<i>lacZ</i> YA- <i>argF</i>)U169 <i>recA1 endA1 hsdR17</i> (rK–, mK+) <i>phoA supE44 λ-thi-1 gyrA96 relA1</i>	Plasmid purification	(Hanahan, 1983)
HT115 (DE3)	F–, <i>mcrA</i> , <i>mcrB</i> , IN(<i>rrnD-rrnE</i>)1, <i>mrc14::Tn10</i> (DE3 lysogen: <i>lacUV5</i> promoter -T7 polymerase	dsRNA expression	(Timmons & Fire, 1998)
BL21	F– <i>ompT hsdSB</i> (rB–, mB–) <i>gal dcm</i>	Protein expression	(Studier & Moffatt, 1986)

2.3 Molecular techniques

2.3.1 DNA assembly

DNA assembly involves the joining of multiple DNA fragments to construct a desired DNA sequence. This section outlines the different methods used for DNA assembly in this study, including *in silico* codon optimization, Golden Gate assembly, site-directed mutagenesis (SDM), phosphorylation and dephosphorylation, and T4 ligation.

2.3.1.1 *In silico* codon optimisation

In silico codon optimization involves modifying the DNA sequence of a gene to maximise the expression of the target gene in the chloroplast of microalga *C. reinhardtii*. This process takes into account the codon usage bias of the chloroplast genome, avoiding rare codons, and optimizing the GC content for stable mRNA structure. The optimization process was carried out using the Codon Usage Optimizer (CUO) tool developed by the Purton Lab. The CUO tool analyses the codon usage preferences of *C. reinhardtii* chloroplast and adjusts the DNA sequence accordingly. It ensures that the optimized gene retains the same amino acid sequence as the original gene but is composed of codons that are more frequently used in the chloroplast genome, resulting in more efficient translation and higher protein yield.

The optimized DNA sequences were synthesized by Integrated DNA Technologies (IDT, Coralville, IA, USA) and subsequently verified through sequencing to confirm the accuracy of the synthesis. The synthetic genes were then cloned into the appropriate expression vectors for further experimentation.

2.3.1.2 Golden Gate

Golden Gate assembly is a molecular cloning method that allows the joining of multiple DNA fragments in a single reaction using Type IIs restriction enzymes and T4 DNA ligase. This method leverages the ability of Type IIs restriction enzymes to cut DNA outside of their recognition sequences, creating unique overhangs that facilitate the precise and directional assembly of DNA fragments. The technique is highly efficient and suitable for the construction of complex plasmids or DNA constructs.

For the Golden Gate assembly performed in this study, DNA fragments with appropriate flanking sequences were digested with the Type IIs restriction enzymes BsaI, SapI, or Esp3I, all obtained from New England Biolabs (NEB, Ipswich, MA, USA). These enzymes recognize specific DNA sequences and cleave outside their recognition sites, generating sticky ends that can be ligated seamlessly. The resulting fragments were ligated using T4 DNA ligase, also sourced from NEB.

For the Golden Gate assembly, the DNA fragments with appropriate flanking sequences were digested with the Type IIs restriction enzyme BsaI, SapI or Esp3I (NEB, Ipswich, MA, USA), and the resulting fragments were ligated using T4 DNA ligase. The reaction was carried out in a single tube with cycling between optimal temperatures for digestion and ligation. The assembled constructs were then transformed into competent cells for further analysis.

The reaction was carried out in a single tube with thermal cycling between optimal temperatures for digestion and ligation. Typically, the reaction conditions involved

alternating between 37°C for restriction enzyme activity and 16°C for ligase activity, repeated for 30 cycles, followed by a final ligation step at 60°C to ensure complete ligation of the DNA fragments. This cycling protocol ensures that the digestion and ligation steps are highly efficient, allowing for the assembly of multiple fragments in a precise manner (Engler et al., 2008).

Following the assembly reaction, the assembled constructs were transformed into chemically competent *E. coli* cells (DH5α or similar strains) using the heat shock method (Section 2.6.1) for further propagation and analysis. *E. coli* strains were grown in LB medium supplemented with 100 µg/mL ampicillin or 50 µg/mL tetracycline when necessary. Successful clones were screened by colony PCR (Appendix 11) and confirmed by sequencing to ensure the accuracy of the assembled constructs.

2.3.1.3 Site-directed mutagenesis (SDM)

Site-directed mutagenesis is a technique used to introduce specific nucleotide changes, deletions, or insertions into a DNA sequence. In this study, site-directed mutagenesis was performed using the Q5® Site-Directed Mutagenesis Kit from New England Biolabs (NEB, Ipswich, MA, USA) (New England Biolabs, 2024). Primers containing the desired mutations were designed according to the manufacturer's guidelines and used to amplify the plasmid DNA. The Q5® High-Fidelity DNA Polymerase was used for amplification to ensure high accuracy and fidelity during DNA synthesis.

Following PCR amplification, the reaction mixture was treated with DpnI enzyme, also provided in the Q5® Site-Directed Mutagenesis Kit, to digest the parental (methylated) DNA template. This step ensures that only the newly synthesized DNA containing the desired mutations remains. The mutated plasmid DNA was then transformed into chemically competent *E. coli* cells (DH5α strain) using the heat shock method (Section 2.6.1). Transformants were plated on selective media and incubated overnight at 37°C. Colonies were picked and screened for the presence of the desired mutation using colony PCR and subsequent DNA sequencing to confirm the successful introduction of the specific nucleotide changes.

2.3.1.4 Phosphorylation and dephosphorylation

Phosphorylation of DNA ends is often required to facilitate ligation, especially when working with DNA fragments generated by restriction digestion. Conversely, dephosphorylation is used to prevent self-ligation of vector DNA, which is crucial for cloning efficiency.

For phosphorylation, DNA fragments were treated with T4 Polynucleotide Kinase (PNK) from New England Biolabs (NEB, Ipswich, MA, USA) in the presence of ATP to add a phosphate group to the 5' ends. This enzymatic reaction is essential for preparing DNA fragments for ligation, ensuring that the 5' ends are phosphorylated, which is a prerequisite for the formation of phosphodiester bonds during ligation.

The phosphorylation reaction was set up by mixing the DNA fragments with T4 PNK and ATP in the appropriate reaction buffer, followed by incubation at 37°C for 30

minutes. This treatment efficiently added phosphate groups to the 5' ends of the DNA fragments, making them suitable for subsequent ligation steps.

Dephosphorylation, on the other hand, was performed using Shrimp Alkaline Phosphatase (rSAP) (NEB, Ipswich, MA, USA) from NEB to remove the 5' phosphate groups from vector DNA, thereby preventing self-ligation. This step is particularly important when preparing vector backbones for cloning, as it reduces the background of empty vectors.

The dephosphorylation reaction involved incubating the vector DNA with rSAP at 37°C for 30 minutes in the recommended reaction buffer. Following the reaction, the enzyme was heat-inactivated at 65°C for 5 minutes to stop the dephosphorylation process.

These enzymatic treatments were crucial for the efficient preparation of DNA fragments and vectors, ensuring successful ligation and cloning experiments.

2.3.1.5 T4 Ligation

T4 DNA ligase is an enzyme that catalyses the formation of phosphodiester bonds between adjacent 3'-hydroxyl and 5'-phosphate termini in DNA. This enzyme is commonly used for the ligation of DNA fragments during cloning.

In this study, T4 ligation was utilized to join DNA fragments with compatible ends. The reaction mixture typically contained the DNA fragments, T4 DNA ligase from New England Biolabs (NEB, Ipswich, MA, USA), and a buffer containing ATP. The ligation

reaction was incubated at room temperature for 10-15 minutes to allow for efficient joining of the DNA fragments.

The reaction was set up by combining the DNA fragments in equimolar ratios, T4 DNA ligase, and the provided 10x T4 DNA ligase reaction buffer. The mixture was then adjusted to a final volume with nuclease-free water and incubated to facilitate ligation. After incubation, the ligated DNA was transformed into chemically competent *E. coli* cells (DH5 α strain) using the heat shock method (Section 2.6.1).

The transformed cells were plated on selective media and incubated overnight at 37°C. Successful transformants were identified by colony PCR and confirmed by sequencing to ensure the correct assembly of the DNA fragments.

2.3.2 Nucleic acids extraction

2.3.2.1 Double-stranded RNA extraction, detection and quantification

Plasmids of dsRNA targets were transformed into the RNase III deficient *E. coli* strain HT115 (DE3) (Gentaur Europe, Kampenhout, Belgium), and colonies were selected on LB agar plates supplemented with 100 μ g/ml ampicillin. A single colony was inoculated into liquid broth supplemented with 100 μ g/ml ampicillin and continuously shaken for 8 hours, followed by cell collection by centrifugation. Total RNA was extracted using the phenol-chloroform (1:1) extraction method, and dsRNA was purified by treating with DNase I (Thermo Fisher Scientific, Waltham, MA, USA, Product code: EN0521) to remove contaminating DNA and RNase A (10 mg, Thermo Fisher Scientific) to remove single-stranded RNA. Purified dsRNA was visualized by

agarose gel electrophoresis and kept at -20°C for further use as a standard for the detection of dsRNA from microalgal transformants.

C. reinhardtii strains were inoculated into 100 mL TAP medium and cultured by shaking at 120 rpm under continuous light (50 µE/m²/s) at 25°C. The cultures were harvested by centrifugation at 4,500 x g for 15 minutes at the late log/stationary phase. Pellets were resuspended using TRIzol™ Reagent (100 mL, Thermo Fisher Scientific) for RNA extraction to obtain total RNA. DNAs and single-stranded RNAs were removed by treatment with TURBO™ DNase (1,000 units, Thermo Fisher Scientific) and RNase A (10 mg, Thermo Fisher Scientific), respectively.

Specific dsRNA was detected by RT-PCR (Appendix 11) using the OneTaq One-Step RT-PCR Kit from New England Biolabs (NEB, Ipswich, MA, USA) (NEB, 2024). dsRNA was diagnostically digested by RNase III (250 units, Thermo Fisher Scientific). Quantitative RT-PCR (qRT-PCR) was performed using the same primers as for RT-PCR. Isolated dsRNA was incubated at 95°C for 5 minutes and immediately chilled on ice for 2 minutes prior to addition into the qRT-PCR reaction to ensure denaturation of dsRNA. A series of ten-fold dilutions of purified dsRNA from the bacterial expression was used to generate a standard curve. The amount of dsRNA was calculated according to a formula obtained from the standard curve.

2.3.2.2 PCR purification

After performing the PCR (Polymerase Chain Reaction), the amplified DNA fragments need to be purified to remove excess primers, nucleotides, enzymes, and other

reaction components that could interfere with subsequent experiments. The purification process can be carried out using a silica column-based purification kit, such as the GeneJET PCR Purification Kit (Thermo Scientific, K0701), according to the manufacturer's instructions.

Briefly, the PCR products were mixed with a binding buffer and loaded onto a silica membrane column. The DNA binds to the silica membrane, while impurities are washed away using a series of wash buffers. The purified DNA is then eluted in a low-salt buffer or water. The concentration and purity of the eluted DNA were determined using a Thermo Scientific NanoDrop Lite, and the quality was assessed by agarose gel electrophoresis.

These steps ensure that the DNA is free from contaminants and suitable for subsequent applications, such as cloning, sequencing, or other molecular biology techniques.

2.4 DNA analysis

2.4.1 Diagnostic restriction enzymes digestion

Restriction enzyme digestion is a fundamental technique in molecular biology used to cut DNA at specific sequences. This technique involves using restriction endonucleases, which recognize and cleave specific palindromic DNA sequences, resulting in DNA fragments with defined ends. The resulting fragments can be analyzed or used in further molecular cloning procedures. Diagnostic restriction enzyme digestion is a method used to verify the identity and integrity of cloned DNA

fragments. This involves cutting the DNA with specific restriction enzymes and analysing the resulting fragment sizes to confirm that the cloning or modification has been successful.

In this study, restriction enzyme digestion was carried out according to the manufacturer's protocols. The reaction mixture typically included the DNA sample, the appropriate restriction enzyme, a compatible buffer, and water to the final volume. The reaction was incubated at the optimal temperature for the enzyme, usually 37°C, for one hour. The digested DNA was then analyzed using agarose gel electrophoresis to confirm the successful cleavage of the DNA.

2.4.2 Agarose gel electrophoresis and gel purification

Agarose gel electrophoresis is a widely used method for the separation and analysis of DNA fragments based on their size. DNA samples are loaded into wells in an agarose gel, and an electric current is applied. The negatively charged DNA fragments migrate towards the positive electrode, with smaller fragments moving faster through the gel matrix than larger ones.

In this study, DNA samples were mixed with a loading dye and loaded into a 1-2% agarose gel prepared with TAE buffer (Appendix 10). The electrophoresis was carried out at 110 V for 45 minutes until the DNA fragments were adequately separated. The gel was stained with ethidium bromide to visualize the DNA under UV light.

For gel purification, the desired DNA fragments were excised from the gel using a clean, sharp blade. The gel slices were then processed using the GeneJET Gel

Extraction Kit (Thermo Scientific) according to the manufacturer's instructions. The purified DNA was eluted in a small volume of elution buffer or water and quantified using a Thermo Scientific NanoDrop Lite.

These steps ensured that the DNA fragments were accurately separated, visualized, and purified for subsequent molecular biology applications.

2.4.3 DNA sequencing

DNA sequencing is the process of determining the precise order of nucleotides within a DNA molecule. This technique is essential for verifying the sequence of cloned DNA fragments and identifying any mutations or errors that may have been introduced during cloning or amplification.

In this study, DNA sequencing was performed using Sanger sequencing and next-generation sequencing (Nanopore) to determine the sequence of the cloned or amplified DNA fragments. Sequencing reactions were set up according to the protocol provided by Source BioScience (Source BioScience, Nottingham, UK; available at sourcebioscience.com). The resulting sequences were analyzed using SnapGene (from GSL Biotech; available at snapgene.com) and Benchling (San Francisco, CA; available at benchling.com) to ensure accuracy and to confirm that the correct sequences had been obtained.

These DNA analysis techniques provided a comprehensive approach to verifying the identity and integrity of the DNA constructs used in this research, ensuring high reliability and precision in the experimental outcomes.

2.5 RNA analysis

2.5.1 Analytical polyacrylamide gel electrophoresis

Analytical polyacrylamide gel electrophoresis (PAGE) is a technique used to separate RNA molecules based on their size and conformation. This method provides higher resolution than agarose gel electrophoresis, making it suitable for analyzing smaller RNA fragments and distinguishing between similar-sized molecules.

In this study, RNA samples were denatured and mixed with a loading dye before being loaded onto a polyacrylamide gel. The electrophoresis was conducted at 110 V for 1 hour, using a 6% polyacrylamide gel prepared with TBE-urea. Following electrophoresis, the RNA was visualized using ethidium bromide, and the gel was analyzed under UV light or with a gel documentation system.

2.5.2 Agarose gel electrophoresis

Agarose gel electrophoresis is also utilized for the analysis of RNA. This technique allows the assessment of RNA integrity and the presence of specific RNA species.

For this analysis, RNA samples were mixed with a loading dye and loaded into a 2% agarose gel prepared with TAE buffer. The electrophoresis was carried out at 110 V for an hour. The gel was stained with ethidium bromide and visualized under UV light to assess the quality and quantity of the RNA samples.

2.5.3 Fluorescent RNA analysis

Fluorescent RNA analysis involves the use of fluorescent labels or dyes to detect and quantify RNA molecules. This method enhances sensitivity and allows for the visualization and quantification of specific RNA species.

2.5.3.1 Fluorescent detection by microplate reader

Fluorescent detection by microplate reader provides a quantitative measure of RNA concentration and allows for high-throughput analysis of multiple samples simultaneously. This method involves using a microplate reader to measure the fluorescence intensity of RNA samples labelled with a fluorescent dye.

For this analysis, RNA samples were labelled with DFHBI (R&D Systems, Catalog #5609). DFHBI was prepared according to the manufacturer's instructions. Briefly, DFHBI was dissolved in DMSO to make a 10 mM stock solution and stored at -20°C. For RNA labelling, the stock solution was diluted to a final concentration of 100 µM in RNA samples.

The fluorescence intensity of the labelled RNA samples was measured using a FLUOstar Omega microplate reader (BMG Labtech, Ortenberg, Germany). The microplate reader was set to the appropriate excitation and emission wavelengths for DFHBI (excitation: 488 nm, emission: 507 nm). The fluorescence readings were then analyzed to determine the concentration and integrity of the RNA samples, using a standard curve for quantification.

These RNA analysis techniques provided comprehensive methods for assessing RNA integrity, concentration, and specific RNA species, ensuring the reliability and accuracy of the experimental outcomes.

2.6 Gene delivery

2.6.1 *E. coli* competent cells and heat shock transformation

The transformation of *E. coli* involves the introduction of plasmid DNA into competent bacterial cells through a heat shock method. Competent *E. coli* cells were prepared using the calcium chloride method, which increases the permeability of the cell membrane to DNA. The plasmid DNA was mixed with the competent cells and kept on ice for 30 minutes. Following this incubation, the cell-DNA mixture was subjected to a brief heat shock at 42°C for 1 minute to facilitate DNA uptake. Immediately after heat shock, the cells were returned to ice for 10 minutes before being incubated in SOC medium at 37°C with 300 rpm shaking for 1 hour to allow for the recovery and expression of antibiotic resistance genes. The transformed cells were then plated on selective LB agar plates containing the appropriate antibiotic and incubated overnight at 37°C. Successful transformants were identified by their growth on selective media.

2.6.2 Chloroplast transformation

Chloroplast transformation involves the delivery of DNA directly into the chloroplast genome. This technique is particularly useful for plants and certain algae, providing an effective way to express foreign genes in these organisms.

In this study, chloroplast transformation was conducted using both biolistic and glass bead DNA delivery methods. Each method was chosen based on the specific requirements of the target cells and the type of DNA construct used.

2.6.2.1 Biolistic DNA delivery

Biolistic DNA delivery, also known as particle bombardment, is a method where DNA-coated particles are physically delivered into cells using high-velocity microprojectiles. This method was utilized for the transformation of *Chlamydomonas reinhardtii*.

C. reinhardtii was transformed by particle bombardment using a Biolistic PDS-1000/He Particle Delivery System (Bio-Rad, Hercules, CA, USA). Transformation cultures were grown to early log phase ($1-2 \times 10^6$ cells/mL) and harvested by centrifugation at $4,500 \times g$. Cells were resuspended in sterile TAP or HSM media as appropriate (see table 2.) to a density of 5×10^8 cells/mL, and 200 μ L was plated directly onto selective plates. DNA was coated onto 0.5 μ m gold DNAdel carrier particles (Seashell Technology LLC, La Jolla, CA, USA) at 5 μ g DNA/mg gold, with 0.5 mg pf particles used per bombardment, with each transformation carried out in triplicate. Plates were sealed with parafilm and incubated under dim light overnight at 25 °C. For transformations based on light restoration, plates were moved from dim light to high light (100 μ Es-1m-2 fluorescent light) following and overnight recovery period. Transformation lines were re-streaked to single colonies three to four times on selective media to obtain homoplasmic lines.

2.6.2.2 Glass beads DNA delivery

For cell-wall deficient recipient cells, chloroplast transformation was performed using a glass beads method (Kindle et al., 1991). This method involves mechanically disrupting the cells with glass beads to facilitate DNA uptake.

Transformation cultures (400 mL) were grown to early log phase ($1-2 \times 10^6$ cells/mL) and harvested by centrifugation at $3,000 \times g$. The pelleted cells were resuspended in an appropriate transformation buffer along with glass beads and the plasmid DNA. The mixture was vigorously vortexed for a defined period to enhance the physical contact between the DNA and the chloroplasts. Following vortexing, the mixture was incubated under optimal conditions to promote DNA integration into the chloroplast genome. Transformants were then selected on appropriate selective media and subjected to multiple rounds of streaking to obtain stable, homoplasmic lines.

These gene delivery methods, tailored for specific organisms and experimental conditions, ensured efficient DNA transfer and stable integration, which were crucial for the subsequent genetic analyses and experimental applications.

2.7 Protein analysis

2.7.1 Protein purification

Protein purification is a series of processes intended to isolate a specific protein from a complex mixture, often involving multiple chromatographic techniques. The objective is to obtain a highly pure protein sample for subsequent analysis.

In this study, the target protein was expressed in the host organism (*E. coli* or *C. reinhardtii*) and harvested by centrifugation. The cell pellet was resuspended in a lysis buffer containing Tris-HCl, NaCl, and protease inhibitors, and subjected to sonication to lyse the cells. The lysate was then clarified by centrifugation at $4,000 \times g$ for 15 minutes at 4°C.

For His-tagged proteins, the clarified lysate was applied to a His-tag purification column (HisTrap™ HP, Cytiva, Marlborough, MA, USA), and the bound proteins were eluted with an imidazole gradient. For Strep-II tagged proteins, the lysate was passed through a Strep-Tactin® Superflow® column (IBA Lifesciences, Göttingen, Germany).

2.7.2 Western blotting

Western blotting is a widely used technique for detecting specific proteins in a sample through the use of antibodies. This method involves the separation of proteins by SDS-PAGE, their transfer to a membrane, and subsequent detection using specific antibodies.

2.7.2.1 *E. coli* protein samples preparation

Protein samples from *E. coli* were prepared by harvesting the cells by centrifugation at $4,000 \times g$ for 15 minutes. The cell pellet was resuspended in lysis buffer containing 50 mM Tris-HCl (pH 8.0), 10 mM EDTA, and 1% SDS, and subjected to sonication to disrupt the cells. The lysate was then clarified by centrifugation at $4,000 \times g$ for 15 minutes at 4°C. The supernatant containing the soluble proteins was collected.

2.7.2.2 *C. reinhardtii* protein samples preparation

Protein samples from *Chlamydomonas reinhardtii* were prepared by harvesting the cells by centrifugation at $4,500 \times g$ for 15 minutes. The cell pellet was resuspended in lysis buffer containing 50 mM Tris-HCl (pH 8.0), 10 mM EDTA, and 1% SDS, and disrupted using sonication. The lysate was clarified by centrifugation at $4,500 \times g$ for 15 minutes at 4°C. The supernatant containing the soluble proteins was collected.

2.7.2.3 SDS-PAGE gel electrophoresis

SDS-PAGE (Sodium Dodecyl Sulfate-Polyacrylamide Gel Electrophoresis) is a technique used to separate proteins based on their molecular weight. Protein samples were mixed with SDS sample buffer and heated at 95°C for 5 minutes to denature the proteins. The samples were then loaded onto a 4-20% Mini-PROTEAN® TGX™ Precast Gel (Bio-Rad, Hercules, CA, USA) and electrophoresed at 150 V for approximately 1.5 hours using Tris-Glycine-SDS running buffer. Following electrophoresis, the gel was either stained with Coomassie Brilliant Blue to visualize the proteins or transferred to a membrane for Western blotting.

2.7.2.4 Signal development

After the transfer of proteins to a nitrocellulose membrane (Amersham Protran, GE Healthcare, Chicago, IL, USA), the membrane was blocked with 5% BSA in PBS-T (PBS with 0.1% Tween 20) to prevent non-specific binding. The membrane was then incubated with a primary antibody specific to the target protein, diluted in blocking buffer, for 1 hour at room temperature. Following incubation, the membrane was

washed with PBS-T and incubated with an HRP-conjugated secondary antibody (Strep-Tactin® HRP for Strep-II tagged proteins, Anti-His HRP for His-tagged proteins, and Anti-HA HRP for HA-tagged proteins) diluted in blocking buffer for 1 hour at room temperature.

Signal development was carried out using an Immun-Star™ HRP Chemiluminescent Kit (Bio-Rad, Hercules, CA, USA). The membrane was incubated with the ECL substrate for 5 minutes, and the chemiluminescent signal was detected using a digital imaging system. The intensity of the bands corresponding to the target protein was quantified using Image Lab™ software (Bio-Rad).

These protein analysis techniques ensured the accurate identification, quantification, and characterization of proteins, providing essential data for the research study.

2.8 Downstream processing

2.8.1 Hanging bag' photobioreactor

The downstream processing of microalgae cultivated in a hanging bag photobioreactor involves several steps to harvest and process the biomass efficiently. This section describes the growth parameters, flocculation, and centrifugation steps required for effective downstream processing (Cui et al., 2022).

2.8.1.1 Growth parameters

Growth parameters in a hanging bag photobioreactor are critical for optimizing biomass yield and quality. According to the methodology described by the study on the characterization of a simple 'hanging bag' photobioreactor for low-cost cultivation of microalgae, cultures were maintained under controlled conditions with a constant light intensity of 150 $\mu\text{E}/\text{m}^2/\text{s}$ and a temperature of 25°C. Aeration was provided through bubbling with compressed air, ensuring adequate mixing and gas exchange. Regular sampling was conducted to monitor growth rates, cell density, and chlorophyll content using spectrophotometric methods.

2.8.1.2 Flocculation

Flocculation is a critical step for the concentration and recovery of microalgal biomass. The process involves aggregating microalgal cells to form larger flocs that can be easily separated from the culture medium. The culture was mixed with the flocculant at a concentration of 10 mg/L and stirred gently for 15 minutes. Floc formation was monitored visually, and the efficiency of flocculation was determined by measuring the reduction in turbidity or cell count in the supernatant after settling (Delrue et al., 2015; Y. Xu et al., 2013).

2.8.1.3 Centrifugation

Following flocculation, the microalgal biomass was further concentrated by centrifugation. This step ensures the removal of remaining culture medium and concentrates the biomass for subsequent processing. Centrifugation was performed

using a Sorvall™ RC 6 Plus Centrifuge (Thermo Fisher Scientific, Waltham, MA, USA) at $4,500 \times g$ for 10 minutes. The pelleted biomass was collected, and the supernatant was discarded. The efficiency of centrifugation was evaluated by measuring the biomass recovery rate and the residual cell concentration in the supernatant.

2.8.2 Freeze drying

Freeze drying, or lyophilization, is employed to preserve and stabilize the harvested microalgal biomass by removing water content under low temperature and vacuum conditions. According to the methodology, the centrifuged biomass was first frozen at -80°C for 12 hours. The frozen biomass was then transferred to a VirTis BenchTop Pro Freeze Dryer (SP Scientific, Warminster, PA, USA), where sublimation of ice occurred under a high vacuum at 0.1 mbar and a condenser temperature of -20°C . The drying process continued until the residual moisture content was reduced to 5%. The freeze-dried biomass was then weighed and stored in airtight containers at room temperature until further use.

2.9 Shrimp feeding trial

The shrimp feeding trial was designed to evaluate the nutritional efficacy of the processed microalgal biomass as a dietary supplement for shrimp. This section outlines the experimental setup, feeding regimen, and the assessment parameters used to determine the impact of the microalgal biomass on shrimp growth and health.

2.9.1 Experimental Setup

The shrimp feeding trial was conducted using juvenile *Litopenaeus vannamei* (Pacific white shrimp). The experiment was set up in a controlled aquaculture facility with multiple replicate tanks for each treatment group. Each tank, with a capacity of 10 L, was stocked with 20 juvenile shrimp, ensuring a stocking density of 0.5 shrimp/L. The tanks were equipped with continuous aeration to maintain dissolved oxygen levels above 5 mg/L, and water temperature was maintained at $28 \pm 1^\circ\text{C}$. Salinity was kept at 30 ± 1 ppt throughout the trial (Charoonnart et al., 2023).

2.9.2 Feeding Regimen

The feeding trial comprised different dietary treatments, including a control diet and diets supplemented with varying levels of microalgal biomass. The diets were formulated based on the nutritional requirements of juvenile shrimp, ensuring they were isonitrogenous and isoenergetic. The control diet consisted of a commercial shrimp feed, while the experimental diets included 10% microalgal biomass.

The shrimp were fed twice daily at 09:00 and 18:00 hours. The feeding rate was adjusted based on the biomass in each tank to ensure approximately 5% of the shrimp biomass was provided as feed per day. Uneaten feed and waste were siphoned out daily, and water quality parameters were monitored regularly to maintain optimal conditions (Charoonnart et al., 2023).

2.9.3 Growth Performance and Health Assessment

The growth performance of shrimp was assessed by measuring initial and final weights, survival rates, and specific growth rates (SGR). Shrimp were individually weighed at the beginning and end of the trial, and the SGR was calculated using the formula:

$$SGR (\% day^{-1}) = \left(\frac{\ln(final\ weight) - \ln(initial\ weight)}{number\ of\ days} \right) \times 100$$

Survival rates were determined by counting the number of surviving shrimps at the end of the trial.

Health assessment included the evaluation of feed conversion ratio (FCR), which was calculated as:

$$FCR = \frac{total\ feed\ intake\ (g)}{total\ weight\ gain\ (g)}$$

Additionally, shrimp samples were collected for biochemical analysis.

2.9.4 Statistical Analysis

Data obtained from the feeding trial were statistically analyzed using GraphPad Prism. Differences between treatment groups were determined using one-way analysis of variance (ANOVA) followed by post-hoc comparisons with Tukey's test. Statistical significance was considered at $p < 0.05$.

The shrimp feeding trial provided comprehensive data on the efficacy of microalgal biomass as a dietary supplement, demonstrating its potential benefits for enhancing growth performance, feed efficiency, and health status of *Litopenaeus vannamei*.

2.10 Bioinformatic analysis

2.10.1 Protein alignment

Protein alignment is a crucial step in bioinformatics that involves comparing protein sequences to identify regions of similarity that may indicate functional, structural, or evolutionary relationships. In this study, protein sequences were aligned using Clustal Omega to ensure accurate comparison and analysis.

The protein sequences of interest were retrieved from the UniProt database and subjected to multiple sequence alignment. The alignment was performed with default parameters, ensuring that gaps and conserved regions were properly accounted for. The results were visualized using Jalview to interpret the alignment and identify conserved motifs, domains, and residues critical for the protein's function.

The alignment data were further used to construct phylogenetic trees to infer evolutionary relationships among the proteins. This comprehensive analysis provided insights into the functional roles and evolutionary history of the proteins studied, contributing to a deeper understanding of their biological significance.

2.10.2 Algal growth data analysis

The algal growth data analysis in this study was conducted using the Algal Data Analyser (ADA) software platform, which is an open-source tool specifically designed for plotting and analysis of data from laboratory photobioreactors, as described by Mapstone et al. (2022).

The process began with the collection and preprocessing of raw abundance data, including normalization to account for sequencing depth differences and log-transformation to stabilize variance. The ADA framework then fitted a generalized linear model to the normalized data, enabling the identification of differential abundance patterns (Mapstone et al., 2022).

Chapter 3

**An improved recipient strain for
simple generation of marker-free
transformants: *psaA*****

3 *psaA*^{**}: an improved recipient strain for simple generation of marker-free transformants

3.1 Introduction

Marker-free genetic transformation represents a pivotal advancement in biotechnology, enabling the creation of genetically modified organisms (GMOs) without the use of antibiotic resistance markers. This approach mitigates ecological and health risks while promoting sustainable genetic engineering practices (Day & Goldschmidt-Clermont, 2011). Marker-free transformation involves integrating genes of interest (GOI) into the host genome using selection methods that result in transgenic lines lacking any antibiotic resistance genes, thereby eliminating the potential for horizontal gene transfer of such genes to other microorganisms such as pathogenic bacteria. This approach supports the commercialisation of GMOs by addressing regulatory restrictions and public concerns regarding GMO safety (E. Specht et al., 2010).

Chlamydomonas reinhardtii serves as an important model organism for chloroplast genetic studies owing to its simple genetics, well-characterized chloroplast genome, and ease of genetic manipulation. Despite these advantages, chloroplast transformation in *C. reinhardtii* faces specific challenges, including achieving high transformation efficiency and ensuring reliable selection of transgenic lines (Harris, 2009; Purton et al., 2013a). Existing transformation methods often require multiple rounds of selection using antibiotic resistance markers and involve complex

procedures such as screening to avoid false-positive lines (*i.e.* those derived from colonies that have acquired natural resistance to the antibiotic) that can limit the applicability and efficiency of the method (Jackson et al., 2022; Taunt et al., 2023; Wannathong et al., 2016). Furthermore, the maintenance and expression of multiple copies of the resistance marker within the polyploid chloroplast of the engineered line represents an unnecessary metabolic burden on the strain. The marker is required simply for the initial selection and to drive the transgenic plastome complement to homoplasmy. Once this is achieved the marker serves no further purpose. It is therefore desirable to create lines that lack (or lose) such transgenic markers and achieve a 'marker-free' state.

As illustrated in Table 3.1 and Figure 3.1, there are currently several strategies for generating marker-free chloroplast transformants of *C. reinhardtii*. The earliest strategies employed non-photosynthetic mutants carrying mutations in key chloroplast genes such as *atpB*, *tscA* or *rbcL* (Esland et al., 2018). These mutants could be rescued to phototrophy by using the cloned wild-type copy of the gene as the marker. Later, knockout lines engineered to disrupt key photosynthetic genes such as *psbH* or *petB* were used as the recipients, with the wild-type gene used as the phototrophic marker whereby it replaces the knockout copy (Cheng et al., 2005; Wannathong et al., 2016). In each case, the mutant allele on the plastome is replaced by the incoming wild-type allele and the linked transgene is incorporated nearby on the plastome (Figure 3.1a and b). An alternative strategy that was not dependent on phototrophic mutants is the CpPos-Neg selection system (Jackson et al., 2022) that can be used with any strain and can be used repeatedly in serial transformations. Here, a dual

marker encoding both resistance to an antibiotic (spectinomycin) and sensitivity to a metabolic analogue (5-fluorocytosine) allows a two-step selection strategy for gain and then loss of the marker during generation of the transgenic line (Figure 3.1c). Improvements have been made for both strategies but still suffer from some limitations (Table 3.1) such as slow colony appearance, restricted targeting loci, potential false positives, and the involvement of antibiotic resistance markers in the initial recipient strains or the selection process. For instance, the CpPosNeg method provides flexibility in targeting GOIs to any locus but necessitates multiple selection rounds and the use of expensive reagents, whereas *psbH* knockout lines TN72 and HT72 allow single-round selection but suffer from slow growth of phototrophic colonies and a single insertion locus located between *psbH* and *trnE2* (Wannathong et al., 2016). The HNT6 strain offers faster colony recovery using selection for light-tolerance on acetate-containing media rather than phototrophic selection on minimal medium, but transgene insertion is again confined to a specific locus upstream of *psaA-3* and the method is susceptible to false positives due to the frequency of light-tolerant mutations (Taunt et al., 2023).

Recipient strain	Selection marker	Advantages	Disadvantages	Reference
WT (e.g. CC-1690)	CpPos-Neg system (e.g., codA-aadA)	<ul style="list-style-type: none"> Gene of interest (GOI) can be targeted to any locus including within the <i>psbA</i> inverted repeat (IR) Serial transformation is possible 	<ul style="list-style-type: none"> Requires two rounds of selection Involves expensive reagents, e.g., spectinomycin and 5-fluorocytosine. Possibility of Spectinomycin resistant (SpecR) false-positive 	(Jackson et al., 2022)
TN72/HT72	<i>psbH</i> gene	<ul style="list-style-type: none"> Requires only single round of selection Simple phototrophic selection using minimal medium, such as High Salt Medium (HSM) No false positives 	<ul style="list-style-type: none"> Colonies appear slowly due to phototrophic growth GOI can be only targeted to <i>psbH-trnE2</i> intergenic locus Serial transformation is impossible 	(Wannathong et al., 2016)
HNT6	<i>psaA-3</i> gene	<ul style="list-style-type: none"> Requires only single round of selection Simple light tolerant selection using Tris-Acetate-Phosphate (TAP) medium Colonies appear fast within 1 week Higher transformation rates than selection on minimal medium 	<ul style="list-style-type: none"> GOI can be only targeted to <i>psaA-3-Wendyll</i> intergenic locus Serial transformation is impossible False-positive due to light-tolerant mutations or incomplete selection (through easily scored upon restreaking on HSM or TAP) 	(Taunt et al., 2023)
<i>psaA**</i> (hypothesis)	trnWUCA	<ul style="list-style-type: none"> Requires only single round of selection Simple light tolerant selection using TAP medium Colonies appear fast within 1 week Higher transformation rates than selection on minimal medium GOI can be targeted to any locus including within the <i>psbA</i> IR Smallest known selectable marker (trnWUCA, 275 bp) An antibiotic resistance gene is not used at any stage 	<ul style="list-style-type: none"> Serial transformation is impossible False-positive due to light-tolerant mutations or incomplete selection (through easily scored upon restreaking on HSM or TAP) 	N.A.

Table 3.1 Comparison of advantages and disadvantages of *psaA*** and other transformation recipient cells developed in the Purton lab.

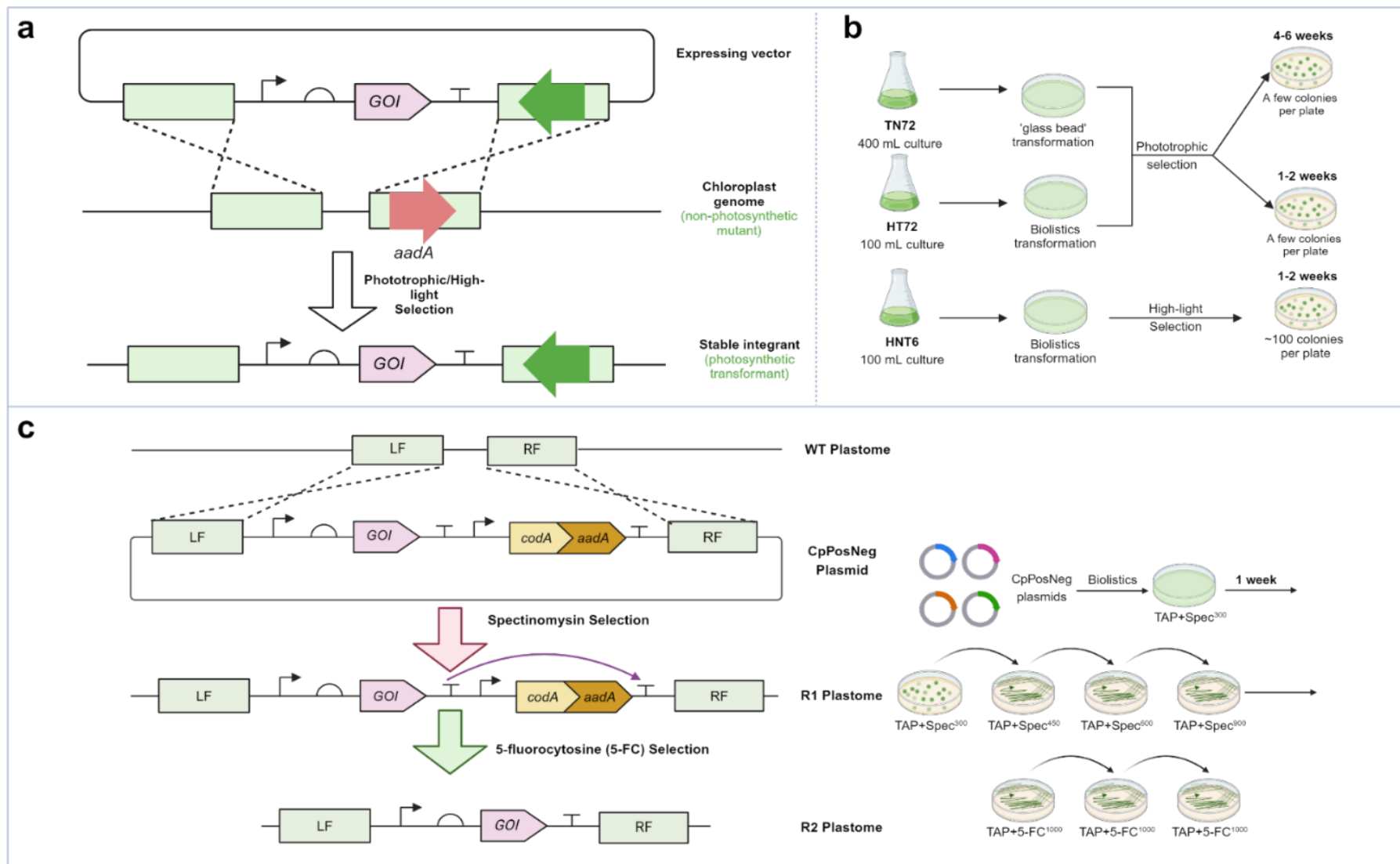


Figure 3.1 Comparison of recipient *C. reinhardtii* strains.

(a) Schematic photosynthetic restoration transformation strategies. The non-photosynthetic mutant (e.g., TN72/HT72 and HNT6 strains) were built by deletion of PSI/PSII genes and insertion of selection marker *aadA* (spectinomycin resistance). GOI expression cassette were integrated to specific neutral site locus (e.g., *psbH* or *psaA-3*) and the transformant cell lines were selected phototrophically (or by high light). (b) Photosynthetic restoration transformation methods and timelines representative strains. (c) CpPos-Neg selection strategy, its transformation methods, and timelines (Jackson et al., 2022).

We hypothesized that the development of a new strategy based on a photosystem I mutant (termed *psaA^{**}*) carrying two nonsense mutations within the *psaA-3* gene could address these critical limitations by providing a more efficient, rapid, and flexible marker-free transformation system for *C. reinhardtii*. Figure 3.2 illustrates the strategy for photosynthetic restoration by inserting genes of interest (GOIs) using codon reassignment with the tRNA marker *trnWUCA*. The diagram shows the integration of the GOI, facilitated by the *trnWUCA* marker, into the plastome. This integration restores photosynthetic functionality by allowing read-through of the two stop codons in *psaA*, enabling the selection of transformants based on their restored photosynthetic ability.

Specifically, the *psaA^{**}* strain is designed to overcome existing challenges through several useful features:

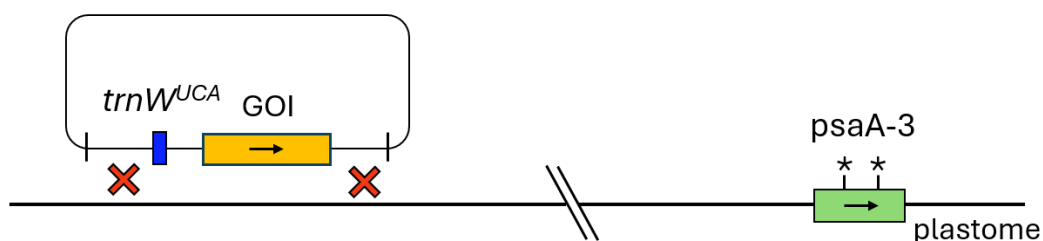


Figure 3.2 Photosynthetic restoration for insertion of GOIs by codon reassignment using tRNA marker *trnWUCA*.

1. A Single Stage of Selection: Unlike the CpPos-Neg strategy, the generation of *psaA^{**}* transformants requires just one stage of selection whereby light tolerance is selected on TAP medium. The *psaA^{**}* strain thereby streamlines the transformation process.

2. **Rapid Recovery:** Unlike selection approaches based on rescue of phototrophic growth on minimal medium, the *psaA*** strategy employs selection for light tolerance under mixotrophic conditions. This is designed to enable the rapid recovery of transformant colonies within one week due to the faster growth of *C. reinhardtii* under mixotrophy, significantly reducing the time to visible colonies compared to the earlier methods.
3. **Higher Transformation Rates:** Taunt et al. (2023) found that selection for light tolerance rather than phototrophy yielded higher transformation rates in addition to faster colony growth. We therefore anticipated that the *psaA*** strain would similarly yield higher transformation rates compared to selection on minimal medium, enhancing overall efficiency.
4. **Minimal Size Marker:** Unlike earlier strategies that use endogenous protein-coding genes as the marker, the *psaA*** approach uses a small tRNA gene engineered to function as an opal suppressor (R. E. B. Young & Purton, 2016). At 275 bp, the *trnWUCA* marker is significantly smaller than all previous markers (Esland et al., 2018).
5. **Targeting to any plastome locus:** The tRNA encoded by the *trnWUCA* marker is designed to work *in trans* to suppress the two UGA stop codons within the *psaA-3* mRNA during translation. Consequently, the marker (together with the linked transgene) can be targeted to any neutral locus including within the inverted repeat (IR) regions, thereby increasing its versatility.

6. Elimination of Antibiotic Resistance Genes: Unlike TN72, HNT6, *etc.* the *psaA*^{**} recipient line is designed to not initially contain any antibiotic resistance marker such as *aadA* that needs to be lost during the drive to homoplasmy. This eliminates the involvement of such antibiotic resistance genes at any stage of the transformation process, offering a more environmentally considerate solution for chloroplast engineering in *C. reinhardtii*.

Another critical aspect of the *psaA*^{**} strain is that it also allows incorporation of a biocontainment strategy into any transgene through codon reassignment - a powerful tool in synthetic biology. Biocontainment refers to the strategic use of genetic elements to prevent the unintended spread or expression of transgenes in non-target organisms. In the context of *C. reinhardtii*, codon reassignment involves modifying the genetic code to utilize an unused codon, such as UGA, within the chloroplast genome. This codon, when reassigned to encode tryptophan (W) specifically within the chloroplast, prevents the functional expression of transgenes in non-target organisms such as *E. coli* (R. E. B. Young & Purton, 2016). This strategy not only addresses the problem of gene toxicity during the cloning process but also significantly enhances the level of biocontainment, ensuring that even if transgenes are horizontally transferred to other organisms, they will not be expressed due to the lack of the specific tRNA required for the reassigned codon. This approach offers a robust solution to potential ecological risks associated with the release of genetically modified microalgae into the environment (R. E. B. Young & Purton, 2016).

The development of the *psaA*^{**} strain and tRNA-based selection method would not only be a significant advance in chloroplast genetic engineering but would also hold considerable potential for the production of high value recombinant proteins.

Chloroplast-based expression systems, particularly in *C. reinhardtii*, have shown promise for the production of therapeutic proteins, vaccines, and bioactive metabolites (Dyo & Purton, 2018; Rasala & Mayfield, 2015). The ability to produce pharmaceutical compounds in a marker-free, biocontained system enhances the safety and acceptability of these products, particularly in medical and therapeutic applications where the use of antibiotic resistance markers is highly discouraged. Additionally, the rapid recovery and high transformation efficiency offered by the *psaA*^{**} strain could streamline the production pipeline, reducing costs and timeframes for the development of new pharmaceutical products.

Objectives and Structure

The primary objectives of this study were to:

1. Develop and validate the *psaA*^{**} strain as an improved recipient for chloroplast transformation.
2. Compare its transformation efficiency and usability against existing recipient strains.
3. Demonstrate the effectiveness of *psaA*^{**} in generating marker-free transformants.

By achieving these objectives, we aimed to establish a robust, efficient, and environmentally considerate system for chloroplast genetic engineering in *C. reinhardtii*, thereby advancing the field of microalgal synthetic biology and expanding its potential applications in biotechnology.

This chapter is structured to provide a comprehensive understanding of the development and advantages of the *psaA*^{**} strain for marker-free transformation of the chloroplast in *C. reinhardtii*. It begins with the creation and validation of the *psaA*^{**} strain, followed by growth analysis under different conditions. The subsequent sections present transformation experiments and their results, concluding with a discussion of the findings and their implications for future research and biotechnological applications.

3.2 Experimental procedures

3.2.1 *C. reinhardtii* strains and growth conditions

To build the *psaA*^{**} strains, a wild type strain of *C. reinhardtii* (CC-1690) and a cell wall-deficient strain (CC-1833) carrying the *cw15* nuclear mutation were used as the starting strains. Both strains were acquired from the Chlamydomonas Resource Centre, University of Minnesota. The CC-1690::*psaA*^{**} and CC-1833::*psaA*^{**} cell lines were maintained in the dark on Tris-acetate phosphate (TAP) plates containing 1.5% agar. The cell lines were cultured for growth tests and western analysis in flasks containing 20 mL TAP, shaking in the dark at 120 rpm and 25 °C. When appropriate, spectinomycin (Spc: sigma-Aldrich; S4014) and 5-fluorocytosine (5-FC: Sigma-Aldrich; F7129) were added to agar plates at a concentration of 300 µg mL⁻¹ and 5 mg mL⁻¹, respectively (Jackson et al., 2022).

3.2.2 Plasmid construction

To construct the unmarked strain *psaA*^{**}, the CpPosNeg strategy was used as described by Jackson et al. (2022). The Start-Stop assembly method was used for

constructing all plasmids, which involves the precise and seamless assembly of genetic constructs (Taylor et al., 2019). Specifically, BsaI was used for generating Level 0 and Level 2 constructs, while SapI was used for Level 1 constructs. In the *psaA*** (pLY410) constructs, two stop codon mutations (TGG to TGA) were introduced to amino acid positions W603 and W611 in the *psaA* exon 3 (*psaA*-3) open reading frame. These constructs were then integrated into the plastome, flanked by 261 bp direct repeats, allowing for the 'loop-out' of the selection marker via homologous recombination and resulting in the unmarked strain. The DNA sequence of *psaA*** (pLY410) is given in Appendix 3; primer sequences are given in Appendix 4.

3.2.3 *C. reinhardtii* transformation

C. reinhardtii strains CC-1690 and CC-1883 were used as the parental cell line for all transformation experiments. With two stop codons introduced to the *psaA* exon 3 making the strains highly light-sensitive, all procedures post-transformation were conducted in a dark environment to prevent light-induced stress. The transformation was carried out using the biolistic method with a PDS-1000/He Particle Delivery System. Plasmid DNA was coated onto gold particles and delivered into the cell under vacuum pressure. Following bombardment, cells were plated on TAP agar medium supplemented with spectinomycin (Spc) for selection of transformants. After initial selection, stable transformants were further analysed for homoplasmy through serial re-streaking on selective media in darkness. Homoplasmic lines were then subjected to negative-selection using 5-Fluorocytosine (5-FC) to facilitate the removal of the marker gene via intramolecular recombination, resulting in marker-free transplastomic lines (Jackson et al., 2022).

3.2.4 Luminescence assays

Luminescence assays were conducted on the CC1690-*psaA^{**}::Nluc* strains. The presence of *trnWUCA* restores the function of *psaA-3^{**}*, enabling transformant strains to grow under light conditions similar to wild-type strains. Cultures were grown in TAP medium under a light intensity of approximately 50 $\mu\text{mol m}^{-2} \text{s}^{-1}$. Mid-log phase cultures were harvested and normalized to the same optical density at 750 nm (OD750). Luminescence was measured using a Steady-Glo Luciferase Assay System (Promega) in a 96-well microplate format. For the assay, 100 μL of normalized culture was mixed with 100 μL of the Steady-Glo reagent, followed by a 5-minute incubation. Luminescence was recorded using a microplate reader, and results were expressed as relative luminescence units (RLU) normalized to OD750 (Jackson et al., 2022).

3.2.5 Western blot analysis

Western blot analysis was performed to detect the expression of the NanoLuciferase (Nluc) protein in the CC1690-*psaA^{**}::Nluc* strains. Cultures were grown under normal light conditions ($\sim 50 \mu\text{mol m}^{-2} \text{s}^{-1}$) and harvested at mid-log phase. Protein extraction was conducted by lysing the cells in an appropriate lysis buffer, followed by SDS-PAGE for protein separation. The separated proteins were transferred onto a nitrocellulose membrane. The presence of Nluc fused with the HA tag was detected using an anti-HA antibody, followed by incubation with a secondary antibody conjugated to a detection enzyme. The resulting signals were visualized using a chemiluminescent substrate, and protein expression levels were quantified by comparing band intensities to those of a standard protein marker.

3.3 Results

3.3.1 Generation of *psaA***— a marker-free *C. reinhardtii* PSI mutant carrying two TGA stop codons in *psaA-3*

Previous studies of PSI mutants of *C. reinhardtii* have shown that they are highly light-sensitive due to the free-radical photo-damage caused by the activity of a PSII complex that is functioning in the absence of a complete electron transfer chain (Erickson et al., 2015). Several groups including ours have exploited this light-sensitivity as a method of selection during chloroplast transformation using mutant lines affected in *psa* genes within the plastome: introduction of the wild-type *psa* gene allowing selection for restored light-tolerance (Taunt et al., 2023). However, rather than using the whole *psa* gene as a marker, a better strategy is to introduce a small mutation in the gene that is complemented by a small DNA element such as the gene for a suppressor tRNA. Young and Purton (2016) demonstrated this by changing a codon for a key tryptophan to an opal stop codon (TGG → TGA) in *psaA-3* and then rescuing the mutant using a *trnW* gene in which the anticodon had been changed to recognise the stop codon. However, the strain that was created in this earlier study also contained the spectinomycin-resistance marker, *aadA* and had just a single base change in *psaA-3* that could revert easily. This strain was therefore not ideal as a recipient for chloroplast engineering studies. We therefore decided to design and construction of a new Δ PSI recipient strain that lacks any markers or unwanted exogenous DNA and contains two Trp→Opal changes in *psaA-3* to greatly reduce the chances of unwanted spontaneous reversion to a wildtype phenotype. This strain is termed *psaA*** (“*psaA* double-stop”).

The generation of *psaA*** leverages the CpPos-Neg strategy (Jackson et al., 2022) to replace the native *psaA* with a *psaA*** cassette in the WT recipient line (CC-1690) such that two stop codons (TGG to TGA) are introduced at amino acid positions W603 and W611 within the open reading frame of exon 3 of the *psaA* gene (*psaA-3*). The same procedure is applied to the cell wall-deficient strain CC-1833 as the parental strain as this allows the use of the same selection method for the ‘glass bead’ method of chloroplast transformation that involves agitating a suspension of a cell-wall deficient strain in the presence of DNA and glass beads (Larrea-Alvarez et al., 2021).

Figure 3.3 illustrates the plasmid construct made and Figure 3.4 plastome integration strategies used for generating the *psaA*** mutant. PCR of total genomic DNA was used to amplify left and right homology arms from the *psaA-3* region of the chloroplast genome with the appropriate *SapI* sites (X, A, Z and Y) at each end to allow assembly with the A-Z DNA part carrying the *codA-aadA* dual marker and a X-Y vector part using the STEP GoldenGate assembly method. Furthermore, the PCR products shared a 261 bp overlap, thereby generating a direct repeat (Figure 3.3, labelled in grey) around the *codA-aadA* that would allow its efficient loop-out following chloroplast transformation when placed under 5-fluorocytosine selection (Jackson et al., 2022). Finally, site-directed mutagenesis of the assembled plasmid using the Kinase-Ligase-DpnI (KLD) method (see: section 2.3) was used to change the two tryptophan codons from TGG to TGA.

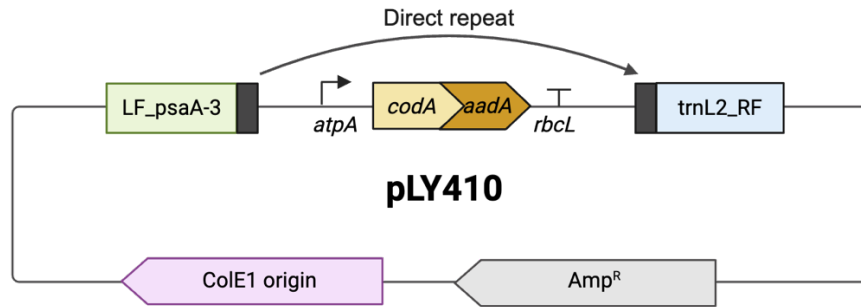


Figure 3.3 The schematic structure of plasmid ppsaA** pLY410.

The final plasmid ppsaA** (pLY410) was introduced into *C. reinhardtii* cells through biolistic transformation. Transformants were selected on TAP medium supplemented with spectinomycin (Spc), which allows only those cells that had successfully integrated the plasmid to survive. Following initial selection, transformants were re-streaked on Spc plates multiple times to guarantee that all chloroplast genome copies within the cells (approximately 83/cell on average) contained the introduced DNA, resulting in a homoplasmic state. This process generated the intermediate transformant line termed R1 (Jackson et al. 2022), where both the dual marker and the site-directed changes are stably integrated into the plastome.

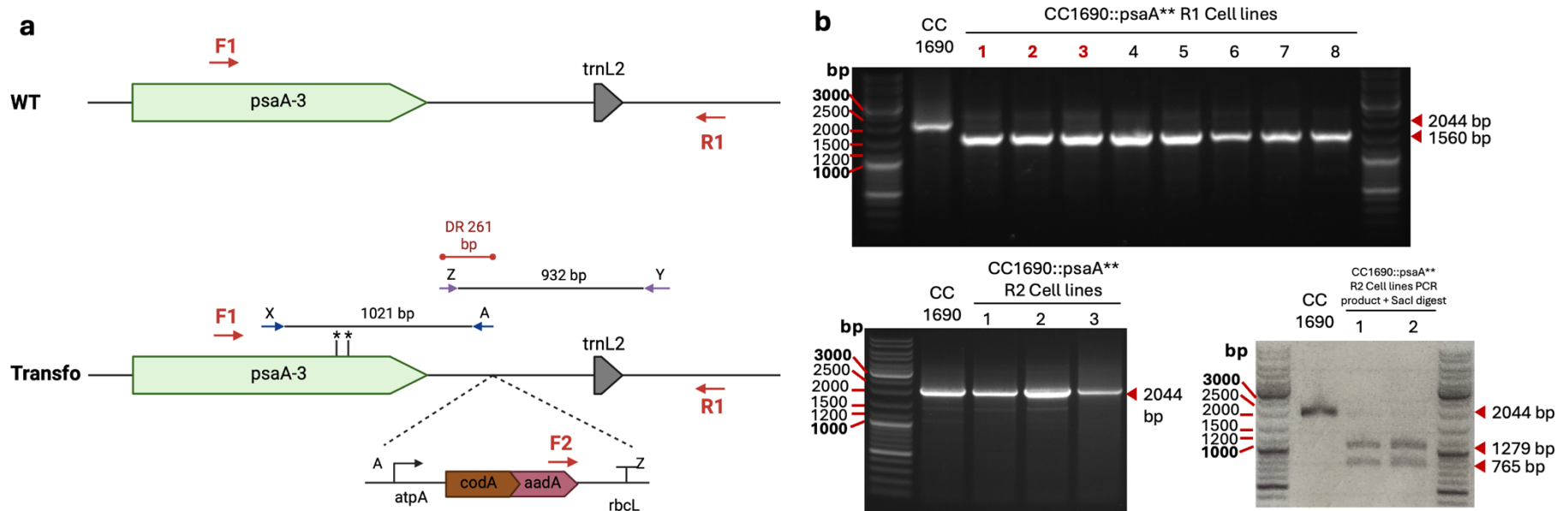


Figure 3.4 Plasmid constructs and plastome integration strategies for the generation of *psaA*, and demonstration of photosynthetic restoration by codon reassignment.**

(a) Schematic of *psaA*** cassette insertion into the intergenic region upstream of *psaA-3* via the CpPos-Neg strategy (Jackson et al., 2022). The cassette contains two TGA stop codons (replacing tryptophan residues at positions W^{603} and W^{611} in the *psaA-3* open reading frame) flanked by 261 bp direct repeats (DRs). These DRs facilitate subsequent excision of the *codA*-*aadA* dual selection marker via intramolecular homologous recombination during 5-fluorocytosine (5-FC) counter-selection. Homologous recombination between the cassette's left/right flanks and the plastome ensures targeted integration upstream of *psaA-3*. (b) Validation of *psaA*** mutation/homoplasmy via '3-primer' PCR, *SmaI* digestion, and Sanger sequencing. PCR primers: F1 (LY314: 5'-GGTTTCCACAGCTTTGG-3'), F2 (LY317: 5'-GAAAGGCGAGATCACTAAG-3'), R1 (LY315: 5'-GCTTGAAACCCGTCAG-3'). Upper gel (R1 transformants): F1+R1 amplify 2044 bp (WT CC-1690) vs. 1560 bp (R1 lines, confirming cassette insertion); F1+F2 verify targeted integration (no WT product). Lower gel (R2 lines, post-5-FC selection): F1+R1 products digested with *SmaI*: 2044 bp (WT, no *SmaI* site) vs. 1279/765 bp (R2 lines, confirming $W^{611} \rightarrow \text{TGA}$ introduces a *SmaI* site). Lane labels: Lane 1 = WT CC-1690; Lanes 2–8 = independent transformants (2–4 = R1; 2–8 = R2).

To confirm homoplasmy in the transgenic cell lines, a 'three-primer PCR' strategy was employed. Panel (b) of Figure 3.4 displays the PCR results for the wild-type (WT) and transformant lines. Specific primers were utilized to amplify regions spanning the *psaA-3* locus and the inserted cassette. The upper portion of Panel (b) shows PCR amplification of the *psaA-3* region using primers F1 and R1. The WT line (CC1690) yielded a single band at 2044 bp, whereas the R1 transformant lines (CC1690::*psaA*** R1) produced a band at 1560 bp, indicating the presence of the *psaA*** insertion. Additional PCR reactions using primers F1, F2, and F3 confirmed the integration of the *psaA*** cassette and the absence of the wild-type *psaA-3* region.

To remove the marker and create a marker-free R2 strain, three independent R1 strains were subjected to a second selection step using 5-fluorocytosine (5-FC). The presence of 5-FC selected for cells that have lost the dual marker via intramolecular recombination between the direct repeat sequences. This recombination event resulted in the excision of the marker cassette, leaving behind only the GOI integrated into the plastome, thereby generating the final R2 strain.

The R2 strains were then confirmed by PCR and phenotypic tests of spectinomycin sensitivity and 5-FC tolerance to ensure that the marker has been completely removed. Unlike a typical design using the CpPosNeg system (which usually including a transgene cassette), the *psaA*** strain was expected to give a PCR product that was the same size as that of the original WT strain following loop-out of the *codA-aadA* cassette, necessitating further analysis to differentiate between *psaA*** and WT strains. Fortunately, the creation of the second TGA codon resulted in the creation of a new *SacI* site at this position allowing this to be used as a diagnostic marker for the R2

transformants. The lower portion of Panel (b) presents this diagnostic enzyme analysis. The PCR products from transformant lines were digested with *SacI* resulting in the predicted band patterns of 2044 bp for the WT, but 1279 bp and 765 bp for the R2 *psaA^{**}* transformants, thereby confirming the successful introduction and homoplasmy of the *psaA^{**}* mutations. Sequencing of the PCR products further validated that the *psaA-3* locus in the R2 transformants was identical to the WT except for the two introduced TGA changes (Appendix 5).

3.3.2 *psaA^{**}* serves as a transformation recipient strain using high light selection

Figure 3.5 illustrates the differential growth capabilities of the parental strain CC-1690 and the *psaA^{**}* transformant line under various chemical conditions. This experiment assessed the *psaA^{**}* strain's potential as a transformation recipient under high light conditions. The *psaA^{**}* mutant showed an inability to grow in the presence of 50 $\mu\text{E}/\text{m}^2/\text{s}$ white light in the absence or presence of acetate, indicating its impaired photosynthetic capacity, unlike the parental strain CC-1690, which grew under the same conditions. These results suggest that the *psaA^{**}* mutant is a suitable candidate for transformation experiments, where successful transformants could be selected based on their ability to grow under high light conditions with acetate, effectively restoring photosynthetic function.

Notably, attempts to apply spectinomycin selection (with the *codA-aadA* marker) in the dark using the cell wall-deficient *cw15* strain as the parental line were unsuccessful. Specifically, under dark conditions, the green background of the algal lawn (from non-transformed *cw15* cells) remained unchanged (no visible clearing or growth of resistant colonies), and no discrete transformant colonies were observed

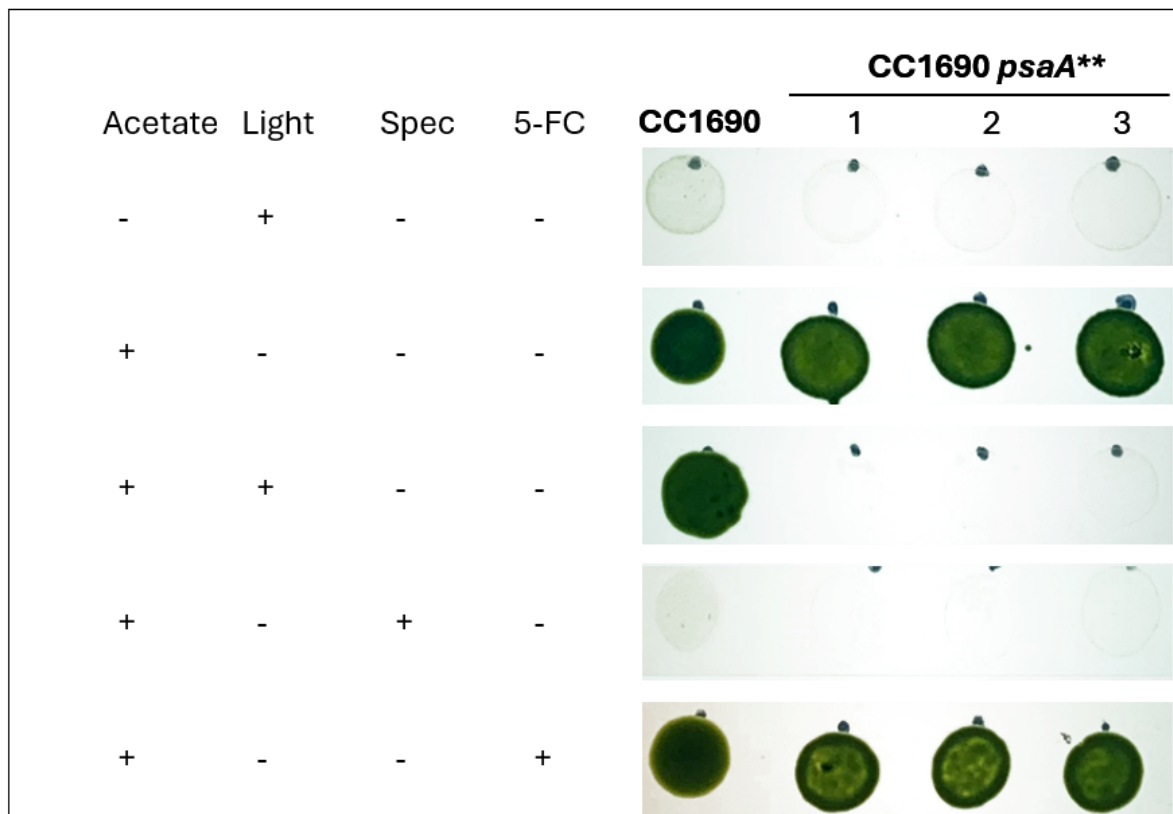


Figure 3.5 Comparative spot test analysis of *C. reinhardtii* *psaA* mutant and parental strain CC-1690 under different conditions.**

(light presence (+): high intensity 50 $\mu\text{E}/\text{m}^2/\text{s}$; light absence (-): light intensity below 1 $\mu\text{E}/\text{m}^2/\text{s}$, covered testing plate with foil; spectinomycin 300 $\mu\text{g}/\text{mL}$, 5-FC: 10 $\mu\text{g}/\text{mL}$).

The figure 3.6 describes the evaluation of the *psaA*** strain as a transformation recipient strain using high light selection. The transformation efficiency was assessed by transforming *psaA*** with an Nluc photosynthetic restoration vector (Appendix 12) under various conditions. In the phototrophic test case, where the transformation was performed on HSM medium with DNA under light conditions, the plate exhibited approximately 10 distinct colonies. This demonstrates that the *psaA*** strain can support transformation under phototrophic conditions, where the cells rely solely on photosynthesis for growth. The presence of distinct colonies indicates successful transformation and photosynthetic restoration. In the negative control, where the

transformation was performed on TAP medium without DNA under light conditions, no colonies were observed. This confirms the specificity and stringency of the selection process, as only transformants with the integrated NLUC gene could grow under the selective conditions. The results of these experiments demonstrate that the *psaA*** strain serves effectively as a transformation recipient strain using high light selection. The high transformation efficiency observed in the mixotrophic test case, combined with the successful colony formation in the phototrophic test case, validates the utility of *psaA*** for genetic transformation. The absence of colonies in the negative control further confirms the specificity of the transformation and selection process. These findings support the use of *psaA*** as a reliable recipient strain for photosynthetic restoration and genetic engineering applications in *C. reinhardtii*.

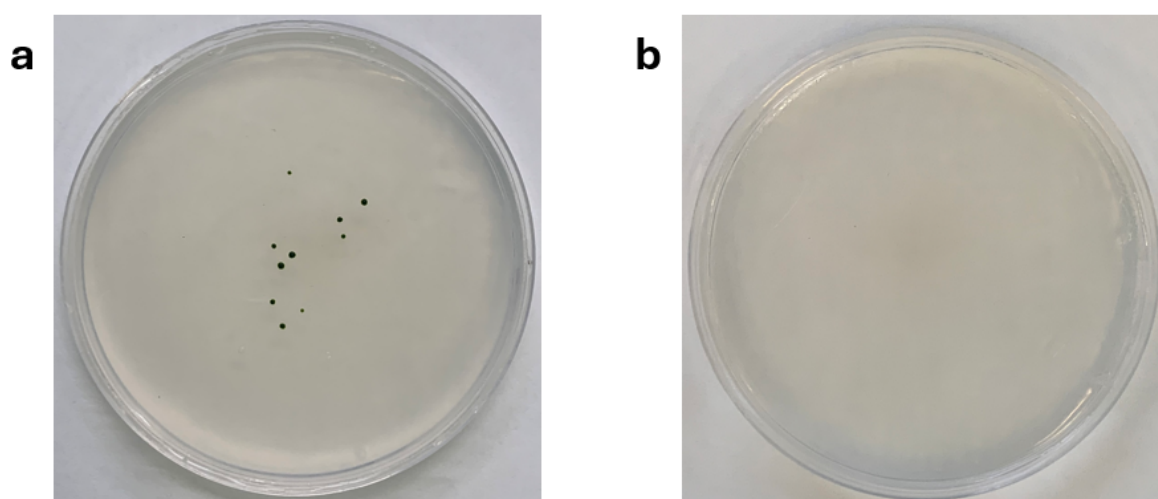


Figure 3.6 Transformation of *psaA* mutant with NLUC in a photosynthetic restoration vector.**

(a) HSM + DNA + Light (phototrophic test case): 10 colonies. (b) HSM – DNA + Light (negative control, with selection): no colony.

3.3.3 *psaA*** as a marker-free recipient cell with rapid transformation feature

To assess whether the *trnW*^{UCA} gene can serve both as a selectable marker and a biocontainment tool for a gene of interest (GOI), two constructs were designed: one in which the *NLUC* gene contains UGA stop codons replacing native tryptophan codons, and a control construct in which the *NLUC* sequence remains unmodified. Figure 3.7 provides a schematic representation of the parental and transformed genotypes, highlighting the location of primers used to discriminate between the two genotypes. The confirmation of homoplasmy in transformant lines was achieved through three-primer PCR, which distinguished between the parental and transformed bands.

In the PCR analysis, the parental *psaA*** line exhibited a band at 2455 bp. In contrast, the transformed lines (*psaA**::NLUC*) showed a distinct band at 1802 bp, indicating successful insertion of the *NLUC* gene. The absence of the parental band in all five transformed lines confirmed homoplasmy, signifying that all chloroplast genomes in the cells contained the inserted gene.

Left Panel: This panel shows the PCR results for the *psaA**::pLY434_HA_nLuc* transformants. The diagram at the top illustrates the integration of the *NLUC* gene into the *psaA*** locus. The PCR gel below confirms the presence of the 1341 bp band in transformants (lanes 4-8), with the parental band (2455 bp) absent, indicating complete homoplasmy.

Right Panel: This panel presents the PCR results for the *psaA**::pLY435_HA_nLuc*** transformants. Similar to the left panel, the integration of the *NLUC* gene into the *psaA*** locus is depicted, and the PCR gel confirms successful transformation and

homoplasmy, with the 1341 bp band present and the parental band absent in the transformant lines.

The results demonstrate that *psaA*** serves as an effective marker-free recipient cell for rapid transformation. The use of the tRNA marker *trnWUCA* for codon reassignment facilitated the accurate insertion of GOIs, enabling efficient photosynthetic restoration. The PCR analysis confirmed the homoplasmy of the transformed lines, validating the reliability and efficiency of the *psaA*** strain for genetic engineering applications in *C. reinhardtii*. This approach offers a robust and marker-free method for transforming chloroplast genomes, advancing the field of synthetic biology and biotechnological research.

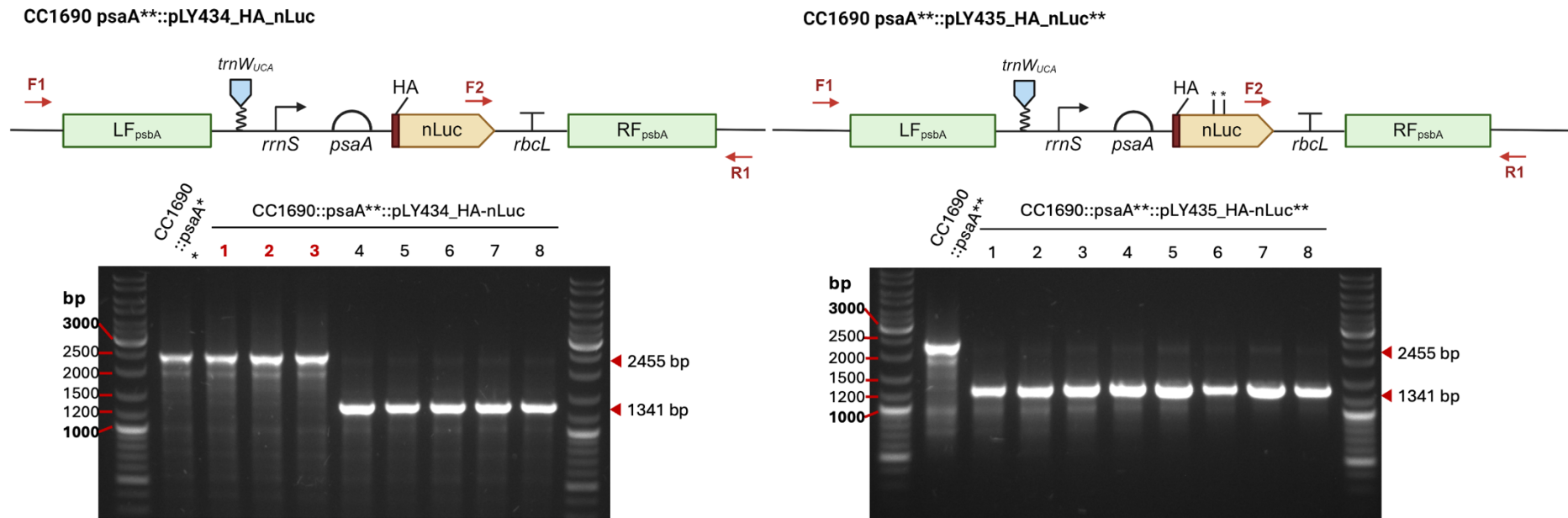


Figure 3.7 PCR and phenotype analysis of the photosynthetically restored line *psaA*^{}::NLUC.**

Left/Right Panels: (Top) Schematic of parental (*psaA*^{**}) and transformed (*psaA*^{**}::nLuc) genotypes, highlighting the location of three primers (F1, F2, R1) used to discriminate between genotypes—primers target regions flanking the nLuc transgene insertion site (within the chloroplast genome) to distinguish parental and transformed loci. (Bottom) Agarose gel of three-primer PCR results confirming homoplasmy in transformant lines. Key bands: Parental *psaA*^{**} strain: A single 2455 bp band (amplified from the unmodified *psaA*^{**} locus). *psaA*^{**}::nLuc transformant lines (5 independent lines shown): A single 1341 bp band (amplified from the locus with integrated nLuc transgene) with no detectable 2455 bp parental band—confirming all chloroplast genome copies carry the nLuc transgene (homoplasmy). nLuc (NanoLuciferase) serves as the reporter gene to validate photosynthetic restoration via *trnW*_{UCA}-mediated readthrough of *psaA*^{**} stop codons, with transgene integration enabling light-tolerant growth of the *psaA*^{**} recipient strain.

3.3.3.1 Analysis of psaA^{**}::NLUC transformants

To demonstrate the protein expression using psaA^{**} strategy, the luciferase assay was conducted. The luminescence assay in Figure 3.8 shows the activity of luciferase in the psaA^{**}::NLUC strains. The luminescence, measured in Relative Luminescence Units (RLU), indicates the functional expression of the NLuc enzyme in these strains. The bar graph presents the mean luminescence values with standard deviations for triplicate readings, offering a reliable measure of the luciferase activity across different samples. The TAP medium and CC1690 wild-type strain exhibit negligible luminescence, as expected, since they do not carry the NLuc gene.

To test whether the presence of stop codons affects the efficiency of protein expression, HA_NLUC and HA_LUC^{**} strains were compared by their luminescence density. Both modified strains show significant luciferase activity, with the CC1690 psaA^{**}_pLY434_HA_NLUC strain demonstrating higher luminescence than the CC1690 psaA^{**}_pLY435_HA_NLUC^{**} strain. This suggests that while both strains effectively express the NLuc enzyme, there may be differences in the efficiency of gene expression or the stability of the protein between the two constructs.

The Western blot in Figure 3.8 displays bands corresponding to the rbcL protein (52.5 kDa) as a loading control and the NLuc protein (22.8 kDa) in the psaA^{**}::NLUC strains. The rbcL bands appear consistent across all lanes, indicating equal protein loading and allowing for accurate comparison of NLuc expression. The intensity of the NLuc bands reflects the protein expression level in each strain. The corresponding bar graph on the right quantifies this expression, showing that the NLuc variant

(_pLY434_HA_NLUC) exhibits stronger band intensity compared to the _pLY435_HA_NLUC** variant. This aligns with the luminescence data, where the _pLY434_HA_NLUC strain also demonstrated higher activity, suggesting a higher expression or better functionality of the luciferase enzyme in this construct.

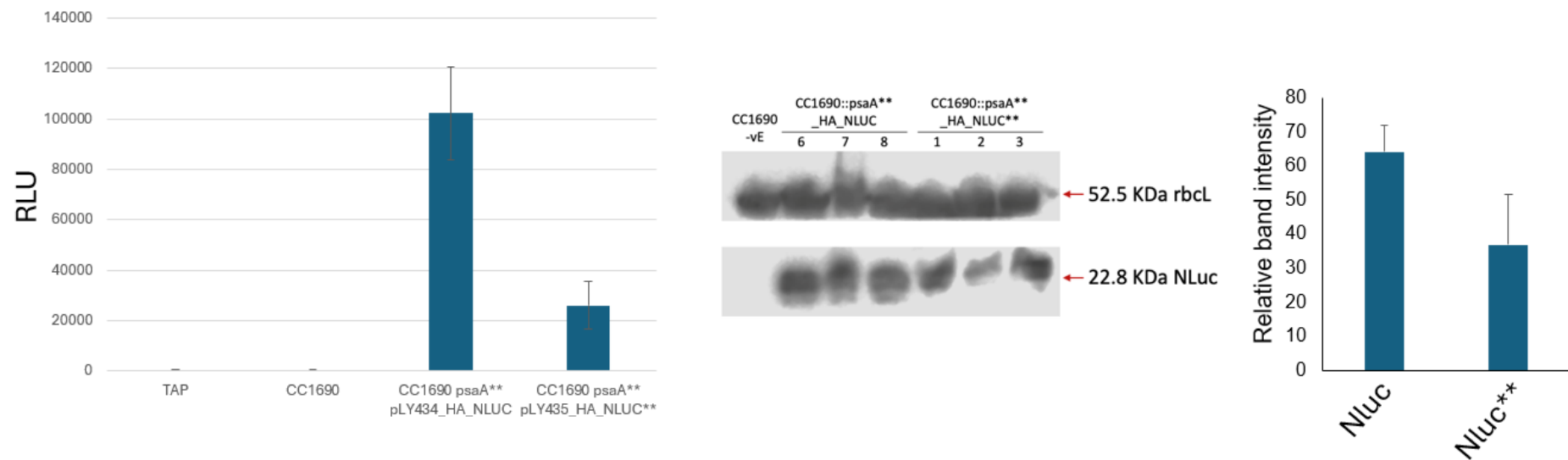


Figure 3.8 Luminescence assay and western blotting analysis of *psaA*::Nluc strains**

(a) Luminescence assay demonstrating luciferase activity in the representative *psaA***::NLUC strain. The bar shows mean and standard deviation of triplicate readings for this strain. (b) Western blotting analysis demonstrating luciferase expression in the representative *psaA***::NLUC strain.

3.4 Discussion

3.4.1 Summary of Key Findings

This study successfully created and validated the CC1690::psaA** strain using the CpPos-Neg strategy (Jackson et al., 2022). The validation of the psaA** strain involved several key steps, including PCR, diagnostic enzyme analysis, and sequencing, all of which confirmed the mutation and homoplasmy of CC1690::psaA**. The successful insertion and confirmation of a test reporter gene (Nluc) indicate that psaA** can serve as a robust recipient for chloroplast genetic studies, providing a reliable basis for further transformations.

The CC1690::psaA** strain exhibited distinct growth characteristics, particularly its inability to grow phototrophically or mixotrophically under high light. Growth analysis spot tests on solid media revealed that psaA** is entirely inhibited by high light (200 μ Em-2s-1). These findings highlight the unique growth responses of psaA** under various light conditions, which is crucial for optimizing transformation protocols.

The CC1690::psaA** strain demonstrated its effectiveness as a recipient strain for transformation. When transformed with Nluc in a photosynthetic restoration vector, the CC1690::psaA** strain showed rapid recovery of colonies under high light selection in phototrophic conditions, as well as the absence of colonies in the negative controls, underscored the high transformation efficiency of CC1690::psaA**. This efficiency is further evidenced by the successful integration and expression of the Nluc gene, making psaA** a valuable tool for genetic engineering.

A significant achievement of this study was the successful generation of marker-free transformants using *psaA***. PCR and phenotype analysis of the photosynthetically restored *psaA**::Nluc* lines confirmed homoplasmy, with the expected band patterns observed in transformant lines. Luminescence assays demonstrated luciferase activity in the representative *psaA**::Nluc* strains, further validating the functionality of the inserted genes.

The failure of spectinomycin selection in the dark when specifically using the more fragile *cw15* as the parental strain suggests a possible dependence on light for full antibiotic efficacy. Whether this reflects a lower level of expression of the *codA-aadA* gene in the dark or lower spectinomycin activity on the chloroplast ribosome in the absence of light, is not clear. A potential approach to overcome this issue could be the use of dim light during selection to maintain some level of chloroplast activity without fully exposing the cells to light, thereby enabling effective selection. Previous studies have shown that the activity of chloroplast-targeting antibiotics like spectinomycin is closely tied to the metabolic state of the chloroplasts, which is regulated by light (Danon & Mayfield, 1991; Harris et al., 2009). Further research could explore this strategy or alternative selection markers that are not reliant on chloroplast activity, ensuring effective selection under varying light conditions.

3.4.2 Comparison with Existing Methods

The *psaA*** strain offers several advantages over the CpPos-Neg method (Jackson et al. 2022) when trying to generate marker-free transformant lines. The latter method requires multiple rounds of selection and involve costly reagents such as spectinomycin and 5-fluorocytosine, which can also lead to false positives (Jackson et

al., 2022). In contrast, *psaA*** requires only a single round of selection and utilizes either acetate-containing (TAP) or minimal salt medium (HSM), significantly reducing the time and cost associated with the transformation process. Additionally, *psaA*** avoids any use of antibiotic resistance markers, thereby addressing public concerns about GMOs and contributing to more sustainable genetic engineering practices.

Notably, the *psaA*** strain builds on and improves the earlier *psaA** system (Young & Purton, 2016)—a single-stop (TGG→TGA) PSI mutant that relied on the *trnW^{UCA}* suppressor tRNA for selection. While *psaA** demonstrated the feasibility of tRNA-mediated translational readthrough for chloroplast transformation, it suffered from two critical limitations: high risk of spontaneous reversion (single TGA codon easily mutates back to TGG) and retention of the *aadA* antibiotic resistance marker in the recipient strain (Young & Purton, 2016). In contrast, *psaA*** introduces two TGA stop codons in *psaA-3*, virtually eliminating reversion events, and uses the CpPos-Neg strategy to remove all exogenous markers (*codA-aadA*) post-selection, resulting in a truly unmarked recipient line. Furthermore, unlike *psaA**, which lacked controllable expression capabilities, *psaA*** can be paired with temperature-sensitive translational readthrough systems such as CITRIC (Cold-Inducible Translational Readthrough In Chloroplasts; Young & Purton, 2018). The CITRIC system employs a temperature-sensitive variant of *trnW^{UCA}* that only functions at permissive temperatures (~20°C), enabling orthogonal control of transgene expression—an advantage not offered by *psaA** or other existing methods like TN72/HT72.

The rescue of the PSII mutant TN72 (or HT72) using the endogenous *psbH* gene as a marker (Wannathong et al., 2016), while requiring only a single round of selection and using simple phototrophic selection on minimal medium, exhibits slow colony

appearance and targeting of GOIs is limited to the *psbH-trnE2* intergenic locus (Wannathong et al., 2016). The PSI mutant strain *psaA***, on the other hand, offers faster colony recovery within one week and allows targeting to any locus, including within the inverted repeat (IR). This flexibility in targeting and rapid recovery makes *psaA*** a superior choice for researchers seeking efficient and versatile transformation methods.

Like *psaA***, the PSI mutant HNT6 that uses the whole of *psaA-3* as a marker (Taunt et al., 2023) offers single-round selection and fast colony recovery using light-tolerant selection with TAP medium. However, a larger transformation construct is required because of the size of the *psaA-3* marker, and GOI targeting is again limited just to one locus: the *psaA-3-wendyll* intergenic locus (Taunt et al., 2023). In comparison, *psaA*** not only offers higher transformation rates but also enables targeting to any locus and uses the smallest known selectable marker (275 bp).

3.4.3 Limitations of *psaA*** strain

Maintaining the *psaA*** strain presents several challenges that have been observed during experimental work:

- **Maintenance Issues:** The *psaA*** strain requires careful handling to keep the cultures fresh and healthy, particularly when transferring from plate to liquid culture. The strain tends to lose viability if not maintained under optimal conditions.
- **Selection Inefficiency:** Heterotrophic selection methods, such as using TAP medium, have not been as effective as anticipated for selecting *psaA***

transformants. This may be due to the specific metabolic requirements of the strain, which are not fully met under heterotrophic conditions.

- **False Positives in Phototrophic Selection:** During phototrophic selection, 'false positives' have been observed, although these are slow-growing and fail to survive after several restreaks and exposure to light. It is possible that a low level of readthrough of the two UGA codons by the native tryptophan tRNA is responsible for this. Such 'leaky' reading of UGA by the tRNA is known to occur in *E. coli* (Grome et al., 2025), and there is some evidence of this occurring also in the *C. reinhardtii* chloroplast (Young & Purton, 2018). This indicates that initial selection may not be stringent enough, allowing non-transformant cells to survive temporarily.
- **Dependency on Light Intensity:** The number of transformants observed on selection plates appears to be highly dependent on the light intensity during the selection process. This suggests that precise control of light conditions is critical for successful transformation and selection.
- **Need for Further Testing:** Given these challenges, further testing is required, particularly focusing on protein expression levels in the *psaA*** strain. Optimizing the conditions for maintenance and selection could lead to more reliable outcomes and better performance in downstream applications.

3.4.4 Future Directions

3.4.4.1 The development of a cell-wall deficient version of the *psaA*^{**}

The development of a cell-wall deficient version of the *psaA*^{**} strain, such as using the *cw15* strain as the parental line, could offer significant advantages in both research and pharmaceutical applications. The *cw15* strain is commonly used in *C. reinhardtii* research due to its ease of transformation and higher rates of DNA uptake, facilitated by the absence of a rigid cell wall (Harris, 2009; Kindle, 1990). Incorporating the *psaA*^{**} cassette into a *cw15* background would likely enhance transformation efficiency and simplify the process of genetic manipulation, making it a more versatile tool for various applications.

One of the most promising potential applications of a cell-wall deficient *psaA*^{**} strain lies in the field of oral delivery systems for animal trials. The absence of a cell wall would allow the *Chlamydomonas* cells to be more easily digested and broken down in the gastrointestinal tract, enhancing the bioavailability of the expressed therapeutic proteins or antigens. This approach has been explored in previous studies, where genetically modified *Chlamydomonas* strains were used to deliver oral vaccines (E. A. Specht & Mayfield, 2014). The *cw15-psaA*^{**} strain could thus serve as an effective vehicle for the delivery of oral vaccines or other therapeutic compounds directly in the gut, offering a non-invasive and cost-effective alternative to traditional injection-based methods.

In the pharmaceutical field, the *cw15-psaA*^{**} strain could be used to produce high-value therapeutic proteins or peptides. The lack of a cell wall facilitates the secretion of these products into the surrounding medium, simplifying purification processes and

reducing production costs (Rasala & Mayfield, 2015). Moreover, the ability to produce complex proteins with proper post-translational modifications in a plant-like system offers an attractive alternative to traditional expression systems like bacteria or yeast, particularly for proteins that require disulphide bonds or other modifications that are challenging in other systems (Taunt et al., 2018).

3.4.4.2 Investigation of the integration of improved version of *trnWUCA*

Future work should focus on investigating the integration and functionality of an improved version of the *trnWUCA* construct. The original design of *trnWUCA* by Young et al. (2015) lacked a portion of its 3' untranslated region (3'UTR) (see figure 3.9, TCTAAAAGGGCATTATGAGCCTAGGTCCTTATGTGCTTTTAGATGTTAGCAAGT TTGCTTACCCACAAAGTGTATTTTGTAACCTTAAGAACAA). These omissions may have impacted the construct's efficiency in facilitating codon reassignment, particularly in the context of highly expressed genes that rely on the UGA codon for tryptophan incorporation. Enhancing the *trnWUCA* design by restoring the full 3'UTR and optimizing the *trnW* gene could potentially improve the stability and functionality of the tRNA, leading to more efficient codon reassignment. This, in turn, may result in higher expression levels of target genes in *C. reinhardtii* and other expression systems. Future studies should evaluate the performance of this improved construct in various

experimental contexts, focusing on its impact on gene expression efficiency.

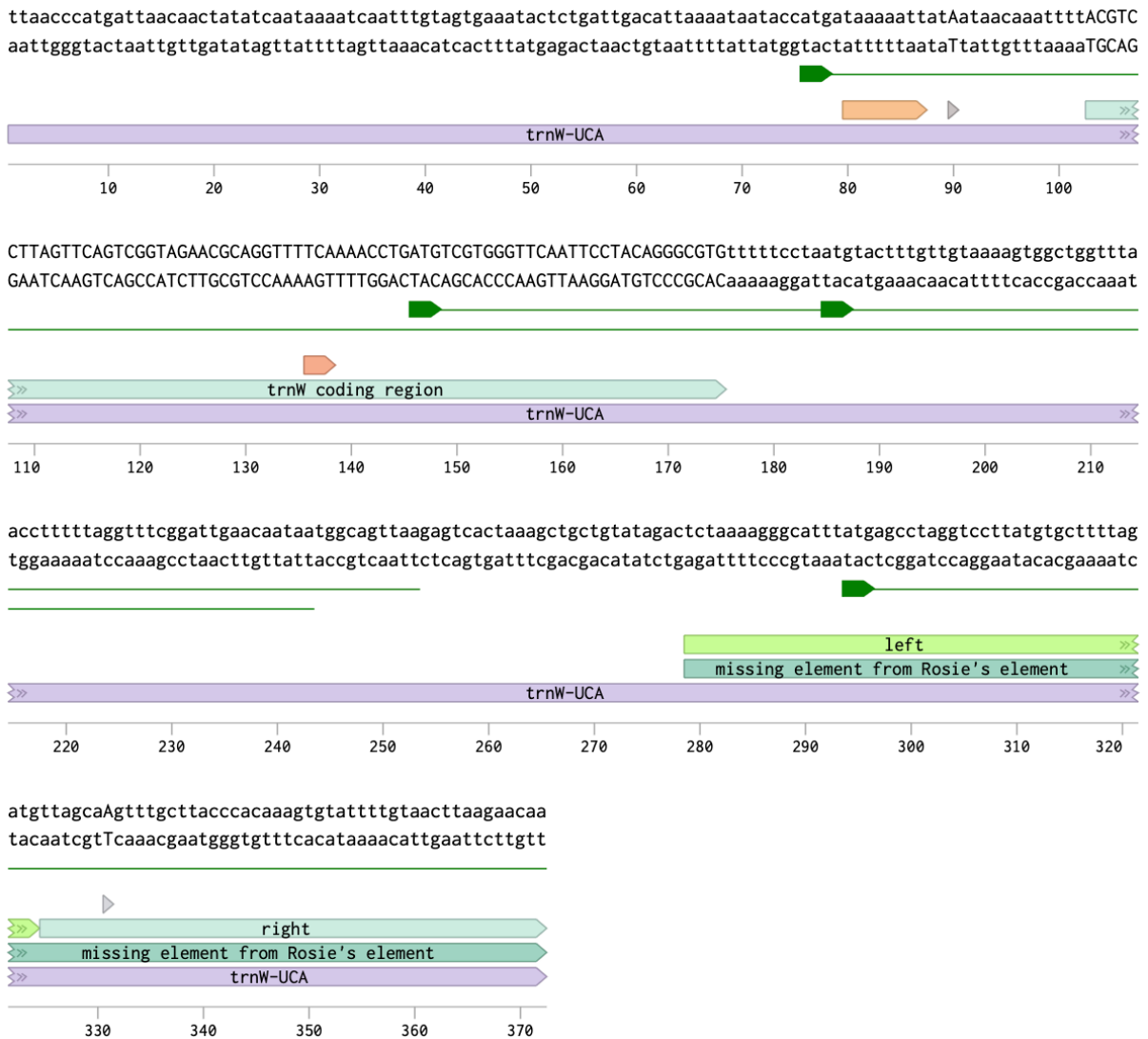


Figure 3.9 The comparison between original design of trnWUCA Young et al. (2015) and full restoring 3' UTR.

3.4.4.3 Temperature-Inducible Systems for Industrial Application: Cold- and Heat-Inducible Strategies

Inducible gene expression systems are essential tools in synthetic biology, offering precise control over protein production, which is particularly beneficial in industrial settings. Commonly used systems include chemical inducers such as IPTG and

tetracycline, as well as temperature-based systems, which provide a cost-effective and scalable alternative in industrial bioreactors.

Temperature-inducible systems activate or repress gene expression in response to temperature changes. A notable example is the CITRIC system (Cold-Inducible Translational Readthrough In Chloroplasts), developed for *C. reinhardtii*, which utilizes a temperature-sensitive version of the modified tryptophan tRNA allowing translation to proceed only at the lower permissive temperature (Young & Purton, 2018). Incorporating such a system in industrial processes enables precise timing of protein production, reducing metabolic burden during growth phases and optimizing yields during production phases.

In addition to cold-inducible systems, heat-inducible systems, which use heat-shock promoters activated at elevated temperatures, offer another layer of control (Morimoto, 1998). These systems are particularly useful for triggering stress-response proteins or other valuable compounds in response to temperature changes. The flexibility offered by both cold- and heat-inducible systems makes them valuable tools for industrial biotechnology, enhancing the efficiency and scalability of protein production processes.

The integration of these inducible systems into *psaA*^{**} strains could further improve their industrial applications. By combining the robust photosynthetic capabilities of the *psaA*^{**} strain with the precise control provided by inducible systems, it would be possible to finely tune gene expression in response to environmental conditions. This integration could optimize the production of valuable biomolecules, reduce metabolic stress during non-production phases, and allow for the scalable production of complex

proteins in *C. reinhardtii*. Such a strategy represents a promising direction for future research and development in the field of synthetic biology and industrial biotechnology.

3.4.4.4 Enhancing expression yield through circular mRNA technology

Recent advances in RNA technology have highlighted the potential of circular mRNA for boosting recombinant protein expression. Circular mRNA is generated through a process known as back-splicing, where the ends of a linear mRNA are joined together, resulting in a molecule that is more stable and resistant to degradation by exonucleases. This increased stability allows for prolonged translation and higher protein yields, as demonstrated in various eukaryotic systems (Litke & Jaffrey, 2019; Zhang et al., 2018).

Studies have also identified native circular RNAs in plant chloroplasts, which are likely the result of mis-splicing events due to the high prevalence of introns in these genomes (Oldenkamp et al., 2019). Leveraging this natural phenomenon, we propose the use of the *rrnS* intron from *Chlamydomonas moewusii*, which is not present in the *C. reinhardtii* plastome. This intron, the smallest of the group I introns and free of *Bsa*I or *Sap*I restriction sites, has been well-characterized in the context of splicing (Durocher et al., 1989).

One of the proteins of interest that could benefit from this enhanced expression strategy is the Pal endolysin, a bacteriophage-derived enzyme with strong antibacterial properties. Endolysins like Pal degrade bacterial cell walls by cleaving specific bonds in peptidoglycans, leading to cell lysis. Pal endolysin, derived from bacteriophage ϕ KMV, specifically targets Gram-negative bacteria, making it a

promising candidate for developing novel antibacterial therapies. Given its potential therapeutic applications, achieving high yields of Pal endolysin through circular mRNA technology could significantly enhance its feasibility as a biopharmaceutical product (Young & Purton, 2016).

To test the efficacy of circular mRNA in enhancing expression, we will construct test and control plasmids for the transformation of the *psaA*** strain. Circular mRNA formation will be confirmed by RT-PCR using primers flanking the expected splice junction. Expression levels of the Nluc reporter gene will then be compared between strains with functional splice sites and those without. If successful, this approach could be extended to the expression of other proteins, such as the Pal endolysin, demonstrating the broad applicability of circular mRNA technology in boosting protein production in *C. reinhardtii*.

Chapter 4

Production of recombinant fish growth hormone (fGH) in the chloroplast of microalga *C. reinhardtii*

4 Production of recombinant fish growth hormone (fGH) in the chloroplast of microalga *C. reinhardtii*

4.1 Introduction

The global population is projected to reach 10 billion by 2050, significantly increasing the demand for food production (Graham, 2019). Aquaculture, the farming of aquatic organisms, is a critical sector in meeting this demand due to its efficiency and sustainability compared to traditional livestock farming (FAO, 2024). Enhancing growth rates of aquatic animals, particularly fish and mollusks, through biotechnological interventions, such as genetic engineering strategies to increase the level of growth hormones (GHs) has become a focal point in aquaculture research (Acosta et al., 2009; Arenal et al., 2008; Santiesteban et al., 2010; Sarker et al., 2020). Strategies for increasing GH levels can involve the production of transgenic animals engineered to over-express the GH at an early growth stage, or by injection or oral delivery of recombinant GH to juvenile animals (Antoro et al., 2016).

Growth hormones play a crucial role in regulating growth, metabolism, and overall development in animals. The use of GH and insulin-like growth factors I and II (IGF-I and II) is considered to accelerate the growth of fish (Farmanfarmaian & Sun, 1999). In aquaculture, the application of GHs has been shown to increase growth rates, improve feed conversion ratios, and enhance the overall productivity of fish farming operations. Researchers have made significant efforts in producing recombinant GHs over the past decades. Previous studies have successfully produced recombinant fish Growth Hormone (fGH) in *Escherichia coli* and shown that injection significantly increasing the

growth of juvenile Nile tilapia (*O. niloticus*) and Rohu (*Labeo rohita*) (Alimuuddin et al., 2010; Sekar et al., 2015).

Previous studies have shown that fish growth hormone (fGH) can stimulate somatic growth not only in fish but also in crustaceans. For example, the transfer of the *tilapia* growth hormone gene into *Litopenaeus schmitti* resulted in significant growth enhancement, demonstrating the cross-species activity of fish GH in shrimp (Arenal et al., 2008). In addition, successful molecular cloning and expression of growth hormone cDNA from yellowfin porgy (*Acanthopagrus latus*) have laid the groundwork for functional studies and potential biotechnological applications in aquaculture (Tsai et al., 1993). These findings support the rationale for evaluating heterologous expression of fGH as a tool for enhancing growth in both vertebrate and invertebrate aquaculture species.

Species	Common Name	GH Name	Accession Number	Amino Acid Sequence Length	Source Reference
<i>Homo sapiens</i>	Human	hGH	P01241	191	https://www.ncbi.nlm.nih.gov/protein/P01241
<i>Sus scrofa</i>	Pig	pGH	P01243	190	https://www.ncbi.nlm.nih.gov/protein/P01243
<i>Gallus gallus</i>	Chicken	chGH	P01244	190	https://www.ncbi.nlm.nih.gov/protein/P01244

<i>Rattus norvegicus</i>	Rat	rGH	P01242	191	https://www.ncbi.nlm.nih.gov/protein/P01242
<i>Capra hircus</i>	Goat	gGH	P01246	191	https://www.ncbi.nlm.nih.gov/protein/P01246
<i>Oncorhynchus mykiss</i>	Trout/Salmon	t/sGH	P01245	188	https://www.ncbi.nlm.nih.gov/protein/P01245
<i>Cyprinus carpio</i>	Carp	cGH	P01247	204	https://www.ncbi.nlm.nih.gov/protein/P01247
<i>Anguilla anguilla</i>	Eel	eGH	P01248	211	https://www.ncbi.nlm.nih.gov/protein/P01248
<i>Acanthopagrus latus</i>	Yellow Porgy	ypGH	Unavailable	191	(Palanivelu & Dharmalingam, 1993)
<i>Oreochromis niloticus</i>	Tilapia	tiGH	P01249	191	https://www.ncbi.nlm.nih.gov/protein/P01249

Table 4.1 GHs of different species

Yeast and other Generally Recognized As Safe (GRAS) organisms have been explored as whole-cell oral delivery systems for GHs. For instance, yeast *Pichia pastoris* has been used to produce tilapia growth hormone (GH), which was shown to boost the growth of other species, including goldfish, carp, and angelfish (Acosta et al., 2009). More recently, microalgae have emerged as promising alternative platforms, serving as whole-cell bioencapsulation and oral delivery systems (Rosales-Mendoza et al., 2020). As discussed in chapter 1, microalgae are considered attractive systems for recombinant protein production due to several advantages: cost-effective

cultivation (Spolaore et al., 2006), scalability (Mata et al., 2010), sustainability (Wijffels & Barbosa, 2010), and safety (Rasala & Mayfield, 2015). Importantly, the use of GRAS platforms such as edible microalgae allows the use of the whole cell biomass as a feed additive, eliminating the need for complex and costly purification processes that are necessary for traditional platforms such as *E. coli* or CHO cells (Rosales-Mendoza et al., 2020). Such traditional methods for manufacturing therapeutic proteins involve not only their purification but also cold chain storage, and manual injection. This makes their use technically challenging and prohibitively expensive for aquaculture, and hinders widespread use.

More specifically, the microalgal chloroplast represents an attractive site of synthesis that is not present in other eukaryotic platforms such as yeasts. The chloroplast genome offers several advantages for genetic engineering, including targeted insertion of transgenes through homologous recombination ensuring stable and predictable expression, high-level expression of transgenes, absence of gene silencing mechanisms often encountered in nuclear transformation, and containment of transgenes within the organelle, reducing the risk of horizontal gene transfer (Bock, 2015; Taunt et al., 2018).

Liu et al. (2007) demonstrated the potential of using photosynthetic microorganisms for recombinant fGH production by supplementing fish feed with 1% transgenic *Synechocystis* sp. PCC6803 engineered to produce fGH from olive flounder, resulting in a significant growth improvement in turbot (S. Liu et al., 2007). Similarly, Chen et al. (2008) produced yellowfin porgy fGH in the marine microalga *Nannochloropsis oculata*, leading to substantial weight gain and body length increases in brine shrimp (H. L. Chen et al., 2008). Additionally, the potential of the *C. reinhardtii* chloroplast as a

platform for producing active growth factors has demonstrated with the production of functional Vascular endothelial growth factor (VEGF) and human growth hormone (hGH), showcasing the potential of this system for whole-cell bioencapsulation and oral delivery (Rasala et al., 2010, Wannathong et al., 2016).

Click or tap here to enter text.Despite these promising early studies using the *C. reinhardtii* chloroplast platform, no research has been carried out on recombinant fGHs, and few studies on therapeutic proteins have been conducted at pilot scale (Dyo & Purton, 2018; Gimpel et al., 2015a; Zedler et al., 2016). The project described in this chapter aimed to develop fGH-expressing *C. reinhardtii* cell lines, quantify fGH production, optimize downstream processing methods, and conduct preliminary feeding trials with shrimp as depicted in figure 4.2.

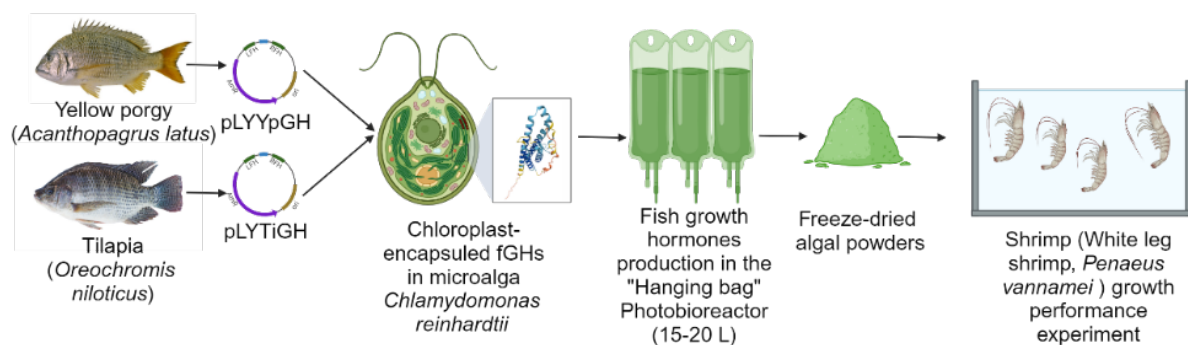


Figure 4.1 The overview of the production of fish growth hormone (fGHs) in the chloroplast of *C. reinhardtii*.

Specifically, the primary objectives of this study were:

1. To achieve high-yield production of recombinant fish growth hormone (fGH) in the chloroplast of *C. reinhardtii*:

- Design and assemble plasmid constructs for the expression of selected fGH in the chloroplast.
- Generate stable, scar-less, and marker-free *C. reinhardtii* strains expressing fGH: This involved comparing two different selective strategies: a 'Chloroplast Positive-negative strategy' (CpPos-Neg) and a 'light restoration strategy' to determine the most efficient method for stable and high-level expression of the fGHs.
- Quantify the expression levels of fGH and assess the growth performance of shrimp larvae fed with the transplastomic algae. This would include scaling up the cultivation using a 'hanging bag' photobioreactor system, optimizing conditions for maximum yield and effective harvesting, and ensuring the process can be implemented under practical, non-sterile conditions for industrial applications.
- Validate the scalability and economic feasibility of producing fGH in *C. reinhardtii*.

2. Conduct preliminary trials in shrimp:

- Evaluate the growth performance and health of shrimp larvae fed with the transplastomic algae expressing fGH.
- Assess the practical application and potential benefits of using fGH-expressing *C. reinhardtii* in shrimp aquaculture.

The development of transgenic *C. reinhardtii* strains expressing fGHs represents a novel approach to enhancing aquaculture productivity. By leveraging the advantages of chloroplast genetic engineering and the natural bioencapsulation properties of

microalgae, this study aims to provide a cost-effective, sustainable, and efficient method for administering growth hormones to fish. The results of this research could have significant implications for the aquaculture industry, contributing to increased food production to meet the demands of a growing global population.

4.2 Results

4.2.1 Choice of fGH sequences

In this study, yellow porgy growth hormone (ypGH) and tilapia growth hormone (TiGH) were selected for transgenic expression due to their relevance in aquaculture and their representation of distinct lineages within teleost fish (Acosta et al., 2009; Arenal et al., 2008). Tilapia is one of the most widely farmed freshwater species globally, known for its rapid growth and adaptability, making TiGH a practical candidate for enhancing growth performance in other species. Yellow porgy, on the other hand, is a marine species with economic value in East and Southeast Asian aquaculture, and its GH (ypGH) provides a useful comparative model from a phylogenetically distant teleost lineage. Including both TiGH and ypGH allows for the evaluation of growth hormone function across diverse genetic backgrounds. Growth hormones across vertebrates, including fish, typically possess a conserved N-terminal secretory signal peptide, which directs the hormone into the secretory pathway for proper biological activity.

4.2.2 Plasmid assembly of fGHs-expressing cassette

The construction of the fish growth hormone (fGH)-expressing cassette was a crucial step in this study, aimed at producing growth hormones from yellow porgy (*Acanthopagrus latus*) and tilapia (*Oreochromis niloticus*) in the chloroplast of *Chlamydomonas reinhardtii*. To achieve this, various plasmid constructs were designed, incorporating both signal peptide-tagged and untagged versions of the growth hormones. Each construct was fused with a hemagglutinin (HA) tag to facilitate detection and quantification of the expressed proteins.

The specific plasmids constructed for this purpose were:

- pLY136: sp-YpGH-HA – This construct contains the signal peptide (SP) sequence fused to the yellow porgy growth hormone (YpGH) and an HA tag. The signal peptide (derived from the native yellow porgy fGH sequence) was included in this construct based on its native role in fish cells—where it mediates secretion of fGH to the extracellular space to exert systemic growth-promoting effects—though its function in the *C. reinhardtii* chloroplast was not pre-validated. At the time of construct design, the signal peptide was tentatively included to test whether it might enhance fGH solubility or stability within the chloroplast stroma (the primary site of chloroplast protein accumulation for non-targeted recombinant proteins), not to direct targeting to a specific sub-chloroplast compartment (e.g., thylakoid lumen). Notably, chloroplast expression of recombinant proteins like fGH often does not require exogenous signal peptides for basic accumulation, as the chloroplast stroma itself provides a compatible environment for folding and retention of many soluble proteins—raising the possibility that this signal peptide may not be strictly necessary for fGH expression in this system.
- pLY180: YpGH-HA – This construct includes the YpGH gene directly fused to an HA tag, without the signal peptide. This version is designed to express the growth hormone in its native form, with the HA tag facilitating its detection.
- pLY151: YpGH – This construct contains only the YpGH gene without any additional tags or signal peptides, providing a baseline for comparison with the tagged versions.
- pLY181: TiGH-HA – This plasmid includes the tilapia growth hormone (TiGH) gene fused to an HA tag, allowing for the detection and quantification of the expressed hormone.
- pLY166: TiGH – This construct contains the TiGH gene without any additional tags, serving as a control to evaluate the effects of the HA tag on expression and functionality.

Each of these constructs was cloned into the *C. reinhardtii* chloroplast genome using plasmids specifically designed for chloroplast transformation. These plasmids contain the coding sequences of the growth hormones, flanked by essential regulatory elements to ensure proper transcription and translation. The regulatory elements used include:

- *rrnS* promoter/*psaA* 5' UTR: This promoter and untranslated region (UTR) are derived from the chloroplast ribosomal RNA gene and *psaA* gene, providing strong and consistent expression of the downstream coding sequence.
- *rbcL* terminator/3'UTR: This terminator and UTR sequence from the chloroplast *rbcL* gene ensures proper termination of transcription and stability of the mRNA.

Additionally, the vectors include homologous regions to facilitate precise integration into the chloroplast genome through homologous recombination. This approach ensures stable and predictable expression of the transgenes, minimizing the risk of gene silencing and positional effects commonly encountered in nuclear transformations.

The inclusion of the HA tag allows for easy detection and quantification of the growth hormone proteins using standard immunological techniques. The use of both tagged and untagged constructs enables a comparison of the effects of the tag on protein expression and functionality. The secretory sequence was retained in one of the YpGH constructs despite the expectation that the sequence would be non-functional in the chloroplast as it might confer stability and activity to the fGH.

The plasmid constructs were validated through restriction digestion and sequencing. These validation steps ensured that the plasmids were correctly assembled and ready for transformation into *C. reinhardtii*.

Figure 4.2 illustrates the schematic design of the fGH-expressing cassettes. Each variant is depicted with its respective elements, including the signal peptide, HA tag, and regulatory sequences. The figure provides a visual representation of the constructs and highlights the strategic placement of each component to optimize expression and functionality within the chloroplast.

In summary, the successful construction and cloning of these plasmid constructs into the *C. reinhardtii* chloroplast genome lay the foundation for the subsequent production and evaluation of recombinant growth hormones. These constructs are expected to produce functional growth hormones, facilitating the enhancement of growth rates in aquatic species through the innovative use of transgenic microalgae.

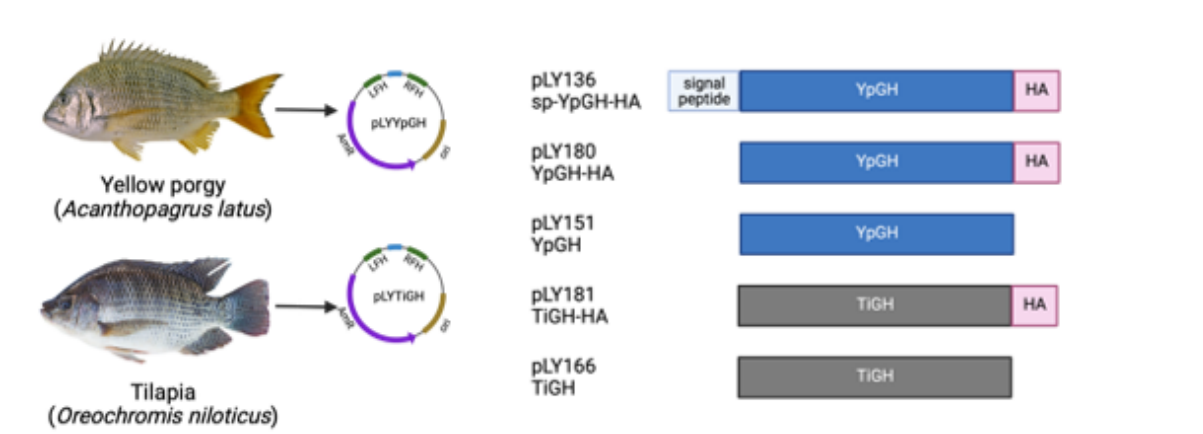


Figure 4.2 Design of fGH-expressing cassette and gene of interests (GOIs) variants used for production of transgenic *C. reinhardtii*.

4.2.3 Generation of stable, scar-less, and marker-free *C. reinhardtii* strainain

To generate stable, scar-less, and marker-free *Chlamydomonas reinhardtii* transformants expressing the fish growth hormone (fGH), a light-restoration strategy was employed. This method ensures the integration of the fGH-expressing cassette into the chloroplast genome without leaving any extraneous genetic markers or sequences.

The light-restoration strategy leverages the ability of certain *C. reinhardtii* strains, such as the HT72 recipient cells, to restore photosynthetic function when a functional gene is integrated into the chloroplast genome. The transformation process involves introducing the fGH-expressing cassette into the HT72 recipient cells via biolistic particle delivery. The homologous recombination machinery of the chloroplast integrates the cassette into the genome, restoring the photosynthetic function of the HT72 cells, which are otherwise photosynthetically deficient. Following transformation, PCR was performed to verify the integration of the gene of interest (GOI) and to ensure homoplasmy of the transformants.

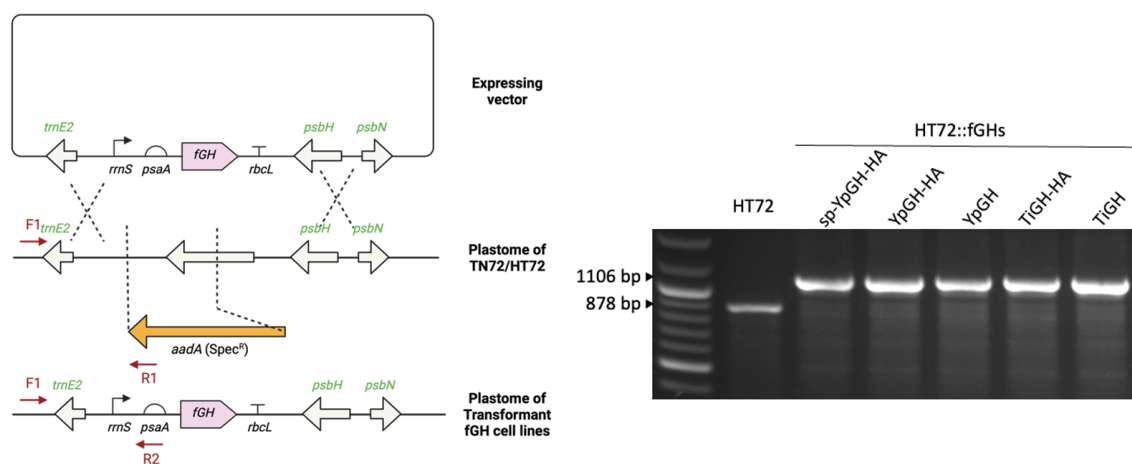


Figure 4.3 Light-restoration Strategy for generation of marker-less transformants using the HT72 recipient cells and PCR confirmation of GOI integration and homoplasmy of pLYfGH transformants.

The transforming plasmid contains the fGHs-expressing cassette which comprises a chloroplast endogenous *rrnS* promoter/promoter/5'UTR element from a chloroplast gene, coding sequence of the fGHs and a chloroplast endogenous *rbcL* terminator/3'UTR. The cassette is flanked by partial *psbH* gene.

Figure 4.4 illustrates the light-restoration strategy used for generating marker-less transformants in the HT72 recipient cells. The figure includes a schematic representation of the transformation process, showing the integration of the fGH-expressing cassette into the chloroplast genome and the subsequent PCR verification steps. The PCR results show successful amplification of the expected product sizes, indicating correct integration and homoplasmy of the transformants. These results confirm that the fGH-expressing cassette has been stably integrated into the chloroplast genome of *C. reinhardtii*.

4.2.4 Western blot analysis of (HA)-tagged fGHs

Western blot analysis was conducted to determine whether the introduced transgenes were being successfully transcribed and translated such that a steady-state level of the recombinant proteins could be detected using antibodies to the HA tag. Crude protein extracts were prepared from the transformants, and equal amounts were fractionated by SDS-PAGE. The proteins were then probed with commercial antibodies against HA to detect the tagged growth hormones. As shown in Figure 4.5, the Western blot results confirmed the expression of the HA-tagged growth hormones in three independent YpGH-HA transformant lines and six independent TiGH-HA transformant lines. Bands corresponding to the expected sizes of the tagged proteins

(22 kDa for YpGH-HA and 24 kDa for TiGH-HA) were detected in the transformed lines but not in the control lines.

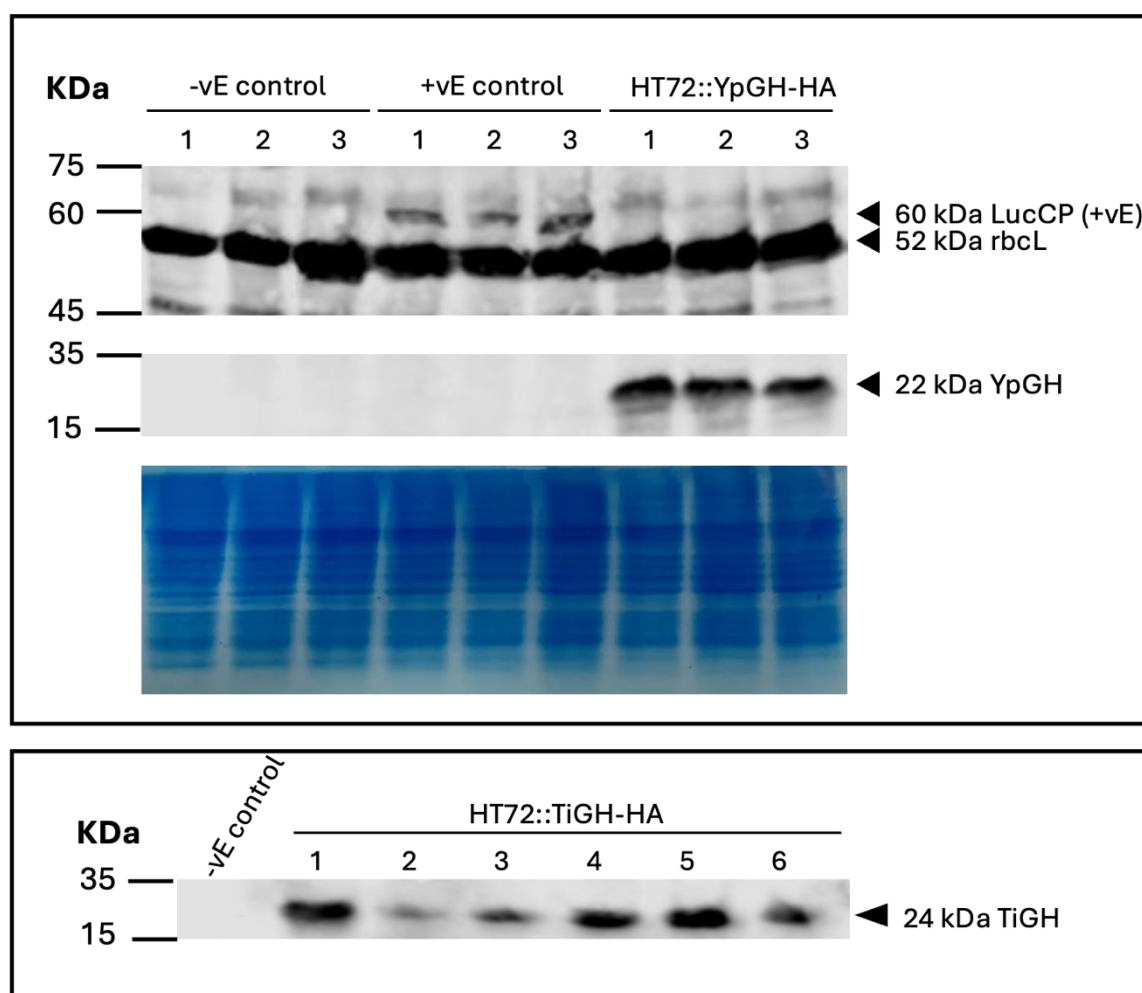


Figure 4.4 Western blot analysis of HA-tagged *C. reinhardtii* FGH transformants.

Crude protein extracts from transformants and control strains were normalized by culture optical density (OD_{750}) to ensure equal loading, fractionated by SDS-PAGE, transferred to a nitrocellulose membrane, and the upper panel was probed sequentially with two primary antibodies—anti-RbcL and anti-HA; the α -RbcL antibody detected a single ~52.5 kDa band in all lanes (controls and transformants), confirming equal protein loading via the constitutively expressed chloroplast protein RbcL; the α -HA antibody showed no reactive bands in the negative control (WT strain CC-1690, no fGH transgene) (confirming no non-specific binding), a single ~60 kDa band in the positive control (transformant expressing HA-tagged lucCP, validating antibody specificity and workflow), single ~22 kDa bands in each of the 3 independent HT72::YpGH-HA lines (matching the predicted size for yellow porgy GH + HA tag), and single ~24 kDa bands in each of the 6 independent HT72::TiGH-HA lines (matching the predicted size for tilapia GH + HA tag), with no non-specific HA-reactive bands detected, confirming specific expression of functional HA-tagged fGHs in the algal chloroplast.

The plasmid assembly and transformation strategy was successful and generated *C. reinhardtii* strains expressing fGHs from yellow porgy and tilapia. The constructs were designed to include regulatory elements for proper expression and an epitope tag for detection of the protein. These results demonstrate the feasibility of producing recombinant growth hormones in *C. reinhardtii*, which could be further explored for applications in aquaculture.

4.2.5 Growth performance of shrimp larvae fed transplastomic microalga *C. reinhardtii*

The growth performance of shrimp larvae fed with transplastomic microalgae was assessed through four dietary treatments: Normal Feed, Feed + WT (wild-type microalga), Feed + YpGH (yellow porgy growth hormone), and Feed + TiGH (tilapia growth hormone). Key performance metrics included weight gain, average daily gain (ADG), feed conversion ratio (FCR), and survival rate. Results showed that the Normal Feed and Feed + TiGH groups achieved the highest weight gain (approximately 0.4 g), while the Feed + WT group had the lowest (about 0.3 g), with the YpGH group showing intermediate results. A similar pattern was observed for ADG, where the Normal Feed and TiGH groups again showed superior daily growth rates (0.021 g/day and 0.02 g/day, respectively), significantly higher than the WT group (0.015 g/day). Although the FCR values did not differ significantly, the Normal Feed group exhibited the lowest FCR, suggesting the most efficient feed utilization, whereas the other groups, particularly those supplemented with microalgae, had higher FCR values, indicating less efficient conversion. Interestingly, the highest survival rate was observed in the WT group (around 70%), followed by Normal Feed (65%), YpGH (60%), and TiGH (50%), with statistical analysis confirming significant differences

across groups. These findings suggest that while transplastomic microalgae expressing growth hormones can enhance growth performance, they may have varying impacts on survival. The results also indicate that feed formulation plays a critical role, not only in promoting growth but also in maintaining shrimp health and viability.

Figure 4.5 presents the performance metrics for each group: weight gain over 30 days, daily growth rate, FCR, and survival percentage. Significant F-values and p-values for final individual weight gain (FIWG), weight gain (WG), and ADG confirm the influence of feed type on shrimp growth performance. Although FCR differences were not statistically significant ($p = 0.063$), the trend suggests potential differences in feed efficiency that may become clearer with more refined measurements or larger sample sizes. The significant variation in survival rates further highlights the impact of feed composition on overall larval health. Several factors could explain these outcomes. First, variability in shrimp sizes may have resulted from cannibalism, a common behavior in carnivorous species, potentially skewing data by allowing larger individuals to consume smaller ones. Second, the 5% inclusion rate of microalgae may have been too low to elicit a strong response, especially if the protein content of the algae was insufficient to support optimal growth. Future experiments should consider increasing the algae supplement concentration, implementing measures to reduce cannibalism (such as size grading or habitat structuring), and performing detailed analyses of the algae's protein content. These adjustments could enhance feed effectiveness and provide more reliable assessments of the impact of transplastomic microalgae on shrimp growth and survival.

The growth performance of shrimp larvae fed with the transplastomic microalgae was assessed through four dietary treatments (each with four biological replicates, $n=4$ tanks per treatment) : Normal Feed, Feed + WT (wild-type microalga), Feed + YpGH (yellow porgy growth hormone), and Feed + TiGH (tilapia growth hormone). Key performance metrics—including weight gain, average daily gain (ADG), feed conversion ratio (FCR), and survival rate—were quantified with standard deviation (SD) to reflect within-group data variability, and standard error of the mean (SEM) was used in Figure 4.5 to visualize the precision of mean estimates ($SEM = SD/\sqrt{n}$, where $n=4$).

- Weight gain: The Normal Feed group achieved the highest weight gain at 0.40 ± 0.04 g (mean \pm SD), followed by the TiGH group at 0.39 ± 0.05 g, the YpGH group at 0.35 ± 0.03 g, and the WT group at 0.30 ± 0.04 g. SEM values for these groups were 0.02 g, 0.025 g, 0.015 g, and 0.02 g, respectively—indicating the mean weight gain for each group is likely within ± 2 –2.5 g of the true population mean.
- Average Daily Gain (ADG): The Normal Feed group had the highest ADG at 0.021 ± 0.002 g/day (mean \pm SD), the TiGH group at 0.020 ± 0.003 g/day, the YpGH group at 0.018 ± 0.002 g/day, and the WT group at 0.015 ± 0.002 g/day. Corresponding SEM values were 0.001 g/day, 0.0015 g/day, 0.001 g/day, and 0.001 g/day, reflecting low variability in daily growth rates across replicates.
- Feed Conversion Ratio (FCR): FCR values did not differ significantly (one-way ANOVA, $p=0.063$), with the Normal Feed group showing the lowest FCR at 1.05

± 0.10 (mean \pm SD), the TiGH group at 1.12 ± 0.12 , the YpGH group at 1.15 ± 0.11 , and the WT group at 1.20 ± 0.13 . SEM values ranged from 0.05–0.065, confirming consistent FCR variability across treatments.

- Survival rate: The WT group had the highest survival rate at $70 \pm 5\%$ (mean \pm SD), followed by the Normal Feed group at $65 \pm 4\%$, the YpGH group at $60 \pm 6\%$, and the TiGH group at $50 \pm 7\%$. SEM values were 2.5%, 2%, 3%, and 3.5%, respectively—with the TiGH group showing the highest SEM (and thus lower precision in the mean estimate) due to greater replicate-to-replicate variability in survival.

These statistical measures (SD and SEM) highlight that while transplastomic microalgae-supplemented diets (YpGH, TiGH) did not significantly outperform the Normal Feed group in weight gain or ADG, the WT group consistently showed lower growth metrics with moderate variability. The higher SEM in the TiGH group's survival rate also suggests that future trials with larger sample sizes ($n > 4$) may be needed to confirm its impact on shrimp viability.

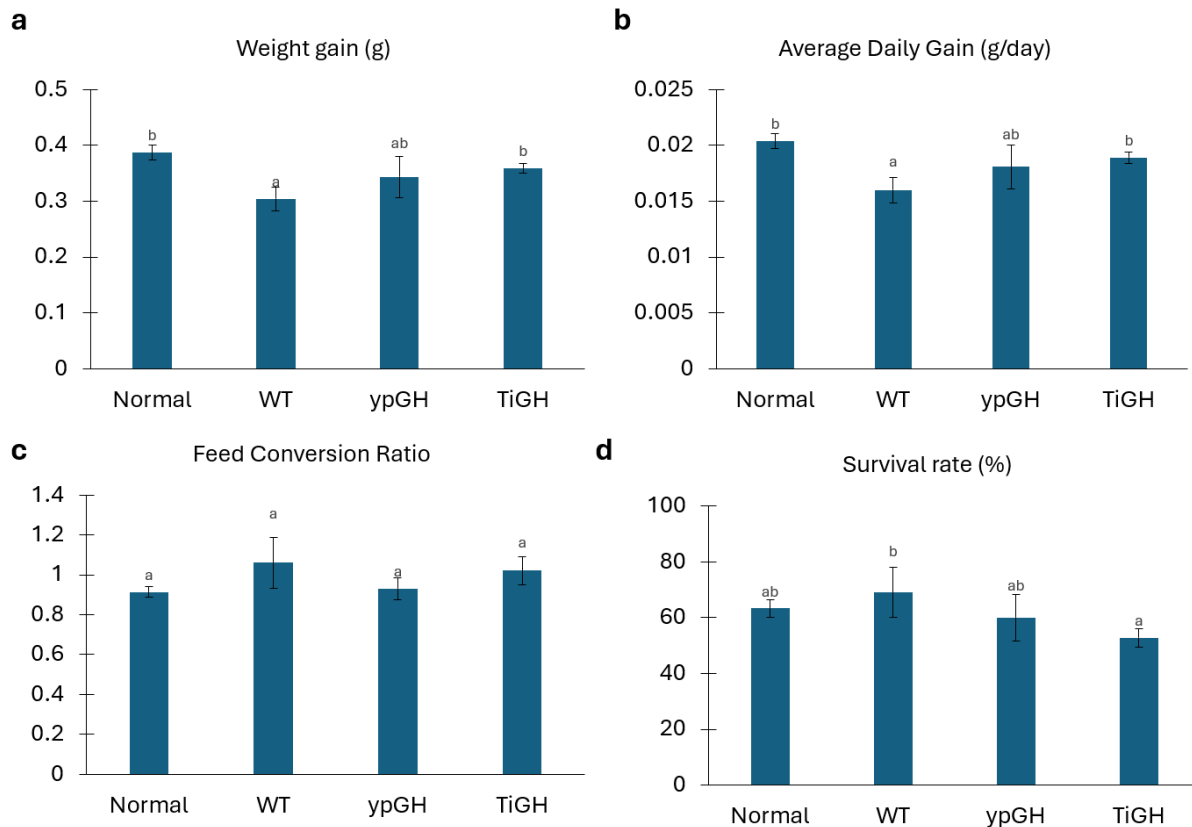


Figure 4.5 Growth performance of shrimp larva fed transplastomic microalga *C. reinhardtii*.

Four different treatment groups were analyzed: Normal Feed, Feed + WT (wild type microalga), Feed + YpGH (yellow porgy growth hormone), and Feed + TiGH (tilapia growth hormone). The performance metrics evaluated include: (a) Represents the average weight gain in grams for shrimp larvae in each treatment group. (b) Shows the average daily gain in grams per day for each treatment group. (c) Depicts the feed conversion ratio for each treatment group. FCR is a measure of the efficiency of the feed in promoting weight gain. (d) Illustrates the survival rate percentage of shrimp larvae in each treatment group. The figure includes four panels (a–d) with error bars representing SEM (to visualize mean estimate precision) and corresponding SD values reported below to quantify within-group data spread ($n=4$): Panel (a): Weight gain (g) – Mean \pm SD: Normal Feed (0.40 ± 0.04 g), TiGH (0.39 ± 0.05 g), YpGH (0.35 ± 0.03 g), WT (0.30 ± 0.04 g); SEM = $SD/\sqrt{4}$. One-way ANOVA: $F=8.72$, $p<0.01$ (significant differences between WT and Normal Feed/TiGH groups). Panel (b): Average Daily Gain (ADG, g/day) – Mean \pm SD: Normal Feed (0.021 ± 0.002 g/day), TiGH (0.020 ± 0.003 g/day), YpGH (0.018 ± 0.002 g/day), WT (0.015 ± 0.002 g/day); SEM = $SD/\sqrt{4}$. One-way ANOVA: $F=9.15$, $p<0.01$ (significant differences between WT and Normal Feed/TiGH groups). Panel (c): Feed Conversion Ratio (FCR) – Mean \pm SD: Normal Feed (1.05 ± 0.10), TiGH (1.12 ± 0.12), YpGH (1.15 ± 0.11), WT (1.20 ± 0.13); SEM = $SD/\sqrt{4}$. One-way ANOVA: $F=2.89$, $p=0.063$ (no significant differences). Panel (d): Survival rate (%) – Mean \pm SD: WT ($70 \pm 5\%$), Normal Feed ($65 \pm 4\%$), YpGH ($60 \pm 6\%$), TiGH ($50 \pm 7\%$); SEM = $SD/\sqrt{4}$. One-way ANOVA: $F=10.36$, $p<0.001$ (significant differences between TiGH and WT/Normal Feed groups). SEM error bars highlight the precision of mean growth/survival estimates (narrower bars = higher precision), while SD values quantify the actual variability in replicate tanks. The WT group showed significantly lower weight gain and ADG ($p<0.01$) and higher FCR than the Normal Feed and TiGH groups, while the TiGH group had significantly lower survival ($p<0.001$) than the WT and Normal Feed groups—suggesting fGH-expressing microalgae do not enhance growth beyond commercial feed but may impact shrimp viability.

4.3 Discussion

The oral delivery of recombinant fish growth hormones (fGH) encapsulated in the dried cells of an edible alga could have a significant impact within the aquaculture industry if growth of the animals was improved but without any impact on animal health or viability. The work in this chapter has demonstrated the successful synthesis of two fGH in the algal chloroplast, and initial feeding trials carried out to evaluate whether oral delivery to shrimp might promote growth.

While the results of this study are promising, several limitations and challenges need to be addressed in future research. Firstly, it is not known whether the fGH chosen for this study are actually functional in the shrimp species with suitable receptors able to transduce the hormone signal into cell growth. Several published studies have indicated that fGH is active in shrimp (Arenal et al., 2008; Laksana et al., 2013; Martínez et al., 2017; Santiesteban et al., 2010) but whether the specific combination of fGH (ypFH or TiGH) and whiteleg shrimp (*Litopenaeus vannamei*) results in activity is unknown. Secondly, it is not known whether a sufficient dose of fGH is taken up from the shrimp gut into the haemolymph following oral delivery. Previously, a subunit vaccine and a specific double-stranded RNA produced in the *C. reinhardtii* chloroplast have been shown to confer protection against White Spot Syndrome Virus when fed to shrimp, but in both these cases a cell-wall deficient strain of *C. reinhardtii* was used (Gimpel & Mayfield, 2013; Specht & Mayfield, 2013). Whether the walled strain using in the FGH study results in enhanced encapsulation such that the dried algal is not broken down in the shrimp gut is a question that should be addressed by studying shrimp tissue and faeces: for example, using a chloroplast transformant expressing a GFP reporter protein (van Wijk, 2024). The digestibility and bioavailability of algal-derived

fGHs are crucial factors for their effectiveness in aquaculture. As discussed earlier, algae can serve as an effective vehicle for delivering nutrients and bioactive compounds to shrimp, enhancing growth and immunity (Ahmad et al., 2022; Fajardo et al., 2020; Han et al., 2019). However, thorough investigations are needed to determine the digestibility and bioavailability of each recombinant product (Annamalai et al., 2021; A. Bélanger et al., 2021). Ensuring that the shrimp can efficiently utilize these products without adverse effects will be essential for the practical application of this technology.

Thirdly, the yield of fGH is low compared to more established cell platforms such as *E. coli* or *S. cerevisiae* and is likely to be below 1% of total soluble protein (TSP) given that the protein is not seen as a visible band on stained SDS gels and requires western blotting for detection (Stoffels et al., 2017). Improvements in the design of *cis* and *trans* regulatory elements for transgenes in the chloroplast are therefore needed to improve promoter strength, mRNA stability, translational efficiency, etc. (Gimpel & Mayfield, 2013; E. A. Specht & Mayfield, 2013), as well as modulation of specific chloroplast proteases to improve protein accumulation (van Wijk, 2024). Fourthly, improving productivity particularly when scaling production. While the current system has demonstrated feasibility at a laboratory scale, scaling up the production to commercial levels will require significant improvements in bioreactor design, nutrient supply, and harvesting techniques (Borowitzka & Vonshak, 2017).

Expanding the production of fGHs to other microalgal species could provide additional benefits and address some of the limitations of using *C. reinhardtii*. Microalgae such as *Nannochloropsis species*, *Phaeodactylum tricornutum*, and *Dunaliella salina* are being explored for recombinant protein production due to their robust growth and ease

of genetic manipulation (E. Specht et al., 2010). Each strain offers unique advantages, such as higher growth rates, different metabolic profiles, and varying abilities to accumulate or secrete proteins, which could be leveraged to optimize fGH production.

In shrimp aquaculture, several microalgal genera are commonly cultured for use as juvenile feed, including *Chaetoceros*, *Skeletonema*, *Thalassiosira*, and *Tetraselmis*. These algae provide essential nutrients and improve water quality by absorbing excess nutrients and producing oxygen (Catarina Guedes, 2012). Integrating genetically engineered strains of these species that express fGHs could potentially enhance the growth rates and health of shrimp, offering a dual benefit of nutrition and hormonal supplementation.

Thalassiosira, a widely used diatom in aquaculture, is a promising candidate for genetic engineering to produce fGHs. Its large cell size and high lipid content make it an excellent vehicle for recombinant protein expression (Kroth et al., 2018). Recent advances in CRISPR/Cas9 and other gene-editing technologies have made it feasible to engineer the nuclear genome of diatoms for specific traits, including the production of therapeutic proteins and growth hormones (Hopes et al., 2016). Engineering *Thalassiosira* to produce fGHs could significantly impact shrimp farming by enhancing growth rates and overall farm productivity.

The production of recombinant fGHs in microalgae, particularly in the chloroplast of *C. reinhardtii*, represents a significant breakthrough in aquaculture biotechnology. This approach offers a sustainable and potentially cost-effective method for enhancing the growth and productivity of farmed shrimp and other aquatic species. The results

presented in this chapter demonstrate the feasibility of this technology and highlight its potential benefits.

In summary, the use of genetically engineered microalgae for oral delivery of growth hormones and other therapeutics is feasible and worthy of further research. However, several challenges and limitations must be addressed to fully realize the potential of this technology. Ensuring the safety and digestibility of algal-derived therapeutics, optimizing production yields, and scaling up the cultivation and harvesting processes are critical areas for future research. Additionally, expanding the production to other microalgal species and integrating genetically engineered microalgae into existing aquaculture systems will be essential for the widespread adoption of this technology.

Chapter 5

Production of recombinant spider silk protein in the chloroplast of *C. reinhardtii*

5 Production of recombinant spider silk protein in the chloroplast of *C. reinhardtii*

5.1 Introduction

The protein that is found in spider silk (termed spider fibroin or 'spidroin'), represents one of nature's most extraordinary materials. This unique fibrous protein is renowned for its exceptional mechanical properties, including unparalleled tensile strength, elasticity, and toughness (Table 5.1). The exceptional mechanical properties of spider silk spidroins stem from their long length and specific protein structure (Ramezaniaghdam et al., 2022).

Table 5.1 Comparative analysis of mechanical properties of spider silk, metals, alloys, and fibre materials.

Material	Tensile Strength (MPa)	Elasticity (Strain at Break %)	Young's Modulus (GPa)	Toughness (MJ/m ³)	Density (g/cm ³)	References
Spider silk	1000-1500	30-40	10-12	150-160	1.3-1.4	(Shao & Vollrath, 2002; Vollrath & Knight, 2003)
High-carbon Steel	1000-2000	1-2	200-210	6-12	7.8	(William D. Callister & David G. Rethwisch, 2018)
Aluminium Alloy	400-550	10-20	69-79	10-25	2.7	(William D. Callister & David G. Rethwisch, 2018)
Titanium Alloy	900-1200	10-15	110-120	20-25	4.5	(William D. Callister & David G. Rethwisch, 2018)
Kevlar	3000-3750	2.5-4	70-125	50-60	1.44	(William D. Callister & David G. Rethwisch, 2018)
Nylon	75-100	15-30	2-4	50-70	1.15-1.35	(William D. Callister & David G. Rethwisch, 2018)

Tensile Strength (MPa): The maximum stress that a material can withstand while being stretched or pulled before breaking. Measured in megapascals (MPa). **Elasticity (Strain at Break %):** The extent to which a material can be stretched relative to its original length before

breaking. Expressed as a percentage (Callister, 2014). Young's Modulus (GPa): A measure of the stiffness of a material. It quantifies the ratio of stress (force per unit area) to strain (proportional deformation) in a material. Higher values indicate a stiffer material. Measured in gigapascals (GPa) (Callister, 2014). Toughness (MJ/m³): The ability of a material to absorb energy and plastically deform without fracturing. It's a measure of the amount of energy a material can absorb before rupturing, often considered a combination of strength and ductility. Measured in megajoules per cubic meter (MJ/m³) (Callister, 2014). Density (g/cm³): The mass per unit volume of a material, indicating how compact the material's molecules are. Measured in grams per cubic centimeter (g/cm³) (Callister, 2015).

Seven types of silk are produced by spiders, each serving a distinct purpose in the construction of their webs (Figure 5.1). Among them, dragline silk functions as the primary structural element and safety line for the spider. Dragline silk stands out due to its exceptional tensile strength, toughness, and elasticity, making it far superior to other silks like flagelliform or tubuliform silk, which are specialized for capture spirals and egg sacs, respectively. This unique combination of properties makes dragline silk the best candidate for biomaterial applications, surpassing the mechanical performance of the other six types (Gosline et al., 1999; Vollrath & Porter, 2006). This silk is renowned for its exceptional tensile strength and resilience and attracts the most attention from scientists (Hayashi et al., 1999; Sponner et al., 2005).

Spider silk, including dragline silk, is synthesised within specialized silk glands located in the spider's abdomen (Figure 5.1). The silk is initially produced as a liquid protein solution and then extruded through spinnerets, where it solidifies into strong, flexible fibres as it exits the spider's body (Hayashi et al., 1999; Vollrath & Knight, 2001). Dragline silk, produced by the major ampullate gland (Figure 5.1), owes its structural superiority to the specific arrangement and composition of protein molecules, which are aligned in a highly ordered crystalline structure, giving the silk its unmatched

strength and toughness (Gosline et al., 1999; Tokareva et al., 2014; Vollrath & Porter, 2006).

This structural complexity is further attributed to the specific proteins that make up spider silk. Among the different types of spider silk proteins, major ampullate spidroin (MaSp) and minor ampullate spidroin (MiSp) have garnered particular attention, as they play a crucial role in determining the mechanical properties of the silk. The major ampullate spidroin (MaSp) in dragline is especially noted for its superior mechanical properties (Table 5.2), which are critical for applications such as in biomedical issues, requiring high strength and durability (Bakhshandeh et al., 2021; Tokareva et al., 2014).

Figure 5.1 Schematic representation of different types of spider silk and their role in spider webs, including an example of the seven types of native silk glands and threads from the spider *Araneus diadematus*: major ampullate silk (blue). Adapted from Zheng & Ling, 2018 and Ramezaniaghdam et al., 2022.

Table 5.2 Comparative analysis of different spider silk proteins in spider draglin. Adapted from Ramezaniaghdam et al., 2022.

Protein	Spider Species	Molecular Mass (KDa)	Number of Amino Acids	Primary Motifs	Tensile Strength (MPa)	Elasticity (Strain at Break %)	Toughness (MJ/m ³)	Young's Modulus (GPa)	References
Major Ampullate Spidroin 1 (MaSp1)	<i>Nephila clavipes</i>	>250	3500-3700	-GGX (X = A, Q, or Y) -GX (X = Q, A or R) -poly-A	875-1094	27-35	150-180.9	9-12.5	(Liu et al., 2008; Vollrath & Knight, 2001; Brooks et al., 2005)
Short Major Ampullate Spidroin 1 (MaSp1s)	<i>Cyrtophora moluccensis</i>	40	439	-GGX (X = A, Q, or Y) -GX (X = Q, A or R) -poly-A	-	-	-	-	(Han et al., 2013)
Major Ampullate Spidroin 2 (MaSp2)	<i>Latrodectus hesperus</i>	>250	3780	-GPX (X = G or S) -QQ -GGX (X = Q, A or R) -GSX (X is usually A) -poly-A	300-800	30-70	100-150	1.5-5.5	(Ayoub et al., 2007; Vollrath & Knight, 2001; Trancik et al., 2006)

Spidroin sequences contain repetitive units of residues capped between non-repetitive N-terminal (NTD) and C-terminal (CTD) domains, whose composition varies among species and thus determines the variety of mechanical properties of spider silks. The CTDs are conserved among spider silk proteins (Gatesy et al., 2001; Hinman & Lewis, 1992; Kovoov, 1987; Rising et al., 2011). The structure of MaSp proteins, including MaSp1 and MaSp2, is characterized by highly repetitive sequences that play a crucial role in the remarkable mechanical properties of spider silk (Table 5.3).

Figure 5.2 The schematic structure of MaSp protein sequences and their structure. Adapted from Van Beek et al., 2002; Gray et al. 2016; Yarger et al., 2018; Ramezaniaghdam et al., 2022

These repetitive regions consist primarily of short motifs such as GGX (where X can be the amino acids alanine (A), glutamine (Q), or tyrosine (Y)), GX (where X is typically glutamine (Q), alanine (A), or arginine (R)), and poly-A (polyalanine) sequences. The GGX and GX motifs contribute to the formation of amorphous regions, providing elasticity and flexibility to the silk, while the poly-A sequences are responsible for

creating β -sheet crystalline structures that impart tensile strength and rigidity (Hayashi et al., 1999; Savage & Gosline, 2008). These repetitive sequences are interspersed with non-repetitive regions that facilitate the solubility and proper folding of the proteins, which is essential during the silk spinning process. The high degree of repetition in these motifs is a key factor in the silk's ability to combine both strength and extensibility, making MaSp proteins some of the most intriguing and studied biopolymers in the field of material science (Vollrath & Knight, 2001).

The potential of spider silk as a biomaterial is further enhanced by its biodegradability and biocompatibility, which align well with the growing emphasis on sustainable and eco-friendly materials. These attributes make it a prime candidate for diverse applications, ranging from biomedical devices to high-performance textiles and composites (Agnarsson et al., 2010; Bini et al., 2004). However, the commercial production of spider silk faces significant hurdles, primarily due to the major difficulties associated with trying to farm spiders, which are territorial and cannibalistic, thus making large-scale silk production unfeasible (Lewis, 2006).

To address these challenges, researchers have turned to genetic engineering to produce recombinant spider silk proteins. This innovative approach involves inserting spider silk genes into alternative host organisms, enabling the scalable production of silk proteins without the need for spider farming. Various expression systems, including bacteria, yeast, plants, and mammalian cells have been explored for this purpose, each offering distinct advantages and challenges (Conrad et al., 2001; Ramezaniaghdam et al., 2022).

To-date, there has been no studies into the recombinant production of spidroin proteins in either plant or algal chloroplasts. As with other recombinant platforms, the production of these proteins in the chloroplast poses significant challenges, particularly due to the unique structural features of spidroins. One major challenge is the genetic assembly of the repetitive regions of the spidroin genes, which are crucial for their mechanical properties. Additionally, the large size of these proteins can constrain the cellular machinery, particularly the tRNA pool, which may be insufficient to efficiently translate the repetitive sequences, especially those repeats requiring high pools of amino-acylated tRNA-Gly and/or tRNA-Ala. This issue has been highlighted in previous studies, in *E. coli*, where similar challenges were encountered (Xia et al., 2010). Addressing these limitations is critical for the successful expression of functional spider silk proteins in *C. reinhardtii*.

This project focuses on the production of MaSp1 using the chloroplast of *Chlamydomonas reinhardtii* as a novel expression system.

- Aim: To express silk proteins with varying numbers of repeats in the chloroplast of *C. reinhardtii*.
 - Objective 1: Develop and implement a novel, 'scar-less' strategy for assembling the repetitive region of the MaSp1 gene.
 - Objective 2: Express and analyse the recombinant MaSp1 protein within the *C. reinhardtii* chloroplast, and further investigate the possibility of incorporating an additional copy of the *trnG* gene into the expression cassette to enrich the tRNA-Gly pool, thereby enhancing protein yield.

- Objective 3: Explore potential methods for downstream upscaling and purification, assessing feasibility for industrial production.

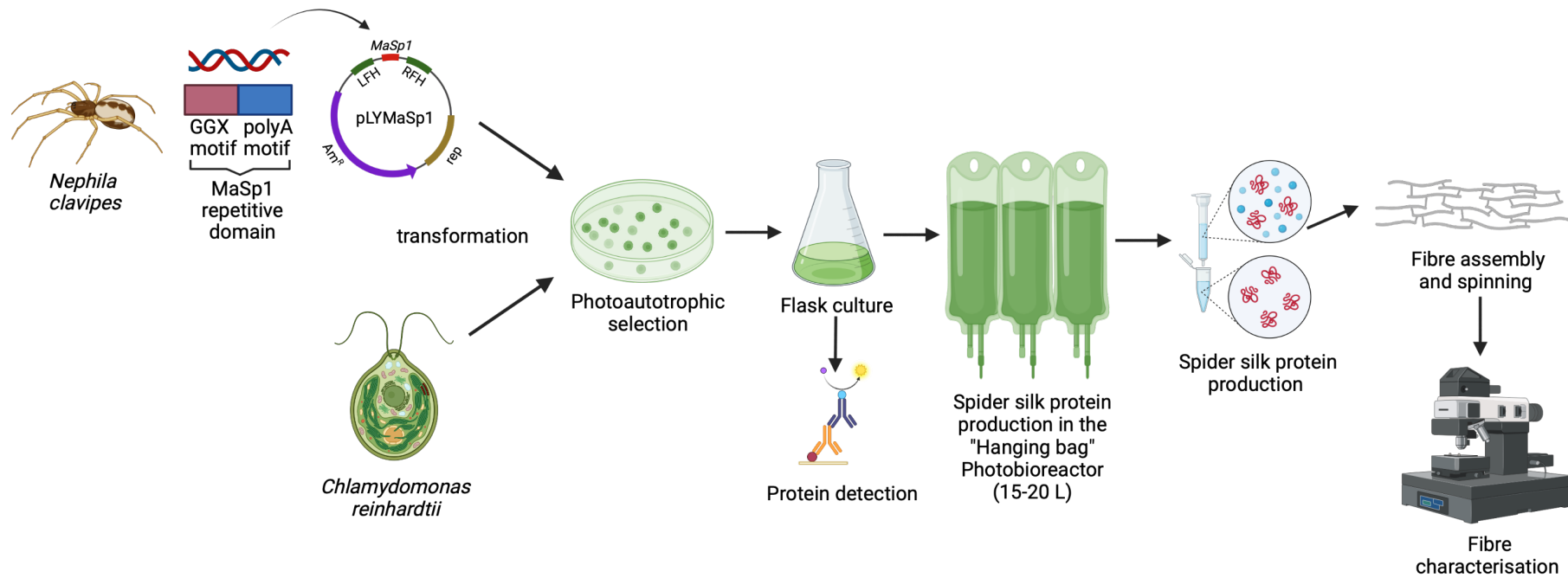


Figure 5.3 Schematic overview of spider silk protein production in *C. reinhardtii*

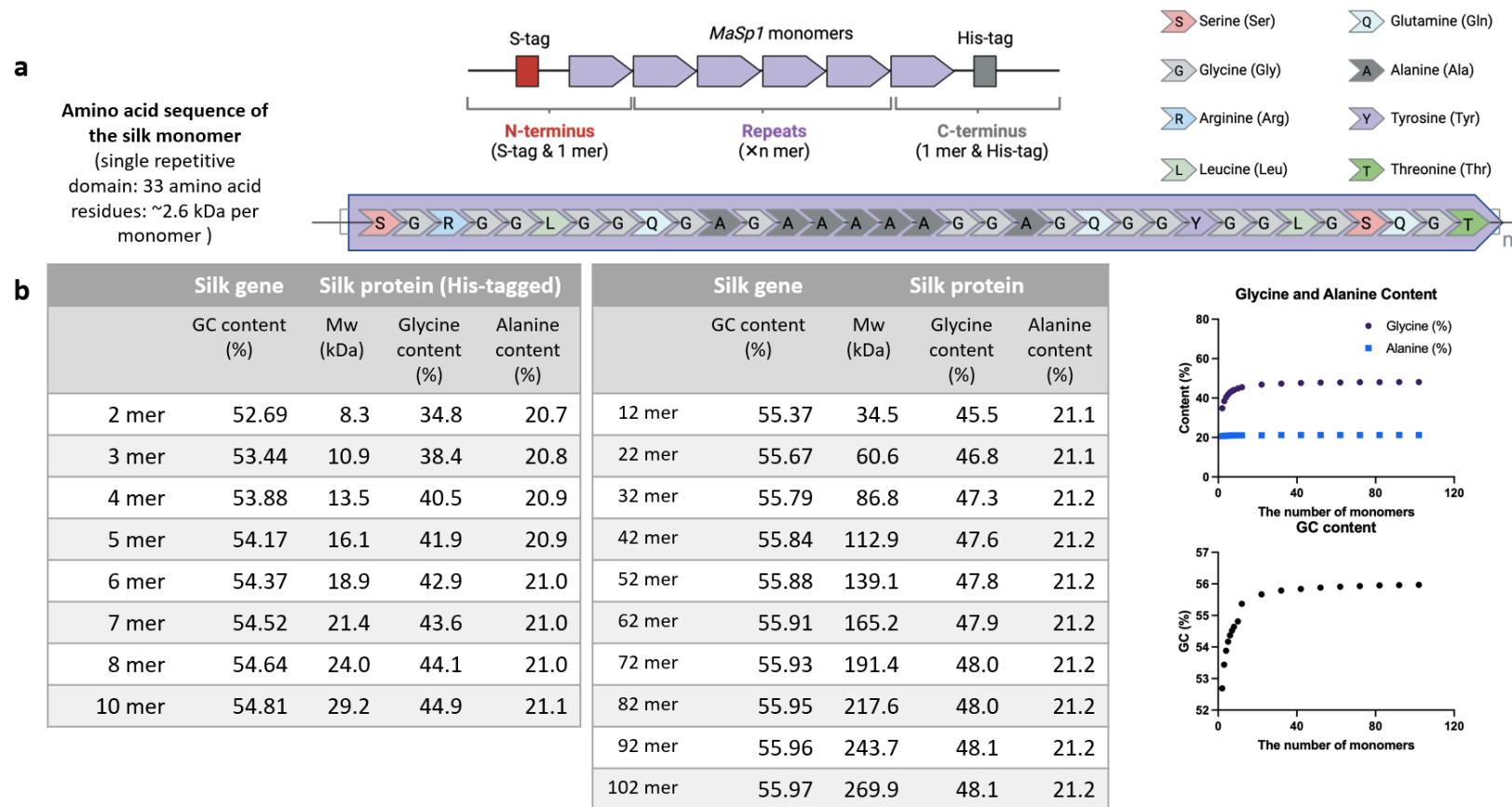


Figure 5.4 Recombinant expression of Spider silk protein (MaSp1) in *C. reinhardtii*.

(a) Recombinant Spider silk protein (MaSp1) expression constructs (Upper) and amino acid sequence of the silk monomer (Lower; single repetitive domain: 33 amino acid residues: ~2.6 kDa per monomer). (b) The GC content of the MaSp1 genes and molecular weight (Mw) along with glycine content of encoded silk proteins.(sequence reference: Foong et al., 2020; data was calculated on benchling

5.2 Results

5.2.1 Construction and assembly strategy of MaSp1-expressing *C. reinhardtii*

To investigate the possibility of recombinant synthesis, the MaSp1 protein from the spider species *Nephila clavipes* was chosen as a model due to its exceptional mechanical properties and its prominence in spider silk research. MaSp1, whose partial cDNA has been sequenced (Foong et al., 2020), is the major protein component of the spider dragline silk. To express recombinant silk proteins of different lengths, several gene constructs were built that each encode different numbers of the iterated peptide motif of MaSp1 (Fig. 5.5). The single repetitive domain in the constructs consists of a 33 residue sequence as follows:

SGRGGLGGQGAGAAAAAGGAGQGGYGGGLGSQGT

The theoretical molecular weights for the target proteins, including a 6xHis-Tag of HHHHHH at the N-terminus and a Strep-Tag of WSHPQFEK at the N-terminus, are 10.5 kDa for the 2-mer (114 aa), 13.1 kDa for the 3-mer (147 aa), and up to 20.9 kDa for the 6-mer (246 aa) (Appendix 7).

As shown in Figure 5.6, the gene of interest (GOI) for MaSp1 is divided into three distinct Level 0 (Lv0) parts that encode the N-terminus, the repetitive unit, and the C-terminus. This modular structure allows each segment to be independently assembled using Golden Gate assembly, with repetitive units linked through identical fusion sites (ACT) at Level 1 (Lv1). In the Lv1 construct, the MaSp1 coding sequence was flanked by a synthetic promoter *rrnS* and *psaA* 5' untranslated region (5'UTR) upstream and a *rbcL* terminator with 3'UTR downstream. The N- and C-termini provide structural

boundaries, while the central repetitive unit can be multimerized to reach the desired length, enabling functional expression of the synthetic MaSp1 construct in *C. reinhardtii*. The number of repetitive units (*i.e.* two to six repeats) was validated by PCR analysis of *E. coli* transformant lines, and selected plasmids were sequenced using Nanopore sequencing to confirm assembly accuracy. Figure 5.6 illustrates the final construction of MaSp1 plasmids designed for the CpPos-Neg selection strategy in which chloroplast transformants are selected on spectinomycin and then the *codA-aadA* dual marker is removed through intramolecular recombination using counter-selection on 5-fluorocytosine. Expression of the MaSp1 genes is achieved by fusion to the endogenous elements: *rrnS* promoter, *psaA* 5' UTR, and *rbcL* terminator/3' UTR.

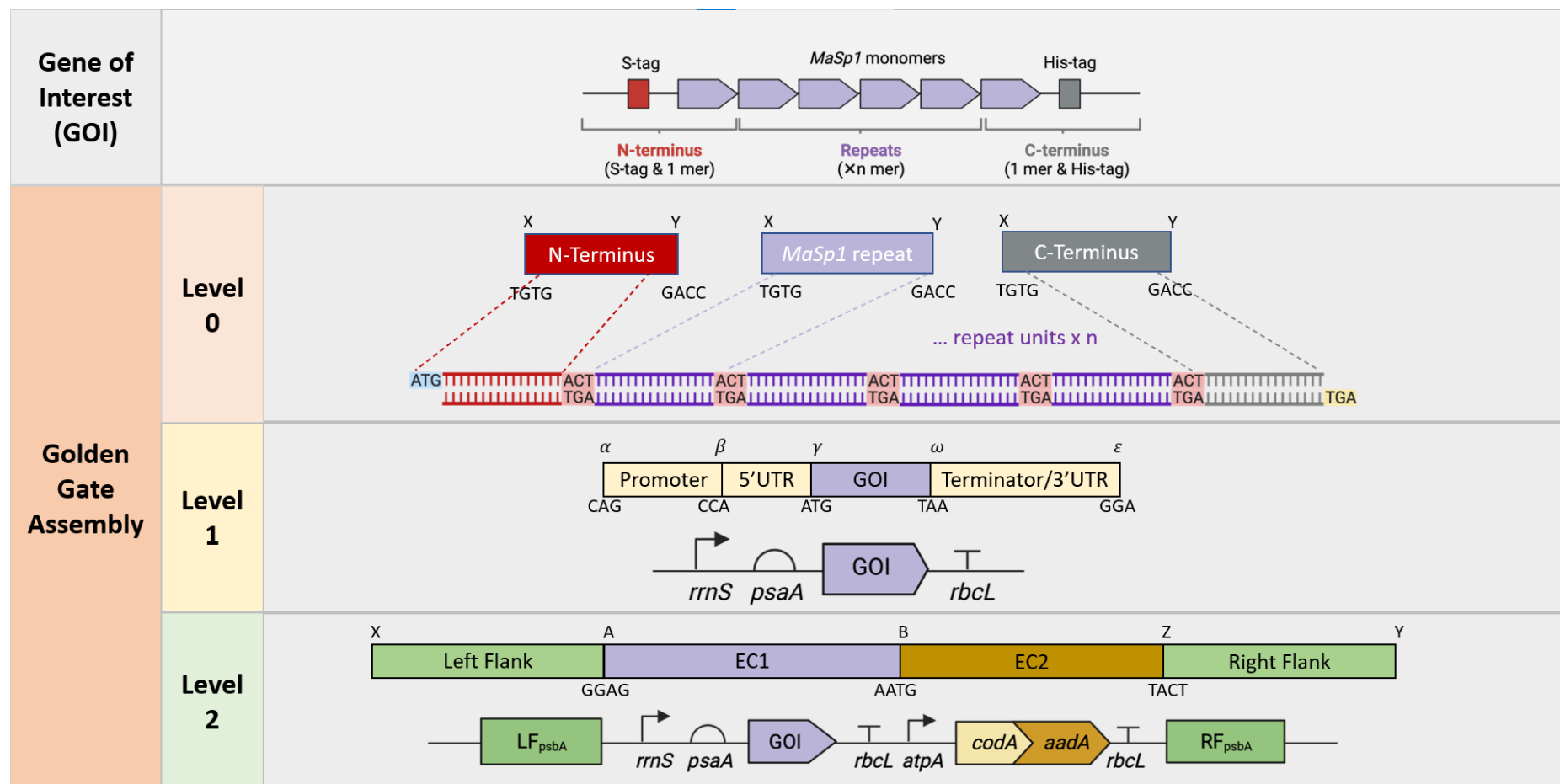


Figure 5.5 Assembly strategy of the vectors with various MaSp1 repetitive domain from *Nephila clavipes* was developed to express spider silk protein.

5.2.2 Construction of MaSp1-expressing *C. reinhardtii*

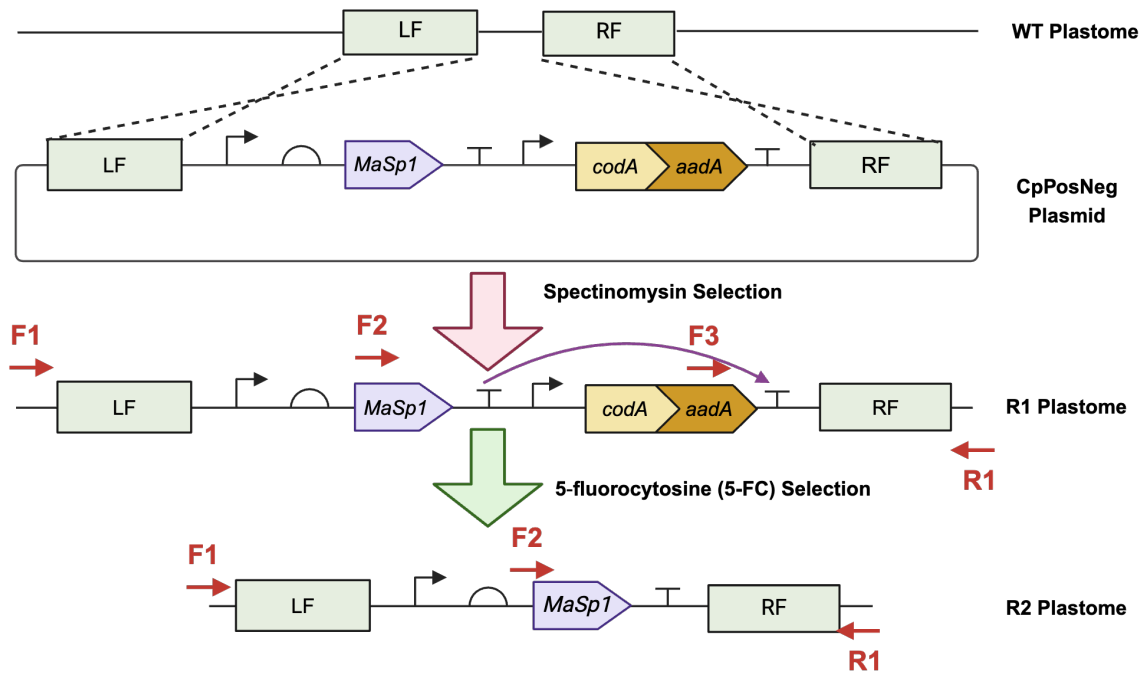


Figure 5.6 PCR confirmation of GOI integration and homoplasmy of MaSp1 transformants.

This figure illustrates the insertion process of the MaSp1 gene into the chloroplast genome via the CpPosNeg strategy, which combines positive (*aadA*) and negative (*codA*) selection. The construct includes left (LF) and right (RF) flanking regions derived from the *psbA-rn5* locus for targeted integration downstream of *psbA* via homologous recombination. Primers F1, F2, F3, and R1 are designed to validate successful integration and determine homoplasmy through PCR analysis. The middle panel outlines the recombination steps leading to MaSp1 insertion, while the lower panel depicts the expected configurations after proper integration and marker excision.

Each construct was used to transform the chloroplast genome of the wild-type strain CC-1690. Transformant lines restreaked under spectinomycin selection were validated by PCR validation using specific primers (F1, F2, F3, R1) to confirm successful integration, correct gene orientation and homoplasmy. A representative

PCR analysis using one selected line for each of the constructs is shown in Figure 5.X. The absence of the 2455 bp WT band from each line and the presence of a band of ~2000 bp confirms that all lines are true R1 transformants and that they have reached homoplasmy.

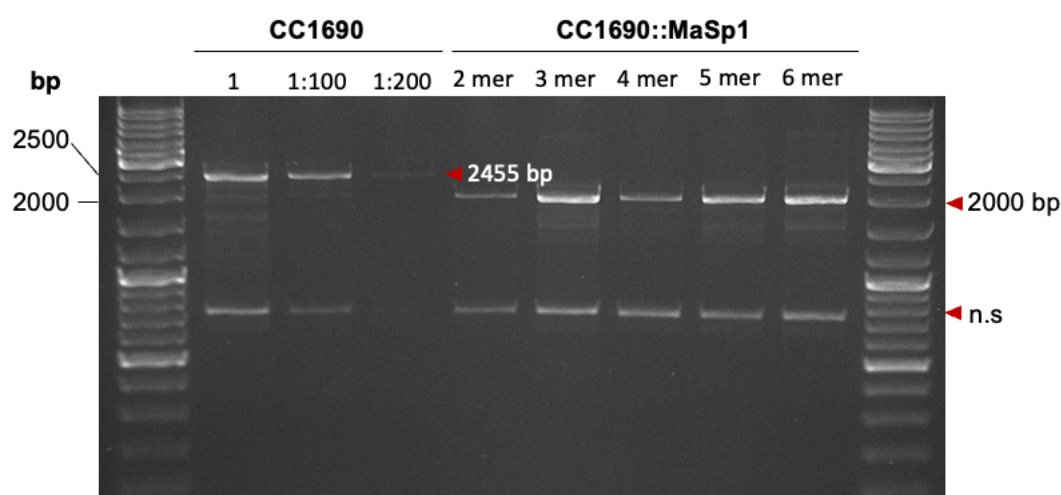


Figure 5.7 PCR confirmation of R1 homoplasmy for CC1690::MaSp1 transformant lines.

Agarose gel image showing PCR results that confirm the insertion of the *MaSp1* transgene in the putative CC1690::MaSp1 transformant lines. Bands corresponding to the expected ~2000 bp for *MaSp1* multimers (2–6 mer) validate successful integration. A nonspecific band (n.s) and the 2455 bp non-transformed (WT) band are also indicated.

To test whether the *MaSp1* transgenes yield detectable levels of their protein product a western blot analysis was carried out using antibodies to the Strep-tag. As shown in Figure 5.9, the analysis confirms the expression of the different *MaSp1* multimers in the *C. reinhardtii* chloroplast, with each construct yielding a band at the expected molecular weight based on the multimer length. Interestingly, there is an apparent correlation between number of repeats and abundance of the protein. The reason for this is not clear and might simply be a technical issue relating to poor transfer efficiency of smaller proteins onto the membrane. However, if it represents a biological effect

then it is likely that this is due to increased copies of the repeat element enhance folding and stability, rather than promoting increased translation. Nevertheless, the results demonstrate that recombinant proteins such as these spidroin proxy proteins that contain highly repetitive motifs can be produced successfully in the algal chloroplast.

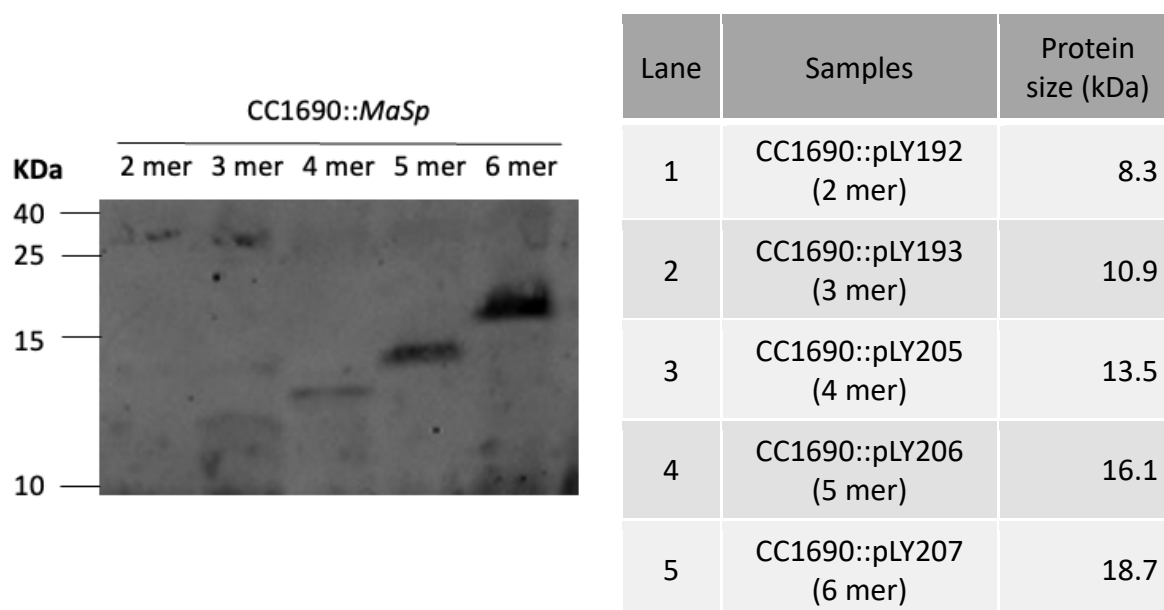


Figure 5.8 Western blot analysis of recombinant MaSp1 multimers (2–6 mer) expressed in the chloroplast of *C. reinhardtii* CC1690.

Each lane represents a different construct (pLY192 to pLY207), with corresponding protein sizes (kDa) as shown in the table (Primary antibody: Anti-His 1:250; Secondary antibody: Goat anti-rabbit IgG Dylight 800 1:25,000).

5.2.3 Improving synthesis of spider silk proteins by enhancing tRNA^{Gly} levels in the chloroplast

Sixteen of the 33 residues in the repetitive spidroin element (SGRGGLGGQGAGAAAAAGGAGQGGYGGLGSQGT) are glycine. If the number of copies of the element in the recombinant protein are increased from the six achieved here to the ~100 found in native MaSp1 then this would represent a significant drain

on the pool of glycyl-tRNAGly, possibly limiting rates of synthesis of the MaSp1 and also affecting the synthesis of the 69 native proteins encoded by the chloroplast genome. One strategy to address this is to try to increase the size of the glycyl-tRNAGly pool. Since the enzyme glycyl-tRNA synthetase is responsible for attaching glycine to the 3' end of tRNA-Gly, then increasing the level of the substrate pools (glycine, tRNA-Gly) or increasing the synthetase activity could all be considered, as shown in Figure 5.10. In *E.coli*, the intracellular pool of glycyl-tRNA is regulated by glycine availability, which depends on extracellular uptake, biosynthesis, and degradation via the glycine cleavage system (Xia et al., 2010). These authors therefore sought to improve spider silk production in *E. coli* by manipulating each of these activities.

Figure 5.9 Strategy for enhancing recombinant expression of *MaSp1* gene by targeting the pathway to Glycyl-tRNAGly.

(a) The glycyl-tRNA metabolic pathway in *E. coli* (adapted from Xia et al., 2010). In this pathway, glycyl-tRNA is synthesized by the attachment of glycine to tRNAGly, catalyzed by glycyl-tRNA synthetase. The intracellular glycine level, crucial for glycyl-tRNA synthesis, is regulated by extracellular glycine uptake, biosynthesis, and degradation via the glycine

cleavage system. This pathway is essential for providing sufficient glycyl-tRNA to support efficient silk protein synthesis. (b) The structure of trnG2UCC, a variant of tRNA^{Gly}, with the structure predicted using the online tool tRNAscan-SE v.2.0. The structure highlights important regions, including the anticodon loop, which is critical for recognizing glycine during translation.

In *C. reinhardtii*, while the glycyl-tRNA synthesis pathway is not fully characterized, introducing an extra copy of the tRNA-Gly gene (*trnG2*) into the chloroplast genome could be hypothesized to enrich the available glycyl-tRNA pool in a similar manner to *E. coli*. This enrichment would be particularly beneficial for expressing glycine-rich proteins like *MaSp1*, especially as the repetitive units increase in length. As the size of *MaSp1* constructs approaches the size of the native protein, the demand for glycyl-tRNA intensifies, potentially creating a bottleneck in translation.

The engineered *trnG2* was modified from the native gene by using the 5' and 3' non-coding elements from another chloroplast tRNA gene, *trnW* as described by Young et al. (2016), adapting both the left and right *cis* elements to optimize expression (Fig. 5.8b). According to the superwobble theory, a tRNA with a U34 base (uracil in the wobble position) can read all codons within a "quartet" codon family. In this context, the glycine tRNA with an unmodified U34 can recognize and pair with all four glycine codons, enabling efficient decoding. This versatility allows one tRNA species to pair with multiple codons, making it ideal for expressing the *MaSp1* protein, where rapid translation of all glycine codons is essential (Fages-Lartaud & Hohmann-Marriott, 2022).

Thus, a new set of *C. reinhardtii* transformant cell lines was generated and analyzed with the goal of improving the translational efficiency of the glycine-rich *MaSp1* proteins. These lines contained both the *MaSp1* construct and the engineered *trnG2*

gene. A different selection strategy was used to create the lines that involved rescuing a photosynthetic mutant (HT72) in which the photosystem II gene *psbH* had been partially deleted. Targeting of the GOI into a neutral site downstream of *psbH*, with the wild-type gene carried on the right-hand flanking element results in marker-free transgenic lines (Wannathong et al. 2016). To compare the effects of tRNA-Gly enrichment, a parallel set of transformant cell lines was generated that lacked the ectopic *trnG2* copy. This set served as a control to evaluate the impact of tRNA-Gly enrichment on *MaSp1* expression.

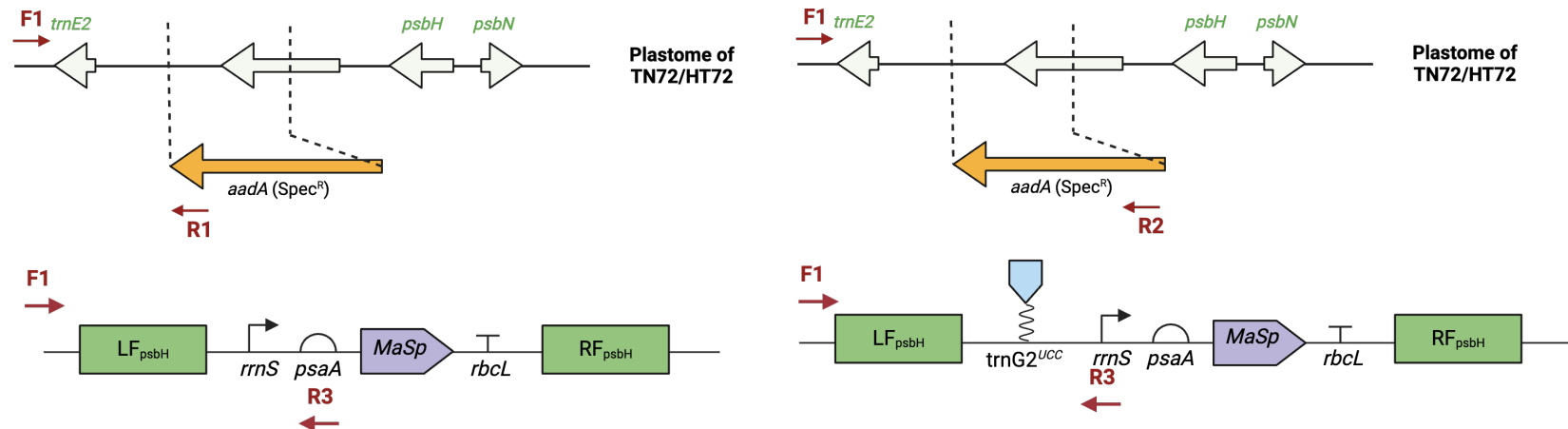


Figure 5.10 Gene insertion for *MaSp1* in the chloroplast genome using a photosynthesis restoration strategy: comparison of *MaSp1* constructs with and without *trnG2*.

This figure illustrates the gene insertion strategy for the *MaSp1* gene using restoration of photosynthesis for selection. It compares two approaches: one with *trnG2* (right panel) and one without (left panel). The construct with *trnG2* aims to increase the glycyl-tRNA pool to enhance the expression of the glycine-rich *MaSp1* protein, while the control construct lacks *trnG2*. The **top diagrams** in each panel represent the native plastome of recipient strain TN72/HT72, showing the deletion of the *psbH* gene and the insertion site flanked by the left and right homology arms (*LF_psbH* and *RF_psbH*). The **bottom diagrams** correspond to the engineered transgene constructs used for integration into this plastome background. Both designs include left (LF) and right (RF) flanking regions for precise targeting into a neutral site downstream of *psbH* and utilize primers (P1, P2, P3) to validate successful integration.

As before, PCR analysis was used to confirm correct insertion of the GOI's and homoplasmy of the transgenic chloroplast genome for each of the transformant lines. As shown in Figure 5.13, representative lines were all homoplasmic with the WT product completely replaced with a PCR product of the expected size for the transgenic genome.

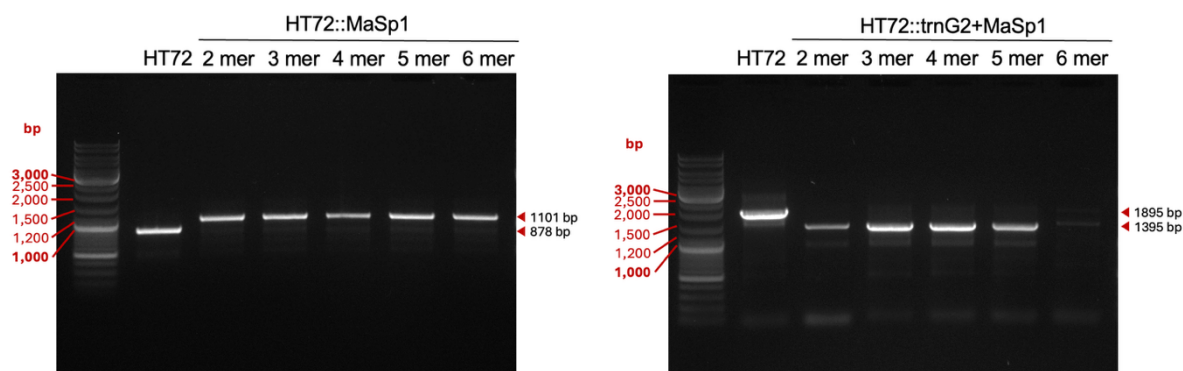


Figure 5.11 PCR Confirmation of MaSp1 integration and homoplasmy in HT72 transformants without (left panel) and with (right panel) the trnG2 gene.

(left panel: without trnG2; right panel: with trnG2, encoding tRNA-Gly), using construct-specific primers as outlined in Figure 5.10—right-panel primers include trnG2-flanking regions, while left-panel primers exclude them. PCR primers target regions flanking the MaSp1 5'UTR integration site, so all 2–6-mer MaSp1 constructs produce consistent amplicon sizes within each panel: ~1100 bp (left panel, no trnG2) and ~1400 bp (right panel, with trnG2), with no size variation by MaSp1 repeat count. Transformant lanes (2–6) show only the target amplicon (no parental HT72 bands), confirming homoplasmy (all chloroplast genomes carry the transgene).

Western blot analysis was conducted to compare the expression of the *MaSp1* multimer genes in both *E. coli* DH5α and *C. reinhardtii* transformants when the chloroplast *trnG2* gene was present or absent. Figure 5.14 presents the Western blot results for the *E. coli* DH5α transformants. The left panel shows protein levels for DH5α::*MaSp1* transformants lacking trnG2, while the right panel depicts DH5α::trnG2-*MaSp1* transformants. Each lane represents a different *MaSp1* multimer length (2 to 6 mer), with bands observed at the expected molecular weights. The results show that the chloroplast *cis* elements (promoter and UTRs) are able to drive expression of *MaSp1* in the bacterium. When comparing the intensity of the MaSp1 4-, 5-mer and 6-mer bands to the endogenous BCCP band there is some evidence that the presence

of the *trnG2* gene has an effect on the level of each protein variant: Particularly, the 4-mer and 5-mer level seem increased in relative intensity compared to the BCCP band. What is not known for certain is whether tRNA-Gly is actually functional in *E. coli* since chloroplast tRNAs are different from their bacterial counterparts (Young and Purton, 2016). Further work is needed to clarify the activity of this foreign tRNA-Gly in *E. coli*.

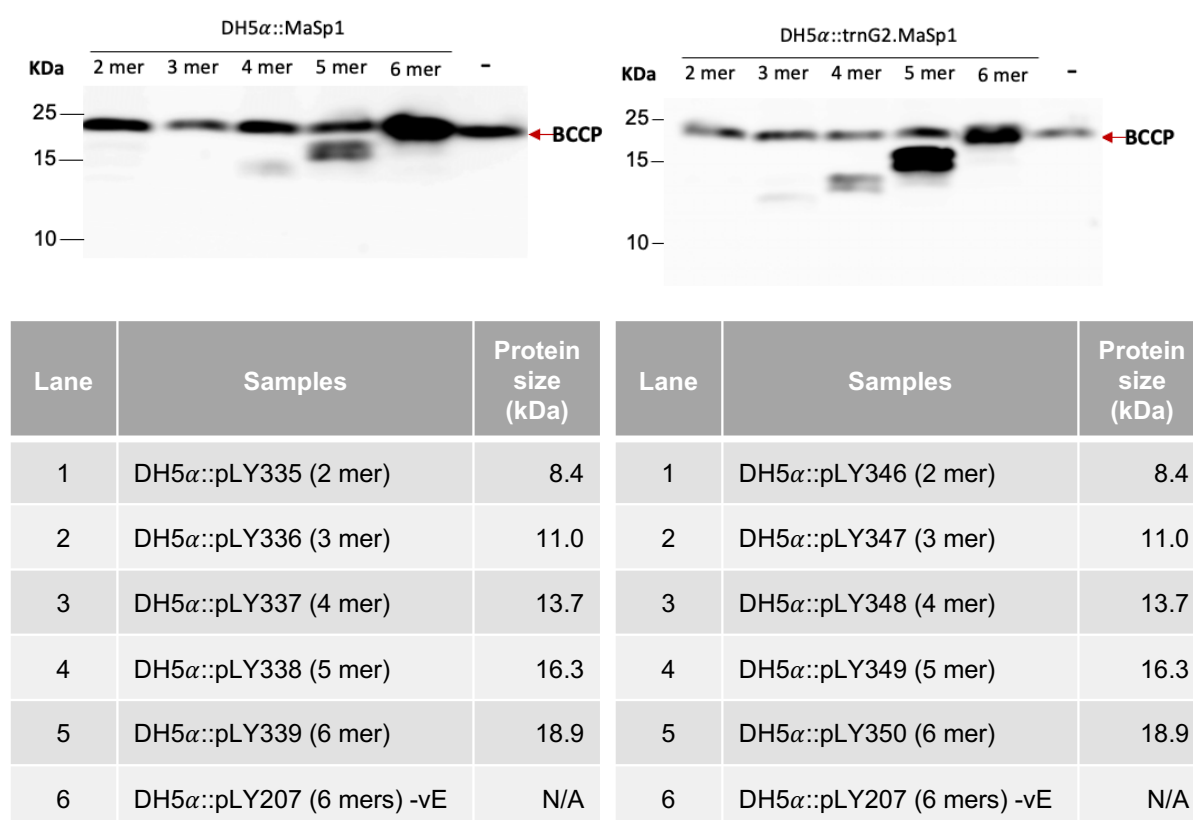


Figure 5.12 Western blot analysis of *MaSp1* multimer expression in *E. coli* DH5α with and without *trnG2* enrichment.

Western blot results for *E. coli* DH5α transformants expressing *MaSp1* multimers, comparing expression levels in samples with and without the *trnG2* transgene. The left panel displays protein expression for DH5α::*MaSp1* transformants without *trnG2*, while the right panel shows DH5α::*trnG2-MaSp1* transformants. Each lane represents a different *MaSp1* multimer length (2 to 6 mer), with bands detected at the expected molecular weights using a Strep-tag II and biotinylation method for clear visualization. The presence of BCCP (biotin carboxyl carrier protein, ~22 kDa) in *E. coli* serves as a loading control, allowing comparison across lanes. Note: Lane 1-5 are Strep-tagged, lane 6 is His-tagged and was used as a negative control.

Additionally, the expression levels of the 2-mer and 3-mer constructs were again significantly lower on the gel than those of the higher multimers, possibly due to the smaller protein sizes affecting transfer efficiency during Western blotting. This trend is consistent with results in other organisms, suggesting that smaller multimers may require optimized conditions for effective detection.

Figure 5.15 shows the Western blot results for *C. reinhardtii* transformants, specifically comparing the expression of the *MaSp1* 6-mer variant in wild-type strain CC1690, HT72::*MaSp1* (without *trnG2*), and HT72::*trnG2* + *MaSp1* (with *trnG2*). Samples were normalised to different cell densities (OD750 values of 20, 10, 4, and 1). Despite successful *MaSp1* expression in *E. coli*, and the previous successful expression in the chloroplast, no detectable expression was observed in these transgenic lines with all of the bands seen in the blot appearing to be due to non-specific binding as they are also seen in the wildtype strain CC-1690 (which was the progenitor of HT72). The reason for this is not clear, but may reflect a lower expression level when transgenes are targeted to the single integration site downstream of *psbH* compared to the duplicated insertion when transgenes are targeted to the *psbA* downstream site within the inverted repeat (Jackson et al. 2022).

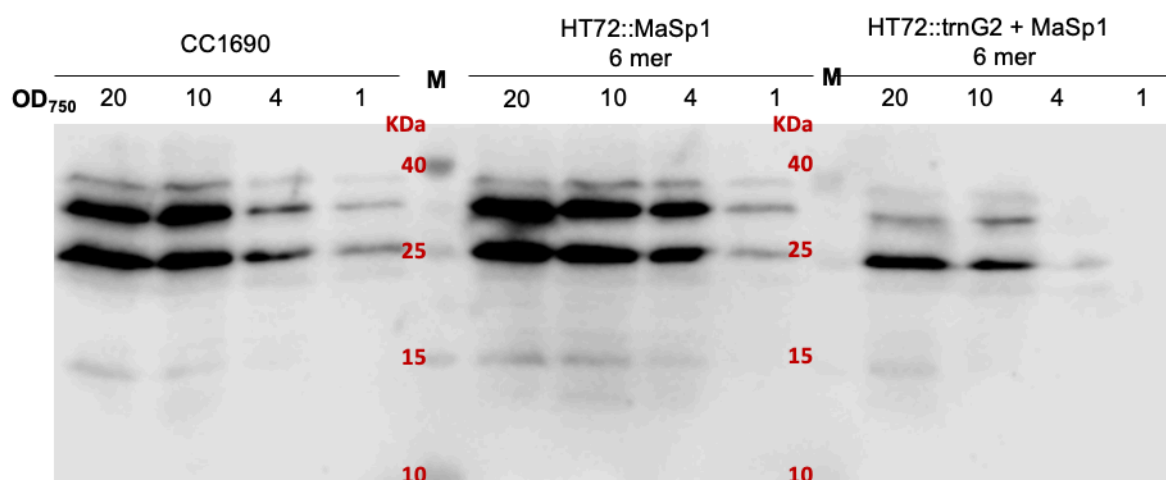


Figure 5.13 Western blot analysis of wild-type *C. reinhardtii* (CC-1690), HT72::*MaSp1* 6-mer, and HT72::trnG2 + *MaSp1* 6-mer transformants at varying cell densities.

Western blot results comparing *MaSp1* 6-mer expression levels in the different strains using antibodies to the StrepII tag on the *MaSp1* protein. Samples were analysed at different cell densities (OD₇₅₀ values of 20, 10, 4, and 1). Molecular weight markers (M) indicate protein sizes in kDa.

5.3 Discussion

The successful expression of *MaSp1* in the chloroplast of *C. reinhardtii* marks a significant advance in the production of recombinant spider silk proteins. This study has demonstrated that *C. reinhardtii* could serve as an effective host for the expression of *MaSp1*, a major ampullate spidroin.

Previous research has shown the potential of *C. reinhardtii* for recombinant protein production due to its well-characterized genetics, ease of manipulation, and capability for high-density cultivation (Purton et al., 2013b). This study builds on these findings by specifically targeting the chloroplast, leveraging its high protein synthesis capacity and the ability to achieve homoplasmy, which ensures that all copies of the chloroplast genome contain the inserted *MaSp1* gene. The results indicate that the chloroplast

transformation approach used in this study is effective for achieving stable and high-level expression of recombinant spider silk proteins.

Despite the successful expression of MaSp1, several limitations were encountered during the study. One of the primary challenges was the purification process of the recombinant spider silk protein. The extraction and purification steps are crucial for obtaining high-quality proteins suitable for further applications. However, these processes can be complex and labour-intensive, often resulting in variable yields and potential degradation of the protein.

The yield and quality of the recombinant spider silk protein were also affected by factors such as the culture conditions and the genetic stability of the transformed *C. reinhardtii* cells. While the chloroplast transformation method offers advantages in terms of homoplasmy and high-level expression, it also presents challenges related to maintaining the genetic stability of the transformed cells over multiple generations (Gimpel et al., 2015b).

Scalability is another significant concern. Although *C. reinhardtii* offers a promising platform for lab-scale production, scaling up the process to industrial levels presents numerous challenges. These include optimizing large-scale culture conditions, ensuring consistent protein quality and yield, and developing cost-effective purification methods. Addressing these challenges is essential for the commercial viability of recombinant spider silk production.

The molecular interactions and bonding within the MaSp1 protein are crucial for its structural integrity and functionality. The semi-crystalline molecular spring

configuration of MaSp1, characterized by a highly organized β -sheet structure with alanine and proline-rich α -helices, is responsible for its exceptional mechanical properties (Scheibel et al., 2010; Vollrath & Knight, 2001). Understanding these molecular interactions is essential for replicating the properties of natural spider silk in recombinant proteins.

Future research should focus on several key areas to enhance the yield and quality of recombinant spider silk proteins. One promising approach is the optimization of genetic constructs to increase expression levels and stability. This could involve the use of stronger promoters, enhanced regulatory elements, and codon optimization to improve translation efficiency (Leon-Banares et al., 2004).

Another area of focus should be the development of more efficient purification methods. Current methods can be labour-intensive and costly, limiting their scalability. Advances in affinity purification techniques, such as the use of novel affinity tags and chromatography resins, could significantly improve the efficiency and cost-effectiveness of the purification process.

Additionally, exploring alternative cultivation methods could help address the scalability challenges. For example, photobioreactors and open pond systems could be optimized for large-scale cultivation of *C. reinhardtii*, providing more consistent and cost-effective production conditions.

The potential industrial applications of recombinant spider silk protein are vast and varied. In the biomedical field, spider silk's biocompatibility and mechanical strength make it ideal for applications such as sutures, wound dressings, and tissue

engineering scaffolds (Altman et al., 2003; Hardy & Scheibel, 2009). In the textile industry, the exceptional strength and elasticity of spider silk fibres could lead to the development of high-performance fabrics and composites (Rising et al., 2011).

However, realizing these applications requires addressing the scalability challenges associated with large-scale production. This includes optimizing cultivation conditions, improving purification processes, and ensuring consistent quality and yield. Collaborations between academia and industry will be crucial for developing scalable production systems and translating laboratory successes into commercial products.

While several challenges remain, including the optimization of purification processes and scalability, the findings of this study provide a solid foundation for future research and development. By addressing these challenges, we can unlock the full potential of recombinant spider silk, paving the way for its widespread application in various industries.

In conclusion, the production of recombinant spider silk protein in *C. reinhardtii* offers a promising solution to the challenges associated with natural spider silk production. By leveraging the genetic and metabolic capabilities of *C. reinhardtii*, we can achieve sustainable and scalable production of this extraordinary biomaterial, opening new possibilities for its use in a wide range of applications.

Chapter 6

The *C. reinhardtii* chloroplast as a platform to produce double-stranded RNA (dsRNA)

6 The *C. reinhardtii* chloroplast as a platform to produce double-stranded RNA (dsRNA)

6.1 Introduction

Double-stranded RNAs (dsRNAs) are critical molecules involved in various biological processes, including antiviral defense and gene regulation through RNA interference (RNAi). These molecules have been identified in a wide range of organisms, spanning a size range from 1.5 to 20 kb. Smaller dsRNAs are particularly notable for their association with virus-like particles, and are essential for viral replication and host interactions [Click or tap here to enter text.\(.\)](#). RNAi has proven to be a versatile tool for gene silencing, enabling both endogenous gene knock-down and antiviral defense in crustaceans. As detailed in the review by Fajardo et al. (2024), dsRNA-mediated RNAi has been successfully employed to silence host genes involved in immune regulation, as well as viral genes critical to pathogen replication, thereby providing both investigative and therapeutic value. Given their significance, the efficient production and accurate detection of dsRNAs are crucial for both fundamental research and practical applications in biotechnology and medicine.

As discussed in Chapter 1, *Chlamydomonas reinhardtii* has emerged as an attractive model organism for various biotechnological applications including synthesis of long dsRNA production in the chloroplast. The chloroplast offers a unique advantage for dsRNA production due to its high copy number and high levels of transgene expression, and the potential for stable accumulation of these RNA molecules in the

absence of any DICER system for processing dsRNAs into small interfering RNAs (Zhang et al., 2015). Previous studies have explored the use of *C. reinhardtii* for producing dsRNAs targeting pathogens such as the White Spot Syndrome Virus (WSSV) in shrimp, demonstrating the feasibility of using this alga as a dsRNA production platform (Charoonnart et al., 2018, 2019, 2023; Fajardo et al., 2024; Saksmerprome et al., 2009).

Despite these advancements, several challenges remain in optimizing dsRNA production in *C. reinhardtii*. Current transformation strategies often result in variable expression levels and stability of the dsRNA gene constructs. Moreover, there is a lack of simple and robust methods for quantifying dsRNA produced in this system, which hampers the scalability and practical application of this technology. These limitations underscore the need for more sophisticated strategies to improve the efficiency and quantification of dsRNA production in *C. reinhardtii*.

The TN72 strain of *C. reinhardtii* is valued in chloroplast engineering, both for dsRNA and protein production, as it has a cell wall-deficient structure that simplifies DNA delivery using methods such as agitation with glass beads, making transformation more accessible and cost-effective (Changko, 2020; Charoonnart et al., 2019, 2023; Vilatte et al., 2023). However, this cell-wall deficiency also leaves TN72 vulnerable to environmental stresses during bioprocessing, such as harvesting, desiccation and storage, limiting its large-scale use (Stoffels et al., 2019). In contrast, strains with a wild-type cell wall offer enhanced stability, crucial for maintaining cell integrity during processes such as disc-stack centrifugation and freeze-drying, and could be better suited for scalable dsRNA production in industrial settings (Vilatte et al., 2023). Additionally, broader adoption in sectors like agriculture and animal health would

benefit from more user-friendly cloning systems, which would make dsRNA technologies accessible to non-specialists (Rosales-Mendoza et al., 2012).

The stability of synthesized double-stranded RNA (dsRNA) within the chloroplast of *C. reinhardtii* is a critical factor for its effective application in aquaculture. While the potential of chloroplast-derived dsRNA has been explored, the mechanisms governing its degradation remain inadequately understood. Research indicates that chloroplast RNA stability is influenced by various factors, including polyadenylation and the activity of ribonucleases. (Schuster et al., 1999). Additionally, the redox state within the chloroplast has been shown to regulate RNA degradation processes. Specific pathways for dsRNA degradation, such as the involvement of an RNA-induced silencing complex (RISC) or other RNA interference (RNAi) appear not to operate in the chloroplast, but understanding what controls dsRNA stability is essential for optimizing dsRNA production for therapeutic and industrial applications in aquaculture and other fields. (Salvador & Klein, 1999).

In *Nicotiana tabacum* (tobacco), plastid-expressed transgenes for dsRNA can induce gene silencing of nuclear-encoded genes through the production of phased small interfering RNAs (phasiRNAs) (S. Bélanger et al., 2023). This research has demonstrated that dsRNA synthesized within chloroplasts can escape into the cytoplasm, where it is processed into 21-nucleotide phasiRNAs. These phasiRNAs then participate in the RNA interference (RNAi) pathway, leading to the degradation or translational inhibition of target nuclear mRNAs. This mechanism enables the silencing of specific nuclear genes without directly altering nuclear DNA sequences, offering a valuable tool for precise gene regulation in plants (S. Bélanger et al., 2023). However, in *C. reinhardtii*, the mechanisms by which plastid-derived dsRNA could

influence nuclear gene expression have not been studied. Pathways for dsRNA transport or escape from the chloroplast to the cytoplasm or nucleus, and the subsequent engagement with the RNAi machinery, remain unexplored in this organism. Further research is needed to elucidate whether similar RNAi-based gene silencing pathways can be harnessed in *C. reinhardtii* for applications in metabolic engineering and gene regulation.

Quantifying dsRNA in *C. reinhardtii* poses significant challenges due to the limitations of current methods, which require complex purification of dsRNA for quantitative RT-PCR analysis involving selective nuclease digestion of contaminating DNA and single-stranded RNA. These techniques often result in substantial dsRNA yield loss, complicating accurate measurement, especially in applications requiring precise dosages, such as therapeutic or agricultural dsRNA products (Charoonnart et al., 2023).

Aptamers are short, single-stranded DNA or RNA molecules selected for their binding specificity to a target molecule, and have gained interest as potential tools for dsRNA quantification due to their high binding affinity, selectivity, and potential for non-destructive binding (R. Xu et al., 2023). In other systems, aptamers have been used effectively for sensitive and selective binding of a fluorescent ligand to dsRNA without requiring purification, thus preserving dsRNA integrity. For instance, aptamer-based biosensors have been developed for the detection of viral dsRNA, simplifying quantification processes (Bouhedda et al., 2018; Hallegger et al., 2006; Kaur et al., 2018; Ouellet, 2016). Trials to apply similar aptamer-based quantification approaches in *C. reinhardtii* have been conducted, though results have been limited. The adaptation process has proven challenging due to the complex intracellular

environment of microalgae (Guzmán-Zapata et al., 2017). Further research is necessary to adapt aptamer technologies more effectively to *C. reinhardtii*. This includes engineering aptamers with improved stability and affinity in the algal chloroplast or cytoplasmic environment and developing robust, standardized protocols for using aptamers as quantification tools. Advances in this area could facilitate accurate dsRNA measurements *in vivo*, thereby supporting broader applications of dsRNA in fields such as aquaculture, biotechnology, and agriculture.

Aims and objectives of this chapter:

1. **Develop a Simplified dsRNA Platform:** Establish a streamlined platform for chloroplast engineering for dsRNA production in the microalga *C. reinhardtii*, optimizing it for ease of use and yield.
2. **Aquaculture Application in Shrimp Therapeutics:** Utilize the dsRNA platform to develop anti-viral therapeutic agents specifically for farmed shrimp within aquaculture, targeting common viral pathogens.
3. **Investigate dsRNA Degradation Mechanisms:** Study the pathways involved in dsRNA degradation within *C. reinhardtii* chloroplasts, with a focus on understanding nuclear-encoded gene silencing mechanisms related to dsRNA stability.
4. **Facilitate dsRNA Quantification with Engineered Aptamers:** Integrate engineered aptamers into the dsRNA expression cassette to enable real-time quantification *in vivo*, using fluorescent signals to accurately represent dsRNA yield.

6.2 Results

6.2.1 'One-step One-pot' platform to clone dsRNA targets

The building of chloroplast transformation plasmids containing dsRNA transgenes typically involves multiple cloning steps. This section reports on the development and application of a 'One-step One-pot' platform for cloning double-stranded RNA targets in *Chlamydomonas reinhardtii*. The platform, based on the pLY118 vector (sequence in Appendix 9), enables efficient assembly and expression of dsRNA constructs with targeting to a specific neutral plastome locus downstream of *psbH*.

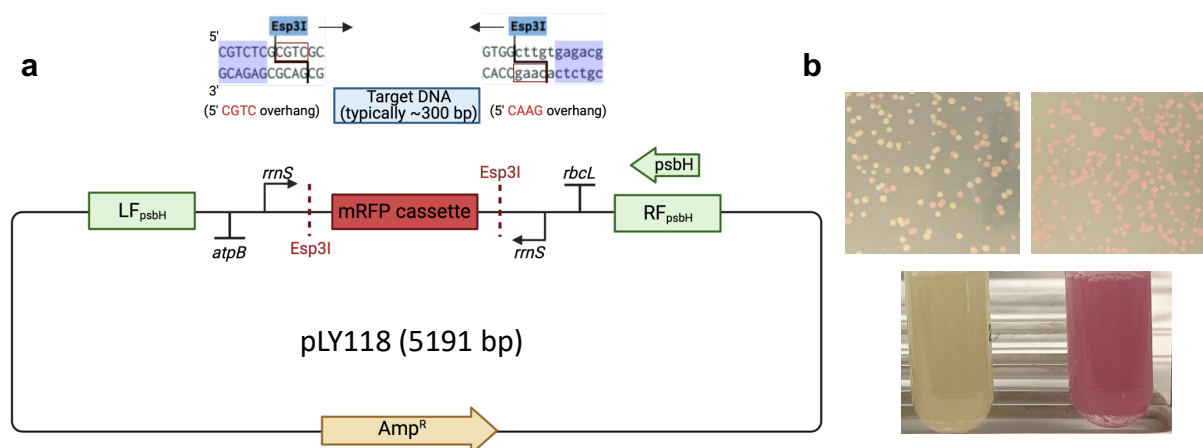


Figure 6.1 The completing p2xTRBL vector allows cloning of any DNA fragment between convergent *rrnS* promoters to create a dual transcription cassette.

(a) Construction of pLY2xTRBL plasmids involved a direct cloning strategy which any target DNA can be cloned using the type IIS enzyme Esp3I, replacing a mRFP reporter gene and creating a dual transcription cassette for the DNA. Flanking chloroplast elements (LF and RF) target the cassette downstream of *psbH*, with selection based on rescue of a *psbH*-deletion mutant. (b) cloning is aided by a simple 'pink/white' screen where *E. coli* transformant colonies and cultures carrying the correctly assembled plasmid have a white phenotype. The experimental plate (left) shows a mix of white and pink colonies: white colonies indicate successful cloning (target DNA replaced the mRFP reporter cassette via Esp3I digestion-ligation, eliminating mRFP expression), while pink colonies retain the original vector with intact mRFP. The control plate (right, no Esp3I added) only has pink colonies, confirming that white colonies in the experimental group result from specific mRFP replacement rather than random

changes. Bottom liquid culture insets further amplify the color difference - pale/colorless for white-colony transformants (correct plasmids) and pink for pink-colony ones (unmodified vectors) - simplifying high-throughput validation.

The construction of pLY118 vector (5191 bp) allows the cloning of any DNA fragment between convergent *rrnS* promoters to create a dual transcription cassette, as illustrated in Figure 6.1a. The pLY118 vector allows direct cloning using the Esp3I enzyme, which generates compatible overhangs for ligating the target DNA fragment. Construction involves a single-step replacement of the mRFP cassette with a PCR product from the target gene that is typically around 300 bp.

Cloning efficiency was evaluated using a simple 'pink/white' screening method. As shown in Figure 6.1a, the vector was designed such that *E. coli* colonies carrying the correctly assembled plasmid would have a white phenotype, while those retaining the original mRFP cassette would be pink. Analysis of a typical cloning experiment (Figure 6.1b) following a one-pot digestion-ligase reaction with both vector and insert DNA, showed a mix white and pink colonies on the experimental plate indicating successful cloning of the DNA construct, whereas the control plate (no Esp3I enzyme) showed only pink colonies. Additionally, liquid cultures from white or pink colonies showed an even clearer colour phenotype, further demonstrating the utility of this simple screen that requires no specialised *E. coli* strain or additions to the nutrient agar plates, unlike traditional cloning vectors based on 'blue-white' selection.

6.2.2 Creating dsRNAs-expressing *C. reinhardtii* for silencing viral genes during shrimp infection

6.2.2.1 Design of transgenic lines against two major viral pathogens of shrimp

Two of the most prevalent and devastating viruses of farmed shrimp are White Spot Syndrome Virus (WSSV) and Yellow Head Virus (YHV) (Charoonnart et al., 2019, 2023). If dsRNA targeting essential genes of these two viruses can be produced in *C. reinhardtii*, then the dried algae can be formulated into the shrimp feed for oral delivery of the dsRNA and protection of the shrimp. Figure 6.2 provides a schematic representation of the process for producing these antiviral dsRNAs in *C. reinhardtii* for use in shrimp, with the VP28 (major envelope protein) and RsRp (RNA-dependent RNA polymerase) genes of WSSV and YHV, respectively selected as targets. Transgenic lines were designed to produce either dsRNA or a combined dsRNA targeting both genes. In the scheme, the transformed algae are cultivated and harvested, and the resulting biomass containing the dsRNA is dried to kill the algae before being formulated into shrimp feed. This approach aims to deliver dsRNA simply and cheaply to shrimp through their diet, providing protection following viral infections.

To investigate RNAi-mediated viral gene silencing in shrimp, we selected specific regions of two key viral genes: WSSV-VP28 and YHV RNA-dependent RNA polymerase (RdRp). VP28 is a major envelope protein essential for WSSV entry into host cells, while RdRp is crucial for the replication of YHV, an RNA virus that significantly impacts shrimp aquaculture. These targets were chosen for their functional importance and established effectiveness in previous RNAi studies. Approximately 500 bp DNA fragments were selected to ensure efficient processing

into siRNAs while maintaining feasibility for synthetic synthesis. The synthetic DNA fragments were cloned into the RNAi expression vector using a one-step cloning strategy to facilitate efficient construct preparation.

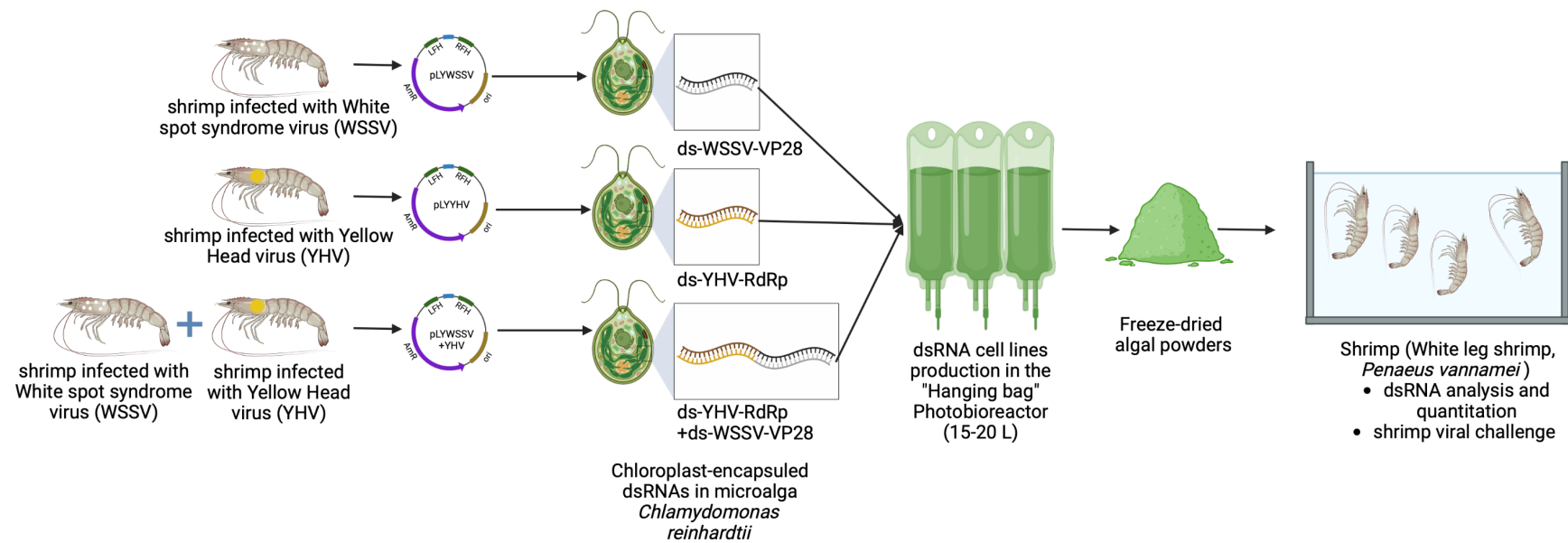


Figure 6.2 Schematic overview of shrimp antiviral dsRNAs production in *Chlamydomonas reinhardtii*.

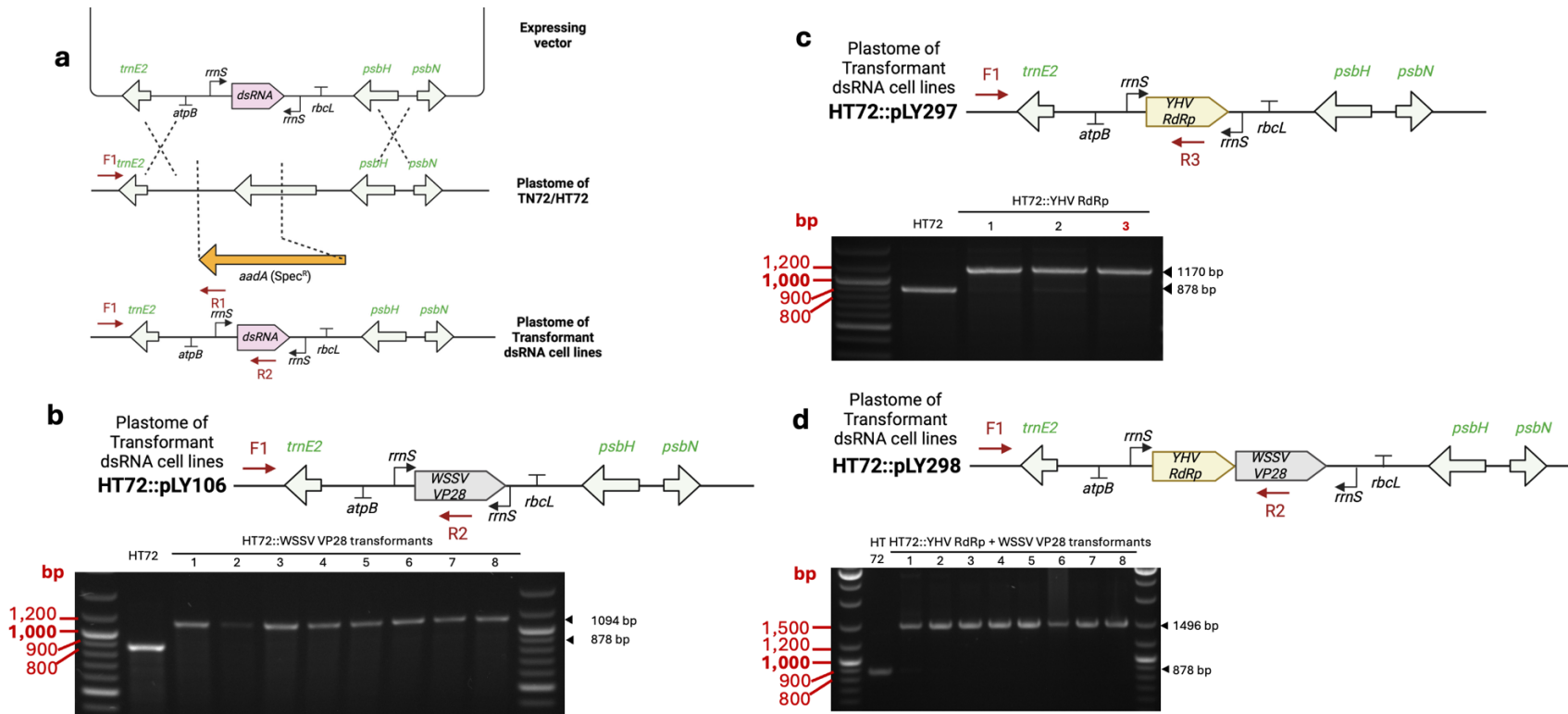


Figure 6.3 Schematic and PCR validation of chloroplast-targeted dsRNA and viral protein expression constructs in *Chlamydomonas reinhardtii* HT72.

(a) Transformation strategy for integrating dsRNA-expressing cassettes into the chloroplast genome: top schematic shows the expression vector, middle depicts the parental plastome (TN72/HT72), and bottom illustrates the transformant plastome with integrated dsRNA cassette and *aadA* selection marker. Primers F1, R1, and R2 are indicated for PCR validation. (b) Plastome schematic and PCR validation of HT72::pLY106 transformants (expressing WSSV VP28). Gel shows WT HT72 (lane 1) and independent transformant lines (lanes 2–8). Amplicons: 1094 bp (transformants, F1 + R2) and 878 bp (WT, F1 + R2). (c) Plastome schematic and PCR validation of HT72::pLY297 transformants (expressing YHV RdRp). Gel shows WT HT72 (lane 1) and independent transformant lines (lanes 2–4). Amplicons: 1170 bp (transformants, F1 + R3) and 878 bp (WT, F1 + R3). (d) Plastome schematic and PCR validation of HT72::pLY298 transformants (co-expressing YHV RdRp and WSSV VP28). Gel shows WT HT72 (lane 1) and independent transformant lines (lanes 2–8). Amplicons: 1496 bp (transformants, F1 + R2) and 878 bp (WT, F1 + R2).

Panel (a) illustrates the strategy for generating dsRNA transformants. The plasmid consists of a dsRNA 'convergent promoters' cassette flanked by the appropriate homologous regions for integration into the chloroplast genome of the $\Delta psbH$ recipient strains, TN72 or HT72. This ensures integration and stable expression of the dsRNA constructs within the chloroplast.

Panel (b) presents the PCR confirmation of the dsRNA-expressing cassette integration into the chloroplast genome. The gel electrophoresis results show DNA bands corresponding to the expected sizes of the dsRNA constructs, confirming successful integration into the chloroplast genome of the TN72::pLY106 strain.

Panel (c) and Panel (d) provide additional PCR confirmations for different dsRNA constructs, such as HT72::pLY297 and HT72::pLY298. These panels display single bands that verify the presence of the dsRNA-expressing cassettes in the chloroplast genome, indicating successful integration and homoplasmy.

6.2.2.2 Mixotrophic dsRNA production using a 'Hanging bag' photobioreactor

6.2.2.3 Shrimp viral challenges

In order to test the efficacy of the dsRNA strains, 15 litres of each strain plus a WT control were grown using a simple hanging bag photobioreactor system (Cui et al., 2022) under mixotrophic conditions using acetate-containing medium. The algal biomass was harvested by flocculation using 2 μ M Ferric chloride and the biomass dried by lyophilisation using a freeze-drier. The dried algae were blended with commercial shrimp feed at a 5% (w/w) inclusion rate using a standard pellet-coating method with fish oil as a binder. A series of challenge trials was set up using shrimp at 12 days post-larvae (12 PL), with each treatment carried out in four replicate tanks (20 L capacity) stocked at a density of 20 shrimp per tank. Tanks were continuously aerated, maintained at 28 ± 1 °C, and received daily partial water exchange.

Figure 6.4 presents the results of the shrimp survival rates following viral challenges.. Panel (a) shows the survival rate of shrimp fed with commercial feed, with or without the addition of the control algal material, and those treated with feed containing algal material with the dsRNA targeting White Spot Syndrome Virus (WSSV). The results indicate that shrimp fed with dsRNA-expressing algae (LY106) show a higher survival rate compared to those fed just with regular commercial feed when challenged with WSSV. However, the survival rate of the dsRNA-treated group does not show a significant difference compared to the WT algae control group when challenged with WSSV. Panel (b) presents survival data for shrimp treated with the multi-target dsRNA construct (dsMulti) compared to a control group and a group treated with WSSV-specific dsRNA. The results suggest that the multi-target dsRNA (LY298) does not

significantly improve survival compared to the WT control when challenged with WSSV. Panel (c) shows survival rates for shrimp treated with dsRNA targeting Yellow Head Virus (YHV). Although the dsRNA treatment group (LY297) appears to have a higher survival rate than the WT group, the difference is not statistically significant. Panel (d) combines data from shrimp treated with the multi-target dsRNA against both WSSV and YHV, showing no significant improvement in survival rates compared to the WT control when challenged with YHV.

The production of antiviral dsRNAs in *C. reinhardtii* offers a promising strategy for controlling viral infections in shrimp through dietary administration. The use of chloroplast-expressed dsRNA ensures stability, as the chloroplast provides a protective environment that prevents degradation by cytoplasmic ribonucleases. This stability is crucial for maintaining the integrity and functionality of dsRNA-based therapeutics when algal cells are consumed by shrimp. The use of whole algal cells as a delivery system simplifies the production process, reducing costs and enhancing the practicality of dsRNA administration.

However, the shrimp survival rate results indicate that the dsRNA-treated groups do not show significant improvement in survival compared to the WT control groups when challenged with WSSV or YHV. Since previous studies have shown that dsRNA produced in the algal chloroplast can be effective in conferring viral protection (Charoonnart et al., 2019, 2023; Saksmerprome et al., 2009), then this lack of significant difference suggests that the current dsRNA constructs and administration protocols may need further optimization to ensure efficacy.

Next steps should focus on several key areas:

- Refinement of dsRNA constructs: Re-design of dsRNA constructs to improve their antiviral efficacy. This could involve targeting alternative viral genes, optimizing the length and sequence of the dsRNA, testing different promoter elements for increased dsRNA synthesis or *cis* elements that increase dsRNA stability in the chloroplast.
- Dosage and administration: Determine the optimal concentration and delivery method for dsRNA to maximize its protective effects. This may include adjusting the dosage of dsRNA in the feed or exploring alternative administration routes.
- Combination therapies: Investigate the potential of combining dsRNA treatments with other antiviral agents or immune modulators to enhance overall efficacy.
- Long-term studies: Conduct long-term studies to assess the sustainability and effectiveness of dsRNA treatments over extended periods and multiple viral challenges.
- Mechanistic studies: Explore the mechanisms by which dsRNA confers antiviral protection, including its stability, uptake, and processing within the shrimp.

Overall, while the initial results are promising, further research and optimization are necessary to fully realize the potential of chloroplast-expressed dsRNA in enhancing disease resistance in aquaculture species.

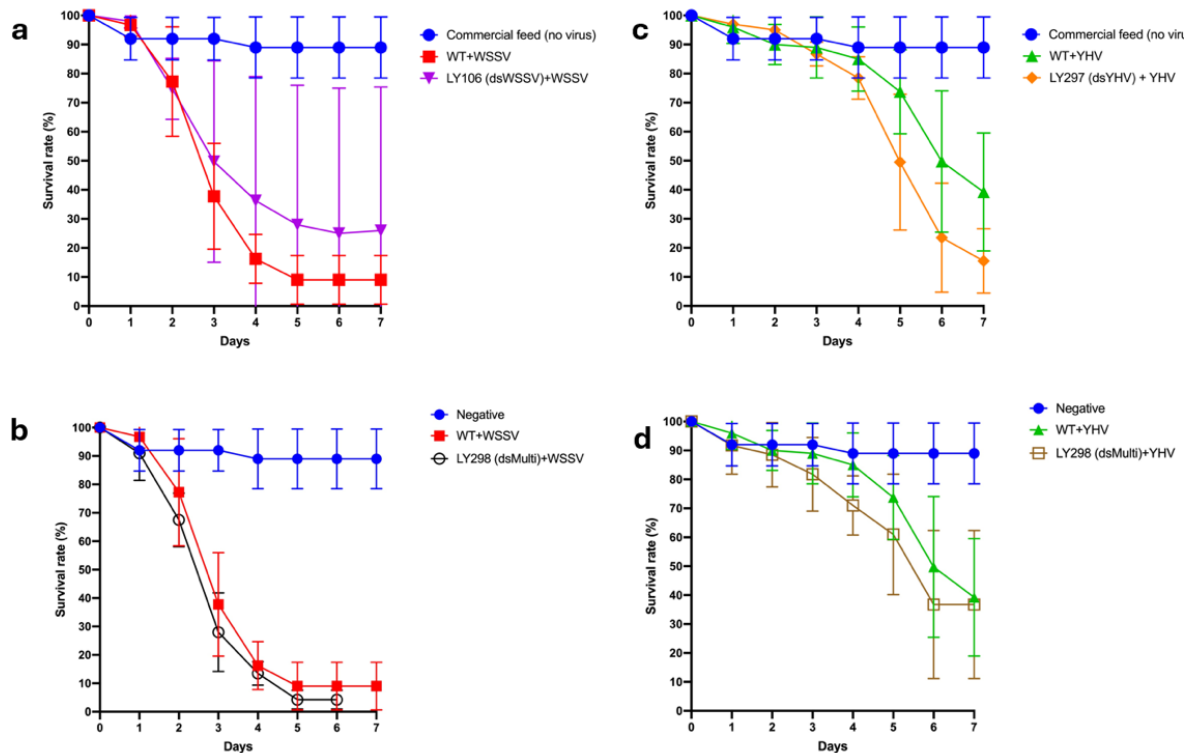


Figure 6.4 Survival rates of shrimp fed with different feeds against WSSV and YHV viral challenges over 7 days.

This figure illustrates the survival rates of shrimp subjected to White Spot Syndrome Virus (WSSV) and Yellow Head Virus (YHV) challenges, comparing the effects of various feeds over a period of 7 days. Panels (a) and (b) show survival rates of shrimp under WSSV infection, while panels (c) and (d) display survival rates under YHV infection. Different feed types are represented: commercial feed without virus (control), wild-type feed (WT) under viral challenge, and genetically modified *C. reinhardtii* feeds (LY296 and LY298) with viral resistance. The error bars indicate variability in survival rates among test groups.

6.2.3 Investigating the gene-silencing mechanism in *C. reinhardtii* chloroplast: Can chloroplast-expressed dsRNAs silence nuclear-encoded genes?

Recent research into RNA escape from tobacco chloroplasts showed that chloroplast-synthesised dsRNA designed to silence specific nuclear genes could induce gene silencing in the cytoplasm resulting in a mutant phenotype (Belanger et al., 2023). This process is presumed to occur through chance lysis of one or more of the multiple chloroplasts in a plant cell, and builds on the observations that chloroplast DNA (cpDNA) also escapes readily leading to integration of cpDNA fragment in the nuclear genome as 'nuclear integrants of plastid DNA' (NUPTs) (Zhang et al., 2020). However, NUPTs are not found in the *Chlamydomonas* nuclear genome and assays for cpDNA transfer indicate that such escape is rare, possibly because the alga has just a single chloroplast, so any lysis event is likely to be lethal (Lister et al., 2003). To further test this hypothesis, I decided to test whether dsRNAs designed to target nuclear genes of *Chlamydomonas* could induce a RNAi phenotype due to escape into the cytoplasm.

Figure 6.5 provides a general overview illustrating the hypothetical process by which dsRNAs expressed in the chloroplast could trigger gene silencing of nuclear-encoded genes. The process spans three cellular compartments: the chloroplast, the cytoplasm, and the nucleus. Within the chloroplast, dsRNA (double-stranded RNA) is produced from a dsRNA expression platform using convergent promoters. High transcriptional activity driven by these promoters leads to the formation of dsRNA. Once synthesised, the dsRNA either escapes or is transported into the cytoplasm where it encounters the Dicer enzyme. Dicer binds to the dsRNA and cleaves it into small interfering RNAs (siRNAs). This processing step is crucial as it converts the long dsRNA into functional

siRNAs that can mediate gene silencing (Doyle et al., 2012; MacRae et al., 2006). One of the siRNA strands (guide RNA) is incorporated into the RNA-induced silencing complex (RISC). The RISC complex is essential for the gene-silencing mechanism, as it guides the siRNA to its complementary mRNA target (MacRae et al., 2006; Meister & Tuschl, 2004). The RISC-siRNA complex searches for and binds to a complementary mRNA molecule in the cytoplasm. This binding is highly specific, dictated by base-pairing interactions between the siRNA and the target mRNA (Elbashir et al., 2001; J. Liu et al., 2004; Meister & Tuschl, 2004). Upon binding, the RISC complex cleaves the target mRNA at a specific site. This cleavage results in the fragmentation of the mRNA, effectively silencing the gene by preventing it from being translated into protein (J. Liu et al., 2004; Yekta et al., 2004). The cleaved mRNA fragments are subsequently degraded within the cell. This degradation ensures that the mRNA cannot be used as a template for protein synthesis, thus silencing the expression of the target gene (Carthew & Sontheimer, 2009; Hannon et al., 2010).

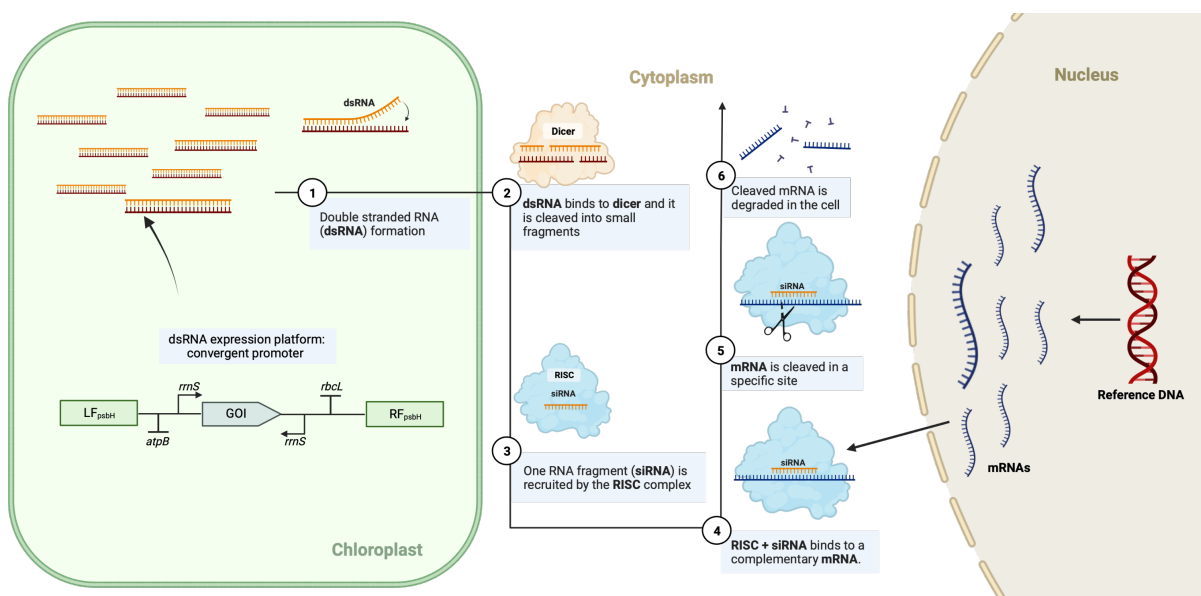


Figure 6.5 Hypothesis schematic overview of chloroplast-expressed dsRNAs trigger gene silencing of nuclear-encoded genes.

However, it is plausible that the dsRNA produced within the chloroplast remains confined and well-protected within the algal chloroplast, preventing it from triggering gene silencing of nuclear-encoded genes. Certainly, the chloroplast double membrane serves as a physical barrier ensures that dsRNA does not Click or tap here to enter text.escape and there is no evidence of Click or tap here to enter text.specific transport mechanisms facilitating movement of RNA across the chloroplast membranes. In the absence of such mechanisms, dsRNA remains trapped within the chloroplast, isolated from the cytoplasmic RNAi machinery. This isolation would prevent the formation of siRNAs and the subsequent gene silencing of nuclear-encoded genes (Breuers et al., 2011; Fuks & Schnell, 1997).

In this study, two nuclear genes with well-documented mutant phenotypes were chosen as targets. The *Y-5* gene is associated with a "yellow in the dark" phenotype due to its role in chlorophyll biosynthesis in the dark, making it a suitable candidate to score a non-lethal phenotypic change resulting from gene silencing. This phenotype would also offer insights into the gene's role in pigment biosynthesis and response to light or dark environments (Ford et al., 1981). The *ARG7* gene, encodes argininosuccinate lyase (ASL), the last enzyme of the arginine biosynthesis pathway. This gene was chosen as it is a well-characterized nuclear marker frequently used in genetic transformation studies in *C. reinhardtii* allowing the rescue of *arg7* mutants to arginine auxotrophy (Debuchy et al., 1989). Targeting *ARG7* allows us to measure silencing effectiveness through established assays and observe arginine auxotrophy. By using *Y-5* and *ARG7* as each other's controls, this setup provides a robust experimental framework to validate the role of chloroplast-produced dsRNAs in silencing nuclear genes. Figure 6.6 illustrates the expression vectors used, the design

of the dsRNA constructs, and the PCR confirmation of gene integration and homoplasmy in the transformants generated.

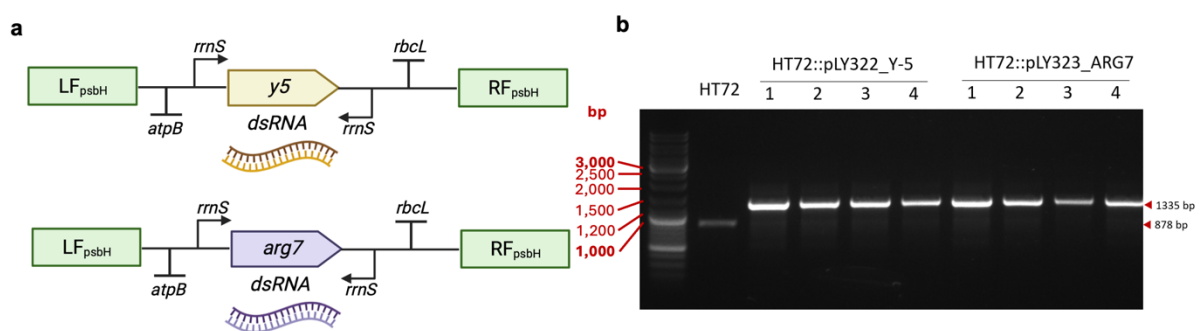










Figure 6.6 Chloroplast-expressed double-stranded RNA expressing Y-5 and Arg7.

(a) Design of expression vectors of pLY118 with Y-5 (associates with yellow-in-the-dark phenotypes have been isolated which were unable to synthesise Chlorophyll in the dark and, as a consequence accumulated Pchlde in their plastids) and ARG7 (encodes the enzyme argininosuccinate lyase and is used to rescue arginine-requiring arg7 mutants to prototrophy) expressing cassette, used for production of transgenic *C. reinhardtii*. (b) PCR confirmation of GOI integration and homoplasmy of *C. reinhardtii* transformants.

Figure 6.7 compares the predicted phenotypes with the actual test results of strains expressing dsRNA for Y-5 and ARG7. The phenotypes were assessed under different light and medium conditions to evaluate the growth and characteristics of the transformant lines.

The predicted phenotypes if gene silencing occurred were based on the known characteristics of the Y-5 and ARG7 mutations. For Y-5 silencing, it was expected that under light conditions, the strain would be green, whereas in the dark, it would exhibit a ‘yellow-in-the-dark’ phenotype due to the inability to synthesize chlorophyll and the consequent accumulation of protochlorophyllide (Pchlde). For ARG7 silencing, in the

absence of L-Arginine, no growth was anticipated due to its requirement for this amino acid. However, in the presence of L-Arginine, the transformant was predicted to grow normally under both light and dark conditions.

Light Medium	Light	Dark
TAP	 Y5 (normal)  ARG7 (no growth)	 Y5 (yellow in the dark)  ARG7 (no growth)
TAP with 300 μM L-Arginine	 Y5 (normal)  ARG7 (normal)	 Y5 (yellow in the dark)  ARG7 (normal)

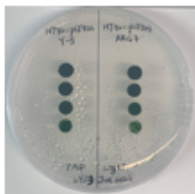
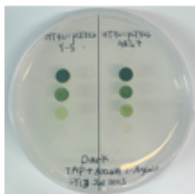
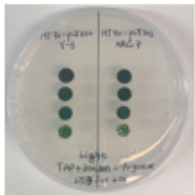
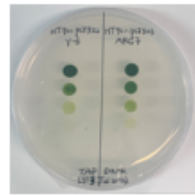
	Light	Dark
TAP		
TAP with 300 μM L-Arginine		

Figure 6.7 Phenotype prediction (upper) and testing results (lower) of the chloroplast-expressed double-stranded Y-5 and ARG7 strains.

Upper panel: Predicted phenotypes if chloroplast-expressed dsRNA silenced nuclear genes, with columns distinguishing strains (first column: Y-5 transformant, second column: ARG7 transformant, optional third column: parental HT72 control strain) and rows distinguishing light conditions (Light vs. Dark); media types are shown on the left (TAP, TAP with 300 μ M L-

Arginine). For Y-5 transformants (first column), predicted phenotypes include green growth in TAP under light, "yellow-in-the-dark" (due to impaired chlorophyll biosynthesis) in TAP under dark, and the same light/dark phenotypes in TAP + L-Arginine; for ARG7 transformants (second column), predicted phenotypes include no growth in TAP (light/dark, due to arginine auxotrophy) and normal growth in TAP + L-Arginine (light/dark); the control (if present) shows parental HT72's baseline traits (e.g., green in light, no yellow-in-dark, arginine auxotrophy in TAP). Lower panel: Actual test results of the same strains (column assignments match upper panel: first column Y-5 transformant, second column ARG7 transformant) across the same media (left) and light conditions (rows), showing no silencing phenotypes (e.g., Y-5 remains green in dark, ARG7 grows in TAP without L-Arginine).

The actual results provide no evidence of dsRNA escape to the cytoplasm leading to gene silencing. On TAP medium under light conditions, both the Y-5 and Arg7 transformants showed normal growth, contrary to the hypothesis that the ARG7 line would not grow due to its requirement for arginine. This indicated that the ARG7 dsRNA was confined within the chloroplast. Similarly, under dark conditions, Y-5 was expected to exhibit a yellow-in-the-dark phenotype due to the accumulation of protochlorophyllide (Pchl_{id}) and the inability to synthesize chlorophyll. However, the results showed that the Y-5 strain like ARG7, grew normally and remained green, further suggesting the confinement of dsRNA within the chloroplast. The results strongly indicate that the dsRNA remains confined within the chloroplast, preventing it from triggering gene silencing of nuclear-encoded genes, unlike gene silencing mediated from nuclear-encoded interfering RNAs (Schroda, 2006). This experimental evidence underscores the importance of considering intracellular barriers and transport or escape mechanisms when designing and interpreting gene-silencing experiments in microalgae.

The potential confinement of dsRNAs within the chloroplast - pending confirmation that dsRNA is indeed present in the organelle (e.g., via chloroplast fractionation with dsRNA-specific RT-PCR or in vivo visualization using RNA aptamers like Spinach) -

—has significant implications for the application of dsRNA-expressing strains in various biotechnological fields. If verified, chloroplasts would provide a protective environment that shields dsRNA from degradation by cytoplasmic ribonucleases, thus preserving the integrity and functionality of dsRNA-based therapeutics. This stability is crucial for maintaining the therapeutic potential of dsRNA when algal cells are consumed by animals, as the organelle's double membrane would prevent premature breakdown before the dsRNA reaches the target site. The use of whole algal cells as a natural delivery system for dsRNA eliminates the need for complex purification and encapsulation processes, reducing production costs and simplifying administration. Moreover, the stability of chloroplast-localised dsRNA within chloroplasts can enhance the efficacy of gene silencing or antiviral treatments, as the protective environment ensures that the dsRNA remains intact until it reaches the target site within the animal's body. This approach, contingent on confirming dsRNA's chloroplast localization, holds promise for sustainable and effective disease management in aquaculture and agriculture, leveraging the unique properties of chloroplast-expressed dsRNA.

To further confirm the expression of dsRNA within the chloroplast and its confinement, additional experiments could be conducted using fluorescent reporter tools, such as RNA aptamers, which were mentioned in section 6.2.4. This method would provide dynamic and real-time visualization of dsRNA localization within the chloroplasts (Guzmán-Zapata et al., 2017). Another approach could involve chloroplast fractionation followed by RNA extraction and RT-PCR to specifically detect dsRNA in chloroplast fractions, ensuring that dsRNA is localized within the chloroplasts (Charoonnart et al., 2019, 2023).

6.2.4 Quantification methods of dsRNA yield in *C. reinhardtii*

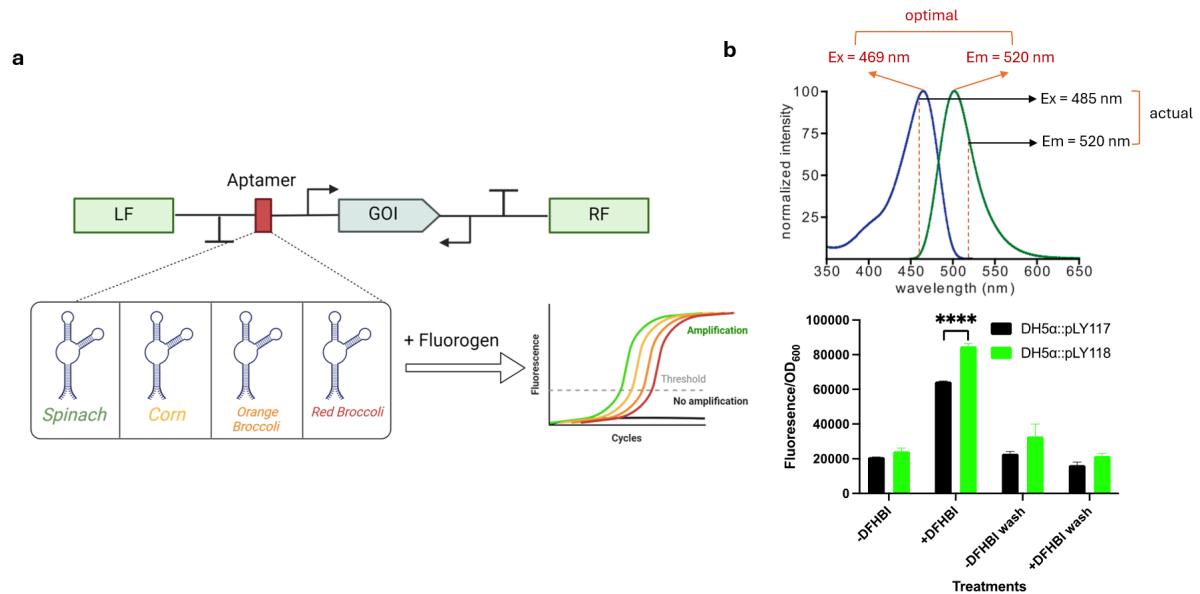


Figure 6.8 Chloroplast-expressed aptamer-integrated double-stranded RNA expressing systems and fluorescent assay.

Figure 6.8 illustrates the design and functionality of an aptamer-tagged double-stranded RNA (dsRNA) expressing system in *Escherichia coli*, along with the results from a fluorescent assay used to detect and quantify dsRNA production.

(a) Design of Aptamer-tagged dsRNA Expressing System

The gene construct used for expressing aptamer-tagged dsRNA within *E. coli* includes several key components necessary for its function. The construct integrates various RNA aptamers such as Spinach, Corn, Orange Broccoli, and Red Broccoli into the sequence, designed to specifically bind to corresponding fluorogens to form a fluorescent complex. This construct also includes the gene of interest (GOI) encoding the dsRNA targeted for expression. When fluorogens are added to the system, they bind to the aptamers, causing a fluorescence signal that indicates the presence and

level of dsRNA expression. The schematic amplification plot shows the increase in fluorescence signal during the assay, with a threshold indicating the point of detectable dsRNA.

(b) Fluorescent Assay Results

The fluorescence spectrum shows the normalized intensity of fluorescence as a function of wavelength, highlighting the optimal and actual excitation (Ex) and emission (Em) wavelengths used in the assay. The optimal wavelengths are Ex = 469 nm and Em = 520 nm, while the actual wavelengths used in the experiment were Ex = 485 nm and Em = 520 nm. The bar graph below the spectrum displays the fluorescence intensity (normalized to OD₆₀₀) for different treatments and strains. Two strains, DH5 α ::pLY117 (represented by black bars) and DH5 α ::pLY118 (represented by green bars), were tested under various conditions, including the presence and absence of the fluorogens DFHBI. The "+DFHBI Wash" condition indicates samples where DFHBI was added and then washed out, assessing the stability of the fluorescence signal.

During the methodology optimization, the concentration of the fluorogens DFHBI to be applied emerged as a critical issue. The experiments revealed significant differences in fluorescence intensity between the control and testing strains, particularly in the presence of DFHBI without washing. These results suggest effective aptamer-fluorogens interactions and successful dsRNA expression. However, it is essential to consider potential technical errors that could contribute to these differences. Ensuring consistent and uniform addition of DFHBI to all samples is crucial to avoid

discrepancies in fluorescence signals. Proper calibration of fluorescence detection instruments before measurements is also necessary to prevent inaccuracies. Additionally, data normalization to OD₆₀₀ must be performed correctly to account for variations in cell density, ensuring accurate comparisons across samples.

Despite these considerations, the significant fluorescence observed in the +DFHBI without washing condition strongly supports the effectiveness of the aptamer-fluorogens system in detecting dsRNA expression. The next steps should involve further optimization of DFHBI concentration to determine the minimal, yet effective amount required for reliable fluorescence detection. Additionally, exploring the dynamic range and sensitivity of the aptamer-fluorogen interaction can provide deeper insights into the system's robustness and potential limitations.

6.3 Discussion

Recent advances in the use of double-stranded RNA have opened promising avenues in various fields, including gene silencing, pest control, and therapeutic applications. This chapter focused on utilizing dsRNA in the model organism *C. reinhardtii*, emphasizing the potential of engineered chloroplast systems for efficient dsRNA production. Despite substantial progress, several challenges remain, including optimizing dsRNA length, understanding gene-silencing mechanisms, and enhancing dsRNA yield through innovative expression systems. This discussion explores these challenges, outlines potential future directions, and considers the broader implications of a dsRNA platform.

6.3.1 Optimizing dsRNA length and multiple dsRNA Constructs

One critical factor affecting dsRNA efficacy is its length, which influences both stability and silencing efficiency. Studies indicate that dsRNA length can impact its uptake by cells, degradation rate, and the effectiveness of the RNA interference (RNAi) response (Tenllado et al., 2003; Yang et al., 2002). While shorter siRNAs (21-25 bp) are traditionally considered the most effective triggers for RNAi, recent work suggests that longer dsRNAs, especially those over 200 bp, may increase stability and persistence, particularly in complex systems (Huvenne & Smagghe, 2010). In *C. reinhardtii*, further research into the optimal dsRNA length for chloroplast expression systems is needed, as longer dsRNA molecules could enhance gene silencing effects but may also increase the risk of degradation or off-target effects. Additionally, the potential of expressing multiple dsRNAs targeting different genes simultaneously could be explored, as this approach may offer more comprehensive gene silencing for applications such as pest control or viral resistance. However, expressing multiple dsRNAs may present challenges in terms of stability and the chloroplast's capacity for dsRNA production, necessitating further investigation into the engineering of chloroplast genomes and transcriptional machinery (Dalakouras et al., 2016).

6.3.2 Gene-silencing mechanisms and the role of dsRNA under stress conditions

In plants and algae, dsRNA triggers gene silencing through a pathway involving Dicer-like enzymes that cleave dsRNA into small interfering RNAs (siRNAs), which then guide the RNA-induced silencing complex (RISC) to complementary mRNA targets,

resulting in degradation (Baulcombe, 2004). While dsRNA-induced silencing has been well-documented in several organisms, the specific gene-silencing mechanisms in *C. reinhardtii* remain partially understood, particularly for nuclear-encoded genes. In the present study, dsRNA production in chloroplasts was utilized to potentially silence nuclear-encoded genes; however, further analysis is necessary to confirm the mechanisms and pathways involved.

Additionally, the role of dsRNA in gene silencing under stress conditions warrants further investigation. Stress factors, such as oxidative stress or nutrient deficiency, can affect gene expression patterns and the RNAi pathway, potentially altering dsRNA efficacy or stability (Baulcombe, 2004). In *C. reinhardtii*, understanding how stress impacts dsRNA-induced silencing is crucial, as environmental stress is common in both natural and industrial settings. Collaborative research with specialists in RNAi and stress physiology would be valuable to dissect these mechanisms, providing insights into the robustness and reliability of chloroplast-derived dsRNA under varying environmental conditions.

6.3.3 Enhancing dsRNA yield with *psaA*** expression system

A promising direction for increasing dsRNA production in *C. reinhardtii* involves developing a novel expression system based on the new, synthetic promoters. The 'psaA** plus dsRNA' system aims to boost dsRNA yield by leveraging alternative promoters that out-perform the *rns* promoter used in this work. By coupling this with optimized dsRNA constructs, this approach could significantly increase dsRNA levels, enhancing the effectiveness of gene silencing applications. Such a system would be

particularly beneficial for large-scale applications, where high dsRNA output is essential, such as in bioinsecticide production or antiviral therapies. Future work should focus on testing this system across different strains and environmental conditions to assess its effectiveness and stability. Additionally, optimizing the dsRNA structure and processing within chloroplasts will be necessary to maximize yield and minimize degradation.

6.3.4 Broad Implications of a dsRNA Platform

The development of a robust dsRNA platform in *C. reinhardtii* holds vast potential beyond the model organism itself. A chloroplast-based dsRNA production system offers an eco-friendly and scalable method for generating dsRNA, which could have diverse applications in agriculture, environmental biology, and medicine.

One major application lies in the use of dsRNA as a biopesticide. Traditional pesticides are often associated with environmental damage and the development of resistance in target pests. By contrast, dsRNA-based pesticides provide a highly specific mode of action, as dsRNA can be designed to target specific genes in pest species, minimizing off-target effects on non-target organisms and reducing environmental impact (Baum et al., 2007; Gordon & Waterhouse, 2007). Recent research has shown that dsRNA-based pesticides can effectively control agricultural pests, such as the Colorado potato beetle and Western corn rootworm, without harming beneficial insects (Xue et al., 2012). Using *C. reinhardtii* as a platform to produce these dsRNA-based pesticides could lower production costs and provide a renewable source of pest control agents.

Another promising area is in mosquito and insect research, particularly in controlling vector-borne diseases. Mosquito-borne diseases, such as malaria and dengue, continue to pose significant public health challenges worldwide. dsRNA can be used to silence genes critical for mosquito survival, reproduction, or disease transmission (Gordon & Waterhouse, 2007). By producing mosquito-specific dsRNA in *C. reinhardtii*, this approach could offer a novel method for population control of mosquito larvae or for reducing their capacity to spread pathogens (Kumar et al., 2013). Additionally, as chloroplast-derived dsRNA is relatively stable, it could be administered in outdoor environments, making it suitable for field applications in vector control.

In a more novel application, dsRNA could be used in tardigrade research. Tardigrades are microscopic animals known for their remarkable ability to survive extreme conditions, including desiccation and radiation. Studying dsRNA-based gene silencing in tardigrades could offer insights into the genetic basis of their resilience, with implications for understanding stress tolerance mechanisms in other organisms (Tenlen et al., 2013). Leveraging *C. reinhardtii* to produce tardigrade-specific dsRNA would provide a renewable and flexible tool for investigating the genes responsible for tardigrade survival strategies, opening new avenues in extremophile biology.

Chapter 7

Final discussion

7 Final discussion

7.1 Summary of main findings

This thesis presents advances in chloroplast engineering using *Chlamydomonas reinhardtii* and their application to produce high-value recombinant products such as fish growth hormone (fGH), spider silk proteins, and double-stranded RNA (dsRNA)-based therapeutics. These advances support the overarching objective of demonstrating *C. reinhardtii*'s utility as a scalable, sustainable bio-factory for diverse biotechnological applications (Einhaus et al., 2024; Liang et al., 2023). The main results of this thesis are summarised as follows:

- **Creation and validation of *psaA***:** The *psaA*** strain was designed as a marker-free transgenic line in which two tryptophan codons (TGG) within the *psaA* gene of Photosystem I are changed to the unused TGA stop codon. This would allow a modified tRNA-Trp gene (*trnW^{UCA}*) to be used as a small, portable and endogenous marker for chloroplast transformation, with selection based on phototrophic rescue due to translational readthrough of the UGA's within the *psaA* mRNA as tryptophan codons. The *psaA*** strain was successfully created and shown to be a stable, homoplasmic line as confirmed by genotyping (PCR analysis, diagnostic enzyme analysis and sequencing) with the expected non-photosynthetic phenotype as determined by growth analysis under different trophic modes. Its application as a recipient line was demonstrated by using the *trnW^{UCA}* marker to introduce the nLuc reporter gene. Furthermore, it was shown that *trnW^{UCA}* could support the translational readthrough of the reporter gene if

UGA stop codons are present within the coding sequence. Consequently, this small gene can serve both as a portable marker for antibiotic-free selection and as a system for biocontainment of introduced transgenes.

- **Expression of fish growth hormone (fGH):** Two different fGH were successfully expressed in *C. reinhardtii* chloroplasts and the whole algal biomass used in preliminary feeding trials using shrimp larvae. Whilst no significant growth improvement was seen – possibly due to degradation of the fGH in the gut or a lack of activity of these fish hormones in shrimp tissue – the work underscores the potential application of such oral delivery in aquaculture, offering a low cost and simple method for producing and administering bioactive hormones for enhanced fish growth and development.
- **Production of recombinant spider silk:** Recombinant production of large proteins such as spidrions that contain multiple repeats of a peptide module presents particular challenges, both in synthetic gene construct an efficient expression without depletion of pools of specific amino acids. The work presented in chapter 5 showed that a modified Golden Gate assembly method could be used to build genes with multiple modules, and delivery of these into the chloroplast allowed the synthesis of spidrions with at least six repeats. This initial work demonstrates the potential of the algal chloroplast as a platform for production of repetitive proteins that have applications as sustainable biomaterials.
- **dsRNA-based therapeutics:** The chloroplast not only represents an attractive chassis for synthesis of recombinant proteins, but also novel RNA molecules. In chapter 6, the synthesis of long double-stranded RNA (dsRNA) that can be used as therapeutics for targeted gene silencing via RNAi. The work shows that *C.*

reinhardtii is an efficient platform for scalable dsRNA production, leveraging its chloroplast genome's high copy number, high transcriptional activity, and the stable accumulation of long dsRNAs. As with the protein vaccines, the dsRNAs could be delivered orally to shrimp and fish to either silence viral gene expression before a viral infection becomes established (e.g. White Spot Syndrome Virus infection in shrimp aquaculture) or silence host genes associated with susceptibility to viral or bacterial pathogens (add Carlos' review on Rab7).

7.2 Further research

7.2.1 Future directions of psaA** system

Building on recent thesis findings, several targeted enhancements could optimize the psaA** expression system in *C. reinhardtii* for a wider range of applications. The psaA** system has shown promise in expressing recombinant proteins in chloroplasts, and further developments could unlock its potential for diverse biotechnological uses. Future work should investigate its versatility for producing advanced recombinant proteins, therapeutic RNA molecules, and high-performance biomaterials. For example, proteins like fish growth hormones and complex biomaterials like spider silk could be efficiently produced using the psaA** system, catering to biomedicine, agriculture, and sustainable manufacturing. Click or tap here to enter text.

Combining an inducible promoter system for the GOI with the psaA** system would offer enhanced control over transgene expression, enabling protein synthesis to be initiated only under specific conditions. This strategy is particularly advantageous when producing complex or high-demand biomolecules such as spidrons, as it

reduces unnecessary metabolic burden on cells and minimizes the risk of growth inhibition due to continuous protein production (Young & Purton, 2018). Robust inducible promoter systems have yet to be developed for the algal chloroplast as none of the ~35 promoters on the plastome is specifically regulated through transcriptional suppression/activation, unlike the situation in bacteria. An early attempt to incorporate the bacterial Lac repressor/IPTG system into a *C. reinhardtii* chloroplast promoter was only partially successful with some leakiness under non-induced conditions. Recently, an effective system for regulating transgenes at the translational level has been developed. This system targets the functioning of specific 5'UTR elements from *rbcL* or *psbD* through the vitamin-regulated expression of nuclear transgenes encoding endogenous protein factors, Mrl1 and Nac2, that specifically bind these respective 5'UTR, and are required for translation (Mordaka et al., 2024). Combining this system with the *psaA***/*trnW* selection system would require re-introducing the TGA stop codons into *psaA* in the nuclear-engineered strains but would allow marker-free transformation and tight regulation of GOI through the addition/removal of micromolar amounts of thiamine or vitamin B₁₂ to the media (Mordaka et al., 2024). This would make *psaA*** a versatile platform for a range of applications.

The *psaA*** system, initially developed as a versatile, marker-free system for high-level expression of recombinant proteins in *C. reinhardtii*, also holds considerable potential for advancing photosynthetic research through manipulations of *psaA* expression and PsaA structure. The *psaA* gene encodes a core component of PSI, a major protein complex in chloroplasts responsible for the initial stages of light energy conversion. The biogenesis of PSI is dependent on efficient synthesis of PsaA, and indeed the assembly of the complex involves an assembly-governed regulation where the rate of

synthesis of PsaA is dependent on the presence of its partner subunit, PsaB, and the rate of synthesis of PsaC is dependent on the presence of PsaA (Wostrikoff et al., 2004). Since a temperature-sensitive version of trnW^{UCA} has been developed where the tRNA is non-functional at the higher temperature (Young & Purton, 2016), then the PsaA** strain could be used to explore this assembly process by manipulating the synthesis of PsaA using a temperature switch. Similar Trp->Stop codon changes in other photosystem genes could similarly be used to turn on/off the biosynthesis of a target subunit using temperature, allowing detailed studies of complex biogenesis using a single strain.

Furthermore, the tryptophans targeted in the PsaA** strain are known to be critical for the binding and redox state of the phylloquinone electron acceptor (Ali et al., 2006; Purton et al., 2001). The strain could therefore be used to study these processes further if non-canonical amino acids (ncAA) such as hydroxy-tryptophan were introduced at these positions. Research to introduce such ncAA systems into the chloroplast where an orthogonal tRNA charged with a ncAA recognises the UGA stop codon are being explored in the Purton group.

7.2.2 Future direction of fish growth hormone (FGH)

To advance the application of chloroplast-engineered microalgae for oral delivery of fish growth hormone (FGH) in aquaculture, further research is essential, particularly to understand the hormone's stability, production levels, and digestibility. This research will enable the optimization of production conditions and dosing strategies, while also exploring the potential of other microalgal species as production hosts.

The stability of chloroplast-produced FGH under aquaculture-like conditions is critical. The hormone must remain active across a range of temperatures and pH levels typical of aquaculture environments. Stability studies at varied temperatures (e.g. 18°C-28°C) and pH levels (6.5-8.0) will help ensure that the hormone retains its efficacy when integrated into fish feed, thereby promoting consistent growth rates in aquaculture. A pertinent reference on this topic is the study by Barry et al. (2007), which investigated the stability of 17 α -methyltestosterone (MT) in fish feed under different storage conditions. The researchers found that MT concentrations remained stable for several months when feed was stored at 4°C or lower, but declined linearly at higher temperatures, with half-lives of 1.1 and 4.8 months at 40°C and 22°C, respectively (Barry et al., 2007). Moreover, this stability testing should account for fluctuations that may occur in open aquaculture settings, providing a realistic assessment of FGH durability.

Quantifying FGH production in the algal biomass is necessary for establishing effective dosage levels for fish feed applications. Protein production analysis, coupled with dosage trials using dried biomass, will provide insights into the required amount of FGH per unit of fish body weight. Establishing optimal doses will maximize growth benefits while reducing production costs (Moriyama et al., 2000). Standardized assays for measuring protein yield per gram of algae will be instrumental in defining practical dosage recommendations.

Digestibility is another crucial factor, especially given that algal cell walls can impact nutrient bioavailability. Trials comparing cell wall-containing and cell wall-deficient *Chlamydomonas* strains are essential to determine which variant allows for the better

nutrient absorption in fish and shrimp. Collaborating with aquaculture experts specializing in shrimp and fish nutrition can further validate the digestibility of FGH in these models (Pulz & Gross, 2004). Effective digestibility could potentially reduce feed conversion ratios, enhancing the economic viability of using FGH in commercial aquaculture.

While *Chlamydomonas* has proven effective, alternative microalgal species, such as the diatom genus *Thalassiosira*, offer distinct advantages, including robust growth in marine conditions and potentially higher yields of fish growth hormone (FGH), as fish naturally feed on *Thalassiosira* (Tam et al., 2021). Future studies could explore diatom-based systems to broaden FGH production platforms, enabling tailored growth conditions for various aquaculture environments and potentially enhancing production flexibility and scalability.

7.2.3 Future directions of spider silk protein

Producing spider silk proteins in the chloroplast of *C. reinhardtii* offers an innovative approach to creating sustainable, bio-based materials. However, synthesising full-length spidrions and achieving sufficient yields remains a challenge, limiting the scope of current applications and analysis. To overcome this, future research should focus on optimizing expression systems, enhancing autotrophic growth conditions, and determining whether the isolated protein can be converted into silk fibres. These steps are expected to improve yield, stability, and functionality of spider silk proteins for broader applications.

Integrating the spider silk expression system with the psaA** platform could significantly enhance protein yield. As discussed above, the psaA** system could be further developed for high-level gene expression in *C. reinhardtii* chloroplasts, offering stable and efficient control of production. Moreover, the psaA** platform enables site-specific, marker-free expression, allowing transgenes for spider silk proteins to be targeted precisely within the chloroplast. This approach not only reduces the metabolic burden on *C. reinhardtii* cells, but also eliminates the need for antibiotic resistance markers, which can be problematic in large-scale applications. Marker-free systems are particularly advantageous as they meet regulatory standards for biosafety, especially in applications such as biomaterials for medical use or sustainable manufacturing.

Detailed analysis of spider silk fibre properties is essential for determining their potential applications in biomaterials. Properties such as tensile strength, elasticity, and biodegradability can vary depending on the protein's post-translational modifications and fibre formation process. Future experiments should focus on extracting, purifying, and spinning the silk proteins into fibres, followed by mechanical testing to assess these characteristics. Such characterization will allow for comparisons with natural spider silk, identifying areas for further refinement or potential applications.

7.2.4 Future directions of dsRNA platform

The development of double-stranded RNA (dsRNA) platforms in algal systems holds substantial potential for advancing both fundamental research and applied

biotechnology. By harnessing the RNA interference (RNAi) pathway, dsRNA platforms can be adapted for various applications, ranging from basic studies of developmental biology to pest control in the environment. Here, I outline the potential directions for improving the dsRNA platform, focusing on both integration with existing systems and specific applications in agriculture and beyond.

Firstly, Integrating the dsRNA expression system with the *psaA*^{**} chloroplast transformation platform offers exciting possibilities, yet initial experiments indicate challenges that need to be addressed. Preliminary trials aimed at producing transformant lines have thus far been unsuccessful. This possibly relates to the repeated occurrence of the same *rrnS* promoter element within the inverted repeat region of the plastome, and highlights the need for further experimentation with alternative regulatory elements. Specifically, testing different heterologous or synthetic promoter and terminator sequences, or even combinations of these, could enhance the synthesis of dsRNA in transformed cells. Stability of the dsRNA pool could also be improved through the use of cis elements known to limit ribonuclease activity. For example, terminal polyG elements have been shown to limit digestion of mRNAs by exonucleases in the *C. reinhardtii* chloroplast. By tailoring these genetic components to the *psaA*^{**} system, we may overcome current transformation challenges, thus opening new avenues for the application of dsRNA in algae.

Building on the versatility of RNAi-based gene silencing, the dsRNA expression platform offers extensive application possibilities. Below are potential uses in various fields:

- **Agricultural Pest Control:** One of the most promising applications of algal dsRNA is in sustainable agriculture. The dsRNA expression systems can target pest insect species such as the Colorado potato beetle (*Leptinotarsa decemlineata*), which has developed resistance to many traditional insecticides (Alyokhin et al., 2008; W. He et al., 2020; Rodrigues et al., 2021). By spraying crops with dried algae expressing dsRNA against an essential gene of the beetle (e.g. the actin gene) we can target this leaf-feeding insect without the need for producing transgenic crops engineered to produce a bioinsecticide. Ingestion of the algal powder would silence the essential gene, resulting in pest mortality without affecting non-target organisms (Rodrigues et al., 2021).
- **Neural Development in Tardigrades:** Tardigrades, known for their unique resilience, have recently become model organisms for studying neural development due to their distinct gene expression patterns and simple nervous system. Tardigrades naturally feed on freshwater algae such as *C. reinhardtii* and dsRNA-containing prey could be designed to knock down specific genes involved in neural development, providing a novel approach to study gene function in these microscopic animals (Tenlen, 2018). This could have implications for understanding neural development and resilience in broader biological contexts.
- **Mosquito Control and Research:** With the rising incidence of mosquito-borne diseases, dsRNA platforms could be applied in mosquito research and control. As in the case of tardigrades, mosquito larvae also feed on live microalgae. By designing dsRNA sequences that silence genes critical for mosquito survival or

reproduction, it may be possible to use algae as a bio-safe, sustainable control method that minimizes the environmental impact associated with conventional insecticides (Balakrishna Pillai et al., 2017).

- **Other Animals that Consume Algae:** Beyond targeted applications, dsRNA expression in algae presents a unique delivery method for animals that naturally feed on algae. Provided the target animal is able to take up the dsRNA from the gut into the tissue, and this then results in an RNA interference cascade, then oral delivery of a low-cost and bioencapsulated dsRNA payload represents an attractive general mechanism for silencing of gene targets. For example, aquaculture and controlled environments where algae serve as a primary food source could benefit from the integration of dsRNA for disease management or pest deterrence. Species-specific dsRNA could be tailored to target diseases or pests in these controlled ecosystems, enhancing productivity and health while reducing chemical inputs.

7.3 Concluding remarks

This thesis underscores the potential of chloroplasts as versatile bio-factories in various biotechnological sectors:

- **Therapeutics:** Chloroplast-produced proteins, such as fGH, could offer scalable solutions for therapeutic and aquaculture industries, reducing dependency on conventional protein production systems and advancing pharmaceutical biotechnology.

- **Agricultural Biotechnology:** The expression of dsRNA and other bio-pesticides in chloroplasts aligns with sustainable agriculture goals, providing pest management tools that are safer for ecosystems and more environmentally friendly than synthetic chemicals.
- **Industrial Biomanufacturing:** Chloroplast-based biomaterials, such as recombinant spider silk, can contribute to greener production methods across industries like textiles and medical devices. These advancements demonstrate the applicability of synthetic biology in environmental sustainability.

The research presented in this thesis advances our understanding of chloroplast engineering in *C. reinhardtii*, demonstrating its potential as a high-yield, marker-free production platform. These advancements contribute to synthetic biology by establishing new avenues for scalable, safe, and cost-effective recombinant protein production. This work underscores chloroplast engineering's transformative potential in creating sustainable biomanufacturing solutions. By advancing the *psaA*** platform, this thesis lays a foundation for future innovations that leverage synthetic biology to address challenges across health, agriculture, and environmental sustainability.

Appendices

Appendices

Appendix 1 Composition of Tris-acetate-phosphate (TAP) medium modified from (Gorman and Levine, 1965; Harris, 2009)

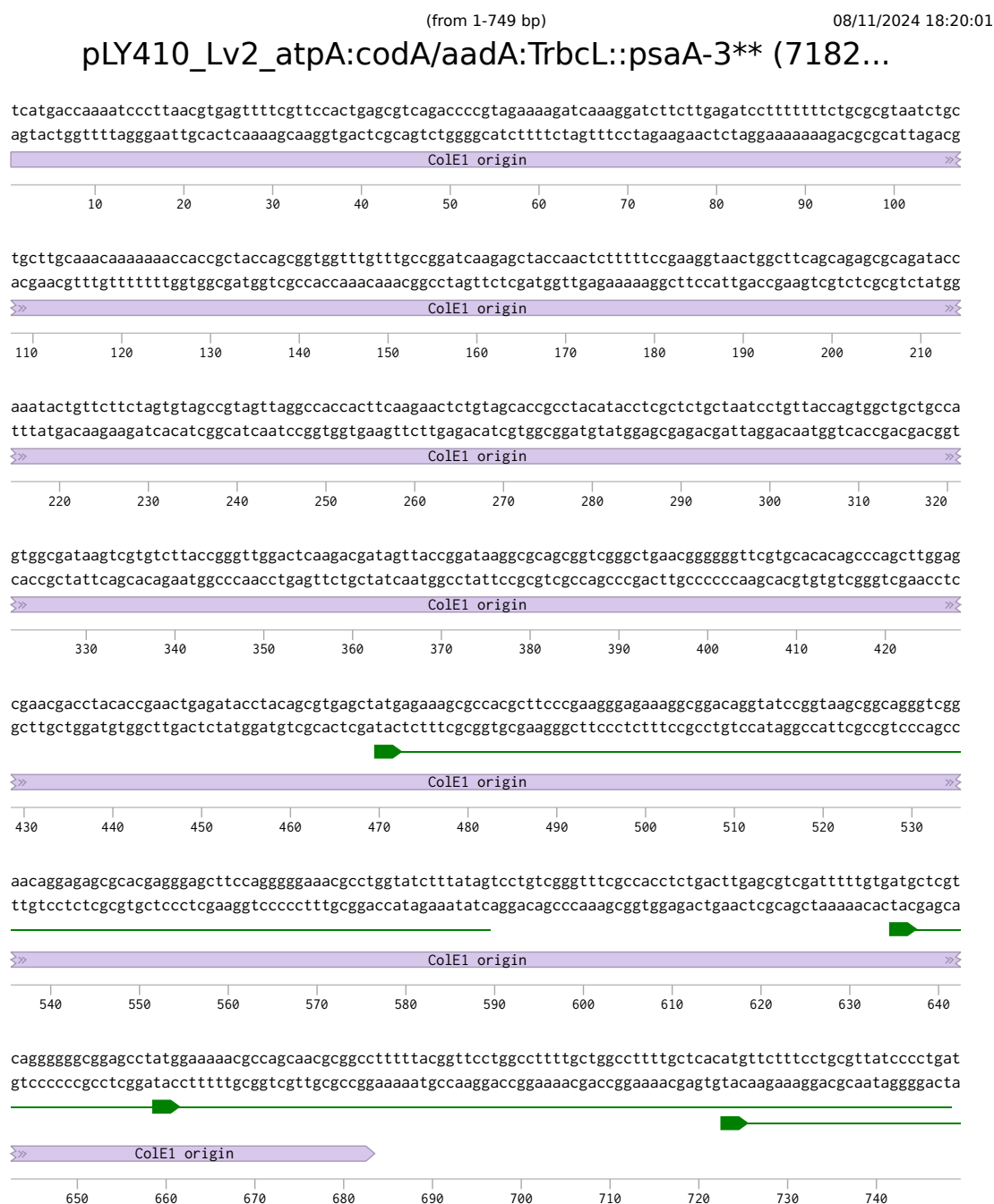
Component	Concentration (per liter)
Tris (Tris base)	2.42 g (20 mM)
Acetic acid (glacial)	1.0 mL (17.4 mM)
NH ₄ Cl	0.375 g (7 mM)
MgSO ₄ ·7H ₂ O	0.1 g (0.4 mM)
CaCl ₂ ·2H ₂ O	0.05 g (0.34 mM)
K ₂ HPO ₄	0.288 g (1.65 mM)
KH ₂ PO ₄	0.144 g (1.06 mM)
Trace elements (Hutner's)	1 mL
Optional: Fe-EDTA	20 µM
Final pH	Adjust to 7.0 with HCl or NaOH

Appendix 2 Composition of Sueoka high-salt (HSM) medium modified from (Harris, Stern and George N., 2009)

Component	Concentration (per liter)
NH ₄ Cl	0.375 g (7 mM)
MgSO ₄ ·7H ₂ O	0.1 g (0.4 mM)
CaCl ₂ ·2H ₂ O	0.05 g (0.34 mM)
K ₂ HPO ₄	0.288 g (1.65 mM)
KH ₂ PO ₄	0.144 g (1.06 mM)
NaCl	2.0 g
Tris (Tris base)	1.21 g (10 mM)
Trace elements (Hutner's solution)	1.0 mL
Final pH	Adjust to 7.0 with HCl

Appendix 3 DNA sequence of plasmid pLY410 (for making *psaA***)

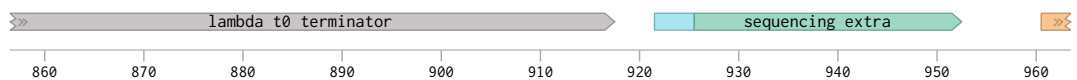
Sequence link: <https://benchling.com/s/seq-ZuSAhJcpxFfo789C4Vuh?m=slm-nCgT6kz9F5t0RiGXe7fp>



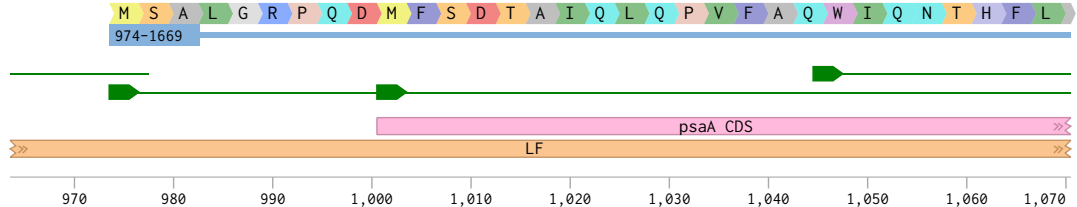
tctgtggataaccgtattaccgcctttgagtgagctgataccgtcgcgcgagccgaacgaccgagcgcttggactcctgttgatagatccagtaacacctcaga
agacacctattggcataatggcggaactcactcgactatggcgagcggtcggttgcgtgcgcgaacctgaggacaactatctaggtcattactggagctct



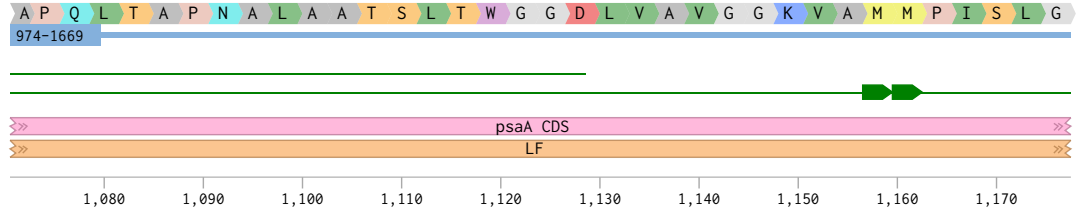
actccatctggattgttcagaacgctcggttccgcccggcggtttttattggtgagaatCCAGtggtCAGCCACAACGATACAATGAGTCAGCTCTTCCCAGCCA
tgaggtagacctaacaagtcttgcgagcaacggcgccgcaaaaaataaccactcttaGGTCacacGTCGGTGTGCTATGTTACTCAGTCGAGAAGGTCGGT



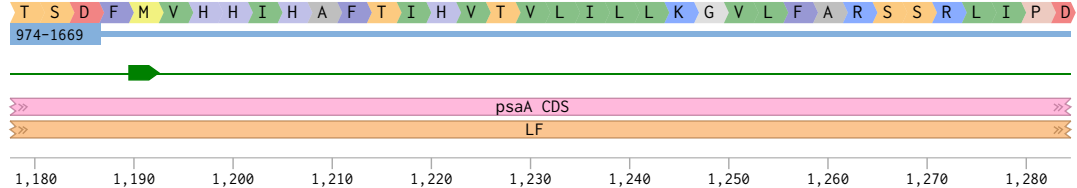
CAACGATACAATGAGTGCTTTAGGTCGTCCTCAAGACATGTTCTCAGATACTGCTATCCAACCTCAACCAGTATTTGCTCAATGGATTCAAATACACACTTCTTAG
GTTGCTATGTTACTCAGCAATCCAGCAGGAGTTCTGTACAAGAGCTATGACGATAGTTGAAGTTGGTCATAAACGAGTTACCTAAGTTTTATGTGTGAAGAATC

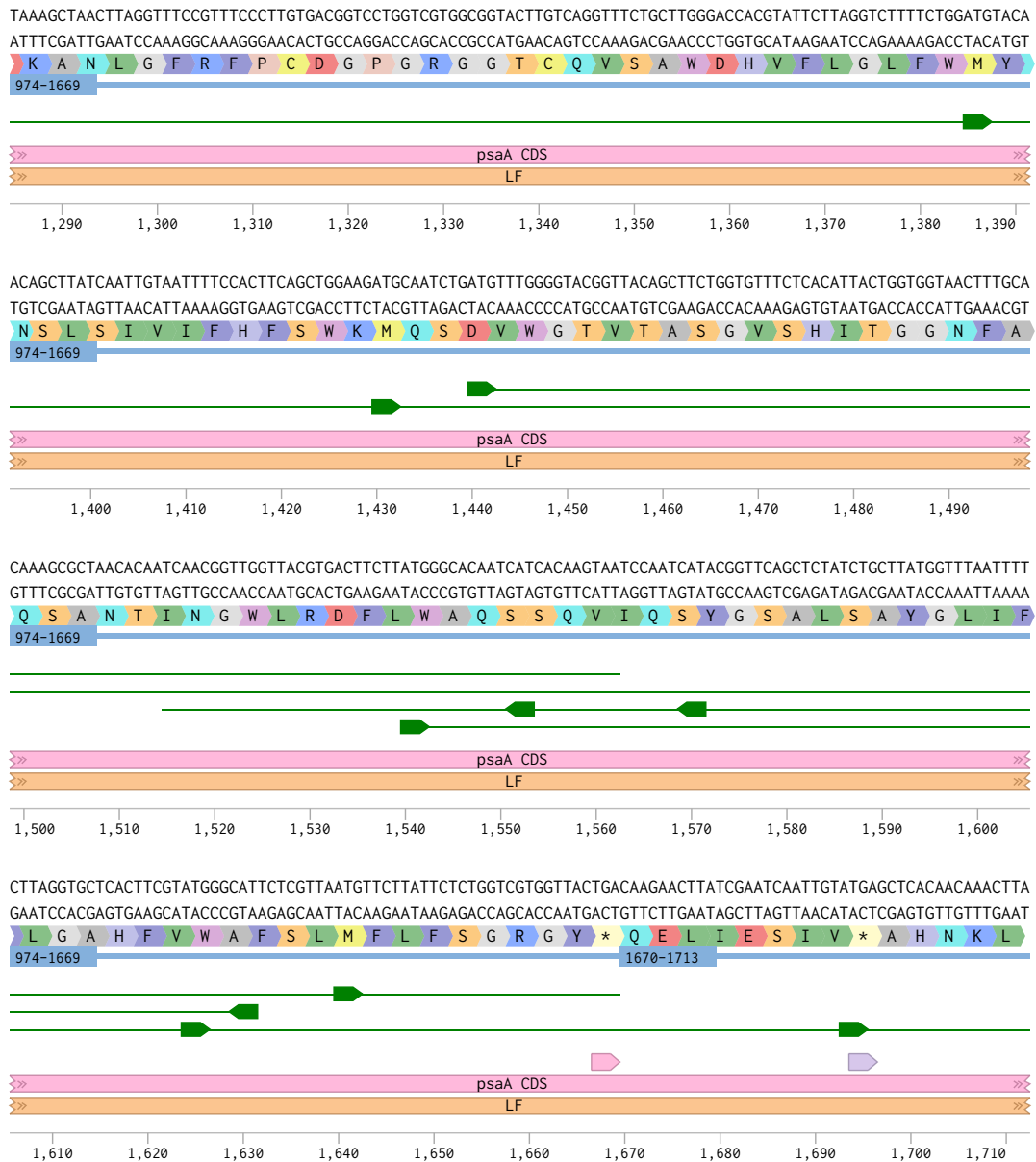


CTCCACAATTAAACAGCACCAATGCTTTAGCTGCTACAAGTTTAACTTGGGGTGGTGATTAGTTGCTGTTGGCGGTAAAGTAGCTATGATGCCTATTTCTTTAGGT
GAGGTGTTAATTGTCGTGGTTTACGAAATCGACGATGTTCAAATTGAACCCCAACCTAAATCAACGACAACGCCATTTCATCGATACTACGGATAAAGAAATCCA

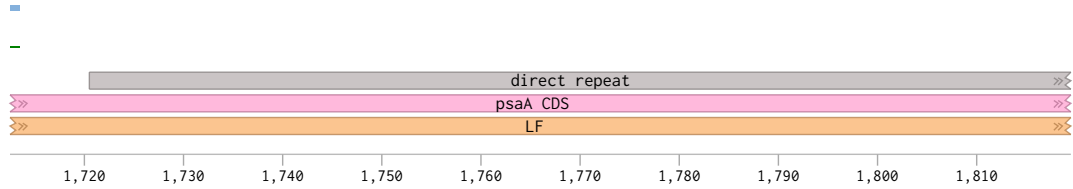


ACTTCTGACTTTATGGTTACCAACATTACGCTTTTACAATTACGTAACGTGTTAATTTCTTCTGAAAGGTGTTTATTTGCTCGTAGCTCTCGTCTTATCCAGA
TGAAGACTGAAATACCAAGTGGTGAAGTGCAGAAAGTGTAAAGTGCAATTGACACAATTAAAGAGACTTTCCACAAAATAACGAGCATCGAGAGCAGAATAGGGTCT

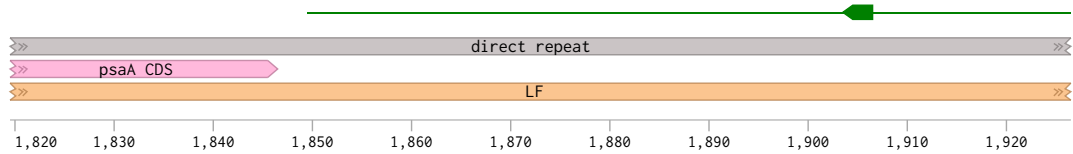




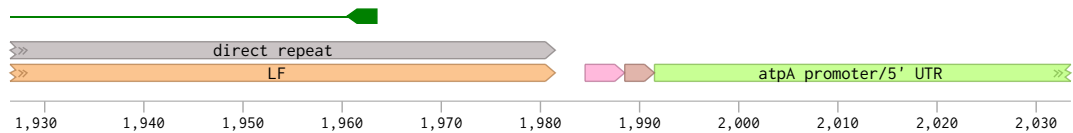
AAGTTGCACCTGCAATTCAACACGTCGCTTTAAGTATTACTCAAGGTCGTGCTGTTGGTGTAGCTCACTACCTTTTAGTGGTATTGCTACTACATGGTCGTTCTTC
TTCACGTGGACGTTAAGTTGGTGCACGAAATTCATAATGAGTTCAGCAGCACAACACATCGAGTGATGGAAAAATCCACCATAACGATGATGACCAGCAAGAAG



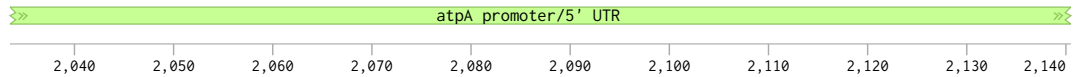
TTAGCAGTATCATTCTGTAGGTTAACATTTAATACTTTTTAATACATATATGCCTAAGTTTATCTTTAAAGATAAAGTATGCCATATGTTTAAGTTATCTAACA
AATCGTGCATAGTAAAGACATCCAATTGTAAATTATGAAAAATTATGTATATACGGATTCAAATAGAAATTTCTATTGTAATCGGTATACACAATTCAATAGATTGT



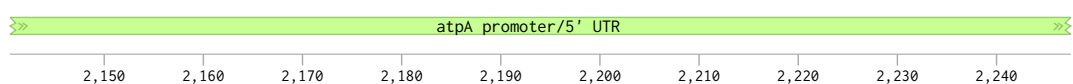
AGGTTACCTTTTTATTCTCTTTAGATATATAACATTAACCTACCGTGATCGGGAGGAGCAGACGCGTCTCCAATATAGTAGACTTTATTAGAGCAGTGTTTA
TCCAATGGAAAAATAAGAGAAATCTATATTTGTAATTTTGATGGCACTAGCCCTCTCGTCTGCGCAGAGGTTATCATCTGAAATAATCTCCGTCACAAAT



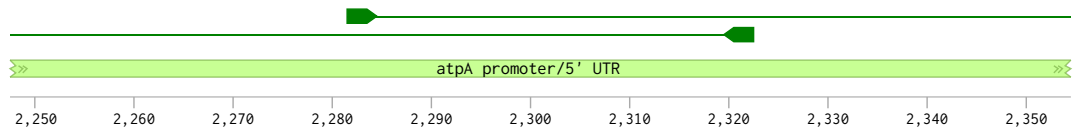
TATACCATAAACGCTCAAAAGTCATTTTATAACTGGATCTCAAAATACCTATAAACCCATTGTTCTTCTCTTTAGCTCTAAGAACATCAATTTATAAATATATTT
ATATGGTATTTCAGTATTTTCAGTAAAAATTTGACCTAGAGTTTATGGATATTGGGTAACAAGAAGAGAAAAATCGAGATTCTTGTTAGTTAAATATTATATAAA



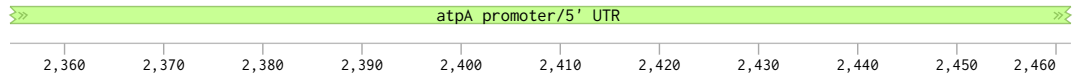
ATTATTATGCTATAATATAAATACTATATAAATACATTTACCTTTTTATAAATACATTTACCTTTTTTTAATTTGCATGATTTTAAATGCTTATGCTATCTTTTTTA
TAATAATACGATATTATATTTATGATATATTTATGTAATGGAAAAATTTATGTAATGGAAAAAAATTAACGTAATAAATACGAATACGATAGAAAAAT



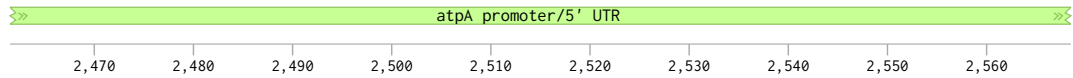
TTTAGTCCATAAAACCTTTAAAGGACCTTTTCTTATGGGATTTTATATTTTCTCAACAAAGCAATCGGCGTCATAAATTTAGTTGCTTACGACGCTGTGGACGT
AAATCAGGTATTTTGGAAATTTCTGAAAAAGAAATACCTATAAATATAAAGGATTGTTTCGTTAGCCGAGTATTTGAAATCAACGAATGCTGCGGACACCTGCA



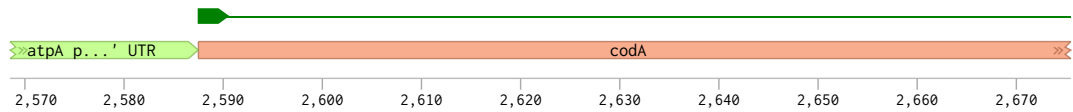
CCCCCCTTCCCTTACGGGCAAGTAACTTAGGGATTTAATGCAATAATAAATTTGCTCTTTCGGGCAAATGAATTTTAGTATTTAAATATGACAAGGGTGAA
GGGGGGGAAGGGAATGCCCGTTTCATTGAAATCCCTAAATTTACGTTATTTATTTAAACAGGAGAAGCCCGTTTACTTAAAAATCAAAATTTATACGTTCCCACTT



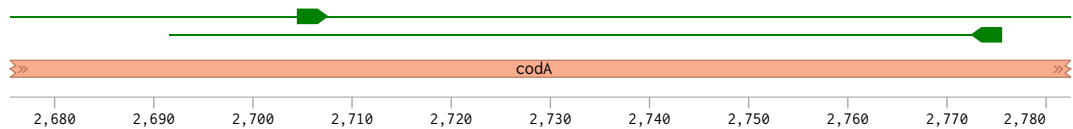
CCATTACTTTTGTTAAACAAGTGATCTTACCACTCACTATTTTGTGAATTTTAACTTATTTAAATTTCTCGAGAAAGATTTTAAAAATAAATTTTAACTTTTAACTTTT
GGTAATGAAAACAATTTGTTCACTAGAATGGTGAGTGATAAAAACAACCTTAAATTTGAATAAATTTTAAAGAGCTCTTCTAAATTTTATTTGAAAAATTAGAAA



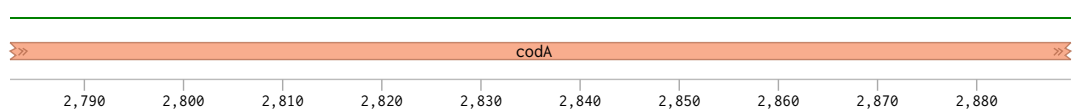
TATTTATTTTTCTTTTTATGtctaacaacgctttacaacAATTATTAACGCTCGTTTACCAGGTGAAGAAGTTTATGGCAAATTCACCTTACAAGACGGTAAAA
ATAATAAAAAAGAAAAATACagattgttgcaaatgtttgTTAATAATTGCGAGCAATGGTCCACTTCTCCAAATACCGTTTAAAGTGAATGTTCTGCCATTTT



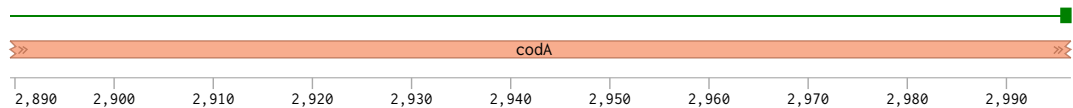
TTTCAGCTATTGATGCTCAATCTGGTGAATGCCAATTACTGAAACTCTTTAGATGCTGAACAAGGTTTAGTTATTCCACCATTGTTGAACCACACATTCACCTTA
AAGTCGATAACTACGAGTTAGACCACATTACGGTTAATGACTTTTGAGAAATCTACGACTTGTCCAAATCAATAAGTGGTAAGCAACTGGTGTGAAGTGAAT



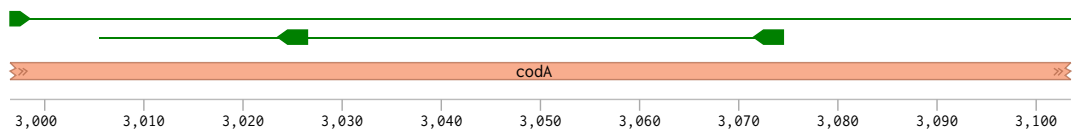
GATACTACACAACAGCTGGTCAACCAACTGGAACCAATCAGGTACTTTATTTGAAGGTATTGAGCGTTGGGCTGAACGTAAGCTTTATTAACACACGACGACGT
CTATGATGTGTTTGTGACCAAGTTGGTTGACCTTGGTTAGTCCATGAATAAACTTCCATAACTCGCAACCCGACTTGCATTTTCAAATAATGTGTGCTGCTGCA

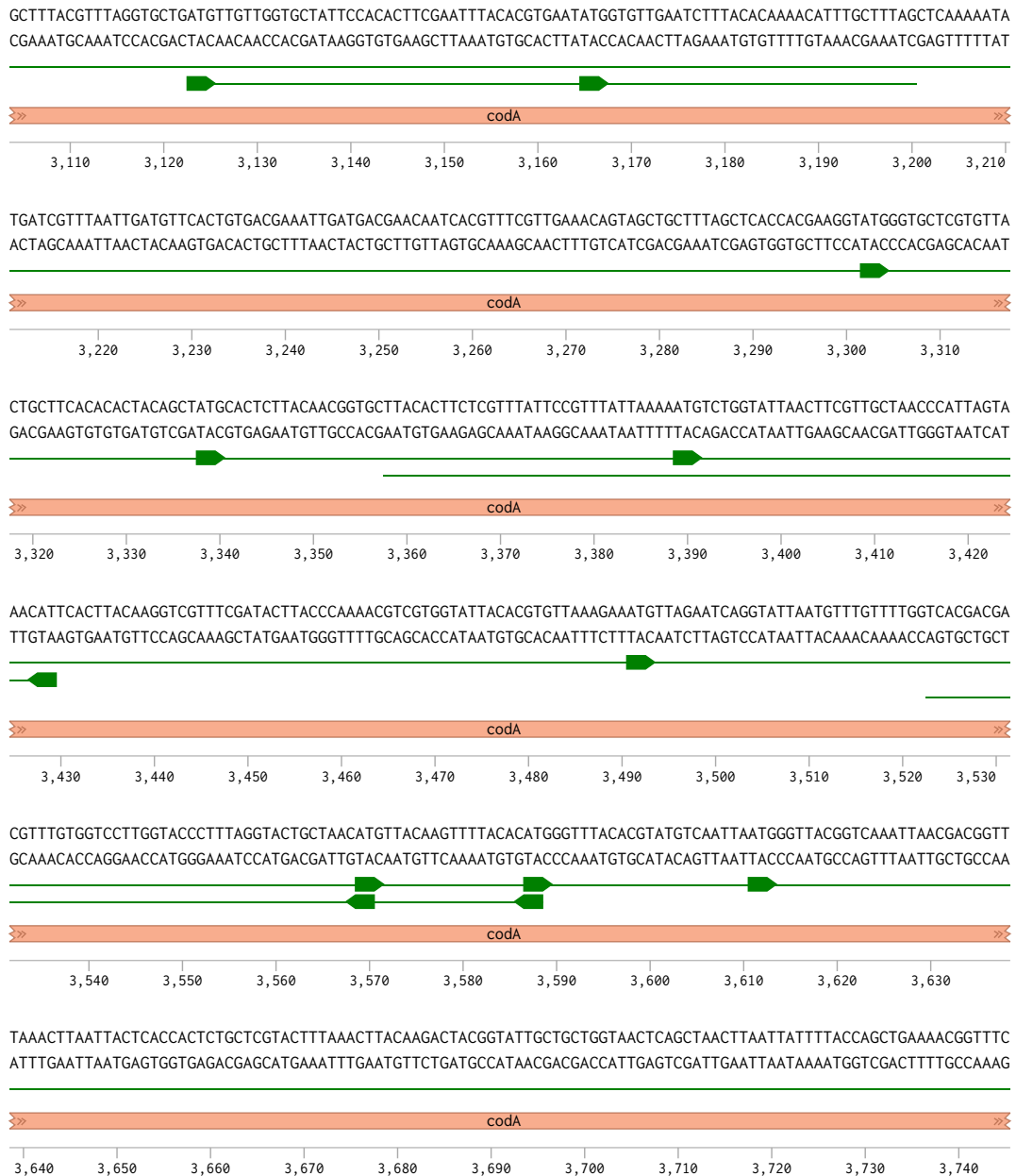


TAAACAACGTGCTTGGCAACATTAAATGGCAAATTGCTAACGGTATTCAACACGTACGTACTCAGTAGACGTTTCTGATGCTACTTTAACAGCTTTAAAGCTA
ATTTGTTGCACGAACCGTTTGAATTTTACCCTTAACGATTGCCATAAGTTGTGCATGCATGAGTGCATCTGCAAAGACTACGATGAAATTTGCGAAATTTTCGAT

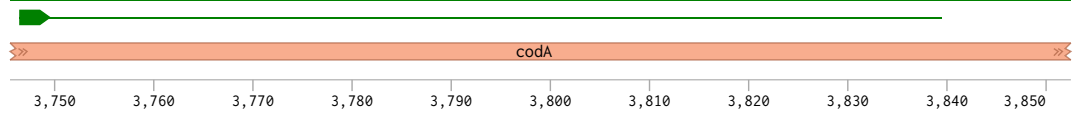


TGTTAGAAGTTAAACAAGAAGTAGCTCCATGGATTGACTTACAAATTTGCTGCTTTCCACAAGAAGGTATTTATCATACCAAACGGTGAAGCTTTATTAGAAGAA
ACAATCTTCAATTTGTTCTTCATCGAGGTACCTAATGAATGTTTAAACGACGAAGGGTGTCTTCCATAAAATAGTATGGGTTTGCCACTTCGAAATAATCTTCTT

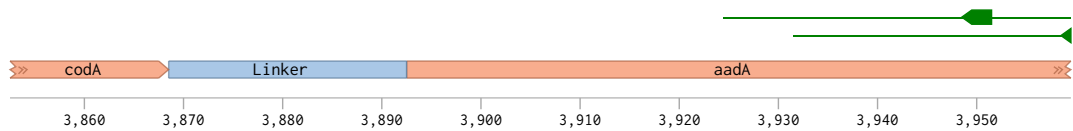




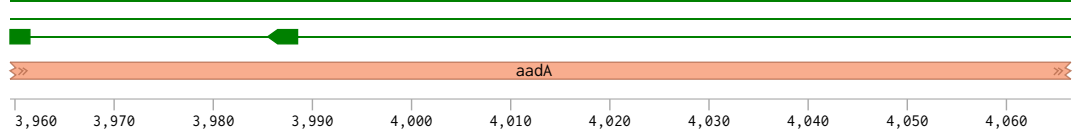
GATGCTTTACGTCGTCAGTTCCAGTACGTTACTCAGTTCGTGGTGGTAAAGTTATTGCTTCAACTCAACCAGCTCAAACTGTTTATTAGAACCAACCAgaagc
CTACGAAATGCAGCAGTTCAAGGTCATGCAATGAGTCAAGCACCACCATTTCAATAACGAAGTTGAGTTGGTCGAGTTTGTGACAAATAAATCTTGTGGTcttcg



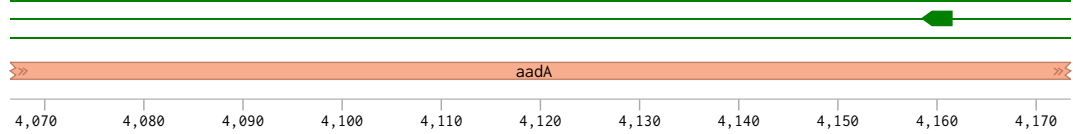
tattgactacaAACGTGGTGGTCTGGTGGTGGTCTGGTgctcgtgaagcggttatcGCCGAAGTATCAACTCAACTATCAGAGGTAGTTGGCGTCATCGAGCGCC
ataactgatgtTTGCACCACCAAGACCACCACCAAGACCAcagcacttcgccaatagCGGCTTCATAGTTGAGTTGATAGTCTCCATCAACCGCAGTAGCTCGCGG



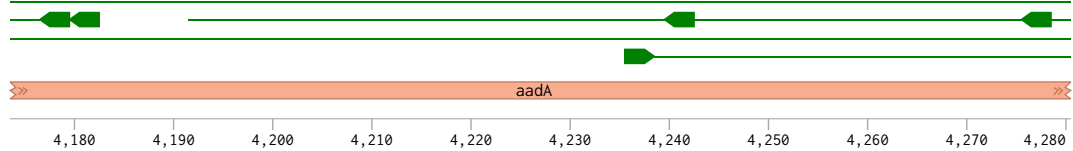
ATCTCGAACCGACGTTGCTGGCGGTACATTTGTACGGCTCCGCAGTGGATGGCGGCCTGAAGCCACACAGTGATATTGATTGCTGGTTACGGTGACCGTAAGGCTT
TAGAGCTTGGCTGCAACGACCGGCATGTAACATGCCGAGGCGTCACCTACGCCGGACTTCGGTGTGTCACTATAACTAAACGACCAATGCCACTGGCATTCCGAA



GATGAAACAACGGCGGAGCTTTGATCAACGACCTTTTGAAAACCTTCGGCTTCCCTGGAGAGAGCGAGATTCTCCGCGCTGTAGAAGTCACCATTGTTGTGCACGA
CTACTTTGTTGCCGCGCTCGAACTAGTTGCTGAAAACCTTTGAAGCCGAAGGGGACCTCTCTCGCTCTAAGAGGCGGACATCTTCAGTGGTAACAACACGTGCT



CGACATCATTCGTTGGCGTTATCCAGCTAAGCGGAACTGCAATTTGGAGAATGGCAGCGCAATGACATTCTTGCAGGTATCTTCGAGCCAGCCACGATCGACATTG
GCTGTAGTAAGGCAACCGCAATAGGTCGATTCCGCGTTGACGTTAAACCTCTTACCGTCGCGTTACTGTAAGAACGTCATAGAAGCTCGGTCGGTGCTAGCTGTAAC



Genomic map of the *aadA* gene region. The map shows a scale from 4,290 to 4,380 bp. A green arrow indicates the direction of transcription for the *aadA* gene, which is located between approximately 4,315 and 4,325 bp. The gene is labeled 'aadA' in the center of the map.

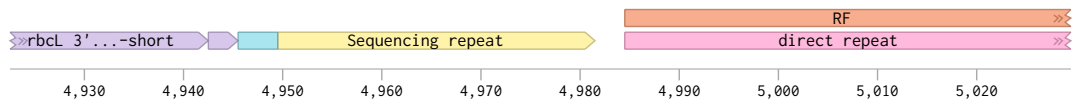
Genomic map of the *aadA* gene. The map shows a scale from 4,500 to 4,600. A green arrow indicates the direction of transcription, starting at approximately 4,510 and ending at 4,530. An orange bar labeled *aadA* spans from approximately 4,510 to 4,600.

rbcL 3'UTR-short

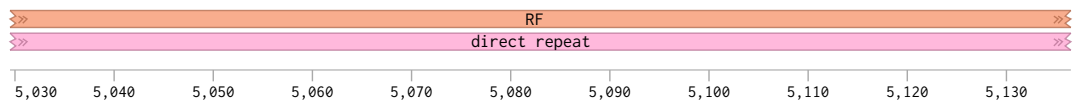
4,710 4,720 4,730 4,740 4,750 4,760 4,770 4,780 4,790 4,800 4,810

Genomic map of the *rbcL* gene region. A green arrow indicates the direction of transcription. A purple bar represents the *rbcL* 3'UTR-short region, spanning from approximately 4,835 to 4,920 bp. The x-axis is labeled with positions from 4,820 to 4,920 in increments of 10.

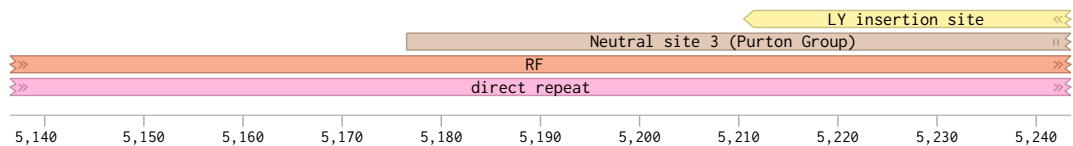
aacataactaaagcgatgtaGGAtactCAGCCTGCAATTCAACCACGTGGAGCTCTTCACAGCCTGCAATTCAACCACGTGCTTTAAGTATTACTCAAGGTCGTGCT
ttgtatgatttcgcctacatCCTatgaGTCGGACGTTAAGTTGGTGACCTCGAGAAGTGTGGACGTTAAGTTGGTGACGAAATTCATAATGAGTTCCAGCACGA



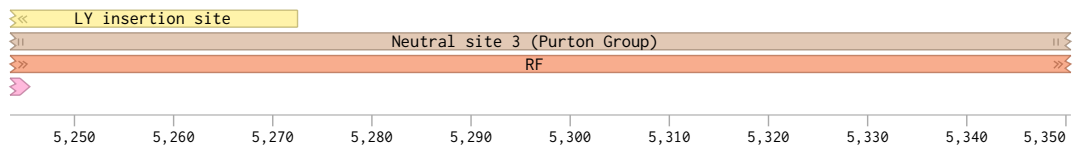
GTTGGTGTAGCTCACTACCTTTTAGGTGGTATTGCTACTACATGGTCTTCTTAGCAGTATCATTCTGTAGGTTAACATTTAATACTTTTAAATACATATAT
CAACCACATCGAGTATGGAAAATCCACCATAACGATGATGACCAGCAAGAAGATCGTGCATAGTAAAGACATCCAATTGTAAATTATGAAAAATTATGTATATA



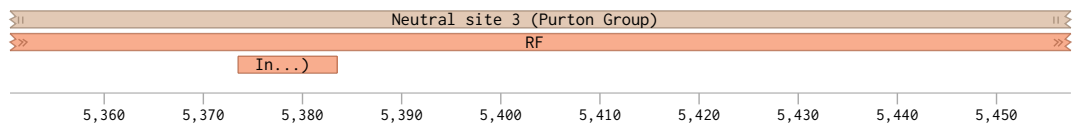
GCCTAAGTTTATCTTTAAAGATAAACTTAGCCATATGTGTTAAGTTATCTAACAAGGTTACCTTTTATTTCTTTAGATATATAAACATTAACCTACCGTGAT
CGGATTCAAATAGAAATTTCTATTTGAATCGGTATACACAATCAATAGATTGTTCCAATGGAAAAATAAGAGAAATCTATATATTTGTAATTTTGTATGGCACTA



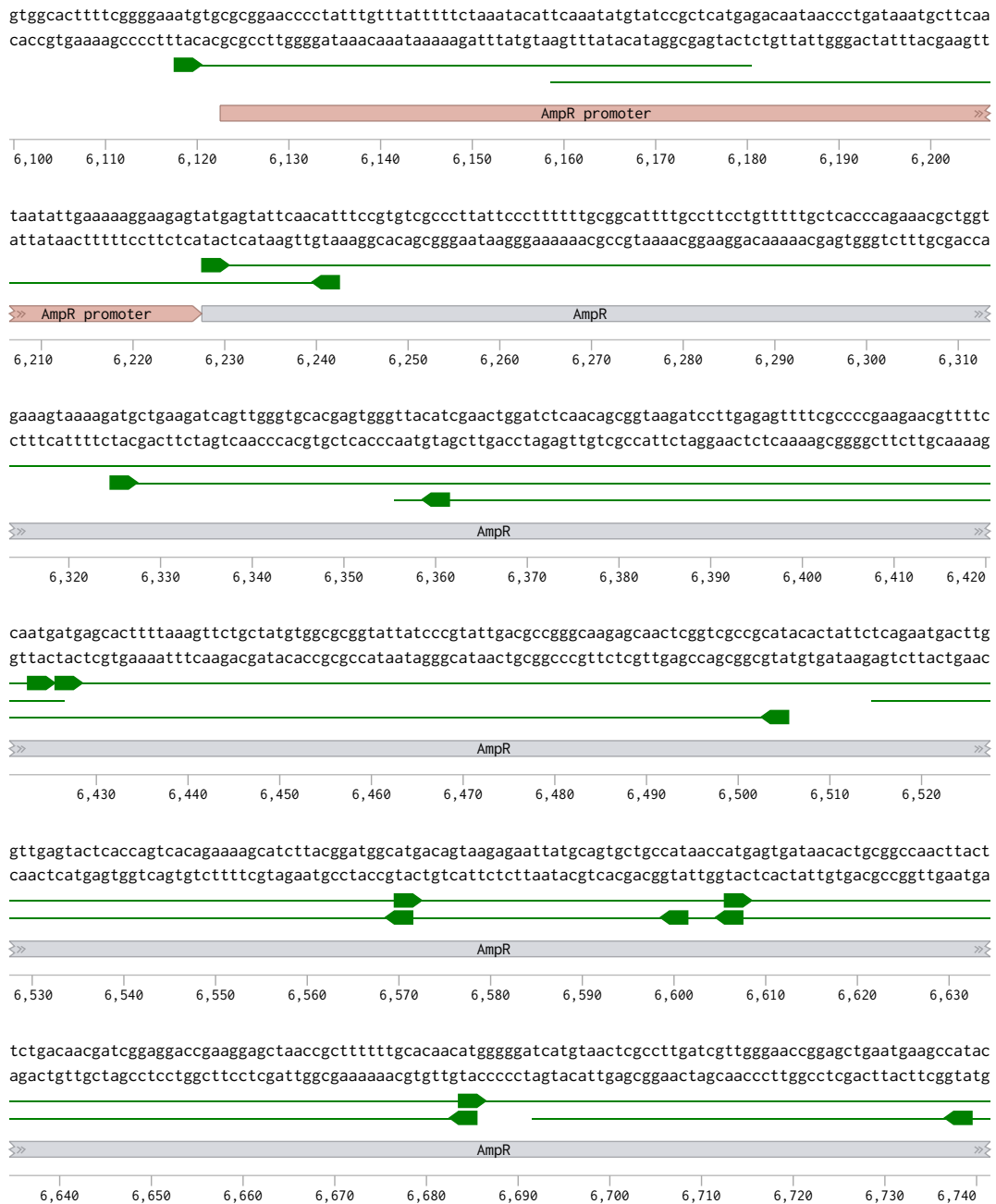
CGTTACACTTTAGATAACTGGAAGGGGAAAAATCATGTATTCGCTGGAAGGCGACCTCCTACTGCCTACTGCGCAGCATTAAATGCTGTAGATATTGGTATCTT
GCAATGTGAAATCTATTGACCTTCCCCCTTTTGTACATAAGCGACCTTCCGCGTGAGGATGACGGATGACGCGTCGTAATTTTACGACATCTATAACCATAGAA

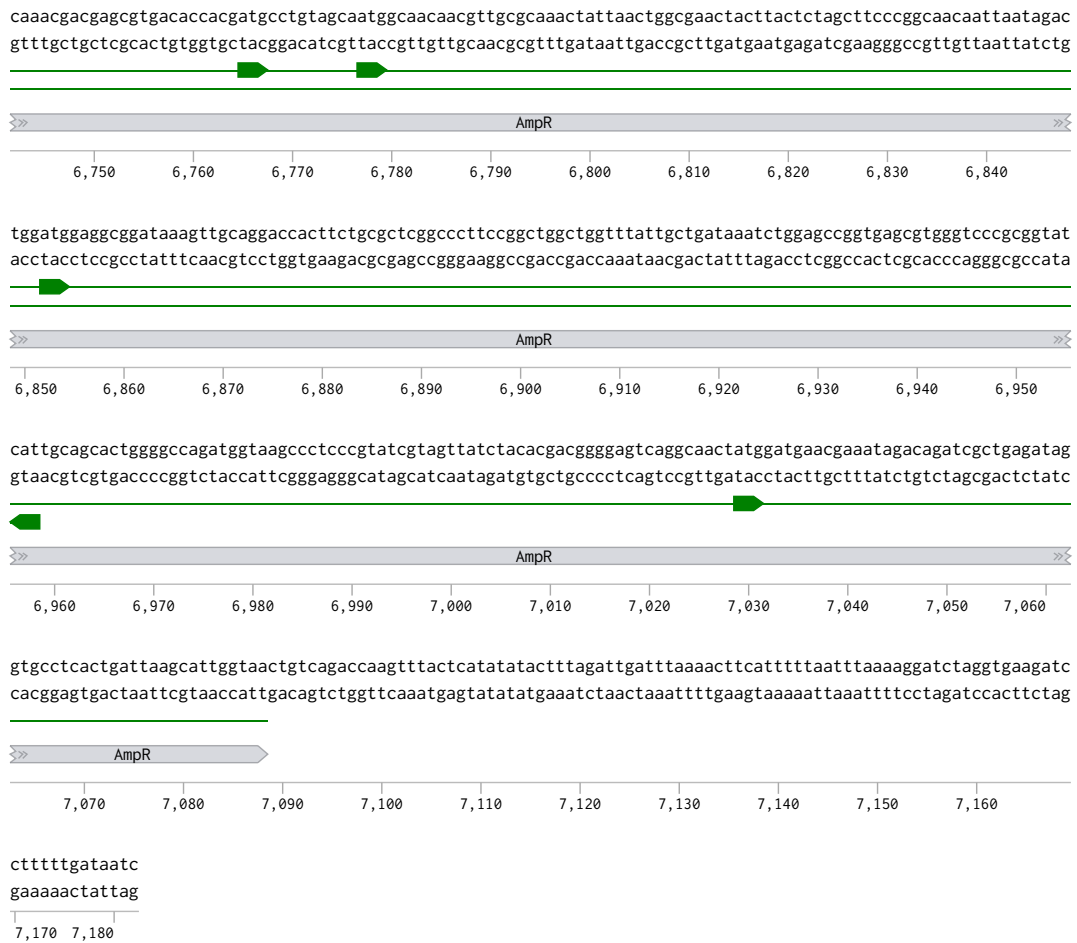


ACAAAGGACAGTAGTACACAATTAACGCGTTGGAATATTTATTTTATTAGAGAAATCCCATATAGCCAATGGCTTAAGGAGTGCATAGGAATAACTAGTCAT
TGTTTCCTGTCATCATGTGTTAATTTGCGCAACCTTATAAATAAAAAGTAATCTCTTAAGGGTATATCGGTTACCGAATTCCTCAGATATCCTTATTGATCAGTA





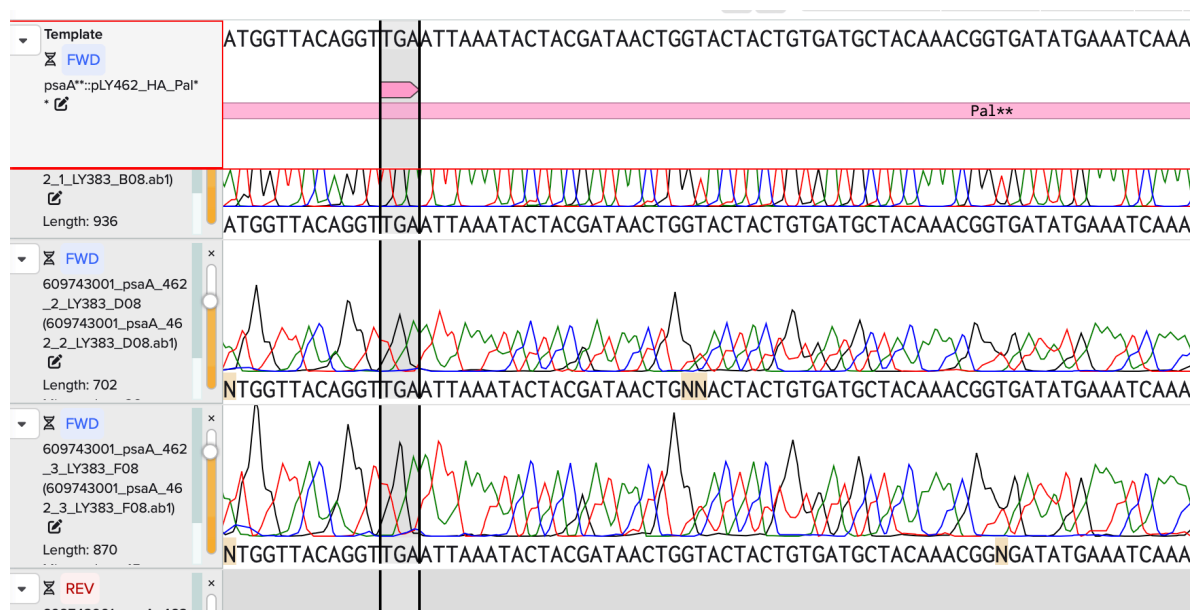




Appendix 4 Summary of primers used for genotyping PCR and DNA sequencing for psaA work.**

Primers	Sequences (5'to 3')	Purpose
LY290	CGCAGAGAAGAGCCCACAACGATACAATGAGTG	Forward, amplify left flank (psaA-3_XA)
LY291	CCTCCTGAAGAGCCGATCACGGTAGTTTTTAATG	Reverse, amplify left flank (psaA-3_XA)
LY292	GGCAGAGAAGAGCCCTGCAATTCAACCACG	Forward, amplify right flank (trnL2_ZY)
LY293	CCTCCTGAAGAGCCCATTCCCCGAGAAAAAG	Reverse, amplify right flank (trnL2_ZY)
LY314 (F1)	GGTTTCCACAGCTTTGG	Genotyping PCR for psaA** strains
LY317 (F2)	GAAAGGCGAGATCACTAAG	Genotyping PCR for psaA** strains
LY315 (R1)	GCTTGAAACCCGTCAG	Genotyping PCR for psaA** strains

1st stop codon: close to forward primer - noise



Appendix 6 Coding sequence and protein sequence of codon optimised *fGH* gene for the *C. reinhardtii* chloroplast.

Names	Coding sequence	Protein sequence	Annotations
Yellow porgy growth hormone (ypGH)	<p>ATGGATCGTGTTGTTTAAATGTTATCAG</p> <p>TATTATCATTAGGTGTTTCTTCACAACCA</p> <p>ATTACAGATGGTCAACGTTTATTTTCAAT</p> <p>TGCTGTATCACGTGTTCAACACTTACACT</p> <p>TATTAGCACAACGTTTATTTTCAGATTTT</p> <p>GAATCAAGTTTACAAACTGAAGAACAAC</p> <p>GTCAATTAAATAAAATTTTTTTACAAGATT</p> <p>TTTGTAATTCAGATTATATTATTTACACCA</p> <p>TTGATAAACATGAAACACAACGTTCAAGT</p> <p>GTTTTAAATTATTATCTATTAGTTATCGT</p> <p>TTAGTAGAATCTTGGGAATTCCTTCTCG</p>	<p>MDRVVLMLSVLSLGVSSQPITDGQRLFSI</p> <p>AVSRVQHLHLLAQRLFSDFESSLQTEEQR</p> <p>QLNKIFLQDFCNSDYIISPIDKHETQRSSVL</p> <p>KLLSISYRLVESWEFPSRSLAGGSAPRNQI</p> <p>SPKLSELKTGIHLLIRANEDGAELFPDSSAL</p> <p>QLAPYGDYYQSPGTDESLRRTYELLACFK</p> <p>KDMHKVETYLTVAKCRLSPEANCTLYPYD</p> <p>VPDYA*</p>	<p>Signal peptide</p> <p>YpGH</p> <p>HA-tag</p>

	TTCATTAGCAGGTGGTTCTGCTCCACGT AATCAAATTTACCAAAATTATCAGAATT AAAAACAGGTATTCATTTATTAATTCGTG CTAATGAAGATGGTGCTGAATTATTTCT GATTCATCTGCTTTACAATTAGCTCCATA TGGTGATTATTATCAATCACCAGGTACA GATGAAAGTTTACGTCGTAATTATGAATT ATTAGCTTGTTTTAAAAAGATATGCATA AAGTAGAAACATATTTAACAGTAGCTAAA TGTCGTTTATCACCAGAAGCTAATTGTAC ATTATATCCATATGATGTTCCAGATTATG CATAA		
Tilapia growth	ATGAACTCAGTAGTATTATTATTATCAG TAGTTTGTTTAGGTGTTTCTTCACAACAA	MNSVLLLLVCLGVSSQQITDSQRLFSIA VNRVTHLHLLAQRLFSDFESSLQTEEQRQ	Signal peptide

hormone (TiGH)	ATTACTGATTCTCAACGTTTATTCTCAAT TGCTGTTAACCGTGTAACACACTTACACT TATTAGCTCAACGTTTATTCTCAGACTTC GAATCTTCTTTACAAACAGAAGAACAAC GTCAATTAAACAAAATTTTCTTACAAGAC TTTTGTA ACTCTGATTACATTATTTCTCCA ATTGACAAACACGAAACACAACGTTTCAT CTGTTTTTAAAATTATTATCAATTCATACG GTTTAGTTGAATCTTGGGAATTCCCTTCT CGTTCATTATCTGGTGGTTCTTCTTTACG TAACCAAATTTCTCCACGTTTATCAGAAT TAAAAACAGGTATTTTATTATTAATTCGT GCTAACCAAGACGAAGCTGAAAACCTACC CAGATACTGATACTTTACAACACGCTCC ATACGGTAACTACTACCAATCTTTAGGTG	LNKIFLQDFCNSDYIISPIDKHETQRSSVLK LLSISYGLVESWEFPSRSLSGGSSLRNQIS PRLSELKTGILLIRANQDEAENYPDTDTL QHAPYGNYYQSLGGNESLRQTYELLACFK KDMHKVETYLTVAKCRLSPEANCTLGGSG GGSG YPYDVPDYA *	TiGH HA-tag
-------------------	--------------------------------------------------------------------------------------------------------------------------------------------------------------------------------------------------------------------------------------------------------------------------------------------------------------------------------------------------------------------------------------------------------------------------------------------------------------------------------------------------------------	-------------------------------------------------------------------------------------------------------------------------------------------------------------------------------------------------	---------------------------

	GTAACGAATCATTACGTCAAACATATGAA TTATTAGCTTGTTTCAAAAAAGACATGCA CAAAGTTGAACTTACTTAACAGTTGCTA AATGTCGTTTATCTCCAGAAGCTAACTGT ACTTTAGGTGGTTCTGGTGGTGGTTCTG GT TATCCATATGATGTTCCAGATTATGC A TAA		
--	-------------------------------------------------------------------------------------------------------------------------------------------------------------------------------------------------------------------------	--	--

Appendix 7 List of components and amino acid sequences in the MaSp1 constructs, adapted from Foong et al., 2020.

Protein component	Amino acid sequence
MaSp1-(2-mer)	<p>MKETAAAKFERQHMDSMAA</p> <p><u>SGRGGLGGQGAGAAAAAGGAGQGGYGGLGSQGT</u></p> <p><u>SGRGGLGGQGAGAAAAAGGAGQGGYGGLGSQGT</u>HHHHHH</p>
MaSp1-(3-mer)	<p>MKETAAAKFERQHMDSMAA</p> <p><u>SGRGGLGGQGAGAAAAAGGAGQGGYGGLGSQGT</u></p> <p><u>SGRGGLGGQGAGAAAAAGGAGQGGYGGLGSQGT</u></p> <p><u>SGRGGLGGQGAGAAAAAGGAGQGGYGGLGSQGT</u>HHHHHH</p>
MaSp1-(4-mer)	<p>MKETAAAKFERQHMDSMAA</p> <p><u>SGRGGLGGQGAGAAAAAGGAGQGGYGGLGSQGT</u></p> <p><u>SGRGGLGGQGAGAAAAAGGAGQGGYGGLGSQGT</u></p> <p><u>SGRGGLGGQGAGAAAAAGGAGQGGYGGLGSQGT</u></p> <p><u>SGRGGLGGQGAGAAAAAGGAGQGGYGGLGSQGT</u>HHHHHH</p>
MaSp1-(5-mer)	<p>MKETAAAKFERQHMDSMAA</p> <p><u>SGRGGLGGQGAGAAAAAGGAGQGGYGGLGSQGT</u></p> <p><u>SGRGGLGGQGAGAAAAAGGAGQGGYGGLGSQGT</u></p> <p><u>SGRGGLGGQGAGAAAAAGGAGQGGYGGLGSQGT</u></p> <p><u>SGRGGLGGQGAGAAAAAGGAGQGGYGGLGSQGT</u></p> <p><u>SGRGGLGGQGAGAAAAAGGAGQGGYGGLGSQGT</u>HHHHHH</p>
MaSp1-(6-mer)	<p>MKETAAAKFERQHMDSMAA</p> <p><u>SGRGGLGGQGAGAAAAAGGAGQGGYGGLGSQGT</u></p> <p><u>SGRGGLGGQGAGAAAAAGGAGQGGYGGLGSQGT</u></p> <p><u>SGRGGLGGQGAGAAAAAGGAGQGGYGGLGSQGT</u></p> <p><u>SGRGGLGGQGAGAAAAAGGAGQGGYGGLGSQGT</u></p> <p><u>SGRGGLGGQGAGAAAAAGGAGQGGYGGLGSQGT</u></p> <p><u>SGRGGLGGQGAGAAAAAGGAGQGGYGGLGSQGT</u>HHHHHH</p>
N-terminus	<p>MKETAAAKFERQHMDSMAA</p> <p><u>SGRGGLGGQGAGAAAAAGGAGQGGYGGLGSQGT</u></p>

MaSp1-mer-repeat	<u>SGRGGLGGQGAGAAAAAGGAGQGGYGGLGSQGT</u>
C-terminus (6xHis-Tagged)	<u>SGRGGLGGQGAGAAAAAGGAGQGGYGGLGSQGT</u> HHHHHH
C-terminus (Strep-tagged)	<u>SGRGGLGGQGAGAAAAAGGAGQGGYGGLGSQGT</u> WSHPQFEK

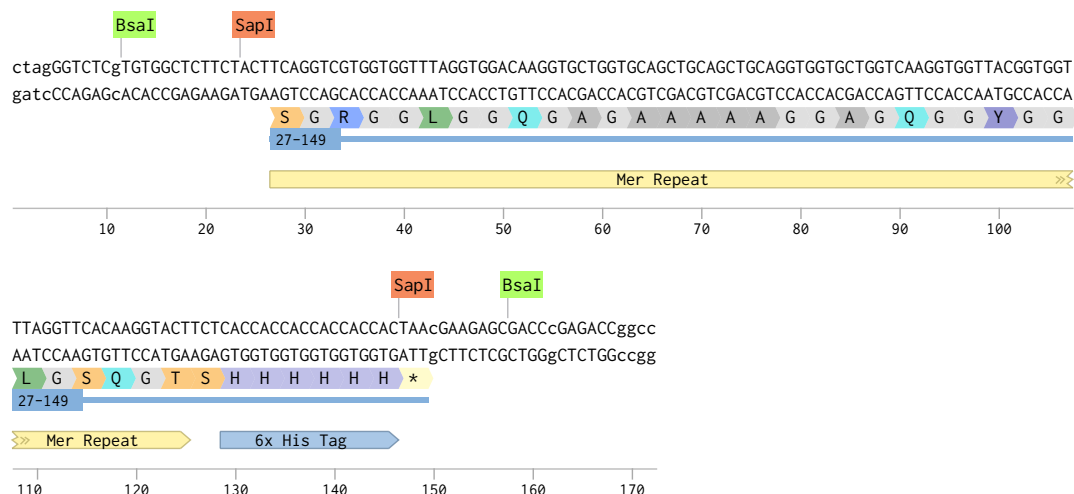
S-Tag
6xHis Tag
Strep tag-II

3. MaSp1 C-Terminus-His Tag

Benchling link: <https://benchling.com/s/seq-fQXmmw0UF5TZ85HvG2Vr?m=sIm-I4LdaYRaQV945stFc2f3>

11/11/2024 13:38:24

LY106 MaSp1 C-terminus opt (repetitive) (172 bp)

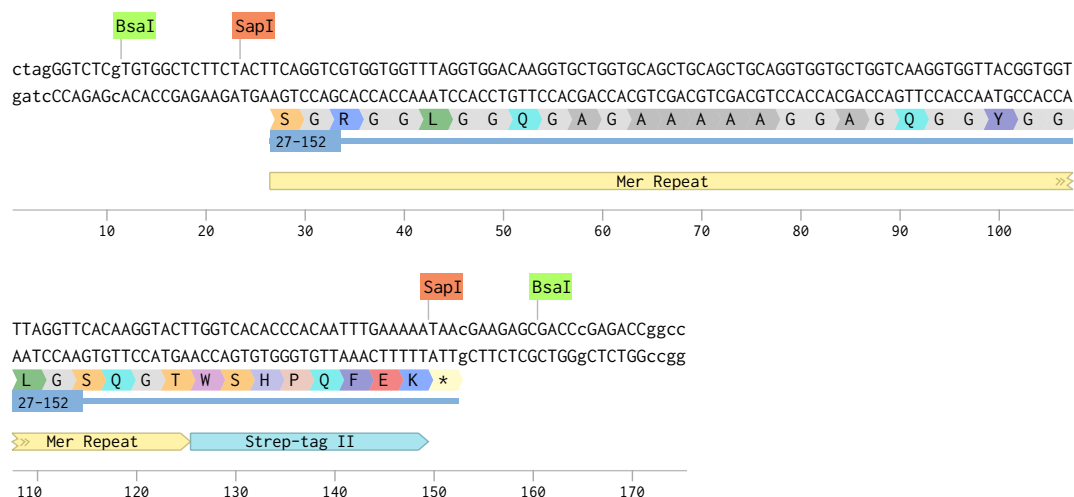


4. MaSp1 C-Terminus-Strep Tag-II

Benchling link: <https://benchling.com/s/seq-oH2x0wKbXFhsBuzpVgNZ?m=slm-W8cq1LJmF1NO2oaKJVuX>

11/11/2024 13:39:07

LY115 MaSp C terminus Strep-tag II (175 bp)



Appendix 9 DNA sequence of plasmid pLY118 (dxTRBL, 5191 bp)

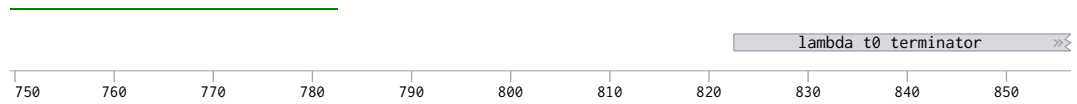
Sequence link: <https://benchling.com/s/seq-KQWYvhWaf3QZjgLYeOjQ?m=sIm-LFuBAmlDoqAPTB4Japdl>



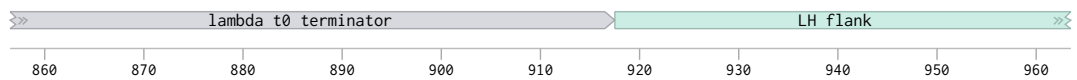
https://benchling.com/purton_lab/f/lib_K02HUnEc-ly_lv2s/seq_QQzs0RrR-ply118_lv2_dxtrbl_sapi_mrfp_esp3i/edit

1/8

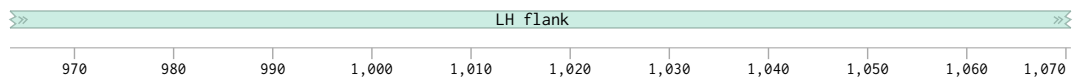
TCTGTGGATAACCGTATTACCGCCTTTGAGTGAGCTGATACCGCTCGCCGACGCCGAACGACCGAGCGCCTTGGACTCCTGTTGATAGATCCAGTAATGACCTCAGA
AGACACCTATTGGCATAATGGCGGAACTCACTCGACTATGGCGAGCGCGCTCGGCTTGTGGCTCGCGGAACCTGAGGACAACTATCTAGTTCATTACTGGAGTCT



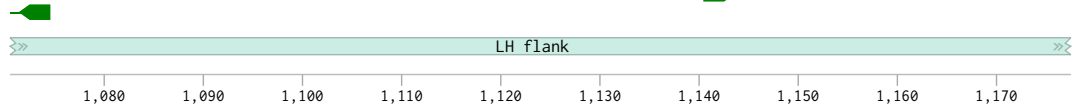
ACTCCATCTGGATTGTTCAGAACGCTCGGTTGCCCGGGCGTTTTTTATTGGTGAGAATgaatccggttttctccgtgaaagggaggtgtcctaggcctctaga
TGAGGTAGACCTAAACAAGTCTTGCGAGCCAACGGCGCCCGCAAAAAATAACCACTCTTActtaggcgcaaaagaggcactttccctccacaggatccggagatct



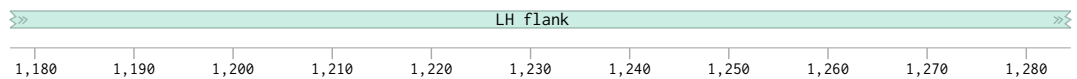
cgatggggccttttgttatattttactaaatatatatataattaaaaaaattgaattgtcaatttttaattgtacacttagttgaaagtgccctgtcccttgg
gctaccccgaaaaacaataaaaatgatttatataataatatttttttaacttaacagttaaaaattacatgtgaatcaactttcacggggacagggaacc



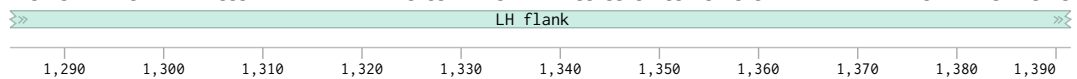
ccatatttaacagaagttatttataacgcagctgttttggagctctataaattataacatcagttactatggatttcccttagttttatggcctaggacgtccc
ggtataaattgtcttcaataaatattgcgtcgacaaaaaacctcagatattttaaatattgtagtcaatgatacctaaagggaatcaaaataccggatcctgcaggg



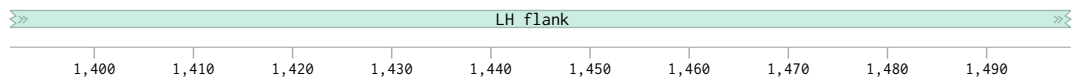
cttcccttcgatgctggaggcatccttttacgggacaataaaatttgttcctcgccatcggtcaacaagttccttcggagtatataaatataggatgttaa
gaagggaagctacgacctccgtaggaaaatgcctgttattttttaaacaacggagcgatgccgattgttcaaggaagcctcatatatttatatcctacaatt

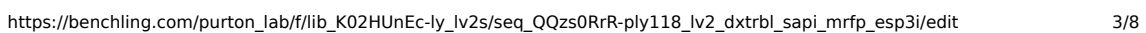


tactgctataaacttttagttgcccaatatttatattaggacgccagtggtaccgacctgcctgcttcgcagtatataaatataggcagttggcaggcaac
atgacgatatattgaaatcaacgggttataaatataatcctgcggtcacctgcacctggcggtgacggacgaagcgtcatatatttatatccgtcaaccgtccgttg

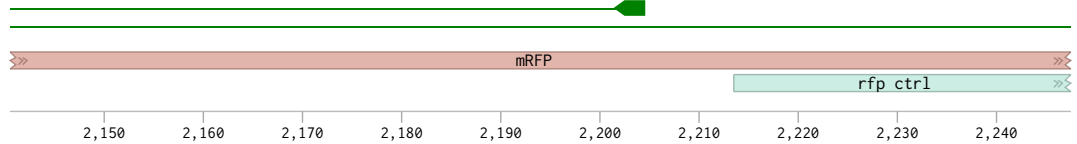


tgccactgacgtcctattttaactccaagtttacttgccctaggcagttggcaggcaacaaattttatgtccactaaaatttttggccgaaggggacgt
acggtgactgcaggataaaattatgagggttcaaatgaacggatccgtcacctgtgttttaataaataacaggtgattttaataaacgggttcccttgca

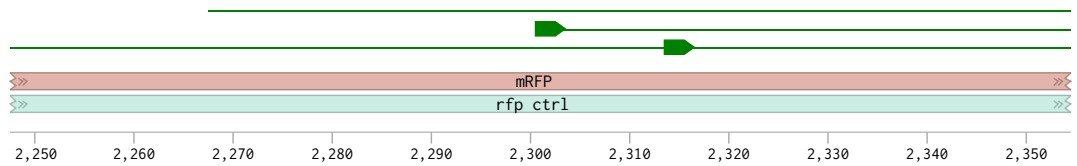




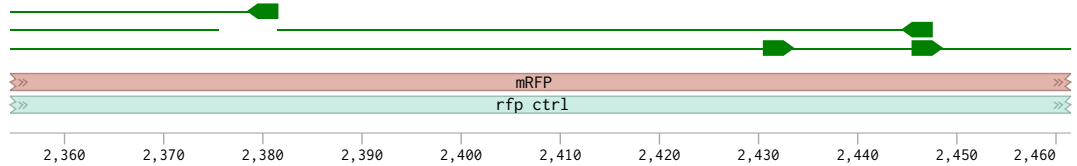
aaggtaccagaccgctaaactgaaagtaccgaaaggtggtccgctgctgcttgggacatcctgtcccgagttccagttacggttccaaagcttacgttaa
ttccatgggtctggcgatttgactttcaatgtttccaccaggcgacggcaagcgaacctgtaggacagggcgctcaaggtcatccaaggtttcgaatgcaattt



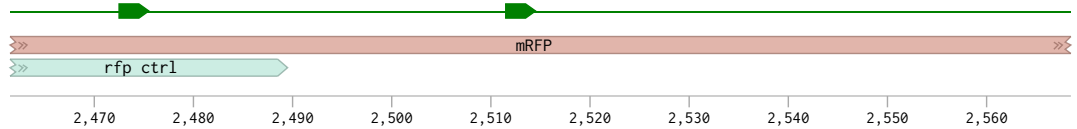
cacccggctgacatccggactacgtgaaactgtccttcccggaaggtttcaaatgggaacgtgttatgaactcgaagacgggtgtgttacggttaccagga
gtggcgagctgtaggcctgatggactttgacaggaaggccttccaaagttaccccttgacaatactgaagcttctgccaccacaacaatggcaatgggtcct



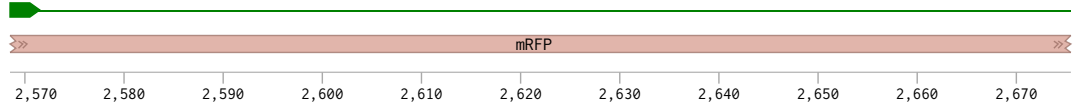
ctctccctgcaagacgggtgagttcatctacaaagttaaactgcgtggttaccaacttcccgctccgacgggtccggttatgcagaaaaaacctgggttgggaagctt
gaggaggacgttctgccactcaagtagatgtttcaatttgacgcacatggttgaaggcgaggctgccaggccaatacgtcttttttggtagccaaccttcgaa



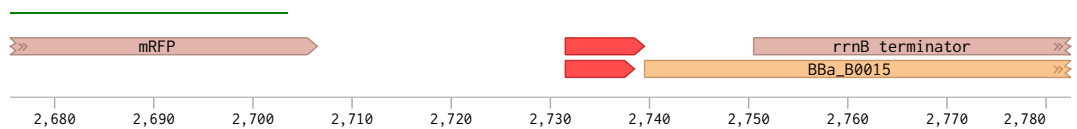
ccaccgaacgtatgtaccgggaagacgggtgctctgaaaggtgaaatcaaatgcgtctgaaactgaaagacgggtggtcactacgacgtgaagttaaaccctac
ggtagcttgcatatcagggccttctgccacgagactttccacttttagttttacgcagactttgactttctgccaccagtgatctgcgacttcaattttggtagg

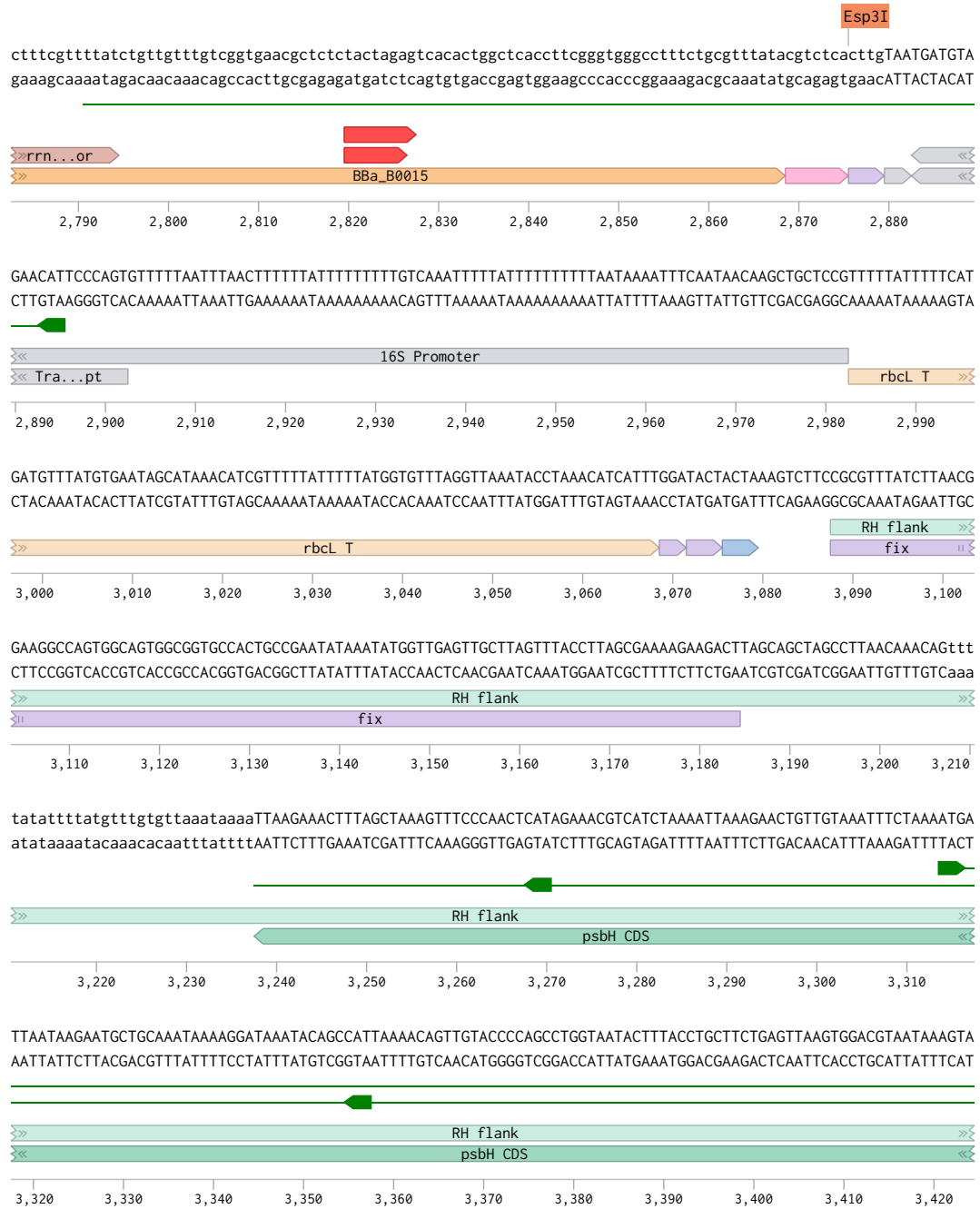


atggctaaaaaacgggttcagctgccgggtgcttacaaaaccgacatcaaactggacatcacctcccacaacgaagactacaccatcggtgaacagtacgaacgtgc
taccgatTTTTGGCCAAGTCGACGGCCACGAATGTTTTGGCTGTAGTTTGACCTGTAGTGGAGGGTGTGCTTCTGATGTGGTAGCAACTGTGATGCTTGCACG

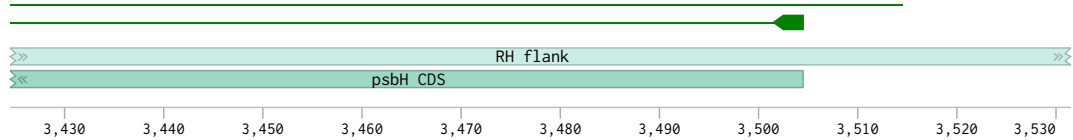


tgaaggtcgtcactccaccggtgcttaataacgtgatagtgttagtgcgtactagagccaggcatcaataaaacgaaaggctcagtcgaaagactgggc
acttccagcagtgagggtggccagaaattatgcgactatcacgatcacatctagcgatgatctcggtccgtagtttttttcttccgagtcagctttctgacccg

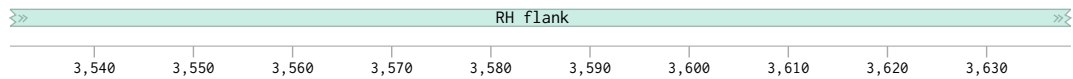




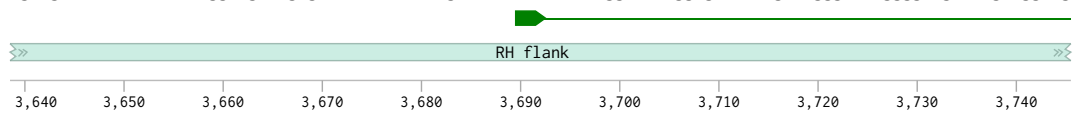
CCTAATGGTGAACATAACCAGGTTCTTGGAAGTCTGAATTTACTTTTGATGGTTAGCTTTAGAAAGTTCCTGTTGCCATaattgattaaatgaattaagcggttatt
GGATTACCACATTGATTGGTCCAAGAACCCTCAGACTTAAATGAAAACCTACCAAACTCGAAATCTTCAAGGACAACGGTAttaactaatttacttaattcgcaataa



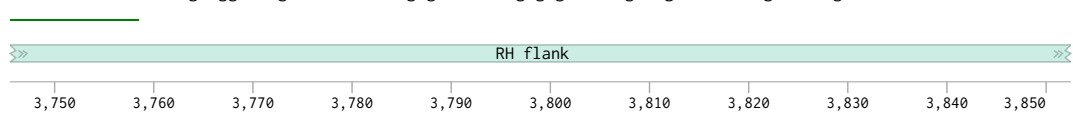
agcgctattttatttactttctgtaaaaaataaggaaaatattcttcagtcattccctctcaggattataaactctgaggataacgttctctcgtaagggtt
tcgcgataaaaaataatgaaagacattttttattcctttataagaagtcacgtacggaagagtcctaatattatgagactcctattgcaagagagcagttcccaaa



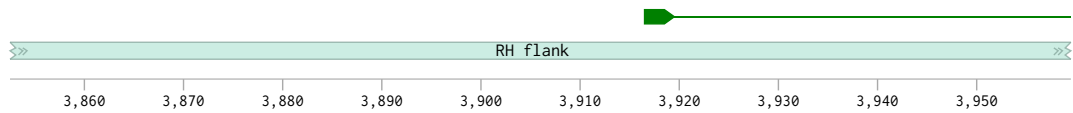
gcttctgtgagtatagaacactactagcacaagaataaattgcataaaatgtatttacctaggaccgcagtaggcagtccttttcccttcagaactgcctgc
cgaagaacactcatatctttggatgatcgtgttctttttaacgtattttatcataaatggatcctggcgtcatccgtcagggaaggggaagcttgcagggaag



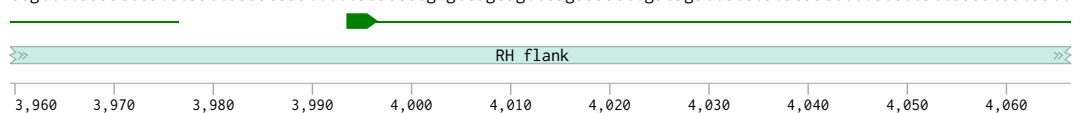
tttaaaagaatgaaaaactgccttctgtgtaagtaaaactctttaattactcactaaagacgatcttagaagttcttcttcttattttatataatattt
aaattttcttacttttttgacggaacagaccattcatittgagaataatgagtgatttctgtagaatcttcaagaacaagtaaaaaataaattatattataaa

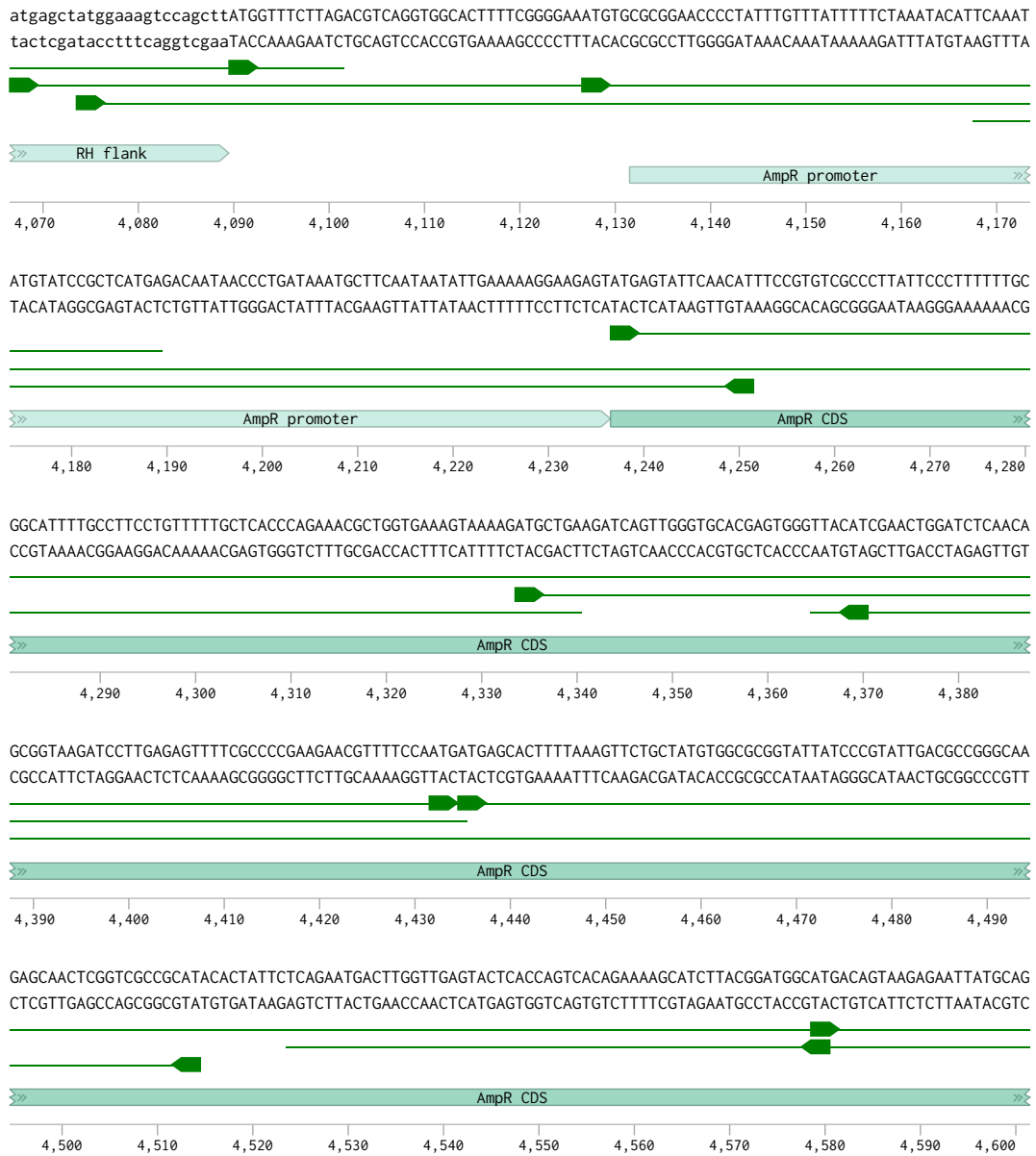


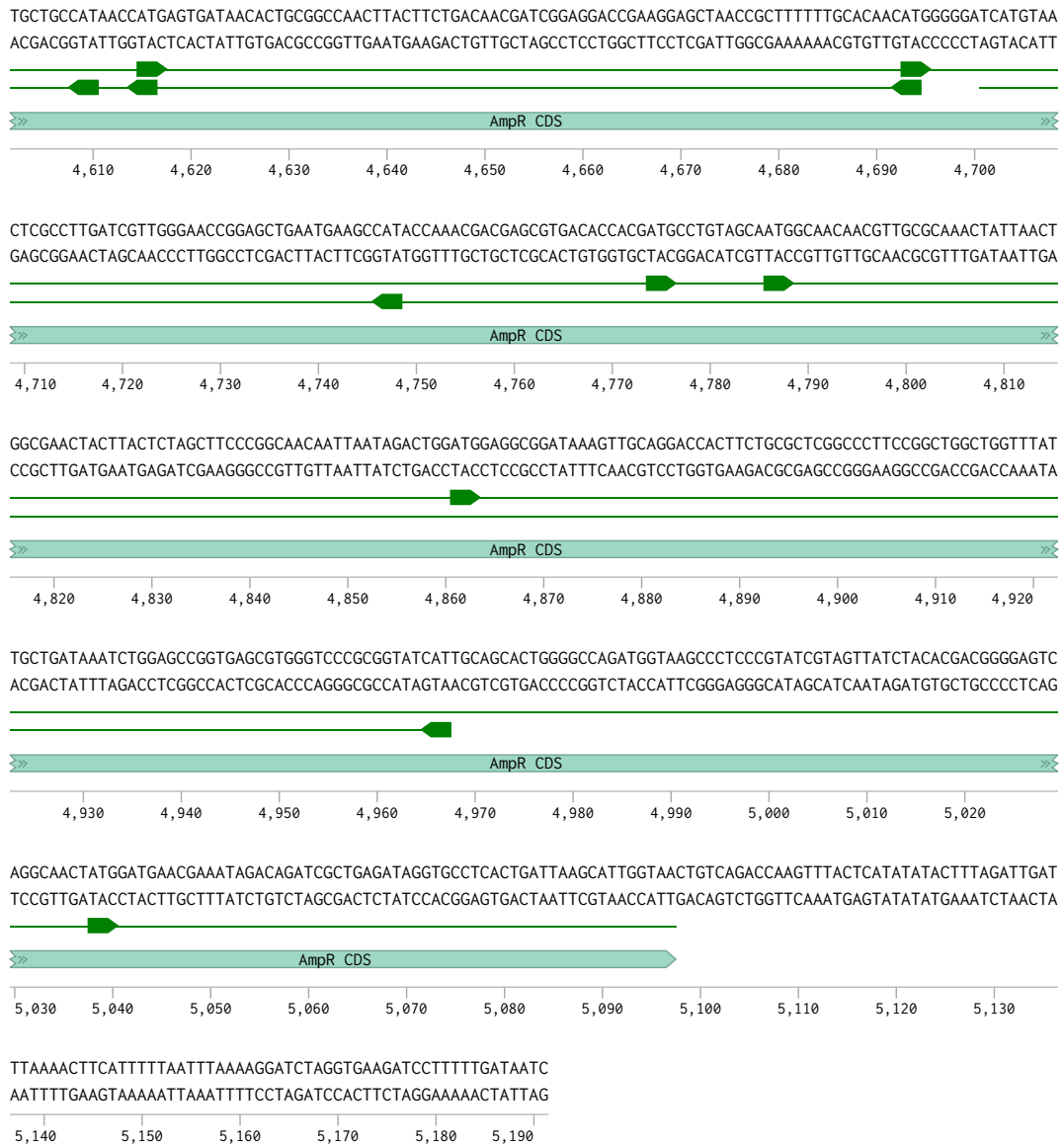
gttatataaaaattaaataatttttaattatgtttaactttgtaaggacagtttcaaagtgacatgaatggctactgcaaaaacgaagtaagttattctttctcag
caatataatttttaattttataaaaatttaatacaaatgaaacattcctgtcaaagtttctgtacttaccgatgacgtttttgcttattcaataagaagagtc



ggcaaaattttgagtagattaattttgtttaaaaatgtgggacacagtcgtcaagtcctttgaaactatctaagagatatgttgaaaagagaataattttattattaa
ccgttttaaaactcatctaattaaacaaattttacaccctgtgtcagcagttcagaaaacttgatagattctctatacaacttttctcttataaaataaatt







Appendix 10 Recipe for 50× Tris-Acetate-EDTA (TAE) Buffer

50× TAE buffer is a concentrated stock solution used for agarose gel electrophoresis of DNA/RNA (e.g., Section 2.4.2; Section 2.5.2). Its high concentration reduces storage volume, making it ideal for large-scale experiments (e.g., screening *C. reinhardtii* transformants, validating dsRNA amplicons). Below is the detailed recipe, preparation steps, and usage guidelines:

1. Component Details (50× Stock Solution)

TAE buffer consists of Tris base (for buffering), glacial acetic acid (to adjust pH), and EDTA (to chelate divalent cations and prevent nuclease activity). The 50× stock is 5× more concentrated than the standard 10× formulation, with final concentrations and volumes per 1 L stock listed below:

Component	Final Concentration (50× Stock)	Amount per 1 L of 50× Stock
Tris base	2000 mM (2 M)	242.28 g
Glacial acetic acid	1000 mM (1 M)	~57.2 mL
EDTA (0.5 M, pH 8.0)	50 mM	100 mL
Deionized water	—	Add to 1 L

2. Preparation Steps

Follow these steps to avoid chemical hazards (glacial acetic acid is corrosive) and ensure buffer stability:

- (1) Dissolve Tris base: Add 242.28 g of Tris base to a 2 L glass beaker. Add ~700 mL of deionized water and stir with a magnetic stir bar until Tris is fully dissolved (no visible crystals remain).
- (2) Add glacial acetic acid: Slowly pour 57.2 mL of glacial acetic acid into the beaker (wear nitrile gloves and a fume hood to avoid fumes/skin contact). Stir gently for 5 minutes to mix evenly.
- (3) Add EDTA: Pour 100 mL of 0.5 M EDTA (pre-adjusted to pH 8.0) into the beaker. Stir for another 5 minutes to ensure homogeneity.
- (4) Adjust volume: Transfer the solution to a 1 L volumetric flask. Rinse the beaker with small portions of deionized water (2× 50 mL) and add rinses to the flask. Add deionized water until the meniscus reaches the 1 L mark.
- (5) Verify pH (optional): The 50× stock will have a pH of ~8.5–8.7. No adjustment is needed—when diluted to 1× working solution, the pH will automatically drop to 8.3 (optimal for electrophoresis).

3. Storage & Usage Guidelines

- Storage: Store 50× TAE stock at room temperature (RT) in a dark, airtight bottle for up to 12 months. Avoid exposure to direct light (EDTA is light-sensitive over long periods).

- Dilution for use: To prepare 1× working solution (for agarose gels), dilute 50× stock 1:50 with deionized water. For example: 100 mL 1× TAE = 2 mL 50× TAE + 98 mL deionized water.
- Agarose gel preparation: Use 1× TAE to dissolve agarose (e.g., 1.5 g agarose + 150 mL 1× TAE for a 1% gel) and as running buffer during electrophoresis.

Appendix 11 Protocols for OneTaq PCR, Q5 High-Fidelity PCR, and OneTaq One-Step RT-PCR

This appendix standardizes protocols for three core nucleic acid amplification techniques - OneTaq PCR (routine amplification), Q5 High-Fidelity PCR (high-accuracy amplification), and OneTaq One-Step RT-PCR (RNA-to-cDNA amplification) - adapted to the thesis's experimental needs (e.g., plasmid validation, genotyping of *Chlamydomonas reinhardtii* transformants, dsRNA detection). All protocols align with NEB's official guidelines for the corresponding reagents.

1. Overview

This appendix addresses three common amplification scenarios in the thesis:

- Routine DNA amplification (e.g., colony PCR for *E. coli* transformants, genotyping of *C. reinhardtii* chloroplast transformants) using OneTaq 2X Master Mix (NEB, Cat. No. M0482);
- High-accuracy amplification (e.g., cloning of codon-optimized genes, site-directed mutagenesis) using Q5 High-Fidelity DNA Polymerase (NEB, Cat. No. M0491);
- RNA-to-cDNA amplification (e.g., detection of chloroplast-expressed dsRNA) using OneTaq One-Step RT-PCR Kit (NEB, Cat. No. M0496).

2. OneTaq PCR Protocol (Routine DNA Amplification)

OneTaq DNA Polymerase is a versatile, cost-effective enzyme for routine amplification of DNA fragments (100 bp–10 kb). Its pre-mixed 2X Master Mix reduces pipetting errors and simplifies reaction setup, making it ideal for high-throughput experiments (e.g., screening *C. reinhardtii* transformants via PCR).

2.1 Reaction Components (25 μ L Volume)

Reagent	Volume (μ L)	Final Concentration	Purpose
OneTaq 2X Master Mix	12.5	1×	Provides buffer, dNTPs (200 μ M each), and OneTaq DNA Polymerase.
Forward Primer (10 μ M)	1	400 nM	Binds to the 5' end of the target sequence.
Reverse Primer (10 μ M)	1	400 nM	Binds to the 3' end of the target sequence.
Template DNA	1–2	10–100 ng	Plasmid DNA, genomic DNA from <i>C. reinhardtii</i> / <i>E. coli</i> , or PCR amplicons.
Nuclease-Free Water	QS to 25	—	Adjusts total volume; avoids nuclease contamination.

2.2 Thermal Cycling Conditions

OneTaq's optimal extension rate is 1 minute/kb (at 68°C). Adjust annealing temperature (T_a) using NEB's T_m Calculator (based on primer sequences) and extension time based on amplicon length:

Step	Temperature	Time	Cycles	Purpose
Initial Denaturation	94°C	30 seconds	1	Unwinds double-stranded template DNA.

Denaturation	94°C	30 seconds	30–35	Separates DNA strands in each cycle.
Annealing	T _a (50–65°C)	30 seconds	30–35	Allows primers to bind to target sequences (adjust T _a ±2°C for specificity).
Extension	68°C	1–5 minutes	30–35	Synthesizes new DNA strands (1 min/kb; e.g., 2 min for 2 kb amplicons).
Final Extension	68°C	5 minutes	1	Ensures complete synthesis of all amplicons.
Hold	4°C	Indefinite	—	Preserves sample integrity post-reaction.

2.3 Key Notes

- For amplicons >5 kb: Add 1 µL of 50% DMSO (final concentration 2%) to the reaction to improve template denaturation and reduce secondary structure.
- For low-template samples (e.g., dilute *C. reinhardtii** genomic DNA): Extend initial denaturation to 2 minutes and increase cycles to 35–40.
- Avoid repeated freeze-thaw of OneTaq 2X Master Mix; store at 4°C for up to 1 month after first thaw.

3. Q5 High-Fidelity PCR Protocol (High-Accuracy Amplification)

Q5 High-Fidelity DNA Polymerase (NEB, Cat. No. M0491) offers ultra-low error rates (~50× lower than Taq) and high processivity, making it ideal for experiments requiring sequence accuracy (e.g., cloning of spider silk MaSp1 genes, site-directed mutagenesis of *psaA*** plasmids).

3.1 Reaction Components (25 µL Volume)

Reagent	Volume (μL)	Final Concentration	Purpose
5× Q5 Reaction Buffer	5	1×	Provides optimal pH, Mg ²⁺ , and stabilizers for high-fidelity amplification.
10 mM dNTP Mix	0.5	200 μM each	Supplies high-purity nucleotides to minimize errors.
Forward Primer (10 μM)	1	400 nM	Specific to the 5' end of the target sequence (design T _m 60–65°C).
Reverse Primer (10 μM)	1	400 nM	Specific to the 3' end of the target sequence (match T _m to forward primer).
Template DNA	1–2	5–50 ng	Use high-purity DNA (e.g., gel-purified PCR products, plasmid DNA) to avoid inhibitors.
Q5 High-Fidelity DNA Pol	0.25	0.02 U/μL	Catalyzes DNA synthesis with high accuracy; avoid excess enzyme.
Nuclease-Free Water	QS to 25	—	Adjusts total volume; use PCR-grade water.

3.2 Thermal Cycling Conditions

Q5 requires higher denaturation temperatures (98°C) to maintain fidelity. Its extension rate is 20 seconds/kb (faster than OneTaq), reducing total reaction time:

Reagent	Volume (μL)	Final Concentration	Purpose
5× Q5 Reaction Buffer	5	1×	Provides optimal pH, Mg ²⁺ , and stabilizers for high-fidelity amplification.
10 mM dNTP Mix	0.5	200 μM each	Supplies high-purity nucleotides to minimize errors.
Forward Primer (10 μM)	1	400 nM	Specific to the 5' end of the target sequence (design T _m 60–65°C).

Reverse Primer (10 μ M)	1	400 nM	Specific to the 3' end of the target sequence (match T_m to forward primer).
Template DNA	1–2	5–50 ng	Use high-purity DNA (e.g., gel-purified PCR products, plasmid DNA) to avoid inhibitors.
Q5 High-Fidelity DNA Pol	0.25	0.02 U/ μ L	Catalyzes DNA synthesis with high accuracy; avoid excess enzyme.
Nuclease-Free Water	QS to 25	—	Adjusts total volume; use PCR-grade water.

3.3 Key Notes for High Fidelity

- For GC-rich templates (>65% GC): Add 1 μ L of 5 M betaine (final concentration 0.2 M) to reduce secondary structure and improve amplification efficiency.
- For site-directed mutagenesis: Use Q5 in conjunction with the Q5 Site-Directed Mutagenesis Kit (NEB, Cat. No. E0554) and include DpnI digestion (to remove parental methylated DNA) post-PCR.
- Store Q5 Polymerase at -80°C ; avoid repeated freeze-thaw (aliquot into single-use volumes if needed).

4. OneTaq One-Step RT-PCR Protocol (RNA Target Amplification)

The OneTaq One-Step RT-PCR Kit (NEB, Cat. No. M0496) integrates reverse transcription (RT) and PCR into a single tube, eliminating cross-contamination risks. It is used in the thesis for detecting chloroplast-expressed dsRNA and validating gene expression.

4.1 Reaction Components (25 μ L Volume)

Reagent	Volume (μ L)	Final Concentration	Purpose
5 \times OneTaq RT-PCR Buffer	5	1 \times	Supports both RT (46–50°C) and PCR (68°C); contains dNTPs and Mg ²⁺ .
Forward Primer (10 μ M)	1	400 nM	Binds to the target RNA (primer-dependent RT; avoid poly-T primers for dsRNA).
Reverse Primer (10 μ M)	1	400 nM	Binds to the complementary cDNA strand post-RT.
Template RNA (purified)	1–2	50–200 ng	Use DNase I-treated RNA (e.g., <i>C. reinhardtii</i> total RNA, purified dsRNA) to eliminate gDNA.
OneTaq RT-PCR Enzyme Mix	0.5	—	Contains M-MuLV reverse transcriptase (RT) and OneTaq DNA Polymerase.
Nuclease-Free Water	QS to 25	—	Use RNase-free water to prevent RNA degradation.

4.2 Thermal Cycling Conditions

Step	Temperature	Time	Cycles	Purpose
Reverse Transcription	46°C	30 minutes	1	Converts RNA to cDNA (adjust to 50°C for GC-rich RNA; avoid >50°C to protect RT activity).
Initial Denaturation	94°C	2 minutes	1	Inactivates RT enzyme and denatures cDNA-template hybrids.
Denaturation	94°C	30 seconds	35	Separates cDNA strands.
Annealing	T _a (52–60°C)	30 seconds	35	Enables primer binding to cDNA.

Extension	68°C	30 seconds–2 minutes	35	Amplifies cDNA (1 min/kb for amplicons >500 bp).
Final Extension	68°C	5 minutes	1	Ensures complete amplicon synthesis.
Hold	4°C	Indefinite	—	Preserves sample integrity.

4.3 Controls and Quality Checks

- Positive Control: Purified dsRNA from *E. coli* HT115 to validate reaction efficiency.
- Negative Control (No Template): Nuclease-free water to detect reagent contamination.
- gDNA Control: Template RNA without OneTaq RT-PCR Enzyme Mix (omits RT) to confirm no residual gDNA.
- Post-PCR analysis: Resolve products on a 1.5% agarose gel (1× TAE buffer) and visualize under UV light to verify target band size.

5. General Guidelines for Amplification Experiments

5.1 Reagent Handling:

- Thaw all reagents on ice (except OneTaq 2X Master Mix, which can thaw at room temperature briefly).
- Mix reagents gently by pipetting; avoid vortexing (especially for Q5 Polymerase and RT enzyme).

5.2 Primer Design:

- Design primers 18–25 bp in length with 40–60% GC content; avoid hairpin structures or self-dimerization (use tools like Benchling or Primer3).

- For *C. reinhardtii* chloroplast targets: Include 1–2 mismatches in primer sequences if amplifying highly conserved regions (e.g., *rbcL*, *psaA*).

5.3 Template Quality:

- For genomic DNA: Use phenol-chloroform extraction to remove proteins and inhibitors.
- For RNA: Store at -80°C in RNase-free tubes; avoid freeze-thaw >3 times.

5.4 Post-PCR Validation:

- For cloning: Purify amplicons using a silica column kit (e.g., GeneJET PCR Purification Kit, Thermo Scientific) before ligation.
- For genotyping: Use restriction enzyme digestion (Section 2.4.1) to confirm amplicon identity (e.g., SacI digestion for *psaA*** mutants).

6. Reagent Information Table

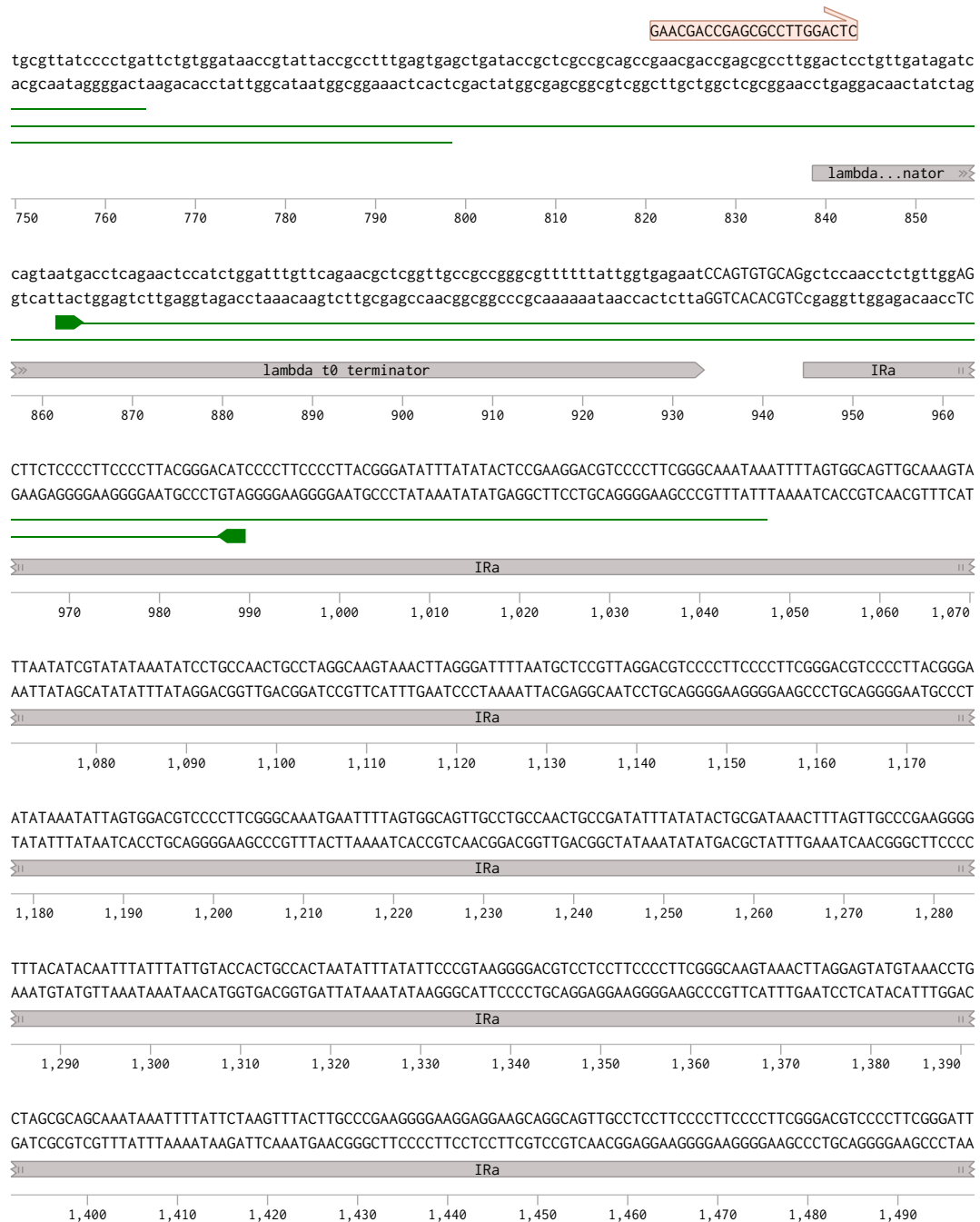
Technique	Reagent Name	NEB Cat. No.	Key Application in Thesis	Storage Condition
Routine PCR	OneTaq 2X Master Mix	M0482	Colony PCR, <i>C. reinhardtii</i> genotyping	-20°C (4°C for 1 month)
High-Fidelity PCR	Q5 High-Fidelity DNA Polymerase	M0491	Cloning, site-directed mutagenesis (<i>psaA</i> **, MaSp1)	-80°C
One-Step RT-PCR	OneTaq One-Step RT-PCR Kit	M0496	dsRNA detection, RNA expression analysis	-20°C
Site-Directed Mutagenesis	Q5 Site-Directed Mutagenesis Kit	E0554	Introducing TGA stop codons in <i>psaA</i> -3	-20°C

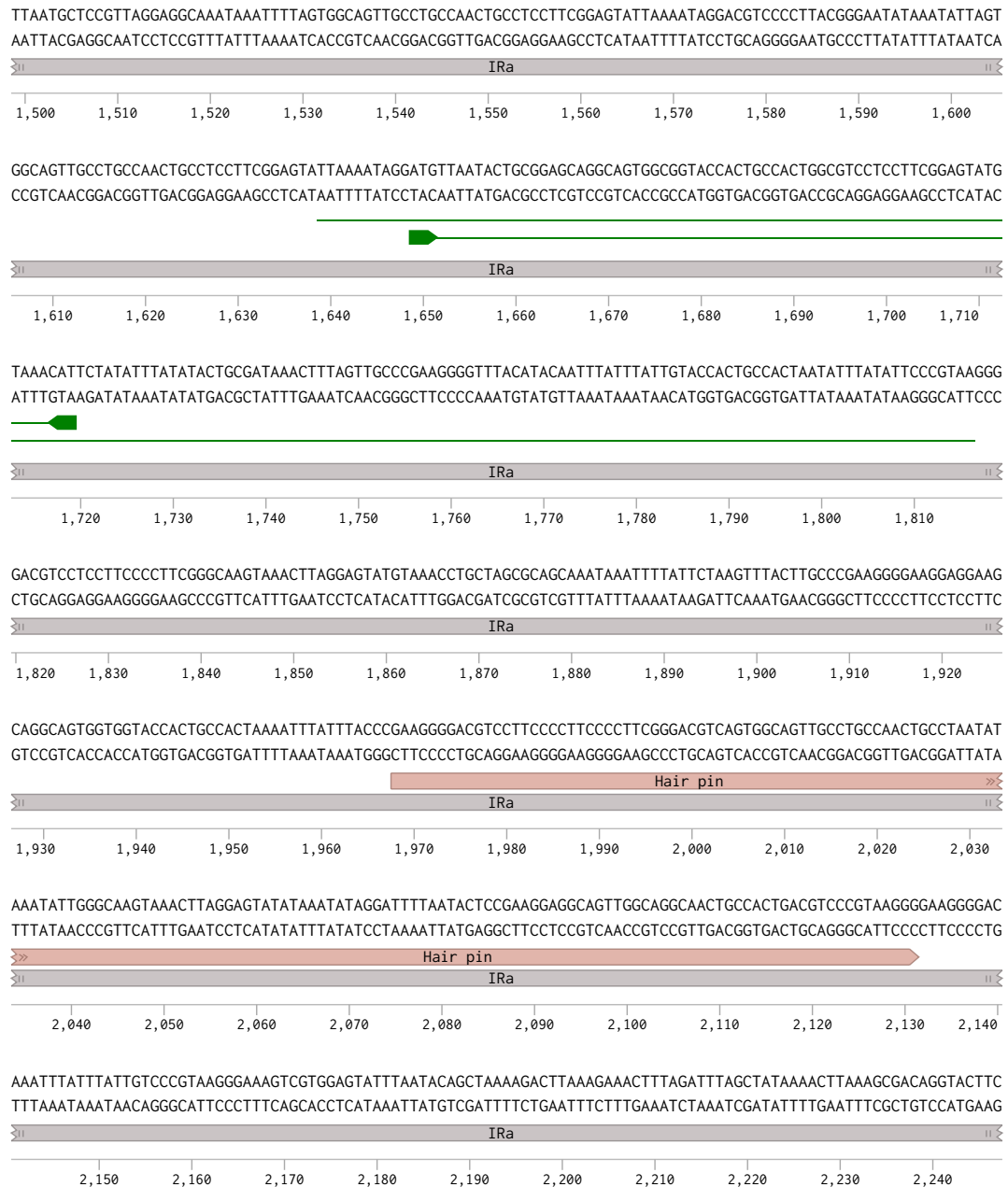
All reagents are compatible with the thesis's experimental workflows and can be referenced via NEB's official product pages (provided in the user's query).

Appendix 12 Plasmid map of NLuc and Nluc**



https://benchling.com/purton_lab/f/lib_K02HUnEc-ly_lv2s/seq_iWjlyhgE-ply434_lv2_trnw-uca_pro-16psa_ha-nluc_ter-rbclps... 1/10





Genomic map of the *trnW* gene region. The map shows a scale from 2,250 to 2,350 bp. A grey bar labeled 'IRa' spans from approximately 2,250 to 2,320 bp. A yellow bar labeled 'trnW' spans from approximately 2,330 to 2,350 bp. Arrows indicate the direction of transcription for both regions.

Gene	Length (nt)
trnW	~2,460
trnW	~2,435

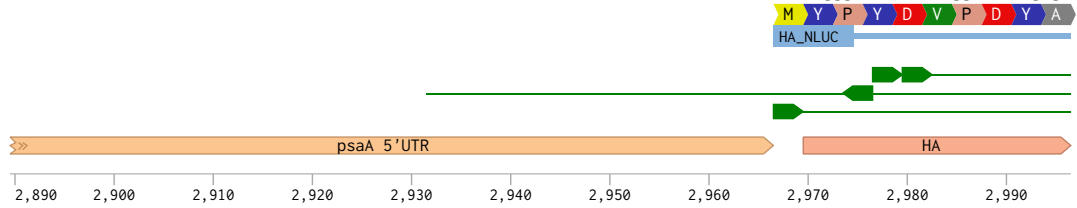
Genomic map of the *trnW* gene region. The top track shows the *trnW* gene structure with exons in green and introns in red. The bottom track shows the *trnW* gene structure with exons in yellow and introns in red. The x-axis represents the genomic position in base pairs, ranging from 2,470 to 2,560.

Genomic map showing the *trnW* gene (yellow arrow) and the 16S rRNA promoter (blue arrow) on a scale from 2,570 to 2,670. The *trnW* gene is located between 2,570 and 2,610, and the 16S rRNA promoter is located between 2,620 and 2,670.

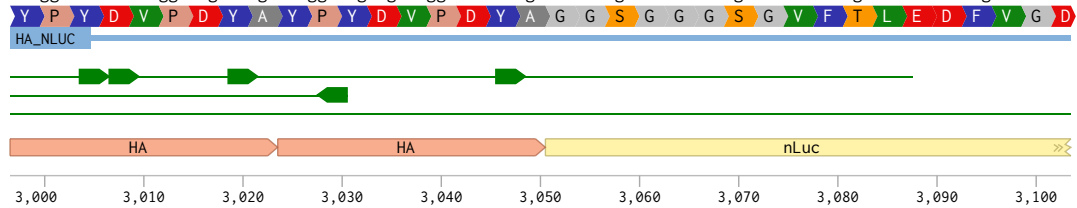
Diagram illustrating the 16S rRNA promoter region. The promoter is located upstream of the 16S rRNA gene, spanning approximately 100 base pairs (from position 2,680 to 2,780). The diagram shows the promoter sequence with a scale from 2,680 to 2,780.

Genomic map of the *psaA* gene region. The 16S rRNA promoter is indicated by a blue arrow pointing right, spanning from approximately 2,790 to 2,835 bp. The *psaA* 5'UTR is indicated by an orange arrow pointing right, spanning from approximately 2,835 to 2,885 bp. The scale bar below the arrows ranges from 2,790 to 2,880 bp with major ticks every 10 bp.

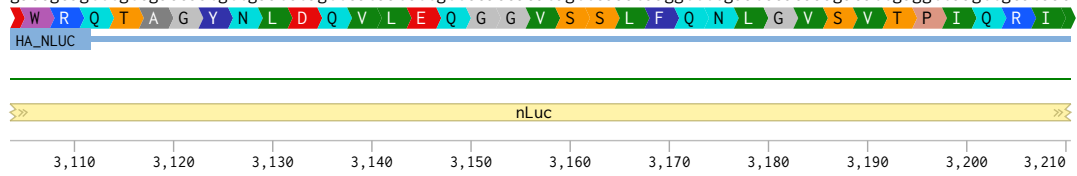
TAATAATTAAAGCGTTGCTAATGGTGAATAATGTATTTATTAATAATAATTGTTATTATAAGGAGAAATCCATGtaccatgatgtgtccagattacgct
ATTATTAATTTTCGCAACGATTACCACATTATTACATAAAATAATTTAATTTATTAACAATAATATTCCTCTTTAGGTACatgggtataactacaaggctaatgcga



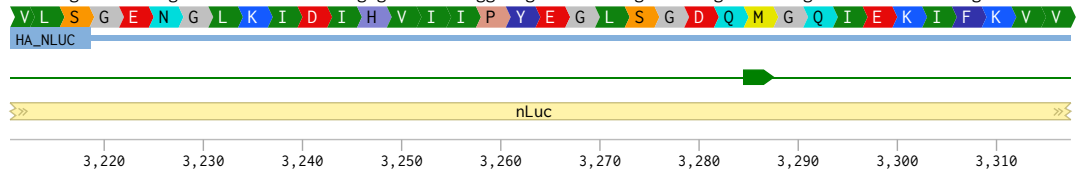
tatccttatgatgtacctgactatgcttatccatcacgcttctgattatgcagggtggttctggtggtggttctggtgttttacttttagaagatttcgtaggtga
atagggaatactacatggactgatacgaataggtatgctgcaaggactaatacgtccaccaagaccaccaccaagaccacaaaaatgaaatcttctaagcatccact



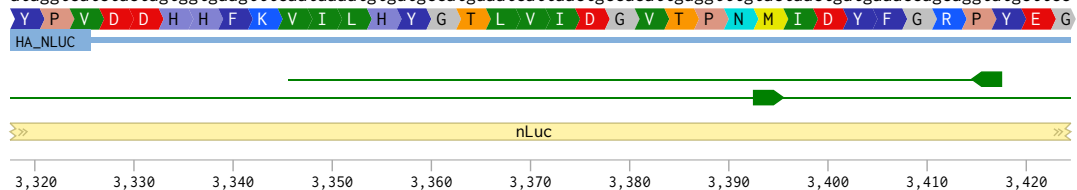
ctggcgtcaaacagctggttacaacttagatcaagtattagaacaagggtgtatcaagtttattccaaaacttaggtgtttctgtaactccaattcaacgtattg
gaccgcagtttgcgaccaatgttgaaatcttagttcataatctgttccaccacatagttcaataaagggtttgaaatccacaaagacattgaggttaagttgcataac

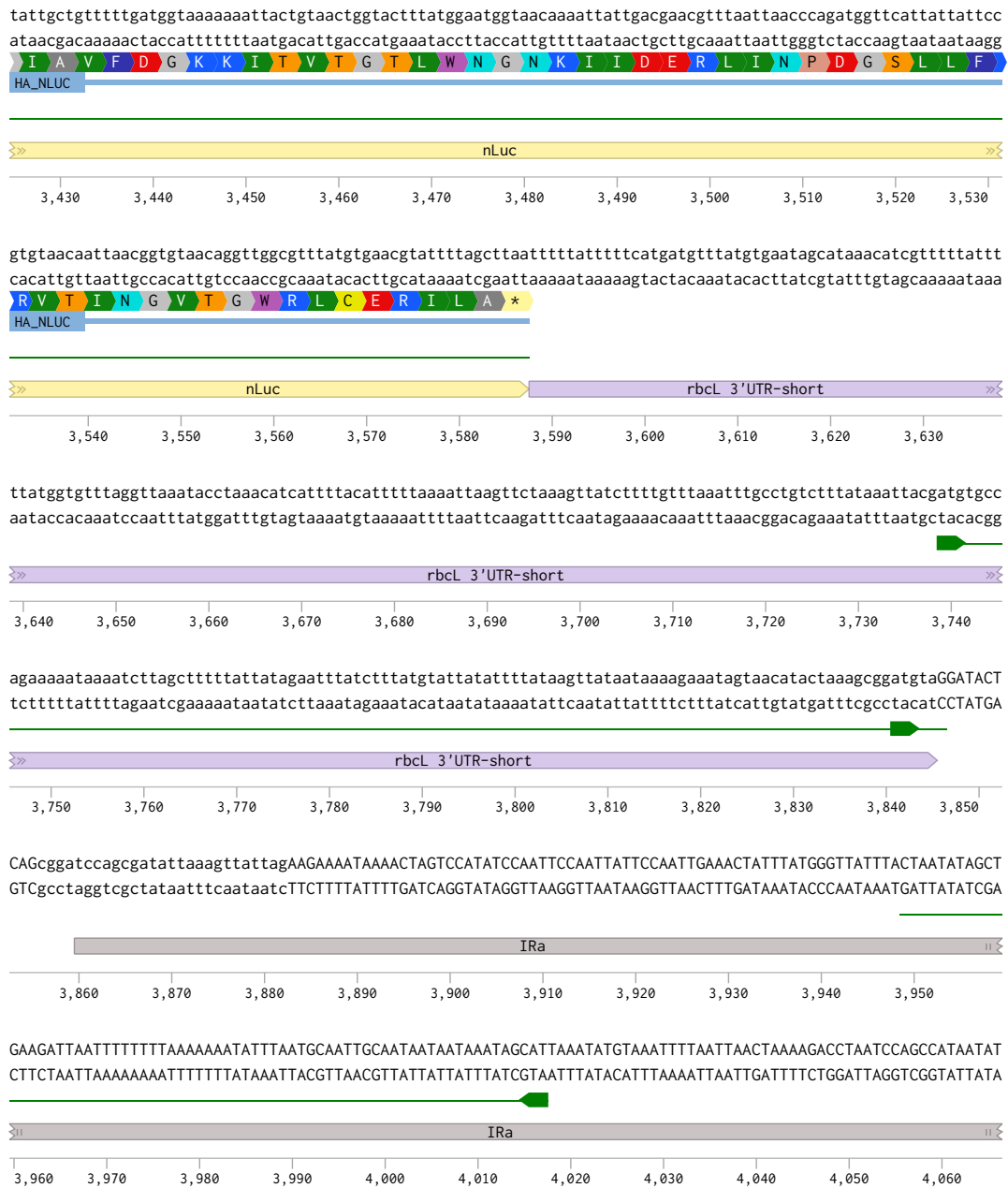


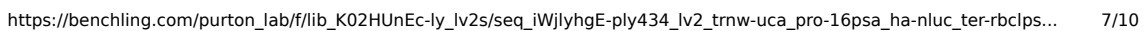
ttttatcagggtgaaacggtttaaaaattgatattcacgtaattattccatcacgaaggtttatctggtgatcaaatgggtcaaattgaaaaattttcaaagttggt
aaaatagtcacacttttgccaaatttttaactataagtgcatataaaggatgcttccaaatagaccactagtttaccagtttaacttttttaaagtttcaacaa



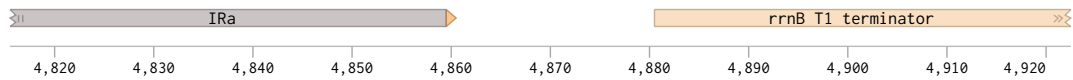
tatccagtagatgatcaccacttcaaagttattttactacgggtacttttagtaattgacgggtgaactccaacatgattgactactttggtcgtccatcacgaagg
ataggatcatctactagttggaagtttcaataaaatgtgatgccatgaaatcatttaactgccacattgaggtttgtactaactgatgaaccagcaggtatgcttcc





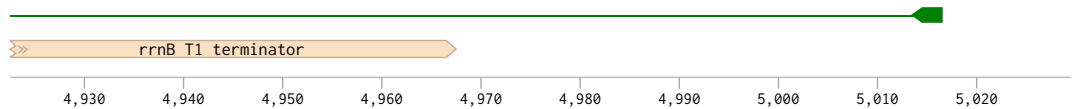


TATCGTAGACGAcagatttacatatcgtagacgacaaatactttgGAAGaccTCTAGGGCGGCGGatttgcctactcaggagagcgttcaccgacaaacaacagat
 ATAGCATCTGCTgtctaagttagcatctgctgtttatgaaacCTTctggAGATCCCGCCGCTaaacaggatgagtcctctcgcaagtggctgtttgtgtcta

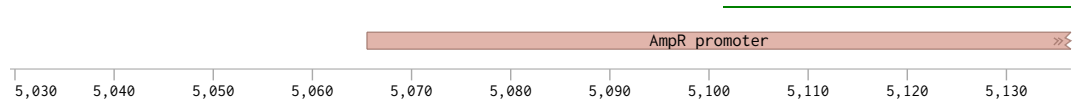


aaaacgaaaggccagcttttcgactgagcctttcgtttatttggatgccgaaaggcctcgtgatacgcctattttatagggttaatgtcatgataataatggtt
 ttttgctttccgggtcagaaagctgactcggaaagcaaaataaactacgggctttccgggagcactatcggtataaaatatccaattacagtactattattacca

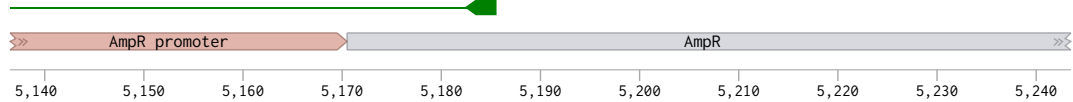
CTACGGGCTTCCCGGAGCACTATG



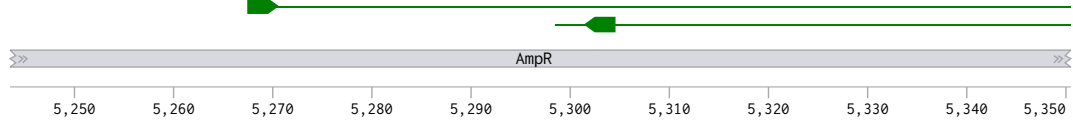
tcttagacgtcaggtggcacttttcgggaaatgtgcgcggaacccctatttggttatttttctaatacattcaaatatgtatccgctcatgagacaataacccctg
 agaactcgcagtcaccgtgaaaagcccctttacacgcgccttggggataaacaataaaaagatttatgtaagttatacataggcgagtactctgttattgggac



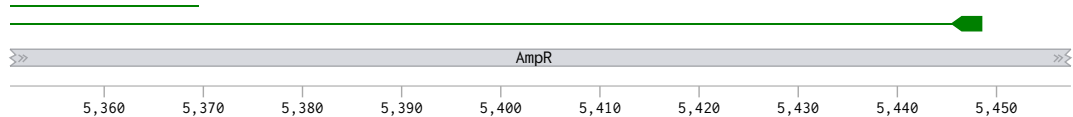
ataaatgcttcaataatattgaaaaggaagagatgatgattcaacatttccgtgtcgccttattccctttttgcggcattttgccttcctgttttgcctacc
 tatttacgaagttattataacttttcttctcatactcataagttgtaaggcacagcggaataagggaataaacgcccgtaaaacggaaggacaaaacgagttg

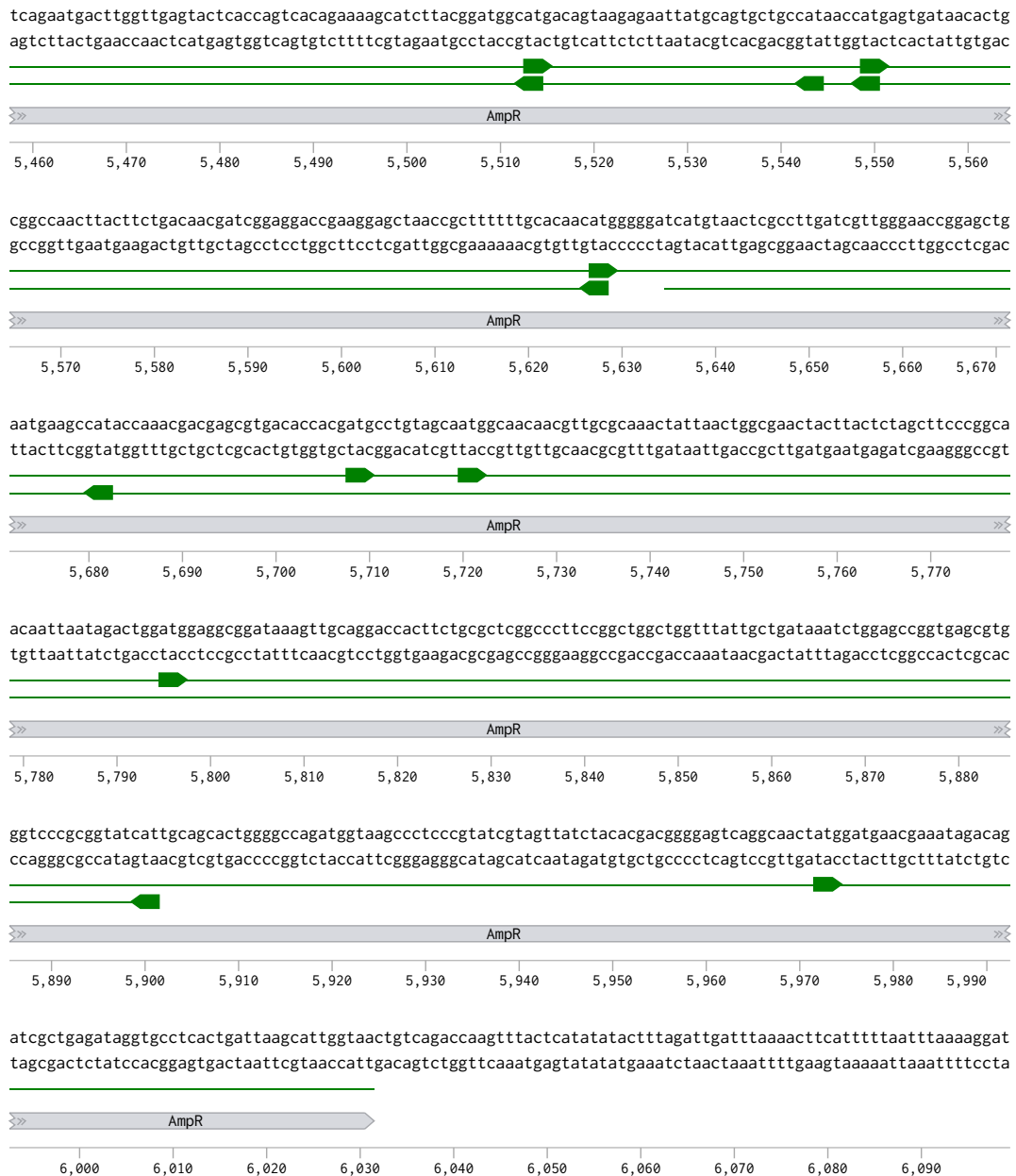


cagaaacgctggtgaaagtaaaagatgctgaagatcagttgggtgcacagtggttacatcgaactggatctcaacagcggtgaagatccttgagagttttgcgcc
 gtctttgcgaccactttcattttctacgacttctagtcaaccacgtgtcaccatgtagcttgacctagagttgtcgccattctaggaactcctaaaacggggg



gaagaacgctttccaatgatgagcacttttaaaagttctgctatgtggcgcggtattatccggtattgacccgggcaagagcaactcggtgcgcgcatacactattc
 ctctttgcaaaaggttactactcgtgaaaattcaagacgatacaccgcgcataatagggcataactgcggcccgttctcgttgaccagcgcggtatgtataag





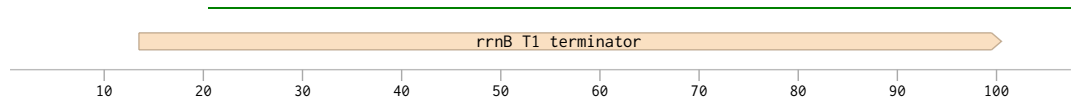
ctaggtgaag
gatccacttc
|
6,100

(from 1-642 bp)

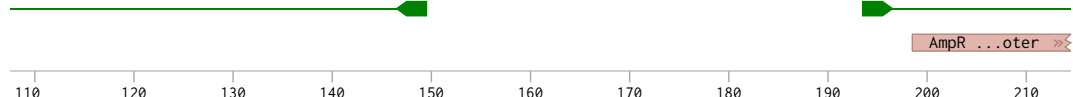
22/11/2025 21:49:35

pLY435_Lv2_trnW-UCA_pro.16/psa_HA-Nluc.2xTGA_te...

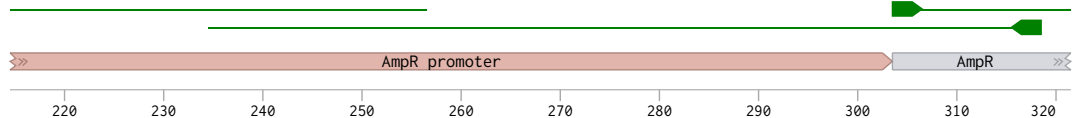
TCTAGGCGCGGCGGatTTgtcctactcaggagagcggttcaccgacaacaacagataaaacgaaaggcccgactctttcgactgagcctttcgtttttatgtgcccg
AGATCCCGCGCCtaaacaggatgagtcctctcgcaagtggctgtttgtgtctatTTgtccttcgggtcagaaagctgactcggaagcaaaaactacgggc



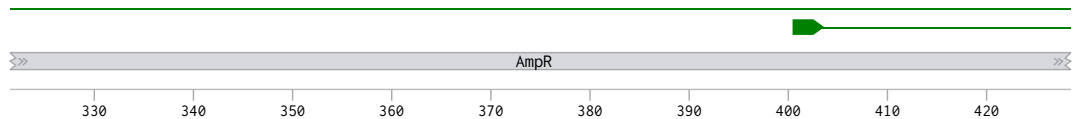
aaagggcctcgtgatacgctatTTttataggttaatgtcatgataataatggTTtcttagacgtcagggtggcactTTtcgggaaatgtgcgcggaaccctatTT
tttcccgagcactatgcggataaaaaatccaattacagtactattattaccaagaatctgcagtcaccgtgaaagccctttacacgcgccttggggataaa



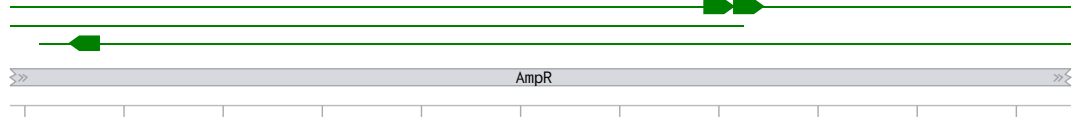
gttttttttctaatacattcaaatatgtatccgctcatgagacaataaccctgataaatgcttcaataattgaaaaaggaagagtatgagtattcaacatttc
caataaaaagatttatgtaagtttatacataggcgagtactctgttattgggactatttacgaagtattataactTTtcttctcatactcataagttgtaaag



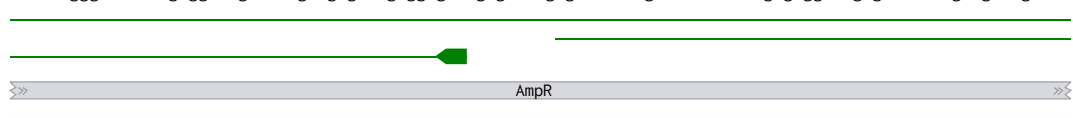
cggtcgccttattccctTTTTtgcggcattTTtccttctgtTTtctcaccagaaacgctggtgaaagtaaaagatgctgaagatcagttgggtgcacgagt
gcacagcgggaataagggaacacgcgtaaaacggaaggacaaaacgagtggtctTTtgcgaccactttcattTTtctacgacttctagtcaaccacgtgctca



gggttacatcgaactggatctcaacagcggtgaagatccttgagagttTTtgcggcgaagaacgctTTtccaatgatgagcactTTtaaagttctgctatgtggcgcg
cccaatgtagcttgacctagagttgtcgccattcttagaactctcaaaagcggggtctTTtgcaaaaggttactactcgtgaaaatttcaagacgataccgcgc

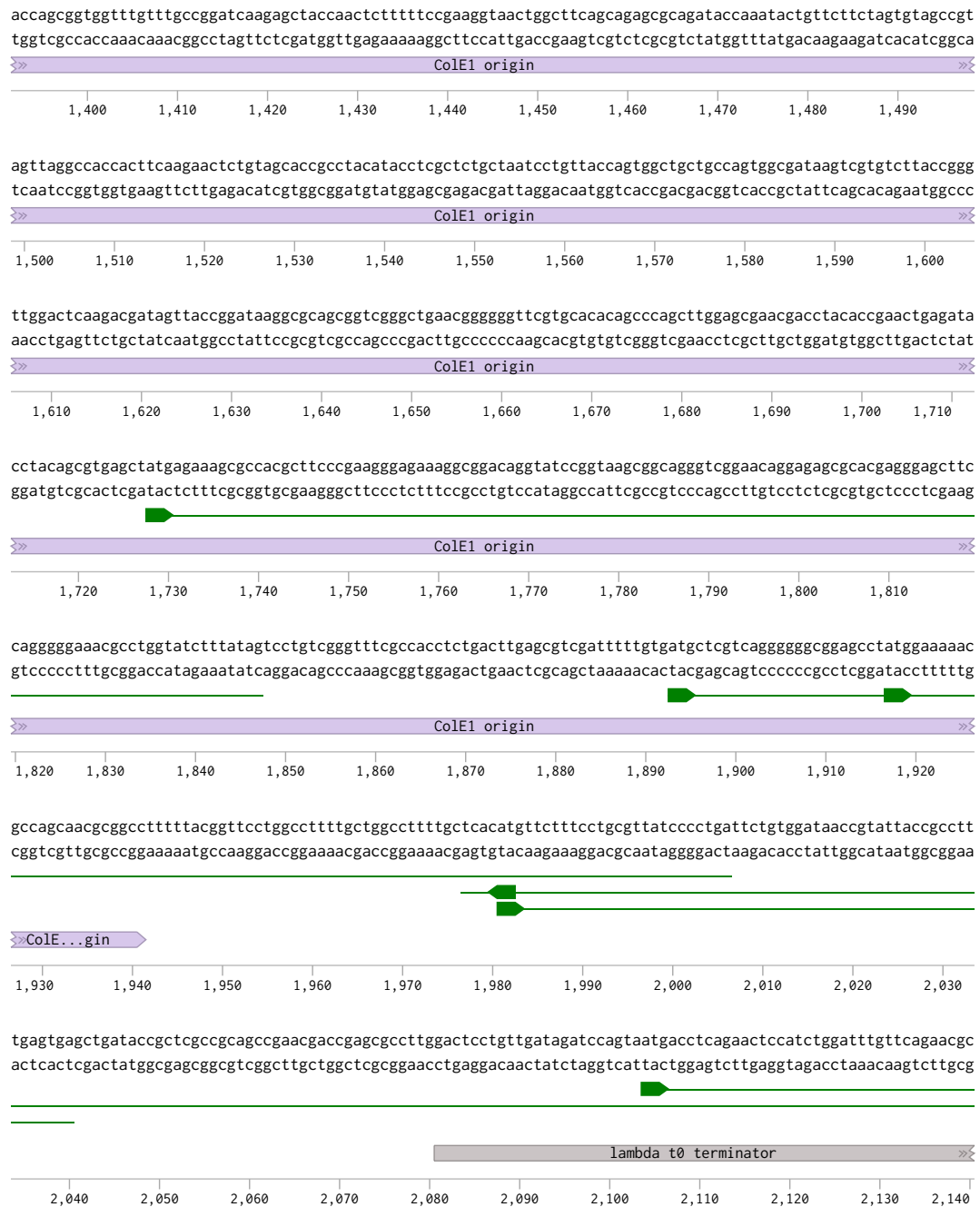


tattatcccgattatgacgccgggcaaggaactcggtcgccgcatacactattctcagaatgacttggttgagtactcaccagtcacagaaaagcatcttacggat
ataatagggcataactgcggccgttctcgttgagccagcggtatgtgataagagtcttactgaaccaactcatgagtggtcagtgctTTtctcgtagaatgccta

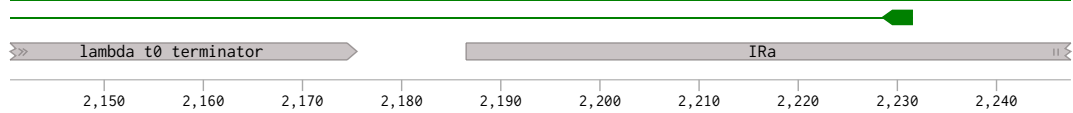


https://benchling.com/purton_lab/f/lib_K02HUnEc-ly_lv2s/seq_WG9fntqT-ply435_lv2_trnw-uca_pro-16psa_ha-nluc-2xtga_ter... 1/9

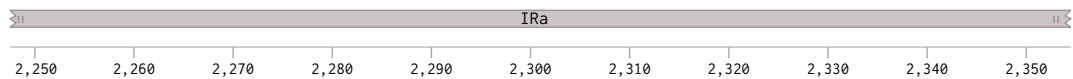




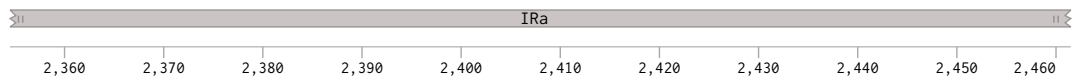
tcggttgccgcccggcggttttttatggtgagaatCCAGTGTGAGctccaacctctgttgAGCTTCTCCCTTCCCTTACGGGACATCCCTTCCCTTACGG
agccaacggcgcccgcaaaaaataaccactcttaGGTCACACGTCcgaggttgagacaaccTCGAAGAGGGGAAGGGGAATGCCTGTAGGGGAAGGGGAATGCC



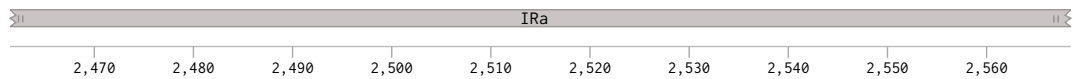
GATATTTATATACTCCGAAGGACGTCCCTTCGGGCAATAAATTTTAGTGGCAGTTGCAAAGTATTAATATCGTATATAAATATCCTGCCAACTGCCTAGGCAAGT
CTATAAATATATGAGGCTTCCTGCAGGGGAAGCCGTTTATTTAAATCACCCTCAACGTTTCATAATTATAGCATATATTTATAGGACGGTTGACGGATCCGTTCA



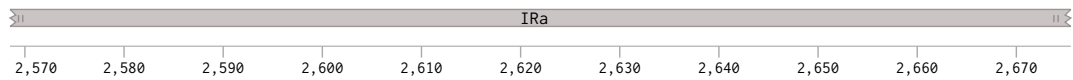
AAACTTAGGGATTTTAAATGCTCCGTTAGGACGTCCCTTCCCTTCGGGACGTCCCTTACGGGAATATAAATATTAGTGGACGTCCCTTCGGGCAATGAATTTT
TTTGAATCCCTAAATACGAGGCAATCCTGCAGGGGAAGGGGAAGCCCTGCAGGGGAATGCCCTTATTTATAATCACCTGCAGGGGAAGCCGTTTACTTAAAA



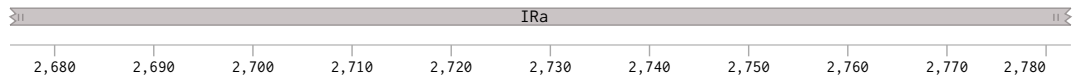
AGTGGCAGTTGCCTGCCAACTGCCGATATTTATATACTGCGATAAACTTTAGTTGCCGAAGGGGTTTACATACAATTTATTTATTGTACCACTGCCACTAATATTT
TCACCGTCAACGGACGGTTGACGGCTATAAATATATGACGCTATTTGAAATCAACGGGCTTCCCAATGTATGTTAAATAAATAACATGGTGACGGTGATTATAAA



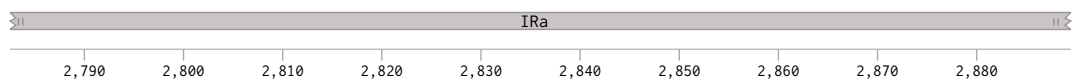
ATATTCCTGAAGGGGACGTCTCTCTCCCTTCGGGCAAGTAACTTAGGAGTATGTAACTGCTAGCGCAGCAAAATAATTTTATTCTAAGTTTACTTGCCCGA
TATAAGGGCATTCCCTGCAGGAGGAAGGGGAAGCCGTTTCAATTTGAATCCTCATACATTTGGACGATCGCGTCGTTTATTTAAATAAGATTCAATGAACGGGCT



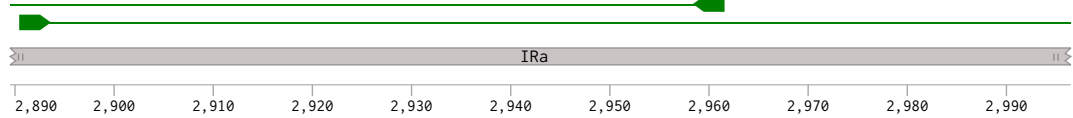
AGGGGAAGGAGGAAGCAGGAGTTGCCTCTCTCCCTTCGGGACGTCCCTTTCGGGATTTTAAATGCTCCGTTAGGAGGCAAAATAATTTTAGTGGCAGTTG
TCCCTTCTCTCTCGTCCGTCACGGAGGAAGGGGAAGCCCTGCAGGGGAAGCCCTAAATACGAGGCAATCCTCCGTTTATTTAAATCACCCTCAAC



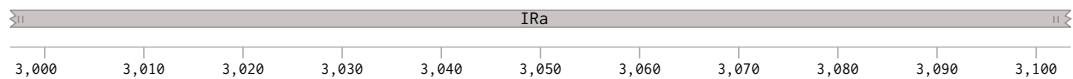
CCTGCCAACTGCCTCTCTCGGAGTATTAATAGGACGTCCCTTACGGGAATATAAATATTAGTGGCAGTTGCCTGCCAACTGCCTCTCGGAGTATTAATAG
GGACGGTTGACGGAGGAAGCCTCATAATTTTATCCTGCAGGGGAATGCCCTTATTTATAATCACCCTCAACGGACGGTTGACGGAGGAAGCCTCATAATTTTATC



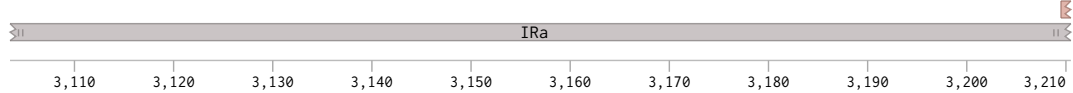
GATGTTAACTACTGCGAGCAGGCAGTGGCGGTACCACTGCCACTGGCGTCTCCTTCGGAGTATGTAACATTCTATTTATATACTGCGATAAACTTTAGTTGCC
CTACAATTATGACGCCTCGTCCGTACCGCCATGGTGACGGTGACCGCAGGAGGAAGCCCTACACATTTGTAAGATATAAATATATGACGCTATTTGAAATCAACGG



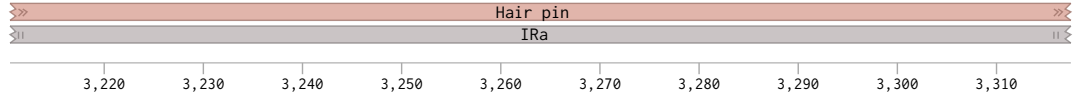
CGAAGGGGTTTACATACAATTTATTTATTGTACCACTGCCACTAATTTATATTTCCCGTAAGGGGACGTCCTTCCCTTCGGGCAAGTAACTTAGGAGTATG
GCTTCCCCAAATGTATGTTAAATAAATAACATGGTGACGGTGATTATAAATATAAGGCATTCCCTGCAGGAGGAAGGGGAAGCCCGTTCATTTGAATCCTCATAC



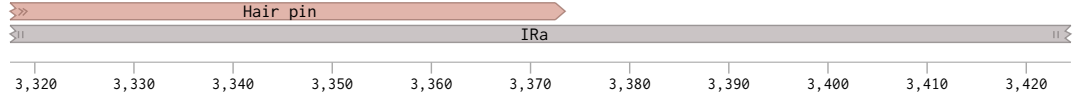
TAAACCTGCTAGCGCAGCAATAAATTTTATTCTAAGTTTACTTGCCGAAGGGGAAGGAGGAAGCAGGCAGTGGTGGTACCACTGCCACTAAAATTTATTTACCCG
ATTTGACGATCGCGTCGTTTATTTAAATAAGATTCAATGAACGGGCTCCCTCTCTCTCGTCCGTACCACCATGGTGACGGTGATTTAAATAAATGGGC



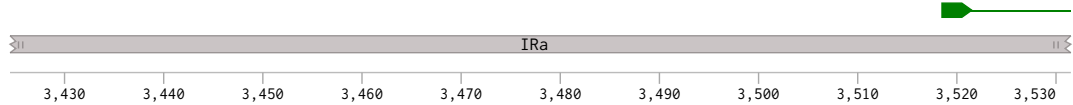
AAGGGGACGTCCTTCCCTTCCCTTCGGGACGTCAGTGGCAGTTGCCTGCCAAGTGCCTAATATAAATATTGGGCAAGTAACTTAGGAGTATATAAATATAGGAT
TCCCTGCAGGAAGGGGAAGGGGAAGCCCTGCAGTCACCGTCAACGGACGGTTGACGGATTATTTATAACCCGTTCAATTTGAATCCTCATATTTTATATCCTA



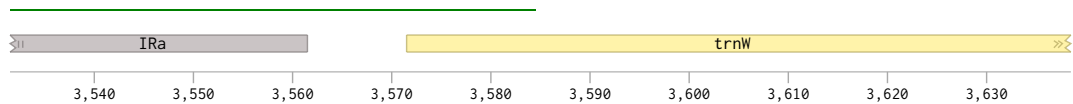
TTTAACTACTCCGAAGGAGGCAGTTGGCAGGCAACTGCCACTGACGTCCCGTAAGGGGAAGGGGACAAATTTATTTATTGTCCCGTAAGGGAAGTCGTGGAGTATTT
AAATTATGAGGCTTCCTCCGTCAACCGTCCGTTGACGGTGACTGCAGGGCATTCCCTTCCCTGTTTAAATAAATAACAGGGCATTCCCTTTCAGCACCTCATAAA

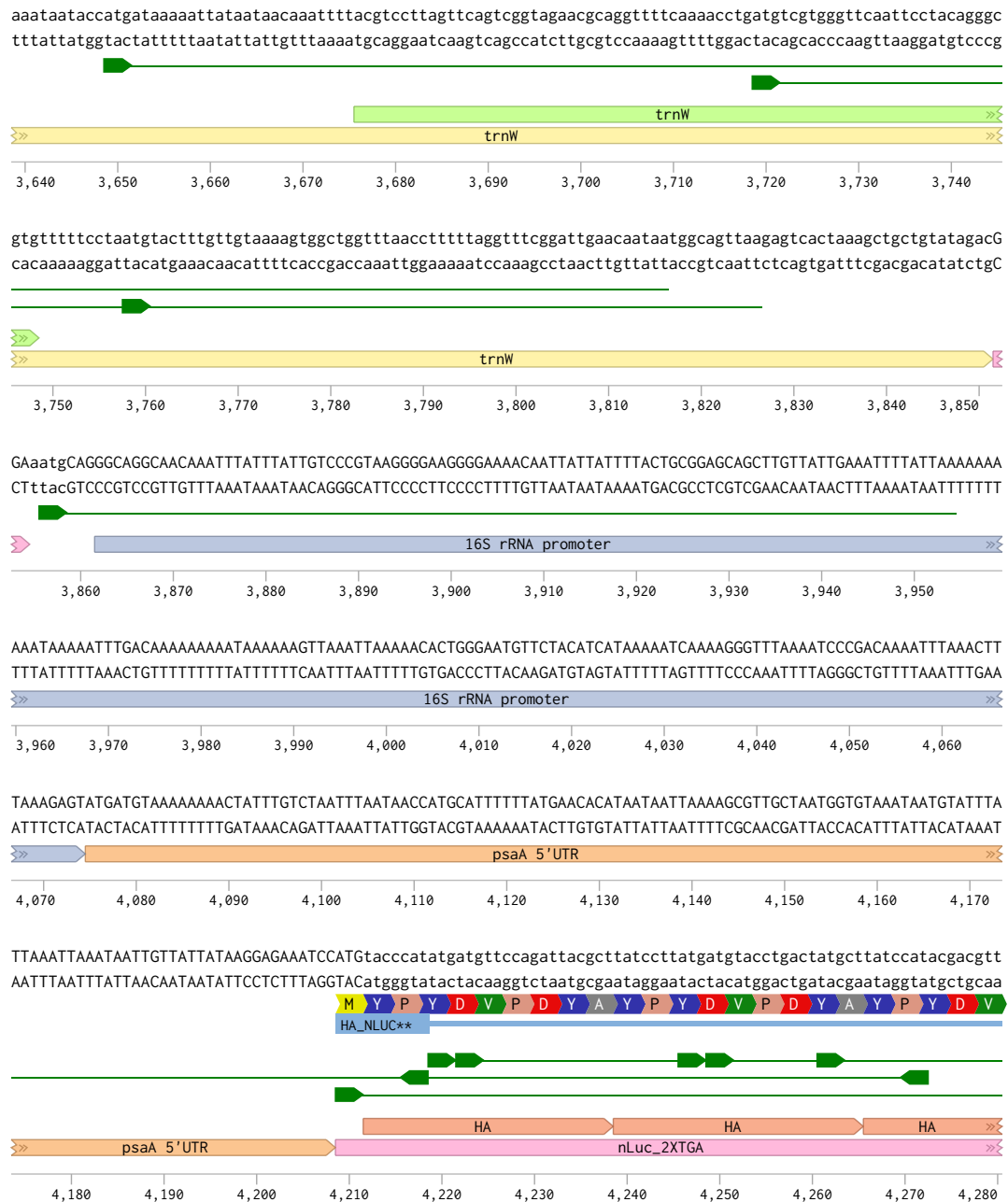


AATACAGCTAAAAGACTTAAAGAACTTTAGATTTAGCTATAAACTTAAAGCGACAGGTACTTCGAAACGGTGATTATCCAGGCCAACTTATGAAATGCAAGT
TTATGTCGATTTTCTGAATTTCTTTGAAATCTAAATCGATATTTTGAATTCGCTGTCCATGAAGGCTTTGCCACCAATAAGTCCGGTTTGAATACTTTACGTTCA

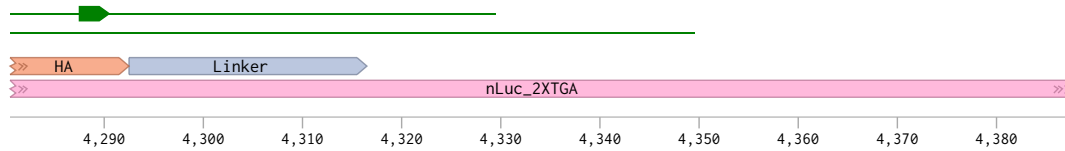


ACCATCAGATATtgctagcatggataggaGGAggagCAGcggttaacccatgattaacaactatatcaataaaatcaattttagtgaaatactctgattgacatta
TGGTAGTCTATAacgatcgctacatgcctCCTcctcGTGcaattgggtataattgttgatagttatTTtagttaacatcactttatgagactaactgtaat

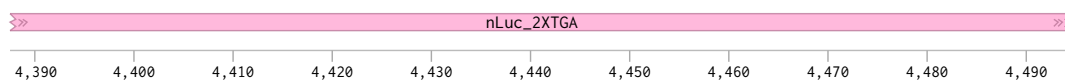




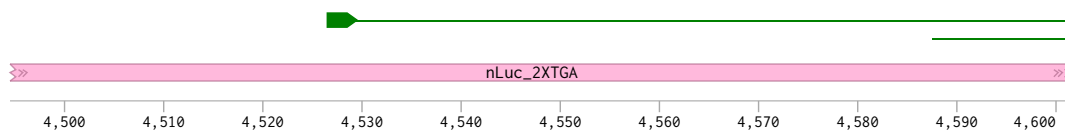
cctgattatgcagggtgtctgtgtgtgtctgtgttttacttttagaagatttcgttagtgactgacgtcaaacagctggttacaacttagatcaagtattaga
 ggactaatcgtccaccaagaccaccacaaagaccacaaaaatgaattctttaaagcatccactgactgcagtttgcgaccaatgttgaatctagttcataatct
 P D Y A G G S G G G S G V F T L E D F V G D * R Q T A G Y N L D Q V L E
 HA_NLUC**



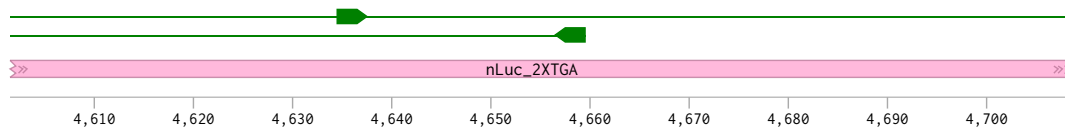
acaagggtgtgtatcaagtttattccaaaacttaggtgtttctgtaactccaattcaacgtattgttttatcagggtgaaacggtttaaaaattgatattcacgtaa
 tgttcaccacatagttcaataaggttttgatccacaaagacattgaggttaagttgcataacaaaatagtcacttttgccaaatttttaactataagtcatt
 Q G G V S S L F Q N L G V S V T P I Q R I V L S G E N G L K I D I H V
 HA_NLUC**



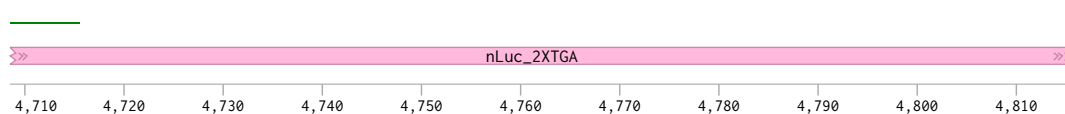
ttattccatacgaagtttatctggtgatcaaatgggtcaaatgaaaaattttcaaagttgtttatccagtagatgacaccacttcaaagttattttacactac
 aataaggtatgcttccaaatagaccactagtttaccagtttaacttttttaaagtttcaacaaataggtcatctactagttggaagtttcaataaaatgtgatg
 I I P Y E G L S G D Q M G Q I E K I F K V V Y P V D D H H F K V I L H Y
 HA_NLUC**

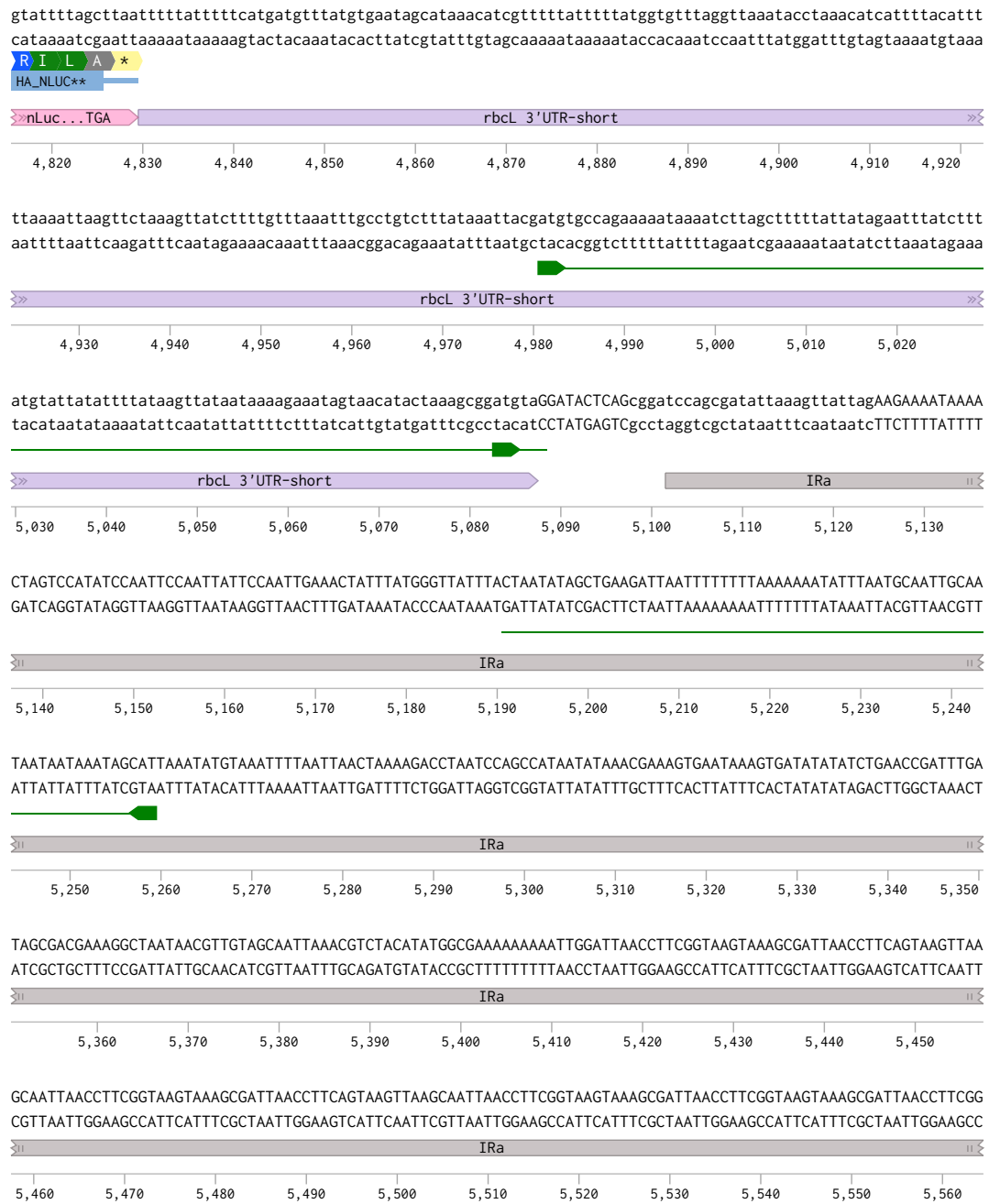


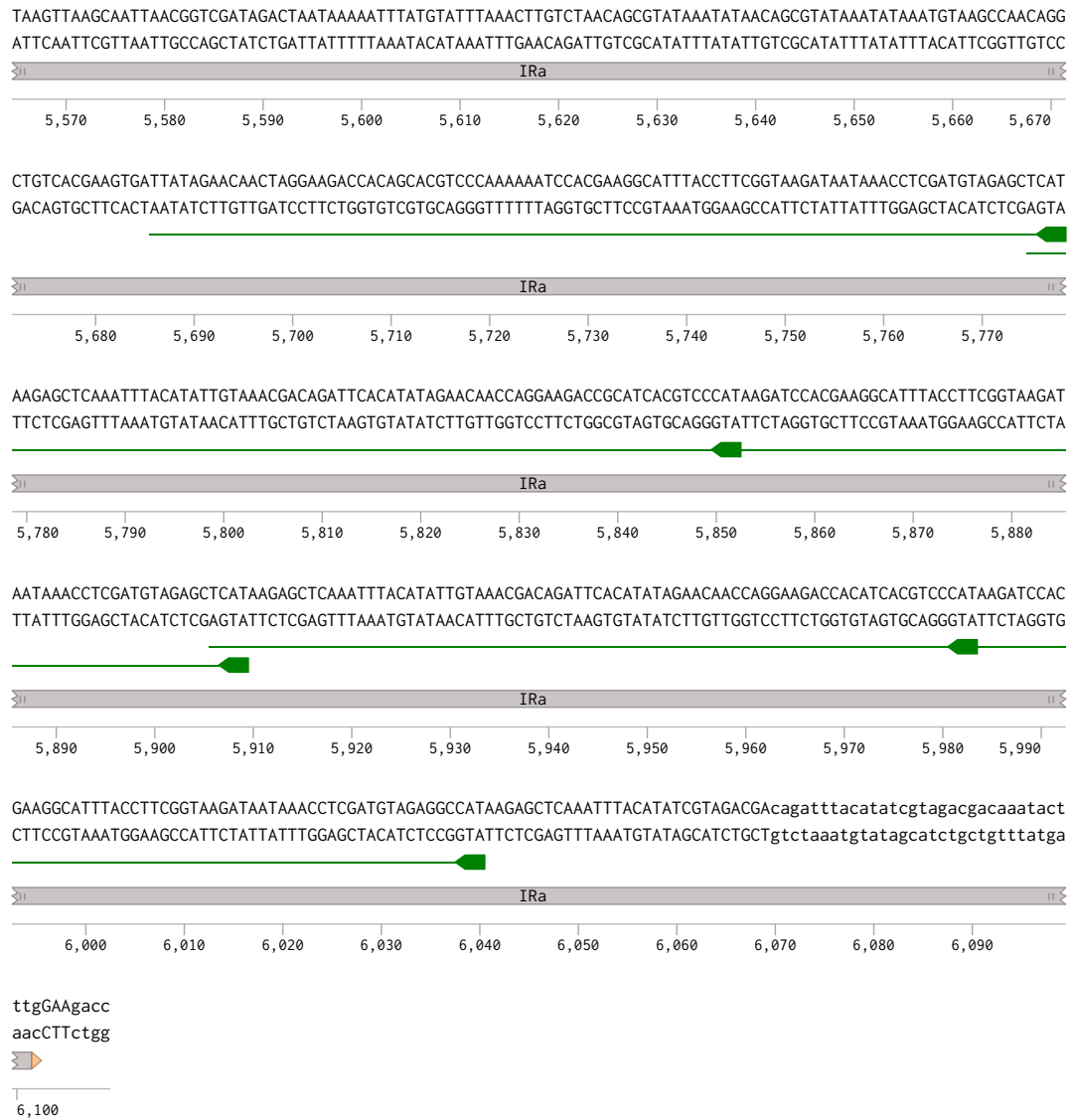
ggtacttttagtaattgacggtgtaactccaacatgatgactacttttgctcgccatacgaaggtattgctgtttttgatggtaaaaaattactgtaactggtac
 ccataaactcattactgccacattgaggtttgtactaactgatgaaccagcaggtatgcttcataacgacaaaaactaccatttttttaagacattgaccatg
 G T L V I D G V T P N M I D Y F G R P Y E G I A V F D G K K I T V T G T
 HA_NLUC**



tttatgaaatggttaacaaaattattgacgaacgtttaattaaccagatggttcattattattccgtgtaacaattaacggtgtaacaggttgccgtttatgtgaac
 aaatactttaccattgttttaataactgcttgcaaatattgggtctaccaagtaataaaggcacattgttaattgccacattgtccaaccgcaatacacttg
 L * N G N K I I D E R L I N P D G S L L F R V T I N G V T G W R L C E
 HA_NLUC**







Reference

- Acosta, J., Estrada, M. P., Carpio, Y., Ruiz, O., Morales, R., Martínez, E., Valdés, J., Borroto, C., Besada, V., Sánchez, A., & Herrera, F. (2009). Tilapia somatotropin polypeptides: Potent enhancers of fish growth and innate immunity. *Biotechnologia Aplicada*, 26(3), 267–272.
- Agnarsson, I., Kuntner, M., Blackledge, T. A., & Lalueza-Fox, C. (2010). Bioprospecting finds the toughest biological material: Extraordinary silk from a giant riverine orb spider [Article]. *PloS One*, 5(9), 1–8. <https://doi.org/10.1371/journal.pone.0011234>
- Ahmad, A., W. Hassan, S., & Banat, F. (2022). An overview of microalgae biomass as a sustainable aquaculture feed ingredient: food security and circular economy. In *Bioengineered* (Vol. 13, Issue 4, pp. 9521–9547). Taylor and Francis Ltd. <https://doi.org/10.1080/21655979.2022.2061148>
- Ali, K., Santabarbara, S., Heathcote, P., Evans, M. C. W., & Purton, S. (2006). Bidirectional electron transfer in photosystem I: Replacement of the symmetry-breaking tryptophan close to the PsaB-bound phylloquinone (A1B) with a glycine residue alters the redox properties of A1B and blocks forward electron transfer at cryogenic temperatures. *Biochimica et Biophysica Acta - Bioenergetics*, 1757(12), 1623–1633. <https://doi.org/10.1016/j.bbabbio.2006.07.006>

- Alimuddin, A., Lesmana, I., Sudrajat, A. O., Carman, O., & Faizal, I. (2010). Production and Bioactivity Potential of Three Recombinant Growth Hormones of Farmed Fish. *Indonesian Aquaculture Journal*, 5(1), 11. <https://doi.org/10.15578/iaj.5.1.2010.11-17>
- Altman, G. H., Diaz, F., Jakuba, C., Calabro, T., Horan, R. L., Chen, J., Lu, H., Richmond, J., & Kaplan, D. L. (2003). Silk-based biomaterials [Article]. *Biomaterials*, 24(3), 401–416. [https://doi.org/10.1016/S0142-9612\(02\)00353-8](https://doi.org/10.1016/S0142-9612(02)00353-8)
- Alyokhin, A., Baker, M., Mota-Sanchez, D., Dively, G., & Grafius, E. (2008). Colorado potato beetle resistance to insecticides. In *American Journal of Potato Research* (Vol. 85, Issue 6, pp. 395–413). <https://doi.org/10.1007/s12230-008-9052-0>
- Annamalai, S. N., Das, P., Thaier, M. I. A., Abdul Quadir, M., Khan, S., Mahata, C., & Al Jabri, H. (2021). Nutrients and energy digestibility of microalgal biomass for fish feed applications [Article]. *Sustainability*, 13(23), 13211. <https://doi.org/10.3390/su132313211>
- Antoro, S., Zairin, M., Alimuddin, Suprayudi, M. A., & Faizal, I. (2016). Growth, biochemical composition, innate immunity and histological performance of the juvenile humpback grouper (*Cromileptes altivelis*) after treatment with recombinant fish growth hormone. *Aquaculture Research*, 47(4), 1238–1250. <https://doi.org/10.1111/are.12581>

- Arenal, A., Pimentel, R., Pimentel, E., Martín, L., Santiesteban, D., Franco, R., & Aleström, P. (2008). Growth enhancement of shrimp (*Litopenaeus schmitti*) after transfer of tilapia growth hormone gene. *Biotechnology Letters*, 30(5), 845–851. <https://doi.org/10.1007/s10529-008-9636-2>
- Arias, C. A. D., Oliveira, C. F. M. de, Molino, J. V. D., Ferreira-Camargo, L. S., Matsudo, M. C., & Carvalho, J. C. M. de. (2023). Production of Recombinant Biopharmaceuticals in *Chlamydomonas reinhardtii*. In *International Journal of Plant Biology* (Vol. 14, Issue 1, pp. 39–52). MDPI. <https://doi.org/10.3390/ijpb14010004>
- Baig, H., Fontanarrosa, P., Kulkarni, V., McLaughlin, J. A., Vaidyanathan, P., Bartley, B., Beal, J., Crowther, M., Gorochofski, T. E., Grünberg, R., Misirli, G., Scott-Brown, J., Oberortner, E., Wipat, A., & Myers, C. J. (2020). Synthetic biology open language (SBOL) version 3.0.0. *Journal of Integrative Bioinformatics*, 17(2–3), 0–62. <https://doi.org/10.1515/jib-2020-0017>
- Bakhshandeh, B., Nateghi, S. S., Gazani, M. M., Dehghani, Z., & Mohammadzadeh, F. (2021). A review on advances in the applications of spider silk in biomedical issues. *International Journal of Biological Macromolecules*, 192(July), 258–271. <https://doi.org/10.1016/j.ijbiomac.2021.09.201>
- Balakrishna Pillai, A., Nagarajan, U., Mitra, A., Krishnan, U., Rajendran, S., Hoti, S. L., & Mishra, R. K. (2017). RNA interference in mosquito: understanding immune responses, double-stranded RNA delivery systems and potential

applications in vector control [Article]. *Insect Molecular Biology*, 26(2), 127–139. <https://doi.org/10.1111/imb.12282>

Barolo, L., Abbriano, R. M., Commault, A. S., Padula, M. P., & Pernice, M. (2024). Proteomic analysis reveals molecular changes following genetic engineering in *Chlamydomonas reinhardtii*. *BMC Microbiology*, 24(1). <https://doi.org/10.1186/s12866-024-03554-4>

Barry, T. P., Marwah, A., & Marwah, P. (2007). Stability of 17 α -methyltestosterone in fish feed. *Aquaculture*, 271(1–4). <https://doi.org/10.1016/j.aquaculture.2007.05.001>

Bateman, J. M., & Purton, S. (2000). Tools for chloroplast transformation in *Chlamydomonas*: Expression vectors and a new dominant selectable marker. *Molecular and General Genetics*, 263(3), 404–410. <https://doi.org/10.1007/s004380051184>

Baulcombe, D. (2004). RNA silencing in plants [Article]. *Nature*, 431(7006), 356–363. <https://doi.org/10.1038/nature02874>

Baum, J. A., Bogaert, T., Clinton, W., Heck, G. R., Feldmann, P., Ilagan, O., Johnson, S., Plaetinck, G., Munyikwa, T., & Pleau, M. (2007). Control of coleopteran insect pests through RNA interference [Article]. *Nature Biotechnology*, 25(11), 1322–1326. <https://doi.org/10.1038/nbt1359>

- Bélanger, A., Sarker, P. K., Bureau, D. P., Chouinard, Y., & Vandenberg, G. W. (2021). Apparent digestibility of macronutrients and fatty acids from microalgae (*Schizochytrium* sp.) fed to rainbow trout (*Oncorhynchus mykiss*): A potential candidate for fish oil substitution [Article]. *Animals (Basel)*, 11(2), 1–10. <https://doi.org/10.3390/ani11020456>
- Bélanger, S., Kramer, M. C., Payne, H. A., Hui, A. Y., Slotkin, R. K., Meyers, B. C., & Staub, J. M. (2023). Plastid dsRNA transgenes trigger phased small RNA-based gene silencing of nuclear-encoded genes [Article]. *The Plant Cell*, 35(9), 3398–3412. <https://doi.org/10.1093/plcell/koad165>
- Belanger, S., Kramer, M. C., Payne, H. A., Hui, A. Y., Slotkin, R. K., Meyers, B. C., & Staub, J. M. (2023). Plastid dsRNA transgenes trigger phased small RNA-based gene silencing of nuclear-encoded genes. *Plant Cell*, 35(9), 3398–3412. <https://doi.org/10.1093/plcell/koad165>
- Bertalan, I., Munder, M. C., Weiß, C., Kopf, J., Fischer, D., & Johanningmeier, U. (2015). A rapid, modular and marker-free chloroplast expression system for the green alga *Chlamydomonas reinhardtii*. *Journal of Biotechnology*, 195, 60–66. <https://doi.org/10.1016/j.jbiotec.2014.12.017>
- Bingham, S. E., Xu, R., & Webber, A. N. (1991). Transformation of chloroplasts with the *psaB* gene encoding a polypeptide of the photosystem I reaction center. *FEBS Letters*, 292(1–2), 137–140. [https://doi.org/10.1016/0014-5793\(91\)80851-S](https://doi.org/10.1016/0014-5793(91)80851-S)

- Bini, E., Knight, D. P., & Kaplan, D. L. (2004). Mapping Domain Structures in Silks from Insects and Spiders Related to Protein Assembly [Article]. *Journal of Molecular Biology*, 335(1), 27–40. <https://doi.org/10.1016/j.jmb.2003.10.043>
- Blankenship, J. E., & Kindle, K. L. (1992). Expression of Chimeric Genes by the Light-Regulated cabII-1 Promoter in *Chlamydomonas reinhardtii*: A cabII-1/nit1 Gene Functions as a Dominant Selectable Marker in a nitI[−] nit2[−] Strain [Article]. *Molecular and Cellular Biology*, 12(11), 5268–5279. <https://doi.org/10.1128/mcb.12.11.5268-5279.1992>
- Blankenship, R. E. (2008). *Molecular Mechanisms of Photosynthesis* (Second edition.) [Book]. Wiley-Blackwell. <https://doi.org/10.1002/9780470758472>
- Bock, R. (2015). Engineering Plastid Genomes: Methods, Tools, and Applications in Basic Research and Biotechnology [Article]. *Annual Review of Plant Biology*, 66(1), 211–241. <https://doi.org/10.1146/annurev-arplant-050213-040212>
- Bock, R. (2022). Transplastomic approaches for metabolic engineering. In *Current Opinion in Plant Biology* (Vol. 66). Elsevier Ltd. <https://doi.org/10.1016/j.pbi.2022.102185>
- Borowitzka, M. A., & Vonshak, A. (2017). Scaling up microalgal cultures to commercial scale. *European Journal of Phycology*, 52(4), 407–418. <https://doi.org/10.1080/09670262.2017.1365177>

- Bouhedda, F., Autour, A., & Ryckelynck, M. (2018). Light-up RNA aptamers and their cognate fluorogens: From their development to their applications. *International Journal of Molecular Sciences*, 19(1). <https://doi.org/10.3390/ijms19010044>
- Boynton, J. E., Gillham, N. W., Harris, E. H., Hosler, J. P., Johnson, A. M., Johnes, A. R., Randolph-Anderson, B. L., Robertson, D., Klein, T. M., Shark, K. B., & Sanford, J. C. (1988). *Chloroplast transformation in Chlamydomonas with high velocity microprojectiles*. 240, 1534–1538.
- Breuers, F. K. H., Bräutigam, A., & Weber, A. P. M. (2011). The plastid outer envelope - A highly dynamic interface between plastid and cytoplasm [Article]. *Frontiers in Plant Science*, 2, 97–97. <https://doi.org/10.3389/fpls.2011.00097>
- Callister, W. D. (2015). *Materials science and engineering*. (D. G. Rethwisch, Ed.; 9th edition, SI v...) [Book]. Wiley.
- Carthew, R. W., & Sontheimer, E. J. (2009). Origins and Mechanisms of miRNAs and siRNAs [Article]. *Cell*, 136(4), 642–655. <https://doi.org/10.1016/j.cell.2009.01.035>
- Catarina Guedes, A. (2012). *Nutritional Value and Uses of Microalgae in Aquaculture* [Bookitem]. IntechOpen. <https://doi.org/10.5772/30576>
- Cavauiolo, M., Kuras, R., Wollman, F. A., Choquet, Y., & Vallon, O. (2017). Small RNA profiling in chlamydomonas: Insights into chloroplast RNA metabolism.

Nucleic Acids Research, 45(18), 10783–10799.
<https://doi.org/10.1093/nar/gkx668>

Cerutti, H., Ma, X., Msanne, J., & Repas, T. (2011). RNA-Mediated Silencing in Algae: Biological Roles and Tools for Analysis of Gene Function [Article]. *Eukaryotic Cell*, 10(9), 1164–1172. <https://doi.org/10.1128/EC.05106-11>

Chaffey, N. (2003). Alberts, B., Johnson, A., Lewis, J., Raff, M., Roberts, K. and Walter, P. Molecular biology of the cell. 4th edn [Article]. *Annals of Botany*, 91(3), 401–401. <https://doi.org/10.1093/aob/mcg023>

Changko, S. (2020). *New tools and strategies for metabolic engineering of the algal chloroplast* (Issue September). <https://discovery.ucl.ac.uk/id/eprint/10119343/>

Changko, S. (2021). *New tools and strategies for metabolic engineering of the algal chloroplast*.

Changko, S., Rajakumar, P. D., Young, R. E. B., & Purton, S. (2020). The phosphite oxidoreductase gene, *ptxD* as a bio-contained chloroplast marker and crop-protection tool for algal biotechnology using *Chlamydomonas*. *Applied Microbiology and Biotechnology*, 104(2), 675–686. <https://doi.org/10.1007/s00253-019-10258-7>

- Charoonnart, P., Purton, S., & Saksmerprome, V. (2018). Applications of microalgal biotechnology for disease control in aquaculture. *Biology*, 7(24). <https://doi.org/https://doi.org/10.3390/biology7020024>
- Charoonnart, P., Taunt, H. N., Yang, L., Webb, C., Robinson, C., Saksmerprome, V., & Purton, S. (2023). Transgenic Microalgae Expressing Double-Stranded RNA as Potential Feed Supplements for Controlling White Spot Syndrome in Shrimp Aquaculture [Article]. *Microorganisms*, 11(8), 1893. <https://doi.org/10.3390/microorganisms11081893>
- Charoonnart, P., Worakajit, N., Zedler, J. A. Z., Meetam, M., Robinson, C., & Saksmerprome, V. (2019). Generation of microalga *Chlamydomonas reinhardtii* expressing shrimp antiviral dsRNA without supplementation of antibiotics. *Scientific Reports*, 9(1), 1–8. <https://doi.org/10.1038/s41598-019-39539-x>
- Chen, H. C., & Melis, A. (2013). Marker-free genetic engineering of the chloroplast in the green microalga *Chlamydomonas reinhardtii*. *Plant Biotechnology Journal*, 11(7), 818–828. <https://doi.org/10.1111/pbi.12073>
- Chen, H. L., Li, S. S., Huang, R., & Tsai, H. J. (2008). Conditional production of a functional fish growth hormone in the transgenic line of *Nannochloropsis oculata* (Eustigmatophyceae). *Journal of Phycology*, 44(3), 768–776. <https://doi.org/10.1111/j.1529-8817.2008.00508.x>

- Chen, H., Yang, Q., Xu, J., Deng, X., Zhang, Y., Liu, T., Rots, M. G., Xu, G., & Huang, K. (2023). Efficient methods for multiple types of precise gene-editing in *Chlamydomonas* [Article]. *The Plant Journal: For Cell and Molecular Biology*, 115(3), 846–865. <https://doi.org/10.1111/tpj.16265>
- Cheng, Q., Day, A., Dowson-Day, M., Shen, G. F., & Dixon, R. (2005). The *Klebsiella pneumoniae* nitrogenase Fe protein gene (*nifH*) functionally substitutes for the *chlL* gene in *Chlamydomonas reinhardtii*. *Biochemical and Biophysical Research Communications*, 329(3), 966–975. <https://doi.org/10.1016/j.bbrc.2005.02.064>
- Chisti, Y. (2007). Biodiesel from microalgae [Article]. *Biotechnology Advances*, 25(3), 294–306. <https://doi.org/10.1016/j.biotechadv.2007.02.001>
- Conrad, U., Scheller, J., Gührs, K.-H., & Grosse, F. (2001). Production of spider silk proteins in tobacco and potato [Article]. *Nature Biotechnology*, 19(6), 573–577. <https://doi.org/10.1038/89335>
- Craig, R. J., Gallaher, S. D., Shu, S., Salomé, P. A., Jenkins, J. W., Blaby-Haas, C. E., Purvine, S. O., O'Donnell, S., Barry, K., Grimwood, J., Strenkert, D., Kropat, J., Daum, C., Yoshinaga, Y., Goodstein, D. M., Vallon, O., Schmutz, J., & Merchant, S. S. (2023). The *Chlamydomonas* Genome Project, version 6: Reference assemblies for mating-type plus and minus strains reveal extensive structural mutation in the laboratory. *Plant Cell*, 35(2), 644–672. <https://doi.org/10.1093/plcell/koac347>

- Cui, J., Purton, S., & Baganz, F. (2022). Characterisation of a simple 'hanging bag' photobioreactor for low-cost cultivation of microalgae. *Journal of Chemical Technology and Biotechnology*, 97(3), 608–619. <https://doi.org/10.1002/jctb.6985>
- Cullen, M., Ray, N., Husain, S., Nugent, J., Nield, J., & Purton, S. (2007). A highly active histidine-tagged *Chlamydomonas reinhardtii* Photosystem II preparation for structural and biophysical analysis. *Photochemical and Photobiological Sciences*, 6(11), 1177–1183. <https://doi.org/10.1039/b708611n>
- Dalakouras, A., Wassenegger, M., McMillan, J. N., Cardoza, V., Maegele, I., Dadami, E., Runne, M., Krczal, G., & Wassenegger, M. (2016). Induction of silencing in plants by high-pressure spraying of In vitro-synthesized small RNAs [Article]. *Frontiers in Plant Science*, 7(2016), 1327–1327. <https://doi.org/10.3389/fpls.2016.01327>
- Daniell, H., Lin, C. S., Yu, M., & Chang, W. J. (2016). Chloroplast genomes: Diversity, evolution, and applications in genetic engineering [Article]. *Genome Biology*, 17(1), 134–134. <https://doi.org/10.1186/s13059-016-1004-2>
- Day, A., & Goldschmidt-Clermont, M. (2011). The chloroplast transformation toolbox: selectable markers and marker removal [Article]. *Plant Biotechnology Journal*, 9(5), 540–553. <https://doi.org/10.1111/j.1467-7652.2011.00604.x>

- Debuchy, R., Purton, S., & Rochaix, J. D. (1989). argininosuccinate lyase gene of *Chlamydomonas reinhardtii*: an important tool for nuclear transformation and for correlating the genetic and molecular maps of the ARG7 locus [Article]. *The EMBO Journal*, 8(10), 2803–2809. <https://doi.org/10.1002/j.1460-2075.1989.tb08426.x>
- DellaPenna, D., & Pogson, B. J. (2006). Vitamin synthesis in plants: Tocopherols and carotenoids [Article]. *Annual Review of Plant Biology*, 57(1), 711–738. <https://doi.org/10.1146/annurev.arplant.56.032604.144301>
- Delrue, F., Imbert, Y., Fleury, G., Peltier, G., & Sassi, J.-F. (2015). Using coagulation–flocculation to harvest *Chlamydomonas reinhardtii*: Coagulant and flocculant efficiencies, and reuse of the liquid phase as growth medium [Article]. *Algal Research (Amsterdam)*, 9, 283–290. <https://doi.org/10.1016/j.algal.2015.04.004>
- Derrien, B., Majeran, W., Effantin, G., Ebenezer, J., Friso, G., van Wijk, K. J., Steven, A. C., Maurizi, M. R., & Vallon, O. (2012). The purification of the *Chlamydomonas reinhardtii* chloroplast ClpP complex: additional subunits and structural features [Article]. *Plant Molecular Biology*, 80(2), 189–202. <https://doi.org/10.1007/s11103-012-9939-5>
- Dobrogojski, J., Adamiec, M., & Luciński, R. (2020). The chloroplast genome: a review. In *Acta Physiologiae Plantarum* (Vol. 42, Issue 6). Springer. <https://doi.org/10.1007/s11738-020-03089-x>

- Dongyu, Q. (2024). 2024 THE STATE OF WORLD FISHERIES AND AQUACULTURE-BLUE TRANSFORMATION IN ACTION [Article]. *The State of World Fisheries and Aquaculture*, R1-232.
- Doyle, M., Jaskiewicz, L., & Filipowicz, W. (2012). Dicer Proteins and Their Role in Gene Silencing Pathways [Bookitem]. In *The Enzymes* (Vol. 32, pp. 1–35). Elsevier Inc. <https://doi.org/10.1016/B978-0-12-404741-9.00001-5>
- Dyo, Y. M., & Purton, S. (2018). The algal chloroplast as a synthetic biology platform for production of therapeutic proteins. *Microbiology (United Kingdom)*, 164(2), 113–121. <https://doi.org/10.1099/mic.0.000599>
- Einhaus, A., Baier, T., & Kruse, O. (2024). Molecular design of microalgae as sustainable cell factories [Article]. *Trends in Biotechnology*, 42(6), 728–738. <https://doi.org/10.1016/j.tibtech.2023.11.010>
- Einhaus, A., Baier, T., Rosenstengel, M., Freudenberg, R. A., & Kruse, O. (2021). Rational Promoter Engineering Enables Robust Terpene Production in Microalgae [Article]. *ACS Synthetic Biology*, 10(4), 847–856. <https://doi.org/10.1021/acssynbio.0c00632>
- Elbashir, S. M., Lendeckel, W., & Tuschl, T. (2001). RNA interference is mediated by 21- and 22-nucleotide RNAs [Article]. *Genes & Development*, 15(2), 188–200. <https://doi.org/10.1101/gad.862301>

- Engler, C., Kandzia, R., Marillonnet, S., & El-Shemy, H. A. (2008). A one pot, one step, precision cloning method with high throughput capability [Article]. *PloS One*, 3(11), e3647–e3647. <https://doi.org/10.1371/journal.pone.0003647>
- Erickson, E., Wakao, S., & Niyogi, K. K. (2015). Light stress and photoprotection in *Chlamydomonas reinhardtii*. *Plant Journal*, 82(3), 449–465. <https://doi.org/10.1111/tpj.12825>
- Esland, L., Larrea-Alvarez, M., & Purton, S. (2018). Selectable markers and reporter genes for engineering the chloroplast of *chlamydomonas reinhardtii*. In *Biology* (Vol. 7, Issue 4). MDPI AG. <https://doi.org/10.3390/biology7040046>
- Fages-Lartaud, M., & Hohmann-Marriott, M. F. (2022). Overview of tRNA Modifications in Chloroplasts [Article]. *Microorganisms (Basel)*, 10(2), 226. <https://doi.org/10.3390/microorganisms10020226>
- Fages-Lartaud, M., Hundvin, K., & Hohmann-Marriott, M. F. (2022). Mechanisms governing codon usage bias and the implications for protein expression in the chloroplast of *Chlamydomonas reinhardtii* [Article]. *The Plant Journal : For Cell and Molecular Biology*, 112(4), 919–945. <https://doi.org/10.1111/tpj.15970>
- Fajardo, C., De Donato, M., Macedo, M., Charoonnart, P., Saksmerprome, V., Yang, L., Purton, S., Mancera, J. M., & Costas, B. (2024). RNA Interference

Applied to Crustacean Aquaculture [Article]. *Biomolecules*, 14(11), 1358.
<https://doi.org/10.3390/biom14111358>

Fajardo, C., Donato, M., Carrasco, R., Martínez-Rodríguez, G., Mancera, J. M., & Fernández-Acero, F. J. (2020). Advances and challenges in genetic engineering of microalgae [Article]. *Reviews in Aquaculture*, 12(1), 365–381.
<https://doi.org/10.1111/raq.12322>

Falkowski, P. G., & Raven, J. A. (2013). *Aquatic photosynthesis* (Second Edition.) [Book]. Princeton University Press.

Farmanfarmaian, A., & Sun, L. Z. (1999). Growth hormone effects on essential amino acid absorption, muscle amino acid profile, N-retention and nutritional requirements of striped bass hybrids. *Genetic Analysis - Biomolecular Engineering*, 15(3–5), 107–113. [https://doi.org/10.1016/S1050-3862\(99\)00012-1](https://doi.org/10.1016/S1050-3862(99)00012-1)

Fields, F. J., Lejzerowicz, F., Schroeder, D., Ngoi, S. M., Tran, M., McDonald, D., Jiang, L., Chang, J. T., Knight, R., & Mayfield, S. (2020). Effects of the microalgae *Chlamydomonas* on gastrointestinal health. *Journal of Functional Foods*, 65. <https://doi.org/10.1016/j.jff.2019.103738>

Foong, C. P., Higuchi-Takeuchi, M., Malay, A. D., Oktaviani, N. A., Thagun, C., & Numata, K. (2020). A marine photosynthetic microbial cell factory as a platform for spider silk production. *Communications Biology*, 3(1). <https://doi.org/10.1038/s42003-020-1099-6>

- Ford, C., Mitchell, S., & Wang, W. yeh. (1981). Protochlorophyllide photoconversion mutants of *Chlamydomonas reinhardtii* [Article]. *MGG Molecular & General Genetics*, 184(3), 460–464. <https://doi.org/10.1007/BF00352523>
- Franklin, S., Ngo, B., Efuet, E., & Mayfield, S. P. (2002). Development of a GFP reporter gene for *Chlamydomonas reinhardtii* chloroplast [Article]. *The Plant Journal: For Cell and Molecular Biology*, 30(6), 733–744. <https://doi.org/10.1046/j.1365-313X.2002.01319.x>
- Fuks, B. (Universite L. de B., & Schnell, D. J. (1997). Mechanism of protein transport across the chloroplast envelope [Article]. *Plant Physiology (Bethesda)*, 114(2), 405–410. <https://doi.org/10.1104/pp.114.2.405>
- Fukuhara, T., & Moriyama, H. (2008). Endornavirus. In *Elsevier Ltd.* <https://doi.org/10.3109/9780203091470-7>
- Gallaher, S. D., Fitz-Gibbon, S. T., Strenkert, D., Purvine, S. O., Pellegrini, M., & Merchant, S. S. (2018). High-throughput sequencing of the chloroplast and mitochondrion of *Chlamydomonas reinhardtii* to generate improved de novo assemblies, analyze expression patterns and transcript speciation, and evaluate diversity among laboratory strains and wild isolates. *Plant Journal*, 93(3), 545–565. <https://doi.org/10.1111/tpj.13788>
- Gatesy, J., Hayashi, C., Motriuk, D., Woods, J., & Lewis, R. (2001). Extreme Diversity, Conservation, and Convergence of Spider Silk Fibroin Sequences

[Article]. *Science (American Association for the Advancement of Science)*, 291(5513), 2603–2605. <https://doi.org/10.1126/science.1057561>

Gimpel, J. A., Hyun, J. S., Schoepp, N. G., & Mayfield, S. P. (2015a). Production of Recombinant Proteins in Microalgae at Pilot Greenhouse Scale. *Biotechnol. Bioeng*, 112, 339–345. <https://doi.org/10.1002/bit.25357/abstract>

Gimpel, J. A., Hyun, J. S., Schoepp, N. G., & Mayfield, S. P. (2015b). Production of recombinant proteins in microalgae at pilot greenhouse scale [Article]. *Biotechnology and Bioengineering*, 112(2), 339–345. <https://doi.org/10.1002/bit.25357>

Gimpel, J. A., & Mayfield, S. P. (2013). Analysis of heterologous regulatory and coding regions in algal chloroplasts. *Applied Microbiology and Biotechnology*, 97(10), 4499–4510. <https://doi.org/10.1007/s00253-012-4580-4>

Goldschmidt-Clermont, M. (1991). Transgenic expression of aminoglycoside adenine transferase in the chloroplast: a selectable marker for site-directed transformation of *Chlamydomonas*. In *Nucleic Acids Research* (Vol. 19, Issue 15). <https://academic.oup.com/nar/article/19/15/4083/1115679>

Goodenough, U. (2023). *The Chlamydomonas Sourcebook: Volume 1: Introduction to Chlamydomonas and Its Laboratory Use* (3rd edition, Vol. 1) [Book]. Academic Press.

- Gordon, K. H. J., & Waterhouse, P. M. (2007). RNAi for insect-proof plants [Article]. *Nature Biotechnology*, 25(11), 1231–1232. <https://doi.org/10.1038/nbt1107-1231>
- Gosline, J. M., Guerette, P. A., Ortlepp, C. S., & Savage, K. N. (1999). The mechanical design of spider silks: From fibroin sequence to mechanical function [Article]. *Journal of Experimental Biology*, 202(23), 3295–3303. <https://doi.org/10.1242/jeb.202.23.3295>
- Graham, F. (2019). Daily briefing: World population will push 10 billion by 2050 [Article]. *Nature (London)*. <https://doi.org/10.1038/d41586-019-01959-0>
- Gray, M. W. (2012). Mitochondrial evolution [Article]. *Cold Spring Harbor Perspectives in Biology*, 4(9), a011403–a011403. <https://doi.org/10.1101/cshperspect.a011403>
- Grome, M. W., Nguyen, M. T. A., Moonan, D. W., Mohler, K., Gurara, K., Wang, S., Hemez, C., Stenton, B. J., Cao, Y., Radford, F., Kornaj, M., Patel, J., Prome, M., Rogulina, S., Sozanski, D., Tordoff, J., Rinehart, J., & Isaacs, F. J. (2025). Engineering a genomically recoded organism with one stop codon. *Nature*. <https://doi.org/10.1038/s41586-024-08501-x>
- Guzmán-Zapata, D., Domínguez-Anaya, Y., Macedo-Osorio, K. S., Tovar-Aguilar, A., Castrejón-Flores, J. L., Durán-Figueroa, N. V., & Badillo-Corona, J. A. (2017). mRNA imaging in the chloroplast of *Chlamydomonas reinhardtii*

- using the light-up aptamer Spinach. *Journal of Biotechnology*, 251(December 2016), 186–188. <https://doi.org/10.1016/j.jbiotec.2017.03.028>
- Hallegger, M., Taschner, A., & Jantsch, M. F. (2006). RNA aptamers binding the double-stranded RNA-binding domain. *Rna*, 12(11), 1993–2004. <https://doi.org/10.1261/rna.125506>
- Han, P., Lu, Q., Fan, L., & Zhou, W. (2019). A review on the use of microalgae for sustainable aquaculture. In *Applied Sciences (Switzerland)* (Vol. 9, Issue 11). MDPI AG. <https://doi.org/10.3390/app9112377>
- Hannon, G. J., Cheloufi, S., Dos Santos, C. O., & Chong, M. M. W. (2010). A dicer-independent miRNA biogenesis pathway that requires Ago catalysis [Article]. *Nature (London)*, 465(7298), 584–589. <https://doi.org/10.1038/nature09092>
- Hardy, J. G., & Scheibel, T. R. (2009). Silk-inspired polymers and proteins [Article]. *Biochemical Society Transactions*, 37(4), 677–681. <https://doi.org/10.1042/BST0370677>
- Harris, : Elizabeth H. (2009). CHAPTER 8 Chlamydomonas in the Laboratory. *The Chlamydomonas Sourcebook*, 241–302. <http://www.sciencedirect.com/science/article/pii/B9780123708731000083>
- Hayashi, C. Y., Shipley, N. H., & Lewis, R. V. (1999). Hypotheses that correlate the sequence, structure, and mechanical properties of spider silk proteins

- [Article]. *International Journal of Biological Macromolecules*, 24(2–3), 271–275. [https://doi.org/10.1016/S0141-8130\(98\)00089-0](https://doi.org/10.1016/S0141-8130(98)00089-0)
- He, S., Crans, V. L., & Jonikas, M. C. (2023). The pyrenoid: The eukaryotic CO₂-concentrating organelle. In *Plant Cell* (Vol. 35, Issue 9, pp. 3236–3259). American Society of Plant Biologists. <https://doi.org/10.1093/plcell/koad157>
- He, W., Xu, W., Xu, L., Fu, K., Guo, W., Bock, R., & Zhang, J. (2020). Length-dependent accumulation of double-stranded RNAs in plastids affects RNA interference efficiency in the Colorado potato beetle. *Journal of Experimental Botany*, 71(9), 2670–2677. <https://doi.org/10.1093/JXB/ERAA001>
- Hinman, M. B. (University of W., & Lewis, R. V. (1992). Isolation of a clone encoding a second dragline silk fibroin: nephila clavipes dragline silk is a two-protein fiber [Article]. *The Journal of Biological Chemistry*, 267(27), 19320–19324. [https://doi.org/10.1016/s0021-9258\(18\)41777-2](https://doi.org/10.1016/s0021-9258(18)41777-2)
- Hopes, A., Nekrasov, V., Kamoun, S., & Mock, T. (2016). Editing of the urease gene by CRISPR-Cas in the diatom *Thalassiosira pseudonana* [Article]. *Plant Methods*, 12(1), 49–49. <https://doi.org/10.1186/s13007-016-0148-0>
- Howe, C., & Barbrook, A. (2007). The remarkable chloroplast genome of dinoflagellates [Article]. *Comparative Biochemistry and Physiology. Part A, Molecular & Integrative Physiology*, 146(4), S215–S215. <https://doi.org/10.1016/j.cbpa.2007.01.466>

- Humby, P. L., Cunningham, M. L., Saunders, H. L., Price, J. A., & Durnford, D. G. (2009). Compartmental cross-talk in the regulation of light harvesting complex transcription under short-term light and temperature stress in *Chlamydomonas reinhardtii* [Article]. *Botany*, 87(4), 375–386. <https://doi.org/10.1139/B09-005>
- Huvenne, H., & Smagghe, G. (2010). Mechanisms of dsRNA uptake in insects and potential of RNAi for pest control: A review [Article]. *Journal of Insect Physiology*, 56(3), 227–235. <https://doi.org/10.1016/j.jinsphys.2009.10.004>
- Jackson, H. O., Taunt, H. N., Mordaka, P. M., Kumari, S., Smith, A. G., & Purton, S. (2022). CpPosNeg: A positive-negative selection strategy allowing multiple cycles of marker-free engineering of the *Chlamydomonas* plastome. *Biotechnology Journal*, 17(10), 1–10. <https://doi.org/10.1002/biot.202200088>
- Jackson, H. O., Taunt, H. N., Mordaka, P. M., Smith, A. G., & Purton, S. (2021). The Algal Chloroplast as a Testbed for Synthetic Biology Designs Aimed at Radically Rewiring Plant Metabolism. *Frontiers in Plant Science*, 12(September), 1–15. <https://doi.org/10.3389/fpls.2021.708370>
- Jia, M., Munz, J., Lee, J., Shelley, N., Xiong, Y., Joo, S., Jin, E., & Lee, J. (2022). The bHLH family NITROGEN-REPLETION INSENSITIVE1 represses nitrogen starvation-induced responses in *Chlamydomonas reinhardtii* [Article]. *The Plant Journal : For Cell and Molecular Biology*, 110(2), 337–357. <https://doi.org/10.1111/tpj.15673>

- Jinkerson, R. E., & Jonikas, M. C. (2015). Molecular techniques to interrogate and edit the *Chlamydomonas* nuclear genome [Article]. *The Plant Journal: For Cell and Molecular Biology*, 82(3), 393–412. <https://doi.org/10.1111/tpj.12801>
- Kaur, H., Bruno, J. G., Kumar, A., & Sharma, T. K. (2018). Aptamers in the therapeutics and diagnostics pipelines. *Theranostics*, 8(15), 4016–4032. <https://doi.org/10.7150/thno.25958>
- Kim, M., Kim, J., Kim, S., & Jin, E. S. (2020). Heterologous gene expression system using the cold-inducible CnAFP promoter in *chlamydomonas reinhardtii* [Article]. *Journal of Microbiology and Biotechnology*, 30(11), 1777–1784. <https://doi.org/10.4014/JMB.2007.07024>
- Kindle, K. L. (1990). High-frequency nuclear transformation of *Chlamydomonas reinhardtii*. *Proceedings of the National Academy of Sciences of the United States of America*, 87(3), 1228–1232. <https://doi.org/10.1073/pnas.87.3.1228>
- Kindle, K. L., Richards, K. L., & Stern, D. B. (1991). Engineering the Chloroplast Genome: Techniques and Capabilities for Chloroplast Transformation in *Chlamydomonas reinhardtii* [Article]. *Proceedings of the National Academy of Sciences - PNAS*, 88(5), 1721–1725. <https://doi.org/10.1073/pnas.88.5.1721>

- Klein, U. (Harvard U., De Camp, J. D., & Bogorad, L. (1992). Two types of chloroplast gene promoters in *Chlamydomonas reinhardtii* [Article]. *Proceedings of the National Academy of Sciences - PNAS*, 89(8), 3453–3457. <https://doi.org/10.1073/pnas.89.8.3453>
- Kovoor, J. (1987). *Comparative Structure and Histochemistry of Silk-Producing Organs in Arachnids*. <https://api.semanticscholar.org/CorpusID:86332869>
- Kroth, P. G., Bones, A. M., Daboussi, F., Ferrante, M. I., Jaubert, M., Kolot, M., Nymark, M., Río Bártulos, C., Ritter, A., Russo, M. T., Serif, M., Winge, P., & Falciatore, A. (2018). Genome editing in diatoms: achievements and goals [Article]. *Plant Cell Reports*, 37(10), 1401–1408. <https://doi.org/10.1007/s00299-018-2334-1>
- Kumar, A., Wang, S., Ou, R., Samrakandi, M., Beerntsen, B. T., & Sayre, R. T. (2013). Development of an RNAi based microalgal larvicide to control mosquitoes. *GCE Special Issue) MalariaWorld Journal, Www.Malariaworld.Org*, 4(6). <https://doi.org/10.5281/zenodo.10894766>
- Laksana, D. P., Subaidah, S., Zairin Junior, M., & Alimuddin, O. C. (2013). Growth of white shrimp post-larvae immersed in recombinant fish growth hormone. *Jurnal Akuakultur Indonesia*, 2, 95–100.
- Larrea-Alvarez, M. (2018). *Molecular tools and approaches for increasing complexity of transplastomic engineering in Chlamydomonas reinhardtii*

[Doctoral thesis (Ph.D.), University College London].

<https://doi.org/https://discovery.ucl.ac.uk/id/eprint/10047617/>

Larrea-Alvarez, M., & Purton, S. (2020). Multigenic engineering of the chloroplast genome in the green alga *Chlamydomonas reinhardtii*. *Microbiology (United Kingdom)*, 166(6), 510–515. <https://doi.org/10.1099/mic.0.000910>

Larrea-Alvarez, M., Young, R., & Purton, S. (2021). A Simple Technology for Generating Marker-Free Chloroplast Transformants of the Green Alga *Chlamydomonas reinhardtii*. In P. Maliga (Ed.), *Chloroplast Biotechnology. Methods in Molecular Biology* (Vol. 2317, pp. 293–304). Humana. https://doi.org/10.1007/978-1-0716-1472-3_17

Lee, W., Matthews, A., & Moore, D. (2022). Safety Evaluation of a Novel Algal Feed Additive for Poultry Production. *Avian Diseases*, 66(3), 1–11. <https://doi.org/10.1637/aviandiseases-D-22-00043>

Leon-Banares, R., GONZALEZ-BALLESTER, D., GALVAN, A., & FERNANDEZ, E. (2004). Transgenic microalgae as green cell-factories [Article]. *Trends in Biotechnology (Regular Ed.)*, 22(1), 45–52. <https://doi.org/10.1016/j.tibtech.2003.11.003>

Lewis, R. V. (2006). Spider Silk: Ancient Ideas for New Biomaterials [Article]. *Chemical Reviews*, 106(9), 3762–3774. <https://doi.org/10.1021/cr010194g>

- Liang, Y., Yu, X., Anaokar, S., Shi, H., Dahl, W. B., Cai, Y., Luo, G., Chai, J., Cai, Y., Mollá-Morales, A., Altpeter, F., Ernst, E., Schwender, J., Martienssen, R. A., & Shanklin, J. (2023). Microalgae. *Plant Biotechnology Journal*, 21(2), 317–330. <https://doi.org/10.1111/pbi.13943>
- Lister, D. L., Bateman, J. M., Purton, S., & Howe, C. J. (2003). DNA transfer from chloroplast to nucleus is much rarer in *Chlamydomonas* than in tobacco. *Gene*, 316(1–2), 33–38. [https://doi.org/10.1016/S0378-1119\(03\)00754-6](https://doi.org/10.1016/S0378-1119(03)00754-6)
- Liu, J., Carmell, M. A., Rivas, F. V., Marsden, C. C., Thomson, J. M., Song, J.-J., Hammond, S. M., Joshua-Tor, L., & Hannon, G. J. (2004). Argonaute2 Is the Catalytic Engine of Mammalian RNAi [Article]. *Science (American Association for the Advancement of Science)*, 305(5689), 1437–1441. <https://doi.org/10.1126/science.1102513>
- Liu, S., Zang, X., Liu, B., Zhang, X., K.K.I.U., A., Zhang, X., & Liang, B. (2007). Effect of growth hormone transgenic *Synechocystis* on growth, feed efficiency, muscle composition, haematology and histology of turbot (*Scophthalmus maximus* L.). *Aquaculture Research*, 38(12), 1283–1292. <https://doi.org/10.1111/j.1365-2109.2007.01796.x>
- Lumbreras, V., Stevens, D. R., & Purton, S. (1998). Efficient foreign gene expression in *Chlamydomonas reinhardtii* mediated by an endogenous intron [Article]. *The Plant Journal : For Cell and Molecular Biology*, 14(4), 441–447. <https://doi.org/10.1046/j.1365-313X.1998.00145.x>

- Ma, K., Deng, L., Wu, H., & Fan, J. (2022). Towards green biomanufacturing of high-value recombinant proteins using promising cell factory: *Chlamydomonas reinhardtii* chloroplast. In *Bioresources and Bioprocessing* (Vol. 9, Issue 1). Springer Science and Business Media Deutschland GmbH. <https://doi.org/10.1186/s40643-022-00568-6>
- MacRae, I. J., Zhou, K., Li, F., Repic, A., Brooks, A. N., Cande, W. Z., Adams, P. D., & Doudna, J. A. (2006). Structural Basis for Double-Stranded RNA Processing by Dicer [Article]. *Science (American Association for the Advancement of Science)*, 311(5758), 195–198. <https://doi.org/10.1126/science.1121638>
- Mapstone, L. J., Taunt, H. N., Cui, J., Purton, S., & Brooks, T. G. R. (2022). ADA : an open-source software platform for plotting and analysis of data from laboratory photobioreactors. *Applied Phycology*, 3(1), 16–26. <https://doi.org/10.1080/26388081.2021.2023632>
- Maréchal, E. (Ed.). (2018). *Plastids* (Vol. 1829). Springer US. <https://doi.org/10.1007/978-1-4939-8654-5>
- Martínez, R., Carpio, Y., Arenal, A., Lugo, J. M., Morales, R., Martín, L., Rodríguez, R. F., Acosta, J., Morales, A., Duconge, J., & Estrada, M. P. (2017). Significant improvement of shrimp growth performance by growth hormone-releasing peptide-6 immersion treatments. *Aquaculture Research*, 48(9), 4632–4645. <https://doi.org/10.1111/are.13286>

- Masi, A., Leonelli, F., Scognamiglio, V., Gasperuzzo, G., Antonacci, A., & Terzidis, M. A. (2023a). *Chlamydomonas reinhardtii*: A Factory of Nutraceutical and Food Supplements for Human Health. In *Molecules* (Vol. 28, Issue 3). MDPI. <https://doi.org/10.3390/molecules28031185>
- Masi, A., Leonelli, F., Scognamiglio, V., Gasperuzzo, G., Antonacci, A., & Terzidis, M. A. (2023b). *Chlamydomonas reinhardtii*: A Factory of Nutraceutical and Food Supplements for Human Health. In *Molecules* (Vol. 28, Issue 3). MDPI. <https://doi.org/10.3390/molecules28031185>
- Mata, T. M., Martins, A. A., & Caetano, Nidia. S. (2010). Microalgae for biodiesel production and other applications: A review [Article]. *Renewable & Sustainable Energy Reviews*, 14(1), 217–232. <https://doi.org/10.1016/j.rser.2009.07.020>
- Mayfield, S. P. (1990). Chloroplast gene regulation: interaction of the nuclear and chloroplast genomes in the expression of photosynthetic proteins [Article]. *Current Opinion in Cell Biology*, 2(3), 509–513. [https://doi.org/10.1016/0955-0674\(90\)90135-2](https://doi.org/10.1016/0955-0674(90)90135-2)
- Meister, G., & Tuschl, T. (2004). Mechanisms of gene silencing by double-stranded RNA [Article]. *Nature*, 431(7006), 343–349. <https://doi.org/10.1038/nature02873>
- Mendez Leyva, A. (2019). *Transformation and Expression of Recombinant Proteins in Microalgae* [PhD Thesis]. The University of Manchester.

- Merchant, S. S., Prochnik, S. E., Vallon, O., Harris, E. H., Karpowicz, S. J., Witman, G. B., Terry, A., Salamov, A., Fritz-Laylin, L. K., Maréchal-Drouard, L., Marshall, W. F., Qu, L.-H., Nelson, D. R., Sanderfoot, A. A., Spalding, M. H., Kapitonov, V. V, Ren, Q., Ferris, P., Lindquist, E., ... Brokstein, P. (2007). The *Chlamydomonas* genome reveals the evolution of key animal and plant functions [Article]. *Science (American Association for the Advancement of Science)*, 318(5848), 245–250. <https://doi.org/10.1126/science.1143609>
- Molnar, A., Melnyk, C. W., Bassett, A., Hardcastle, T. J., Dunn, R., & Baulcombe, D. C. (2010). Small Silencing RNAs in Plants Are Mobile and Direct Epigenetic Modification in Recipient Cells [Article]. *Science (American Association for the Advancement of Science)*, 328(5980), 872–875. <https://doi.org/10.1126/science.1187959>
- Mordaka, P. M., Clouston, K., Gorchs-Rovira, A., Sutherland, C., Zhang, D. Q., Geisler, K., Mehrshahi, P., & Smith, A. G. (2024). Regulation of nucleus-encoded trans-acting factors allows orthogonal fine-tuning of multiple transgenes in the chloroplast of *Chlamydomonas reinhardtii*. *Plant Biotechnology Journal*. <https://doi.org/10.1111/pbi.14557>
- Moriyama, S. (Kitasato Univ., Ayson, F. G., & Kawauchi, H. (2000). Growth regulation by insulin-like growth factor-I in fish [Article]. *Bioscience, Biotechnology, and Biochemistry*, 64(8), 1553–1562. <https://doi.org/10.1271/bbb.64.1553>

- Murbach, T. S., Glávits, R., Endres, J. R., Hirka, G., Vértési, A., Béres, E., & Szakonyiné, I. P. (2018). A Toxicological Evaluation of *Chlamydomonas reinhardtii*, a Green Algae. *International Journal of Toxicology*, 37(1), 53–62. <https://doi.org/10.1177/1091581817746109>
- Nelson, N., & Yocum, C. F. (2006). Structure and Function of Photosystems I and II [Article]. *Annual Review of Plant Biology*, 57(1), 521–565. <https://doi.org/10.1146/annurev.arplant.57.032905.105350>
- Newman, S. M., Boynton, J. E., Gillham, N. W., Randolph-Anderson, B. L., Johnson, A. M., & Harris, E. H. (1990). *Transformation of Chloroplast Ribosomal RNA Genes in Chlamydomonas: Molecular and Genetic Characterization of Integration Events*.
- Newman, S. M., Harris, E. H., Johnson, A. M., Boynton, J. E., & Gillham, N. W. (1992). *Nonrandom Distribution of Chloroplast Recombination Events in Chlamydomonas reinhardtii: Evidence for a Hotspot and an Adjacent Cold Region*.
- Niemeyer, J., Fischer, L., Aylward, F. O., & Schroda, M. (2023). Analysis of Viral Promoters for Transgene Expression and of the Effect of 5'-UTRs on Alternative Translational Start Sites in *Chlamydomonas* [Article]. *Genes*, 14(4), 948. <https://doi.org/10.3390/genes14040948>
- Niklas, K. J., Cobb, E. D., & Matas, A. J. (2017). The evolution of hydrophobic cell wall biopolymers: from algae to angiosperms. In *Journal of Experimental*

- Botany* (Vol. 68, Issue 19, pp. 5261–5269). Oxford University Press.
<https://doi.org/10.1093/jxb/erx215>
- Ouellet, J. (2016). RNA fluorescence with light-Up aptamers. *Frontiers in Chemistry*, 4(JUN), 1–12. <https://doi.org/10.3389/fchem.2016.00029>
- Perozeni, F., & Baier, T. (2023). Current Nuclear Engineering Strategies in the Green Microalga *Chlamydomonas reinhardtii*. In *Life* (Vol. 13, Issue 7). Multidisciplinary Digital Publishing Institute (MDPI).
<https://doi.org/10.3390/life13071566>
- Przibilla, E., Heiss, S., Johanningmeier, U., & Trebst, A. (1991). Site-Specific Mutagenesis of the D1 Subunit of Photosystem II in Wild-Type *Chlamydomonas*. In *The Plant Cell* (Vol. 3).
- Pulz, O., & Gross, W. (2004). Valuable products from biotechnology of microalgae [Article]. *Applied Microbiology and Biotechnology*, 65(6), 635–648.
<https://doi.org/10.1007/s00253-004-1647-x>
- Purton, S., & Rochaix, J.-D. (1995). Characterisation of the ARG7 gene of *Chlamydomonas reinhardtii* and its application to nuclear transformation [Article]. *European Journal of Phycology*, 30(2), 141–148.
<https://doi.org/10.1080/09670269500650901>
- Purton, S., Stevens, D. R., Muhiuddin, I. P., Evans, M. C. W., Carter, S., Rigby, S. E. J., & Heathcote, P. (2001). Site-directed mutagenesis of PsaA residue

W693 affects phylloquinone binding and function in the photosystem I reaction center of *Chlamydomonas reinhardtii*. *Biochemistry*, 40(7), 2167–2175. <https://doi.org/10.1021/bi0019489>

Purton, S., Szaub, J. B., Wannathong, T., Young, R., & Economou, C. K. (2013a). Genetic engineering of algal chloroplasts: Progress and prospects [Article]. *Russian Journal of Plant Physiology*, 60(4), 491–499. <https://doi.org/10.1134/S1021443713040146>

Purton, S., Szaub, J. B., Wannathong, T., Young, R., & Economou, C. K. (2013b). Genetic engineering of algal chloroplasts: Progress and prospects [Article]. *Russian Journal of Plant Physiology*, 60(4), 491–499. <https://doi.org/10.1134/S1021443713040146>

Ramezaniaghdam, M., Nahdi, N. D., & Reski, R. (2022). Recombinant Spider Silk: Promises and Bottlenecks [Article]. *Frontiers in Bioengineering and Biotechnology*, 10, 835637. <https://doi.org/10.3389/fbioe.2022.835637>

Rasala, B. A., Lee, P. A., Shen, Z., Briggs, S. P., Mendez, M., & Mayfield, S. P. (2012). Robust expression and secretion of xylanase1 in *Chlamydomonas reinhardtii* by fusion to a selection gene and processing with the FMDV 2A peptide [Article]. *PloS One*, 7(8), e43349–e43349. <https://doi.org/10.1371/journal.pone.0043349>

- Rasala, B. A., & Mayfield, S. P. (2011). The microalga *Chlamydomonas reinhardtii* as a platform for the production of human protein therapeutics [Article]. *Bioengineered Bugs*, 2(1), 50–54. <https://doi.org/10.4161/bbug.2.1.13423>
- Rasala, B. A., & Mayfield, S. P. (2015). Photosynthetic biomanufacturing in green algae; production of recombinant proteins for industrial, nutritional, and medical uses [Article]. *Photosynthesis Research*, 123(3), 227–239. <https://doi.org/10.1007/s11120-014-9994-7>
- Rasala, B. A., Muto, M., Lee, P. A., Jager, M., Cardoso, R. M. F., Behnke, C. A., Kirk, P., Hokanson, C. A., Crea, R., Mendez, M., & Mayfield, S. P. (2010). Production of therapeutic proteins in algae, analysis of expression of seven human proteins in the chloroplast of *Chlamydomonas reinhardtii*. *Plant Biotechnology Journal*, 8(6), 719–733. <https://doi.org/10.1111/j.1467-7652.2010.00503.x>
- Rasala, B. A., Muto, M., Sullivan, J., & Mayfield, S. P. (2011). Improved heterologous protein expression in the chloroplast of *Chlamydomonas reinhardtii* through promoter and 5' untranslated region optimization [Article]. *Plant Biotechnology Journal*, 9(6), 674–683. <https://doi.org/10.1111/j.1467-7652.2011.00620.x>
- Raven, P. H. (1999). *Biology of plants* (R. Franklin. Evert & S. E. Eichhorn, Eds.; 6th ed.) [Book]. W.H. Freeman.

- Remade, C., Cline, S., Boutaffala, L., Gabilly, S., Larosa, V., Rosario Barbieri, M., Coosemans, N., & Hamel, P. P. (2009). The ARG9 Gene Encodes the Plastid-Resident N-Acetyl Ornithine Aminotransferase in the Green Alga *Chlamydomonas reinhardtii*. *Eukaryotic Cell*, 8(9), 1460–1463. <https://doi.org/10.1128/EC.00108-09>
- Rising, A., Widhe, M., Johansson, J., & Hedhammar, M. (2011). Spider silk proteins: recent advances in recombinant production, structure-function relationships and biomedical applications [Article]. *Cellular and Molecular Life Sciences: CMLS*, 68(2), 169–184. <https://doi.org/10.1007/s00018-010-0462-z>
- Robertson, D., Boynton, J. E., & Gillham, N. W. (1990). Cotranscription of the wild-type chloroplast *atpE* gene encoding the CFI/CFo epsilon subunit with the 3' half of the *rps7* gene in *Chlamydomonas reinhardtii* and characterization of frameshift mutations in *atpE*. *Molecular and General Genetics*, 221, 155–163. <https://doi.org/https://doi.org/10.1007/BF00261715>
- Rochaix, J.-D. (1997). Chloroplast reverse genetics: new insights into the function of plastid genes [Article]. *Trends in Plant Science*, 2(11), 419–425. [https://doi.org/10.1016/S1360-1385\(97\)90025-X](https://doi.org/10.1016/S1360-1385(97)90025-X)
- Rodrigues, T. B., Mishra, S. K., Sridharan, K., Barnes, E. R., Alyokhin, A., Tuttle, R., Kokulapalan, W., Garby, D., Skizim, N. J., Tang, Y., Manley, B., Aulisa, L., Flannagan, R. D., Cobb, C., & Narva, K. E. (2021). First Sprayable Double-Stranded RNA-Based Biopesticide Product Targets Proteasome

Subunit Beta Type-5 in Colorado Potato Beetle (*Leptinotarsa decemlineata*).
Frontiers in Plant Science, 12(November).
<https://doi.org/10.3389/fpls.2021.728652>

Rosales-Mendoza, S., García-Silva, I., González-Ortega, O., Sandoval-Vargas, J. M., Malla, A., & Vimolmangkang, S. (2020). The Potential of Algal Biotechnology to Produce Antiviral Compounds and Biopharmaceuticals. *Molecules*, 25(18), 1–25. <https://doi.org/10.3390/molecules25184049>

Rosales-Mendoza, S., Paz-Maldonado, L. M. T., & Soria-Guerra, R. E. (2012). *Chlamydomonas reinhardtii* as a viable platform for the production of recombinant proteins: current status and perspectives [Article]. *Plant Cell Reports*, 31(3), 479–494. <https://doi.org/10.1007/s00299-011-1186-8>

Rosales-Mendoza, S., Solís-Andrade, K. I., Márquez-Escobar, V. A., González-Ortega, O., & Bañuelos-Hernandez, B. (2020). Current advances in the algae-made biopharmaceuticals field. *Expert Opinion on Biological Therapy*, 20(7), 751–766. <https://doi.org/10.1080/14712598.2020.1739643>

Rosano, G. L., & Ceccarelli, E. A. (2014). Recombinant protein expression in *Escherichia coli*: Advances and challenges. In *Frontiers in Microbiology* (Vol. 5, Issue APR). Frontiers Research Foundation. <https://doi.org/10.3389/fmicb.2014.00172>

Sager, R. (1955). Inheritance in the Green Alga *Chlamydomonas Reinhardi*. *Genetics*, 40(4), 476–489. <https://doi.org/10.1093/genetics/40.4.476>

- Saksmerprome, V., Charoonnart, P., Gangnonngiw, W., & Withyachumnarnkul, B. (2009). A novel and inexpensive application of RNAi technology to protect shrimp from viral disease. *Journal of Virological Methods*, 162(1–2), 213–217. <https://doi.org/10.1016/j.jviromet.2009.08.010>
- Salomé, P. A., & Merchant, S. S. (2019). A series of fortunate events: Introducing chlamydomonas as a reference organism. In *Plant Cell* (Vol. 31, Issue 8, pp. 1682–1707). American Society of Plant Biologists. <https://doi.org/10.1105/tpc.18.00952>
- Salvador, M. L., & Klein, U. (1999). The Redox State Regulates RNA Degradation in the Chloroplast of *Chlamydomonas reinhardtii* [Article]. *Plant Physiology (Bethesda)*, 121(4), 1367–1374.
- Sandoval-Vargas, J. M., Jiménez-Clemente, L. A., Macedo-Orsorio, K. S., Oliver-Salvador, M. C., Fernández-Linares, L. C., Durán-Figueroa, N. V., & Badillo-Corona, J. A. (2019a). Use of the *ptxD* gene as a portable selectable marker for chloroplast transformation in *Chlamydomonas reinhardtii*. *Molecular Biotechnology*, 61(6), 461–468. <https://doi.org/10.1007/s12033-019-00177-3>
- Sandoval-Vargas, J. M., Jiménez-Clemente, L. A., Macedo-Orsorio, K. S., Oliver-Salvador, M. C., Fernández-Linares, L. C., Durán-Figueroa, N. V., & Badillo-Corona, J. A. (2019b). Use of the *ptxD* gene as a portable selectable marker for chloroplast transformation in *Chlamydomonas reinhardtii* [Article]. *Molecular Biotechnology*, 61(6), 461–468. <https://doi.org/10.1007/s12033-019-00177-3>

- Santiesteban, D., Martín, L., Arenal, A., Franco, R., & Sotolongo, J. (2010). Tilapia growth hormone binds to a receptor in brush border membrane vesicles from the hepatopancreas of shrimp *Litopenaeus vannamei*. *Aquaculture*, 306(1–4), 338–342. <https://doi.org/10.1016/j.aquaculture.2010.05.023>
- Sarker, P. K., Kapuscinski, A. R., McKuin, B., Fitzgerald, D. S., Nash, H. M., & Greenwood, C. (2020). Microalgae-blend tilapia feed eliminates fishmeal and fish oil, improves growth, and is cost viable. *Scientific Reports*, 10(1), 1–14. <https://doi.org/10.1038/s41598-020-75289-x>
- Scheibel, T., Kessler, H., Hagn, F., Eisoldt, L., Hardy, J. G., Vendrely, C., & Coles, M. (2010). A conserved spider silk domain acts as a molecular switch that controls fibre assembly [Article]. *Nature (London)*, 465(7295), 239–242. <https://doi.org/10.1038/nature08936>
- Schroda, M. (2006). RNA silencing in *Chlamydomonas*: Mechanisms and tools. In *Current Genetics* (Vol. 49, Issue 2, pp. 69–84). <https://doi.org/10.1007/s00294-005-0042-1>
- Schuster, G., Lisitsky, I., & Klaff, P. (1999). Polyadenylation and degradation of mRNA in the chloroplast [Article]. *Plant Physiology (Bethesda)*, 120(4), 937–944. <https://doi.org/10.1104/pp.120.4.937>
- Sekar, M., Singh, S. D., Angel, R. J., Meena, D. K., Sivakumar, N., Suresh, E., & Kathirvelpandian, A. (2015). Growth promoting activity of *Pangasianodon*

hypophthalmus recombinant growth hormone expressed in Escherichia coli.
Indian Journal of Fisheries, 62(1), 70–77.

Shamriz, S., & Ofoghi, H. (2017). Outlook in the application of Chlamydomonas reinhardtii chloroplast as a platform for recombinant protein production.
Biotechnology and Genetic Engineering Reviews, 32(1–2), 92–106.
<https://doi.org/10.1080/02648725.2017.1307673>

Smith, V. H. (2003). Eutrophication of freshwater and coastal marine ecosystems: A global problem [Article]. *Environmental Science and Pollution Research International*, 10(2), 126–139. <https://doi.org/10.1065/espr2002.12.142>

Song, S.-H., Dick, B., Zirak, P., Penzkofer, A., Schiereis, T., & Hegemann, P. (2005). Absorption and emission spectroscopic characterisation of combined wildtype LOV1–LOV2 domain of phot from Chlamydomonas reinhardtii [Article]. *Journal of Photochemistry and Photobiology. B, Biology*, 81(1), 55–65. <https://doi.org/10.1016/j.jphotobiol.2005.06.003>

Specht, E. A., & Mayfield, S. P. (2013). Synthetic oligonucleotide libraries reveal novel regulatory elements in chlamydomonas chloroplast mRNAs. *ACS Synthetic Biology*, 2(1), 34–46. <https://doi.org/10.1021/sb300069k>

Specht, E. A., & Mayfield, S. P. (2014). Algae-based oral recombinant vaccines. *Frontiers in Microbiology*, 5(FEB), 1–7.
<https://doi.org/10.3389/fmicb.2014.00060>

- Specht, E., Miyake-Stoner, S., & Mayfield, S. (2010). Micro-algae come of age as a platform for recombinant protein production [Article]. *Biotechnology Letters*, 32(10), 1373–1383. <https://doi.org/10.1007/s10529-010-0326-5>
- Sponner, A., Vater, W., Rommerskirch, W., Vollrath, F., Unger, E., Grosse, F., & Weisshart, K. (2005). The conserved C-termini contribute to the properties of spider silk fibroins [Article]. *Biochemical and Biophysical Research Communications*, 338(2), 897–902. <https://doi.org/10.1016/j.bbrc.2005.10.048>
- Stoffels, L., Taunt, H. N., Charalambous, B., & Purton, S. (2017). Synthesis of bacteriophage lytic proteins against *Streptococcus pneumoniae* in the chloroplast of *Chlamydomonas reinhardtii*. *Plant Biotechnology Journal*, 15(9), 1130–1140. <https://doi.org/10.1111/pbi.12703>
- Studier, F. W., & Moffatt, B. A. (1986). Use of bacteriophage T7 RNA polymerase to direct selective high-level expression of cloned genes [Article]. *Journal of Molecular Biology*, 189(1), 113–130. [https://doi.org/10.1016/0022-2836\(86\)90385-2](https://doi.org/10.1016/0022-2836(86)90385-2)
- Sugiura, M. (2003). History of chloroplast genomics [Article]. *Photosynthesis Research*, 76(1–3), 371–377. <https://doi.org/10.1023/A:1024913304263>
- Tam, L. T., Van Cong, N., Thom, L. T., Ha, N. C., Hang, N. T. M., Van Minh, C., Vien, D. T. H., & Hong, D. D. (2021). Cultivation and biomass production of the diatom *Thalassiosira weissflogii* as a live feed for white-leg shrimp in

- hatcheries and commercial farms in Vietnam [Article]. *Journal of Applied Phycology*, 33(3), 1559–1577. <https://doi.org/10.1007/s10811-021-02371-w>
- Taunt, H. N., Jackson, H. O., Gunnarsson, Í. N., Pervaiz, R., & Purton, S. (2023). Accelerating Chloroplast Engineering: A New System for Rapid Generation of Marker-Free Transplastomic Lines of *Chlamydomonas reinhardtii*. *Microorganisms*, 11(8). <https://doi.org/10.3390/microorganisms11081967>
- Taunt, H. N., Stoffels, L., & Purton, S. (2018). Green biologics: The algal chloroplast as a platform for making biopharmaceuticals. *Bioengineered*, 9(1), 48–54. <https://doi.org/10.1080/21655979.2017.1377867>
- Taylor, G. M., Mordaka, P. M., & Heap, J. T. (2019). Start-Stop Assembly: A functionally scarless DNA assembly system optimized for metabolic engineering. *Nucleic Acids Research*, 47(3). <https://doi.org/10.1093/nar/gky1182>
- Tenlen, J. R. (2018). Microinjection of dsRNA in tardigrades [Article]. *Cold Spring Harbor Protocols*, 2018(11), 900–904. <https://doi.org/10.1101/pdb.prot102368>
- Tenlen, J. R., McCaskill, S., & Goldstein, B. (2013). RNA interference can be used to disrupt gene function in tardigrades [Article]. *Development Genes and Evolution*, 223(3), 171–181. <https://doi.org/10.1007/s00427-012-0432-6>

- Tenllado, F., Martínez-García, B., Vargas, M., & Díaz-Ruíz, J. R. (2003). Crude extracts of bacterially expressed dsRNA can be used to protect plants against virus infections [Article]. *BMC Biotechnology*, 3(1), 3–3. <https://doi.org/10.1186/1472-6750-3-3>
- Timmons, L., & Fire, A. (1998). Specific interference by ingested dsRNA [Article]. *Nature (London)*, 395(6705), 854–854. <https://doi.org/10.1038/27579>
- Tokareva, O., Jacobsen, M., Buehler, M., Wong, J., & Kaplan, D. L. (2014). Structure–function–property–design interplay in biopolymers: Spider silk [Article]. *Acta Biomaterialia*, 10(4), 1612–1626. <https://doi.org/10.1016/j.actbio.2013.08.020>
- Torres-Tiji, Y., Fields, F. J., Yang, Y., Heredia, V., Horn, S. J., Keremane, S. R., Jin, M. M., & Mayfield, S. P. (2022). Optimized production of a bioactive human recombinant protein from the microalgae *Chlamydomonas reinhardtii* grown at high density in a fed-batch bioreactor [Article]. *Algal Research (Amsterdam)*, 66, 102786. <https://doi.org/10.1016/j.algal.2022.102786>
- Tsai, H. J., Lin, K. L., & Chen, T. T. (1993). Molecular cloning and expression of yellowfin porgy (*Acanthopagrus latus* houttuyn) growth hormone cDNA. *Comparative Biochemistry and Physiology -- Part B: Biochemistry And*, 104(4), 803–810. [https://doi.org/10.1016/0305-0491\(93\)90216-R](https://doi.org/10.1016/0305-0491(93)90216-R)

- van Wijk, K. J. (2024). Intra-chloroplast proteases: A holistic network view of chloroplast proteolysis. In *Plant Cell* (Vol. 36, Issue 9, pp. 3116–3130). American Society of Plant Biologists. <https://doi.org/10.1093/plcell/koae178>
- Vilatte, A., Spencer-Milnes, X., Jackson, H. O., Purton, S., & Parker, B. (2023). Spray Drying Is a Viable Technology for the Preservation of Recombinant Proteins in Microalgae. *Microorganisms*, 11(2). <https://doi.org/10.3390/microorganisms11020512>
- Vollrath, F., & Knight, D. P. (2001). Liquid crystalline spinning of spider silk [Article]. *Nature (London)*, 410(6828), 541–548. <https://doi.org/10.1038/35069000>
- Vollrath, F., & Porter, D. (2006). Spider silk as archetypal protein elastomer [Article]. *Soft Matter*, 2(5), 377–385. <https://doi.org/10.1039/b600098n>
- Wannathong, T., Waterhouse, J. C., Young, R. E. B., Economou, C. K., & Purton, S. (2016). New tools for chloroplast genetic engineering allow the synthesis of human growth hormone in the green alga *Chlamydomonas reinhardtii*. *Applied Microbiology and Biotechnology*, 100(12), 5467–5477. <https://doi.org/10.1007/s00253-016-7354-6>
- Wehr, J. D., & Sheath, R. G. (2002). *Freshwater algae of North America: ecology and classification* (1st ed.) [Book]. Academic Press. <https://doi.org/10.1016/B978-0-12-741550-5.X5000-4>

- Weiner, I., Atar, S., Schweitzer, S., Eilenberg, H., Feldman, Y., Avitan, M., Blau, M., Danon, A., Tuller, T., & Yacoby, I. (2018). Enhancing heterologous expression in *Chlamydomonas reinhardtii* by transcript sequence optimization [Article]. *The Plant Journal: For Cell and Molecular Biology*, 94(1), 22–31. <https://doi.org/10.1111/tpj.13836>
- Weiner, I., Feldman, Y., Shahar, N., Yacoby, I., & Tuller, T. (2020). CSO – A sequence optimization software for engineering chloroplast expression in *Chlamydomonas reinhardtii* [Article]. *Algal Research (Amsterdam)*, 46, 101788. <https://doi.org/10.1016/j.algal.2019.101788>
- Wijffels, R. H., & Barbosa, M. J. (2010). Outlook on Microalgal Biofuels [Article]. *Science (American Association for the Advancement of Science)*, 329(5993), 796–799. <https://doi.org/10.1126/science.1189003>
- William D. Callister, J., & David G. Rethwisch. (2018). *Materials science and engineering: an introduction* (10th ed) [Book]. Wiley.
- Wostrikoff, K., Girard-Bascou, J., Wollman, F. A., & Choquet, Y. (2004). Biogenesis of PSI involves a cascade of translational autoregulation in the chloroplast of *Chlamydomonas*. *EMBO Journal*, 23(13), 2696–2705. <https://doi.org/10.1038/sj.emboj.7600266>
- Xia, X. X., Qian, Z. G., Ki, C. S., Park, Y. H., Kaplan, D. L., & Lee, S. Y. (2010). Native-sized recombinant spider silk protein produced in metabolically engineered *Escherichia coli* results in a strong fiber. *Proceedings of the*

National Academy of Sciences of the United States of America, 107(32), 14059–14063. <https://doi.org/10.1073/pnas.1003366107>

Xia, X.-X., Qian, Z.-G., Ki, C. S., Park, Y. H., Kaplan, D. L., Lee, S. Y., & Demain, A. L. (2010). Native-sized recombinant spider silk protein produced in metabolically engineered *Escherichia coli* results in a strong fiber [Article]. *Proceedings of the National Academy of Sciences - PNAS*, 107(32), 14059–14063. <https://doi.org/10.1073/pnas.1003366107>

Xu, R., Ouyang, L., Chen, H., Zhang, G., & Zhe, J. (2023). Recent Advances in Biomolecular Detection Based on Aptamers and Nanoparticles [Article]. *Biosensors (Basel)*, 13(4), 474. <https://doi.org/10.3390/bios13040474>

Xu, Y., Purton, S., & Baganz, F. (2013). Chitosan flocculation to aid the harvesting of the microalga *Chlorella sorokiniana*. *Bioresource Technology*, 129, 296–301. <https://doi.org/10.1016/j.biortech.2012.11.068>

Xue, X.-Y., Mao, Y.-B., Tao, X.-Y., Huang, Y.-P., Chen, X.-Y., & Jockusch, E. (2012). New Approaches to Agricultural Insect Pest Control Based on RNA Interference [Bookitem]. In *Advances in Insect Physiology* (Vol. 42, pp. 73–117). Elsevier Science & Technology. <https://doi.org/10.1016/B978-0-12-387680-5.00003-3>

Yang, D., Buchholz, F., Huang, Z., Goga, A., Chen, C.-Y., Brodsky, F. M., & Bishop, J. M. (2002). Short RNA Duplexes Produced by Hydrolysis with *Escherichia coli* RNase III Mediate Effective RNA Interference in Mammalian

- Cells [Article]. *Proceedings of the National Academy of Sciences - PNAS*, 99(15), 9942–9947. <https://doi.org/10.1073/pnas.152327299>
- Yekta, S., I-hung Shih, & Bartel, D. P. (2004). MicroRNA-Directed Cleavage of HOXB8 mRNA [Article]. *Science (American Association for the Advancement of Science)*, 304(5670), 594–596. <https://doi.org/10.1126/science.1097434>
- Young, R. E. B., & Purton, S. (2014). Cytosine deaminase as a negative selectable marker for the microalgal chloroplast: A strategy for the isolation of nuclear mutations that affect chloroplast gene expression. *Plant Journal*, 80(5), 915–925. <https://doi.org/10.1111/tpj.12675>
- Young, R. E. B., & Purton, S. (2016). Codon reassignment to facilitate genetic engineering and biocontainment in the chloroplast of *Chlamydomonas reinhardtii*. *Plant Biotechnology Journal*, 14(5), 1251–1260. <https://doi.org/10.1111/pbi.12490>
- Young, R., & Purton, S. (2018). CITRIC: Cold-inducible translational readthrough in the chloroplast of *Chlamydomonas reinhardtii* using a novel temperature-sensitive transfer RNA. *Microbial Cell Factories*, 17(1). <https://doi.org/10.1186/s12934-018-1033-5>
- Zedler, J. A. Z., Gangl, D., Guerra, T., Santos, E., Verdelho, V. V., & Robinson, C. (2016). Pilot-scale cultivation of wall-deficient transgenic *Chlamydomonas reinhardtii* strains expressing recombinant proteins in the chloroplast. *Applied*

Microbiology and Biotechnology, 100(16), 7061–7070.
<https://doi.org/10.1007/s00253-016-7430-y>

Zhang, G. J., Dong, R., Lan, L. N., Li, S. F., Gao, W. J., & Niu, H. X. (2020). Nuclear integrants of organellar DNA contribute to genome structure and evolution in plants. In *International Journal of Molecular Sciences* (Vol. 21, Issue 3). MDPI AG. <https://doi.org/10.3390/ijms21030707>

Zhang, J., Khan, S. A., Hasse, C., Ruf, S., Heckel, D. G., & Bock, R. (2015). Full crop protection from an insect pest by expression of long double-stranded RNAs in plastids. *Science*, 347(6225), 991–994.
<https://doi.org/10.1126/science.1257856>